UNIVERSITÀ DI NAPOLI FEDERICO II

DIPARTIMENTO DI FARMACIA

Dottorato di Ricerca in "Scienza del Farmaco"

XXIX Ciclo 2014/2017

Identification of new synthetic and semi-synthetic derivatives for the treatment of entero-hepatic disorders

Dott. Dario Masullo

Tutors

Prof.ssa A. Zampella

Prof. Kourosch Abbaspour Tehrani

Coordinatore

Prof.ssa M.V. D'Auria

“You never know what’s around the corner.
It could be everything or it could be nothing.
You keep putting one foot in front of the other.
And then, one day, you look back
and you have climbed a mountain”
Tom Hiddleston

INDEX

ABSTRACT

Bile acids, the end product of cholesterol metabolism, got researchers attention in the last twenty years for their ability to act as signal molecules. They are involved in multiple metabolic processes and, for this reason, they could be interesting lead compounds for the treatment of various diseases linked to metabolic syndrome. Due to their small chemical structure, bile acids are promiscuous molecules; indeed, they are able to bind both nuclear and G-protein coupled receptors, but, in some cases, in an unspecific manner. This promiscuity could lead to an unwanted activation of one of the two mentioned receptor class that could results in undesired side effects. For this reason, it became fundamental to understand the key pharmacophoric portions in that kind of molecules in order to know which part of them is responsible for the activation of one or both that receptors class.

In this context, most of my Ph.D. was spent on the speculation on different bile acid scaffolds, where modifications were done in order understand the selectivity criteria behind the activation of one of the two receptors classes, improving their activity towards them. The modifications carried out generated a first class of novel selective and dual FXR, GPBAR1 (a G-protein coupled receptor) and LXRα agonists, in which some members could be considered as potential lead compounds for the treatment of several aspects of metabolic diseases.

Furthermore, a new class of SHP (an orphan nuclear receptor) agonists was synthesised. This represent the first example reported in literature of synthetic selective agonists for this receptor, with promising results for the treatment of liver fibrosis.

Finally, the last part of my Ph.D. was spent in the organic synthesis laboratories of the Department of Chemistry, Antwerp University, where the direct functionalization of the 2-aza-anthraquinone, a molecule endowed with potential antiplasmodial activity, was carried out.

CHAPTER 1:
INTRODUCTION

1.1. Metabolic syndrome

In the civilized world characterized by a stressful life, where sedentary habits and unhealthy food are a common trend, the metabolic syndrome became a relevant factor for both citizen and public health.

Metabolic syndrome resulted from several factors that are responsible for the increase of cardiovascular diseases and type II diabetes, two conditions that could lead to death.[1] Among these factors, insulin resistance, visceral adiposity, atherogenic dyslipidaemia, endothelial dysfunction, genetic susceptibility, elevated blood pressure, and chronic stress play a critical role in metabolic syndrome. Following the guidelines of World Health Organization, the incidence of metabolic syndrome increases dramatically when diabetes associates with one of the following pathologies: high blood pressure, dyslipidaemia, central obesity, and microalbuminuria.[2] Today, more than 65% of the world population lives in countries where obesity is a life risk factor more than malnutrition,[3] and about 20-25% of world's population shows the typical cluster of risk for metabolic syndrome, numbers that are destined to grow.[4] Actually, the clinical management of both short and long-term effects of metabolic syndrome is difficult, because there is not a univocal method to improve or prevent the syndrome. One of the most used approaches by physicians is to treat separately the syndromes that constitute the metabolic disease. This approach could be useful in the treatment of the short-term effects of metabolic syndrome, but fails in the management of long-term effects. As suggested in the guidelines of the National Cholesterol Education Programme,[5] the treatment of metabolic syndrome should consist in a combination of lifestyle modification, diet, physical activity, weight reduction, behaviour changes, pharmacological approach and bariatric surgery, as final choice. The last one should be actuated only when the patient does not respond anymore to weight loss diet or medication.[6]

Today, the pharmacological approach to the weight loss is based on two classes of drugs, the inhibitors of nutrient absorption and appetite suppressants. Orlistat, the only nutrient absorption inhibitor currently in medical use, associates with several side effects such as flatulence and oil leakage in the stool, which could lead to a poor tolerance and compliance for the long-term use.[1]

Regarding dyslipidaemia, there is a single/combined pharmacological approach which involves statins, considered the most effective class of molecules in lowering LDL,[5] in combination with niacin or fibrates (fenofibrate and gemfibrozil). Niacin, in a long-term exposition, could lead to flushing and hyperglycaemia,[7] thus, in patients affected by diabetes, the dose of niacin should be kept low.[8] However, although cases of myopathy and rhabdomyolysis have been reported, the combination between statin/niacin or statin/fibrate is generally considered save.[9]

Angiotensin converting enzyme (ACE) inhibitors and angiotensin receptor blockers (ARBs) represent the first line treatment of hypertension in metabolic syndrome, especially in the setting of diabetes.[10] Although ACE inhibitors and ARBs could reduce the risk of diabetes,[11] a recent study suggested that the ACE inhibitor ramipril does not prevent the progression of diabetes in people with impaired glucose tolerance (IGT) or impaired fasting glucose (IFG).[12]

About diabetes, the election therapy for its treatment consists in the use of oral hypoglycaemic agents such as metformin, thiazolidenediones, and acarbose.[13,14,15] Whereas these classes of compounds reduce the incidence of type II diabetes mellitus in patients affected by high hematic levels of glucose, no reduction in the risk of cardiovascular events in metabolic syndrome (except for acarbose) has been so far reported.[16]

Considering that one of the most common side effect for all the above reported treatments is the tolerance, alternative pharmacological approaches become fundamental for the treatment of metabolic syndrome. In this sense, an effective therapeutic strategy could be the modulation of the activity of metabolic nuclear and G-protein coupled receptors.

These receptors are involved in the regulation of many physiologic processes through different mechanisms of action that will be discussed in the next paragraphs. The binding of small lipophilic endogenous and exogenous molecules

to metabolic nuclear and G protein coupled receptors, leads to their activation or suppression. As result, a specific modulation of the physiologic pathway in which the receptor is involved, occurs. This accurate activity modulation points out nuclear and G protein coupled receptors as appealing pharmacological targets for the treatment of all the aspect composing the metabolic syndrome.

1.2. Nuclear receptors

Nuclear receptors (NRs) are a class of intracellular protein able to bind specific DNA sequences enhancing the transcription of the adjacent genes after the binding of small molecules, hormones or steroids. After ligand binding, the complex ligand-nuclear receptor transmigrates into the cell nucleus, and, thanks to the linking with other nuclear proteins, binds DNA and activates the gene expression. All nuclear receptors share two high conservative domains in their structure (Figure 1); the N-terminal domain, also called DNA binding domain, responsible for the binding to DNA, and a C-terminal domain, the ligand-binding domain (LBD), responsible of the binding between the ligand and NR. The binding of NR to DNA induces conformational changes that lead to release of a co-repressor, the recruitment of a co-activator, chromatin remodelling and finally the activation of the transcriptional machinery.

Forty-eight genes coding for NRs are present in the human genome; most of them have been characterized during the last twenty years whereas others still require a de-orphanization or a complete explanation of their physiological role. One of the first nuclear receptors classification is based on DNA-binding properties and dimerization preferences. A more recent classification divided NRs in seven classes (from NR0 to NR6) on the base of multiple alignment procedures, phylogenetic-tree construction methods and other evolutionary consideration.[17] In table 1 is reported the latest NRs classification.

While oestrogen receptor like subfamily works as homodimer, subfamilies 1 and 2 of NRs work as heterodimers with the retinoid X receptor (RXR).

Among these last two subfamilies, remarkable are the peroxisome proliferated activated receptor (PPAR), with its two isoforms α and β, vitamin D receptor (VDR), retinoid acid receptor (RAR), pregnane X receptor (PXR), constitutive

androstane receptor (CAR), liver X receptor (LXR) and farnesoid X receptor (FXR). Differently from all the other mentioned receptors, PXR and CAR are orphan receptors, as physiological ligands have not been so far identified. PXR and CAR are called xenobiotic nuclear receptors because their activation from xenobiotics enhances the transcription of Phase I and II enzymes, responsible of liver drug metabolization and elimination.

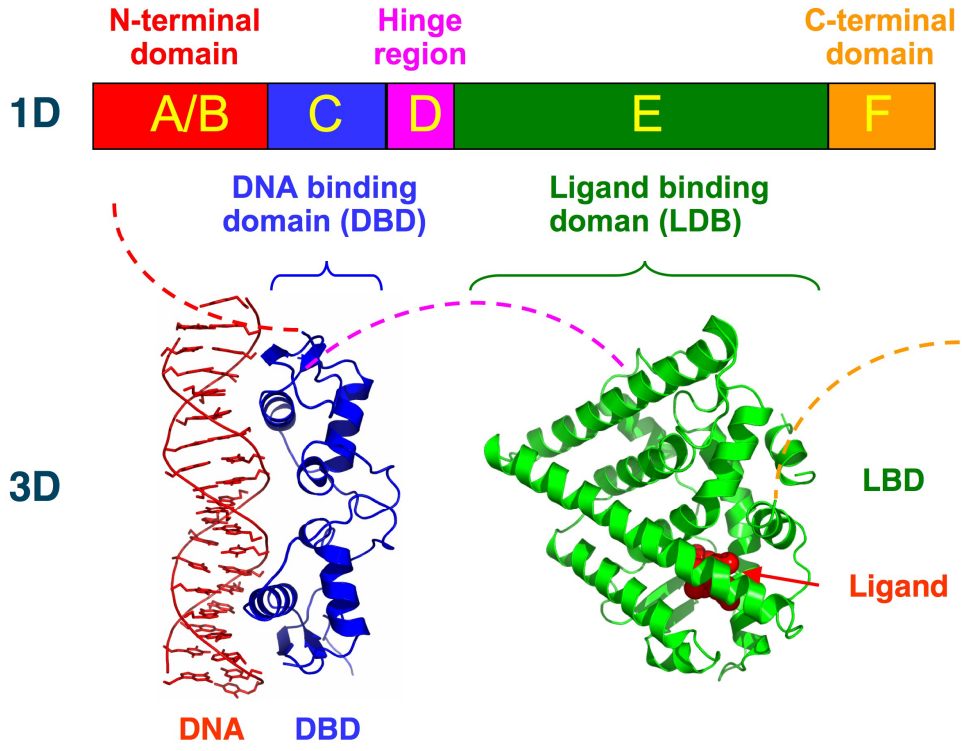

Figure 1. Nuclear receptors structure

In this thesis my attention has been focused on FXR and LXR, two NRs activated by bile acids (BAs) that regulate various metabolic functions.

SUBFAMILY		GROUP
NR1	Thyroid Hormone Receptor-like	•Thyroid hormone receptor •Retinoic acid receptor •Peroxisome proliferator-activated receptor •Rev-ErbA, RAR-related orphan receptor •Liver X receptor-like •Vitamin D receptor-like •NRs with two DNA binding domains
NR2	Retinoid X Receptor-like	•Hepatocyte nuclear factor-4 •Retinoid X receptor •Testicular receptor •TLX/PNR •COUP/EAR
NR3	Estrogen Receptor-like	•Estrogen receptor •Estrogen related receptor •3-Ketosteroid receptors
NR4	Nerve Growth Factor IB-like	•NGFIB/NURR1/NOR1
NR5	Steroidogenic Factor-like	•SF1/LRH1
NR6	Germ Cell Nuclear Factor-like	•GCNF
NR0	Miscellaneous	•DAX/SHP

Table 1: NRs classification

1.2.1. Farnesoid X receptor (FXR)

In 1999, FXR was deorphanized with the identification of bile acids (BA) as endogenous ligands.[18,19,20] FXR, mostly expressed in liver and bowel, functions as the master sensor of BAs concentration in liver (Figure 2).[21] Indeed, by a negative feedback mechanism, FXR reduces BAs concentration, preventing the toxic effects of these molecules.[22] This is the consequence of three different pathways. First, the activation of FXR results in the gene expression of the small heterodimer partner (SHP), an orphan nuclear receptor that lacks DNA-binding domain.[23] SHP dimerizes with both LRH-1 and LXRα, resulting in the inhibition of the expression of CYP7A1, a cytochrome involved in the *de novo* synthesis of bile acids.[24] On the other hand, FXR inhibits BAs uptake in hepatocytes by the repression of Na^+/taurocholate co-transporting polypeptide (NTCP) and organic anion transporting polypeptide 1 (OATP1), and stimulates their elimination in liver, intestine and kidney by enhancing the expression of the bile-salt exporting pump (BSEP), the alternative basolateral efflux transporter multi-drug resistance 3 (MDR3) and organic solute transporters α and β (OSTα/β).[25,26] For these features, FXR appears to be a very attractive target for the treatment of primary biliary cirrhosis (PBC) and primary sclerosing cholangitis (PSC), two disorders characterized by impaired bile acids level in the liver and resulting from progressive bile duct destruction.[27,28]

Beside this canonical function, FXR is also involved in maintaining lipid homeostasis and glucose metabolism. In fact, FXR activation results in the inhibition of triglyceride synthesis through the down regulation of both the transcription factor sterol-regulatory-element-binding protein-1c (SREBP1c) and its target fatty acid synthase (FAS).[29] Furthermore, FXR is able to down-regulate gluconeogenesis by the inhibition of phosphoenol pyruvate carboxy kinase, glucose-6-phosphatase and fructose-1,6-biphosphatase synthesis, all involved in the *de novo* synthesis of glucose.[30,31,32]

For these metabolic effects, FXR could also be an appealing target for the treatment of both non-alcoholic steatohepatitis (NASH) and non alcoholic fatty liver diseases (NAFLD).

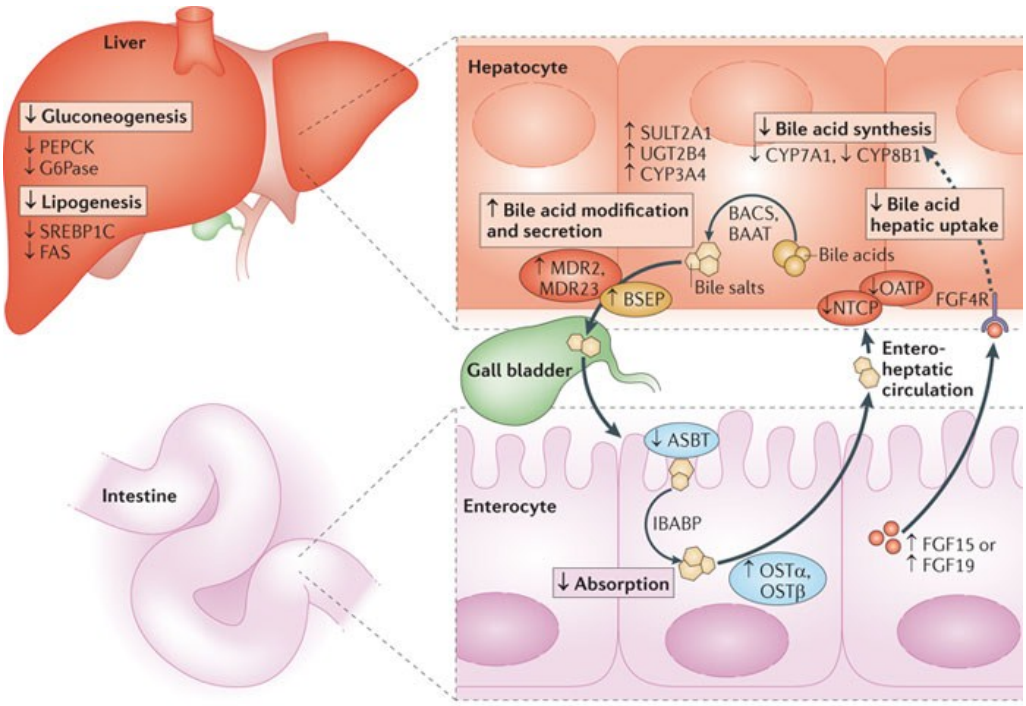

Figure 2. FXR functions

The potential therapeutic application of FXR agonists in the treatment of many metabolic pathologies increased the attention of researchers to identify endogenous and exogenous modulators of this receptor. Among endogenous ligands, the chenodeoxycholic acid (CDCA), one of the most abundant BA contained in the bile, represents the most potent FXR activator. Regarding synthetic molecules (Figure 3), high-throughput screening of several libraries of compounds, showed some potent synthetic FXR agonists, noteworthy GW4064, obeticholic acid (6-ECDCA) and fexaramine.[33,34,35]

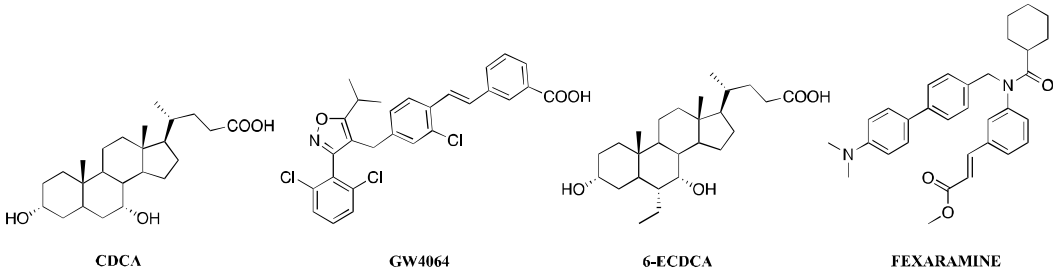

CDCA GW4064 6-ECDCA FEXARAMINE

Figure 3. Natural and synthetic FXR agonists

1.2.2. Liver X receptor (LXR)

The two isoforms of LXR (LXRα and LXRβ) share about 77% aminoacid sequence identity, and are both activated by the same endogenous ligands.[36] While LXRβ is ubiquitously expressed, LXRα is expressed in liver, intestine, adipose tissue, spleen and macrophages. LXR main function is the regulation of lipid and cholesterol metabolism.[37] Their mechanism of action (Figure 4) include the hetero-dimerization with RXR, leading to the activation of LXR responding element (LXRE), which, in turn, activates several genes involved in cholesterol and fatty acids metabolism such as the ATP binding cassettes A1, G5 and G8 (ABCA1, ABCG5, ABCG8), apolipoprotein E and sterol response element binding protein 1 (SREBP-1c).[38,39]

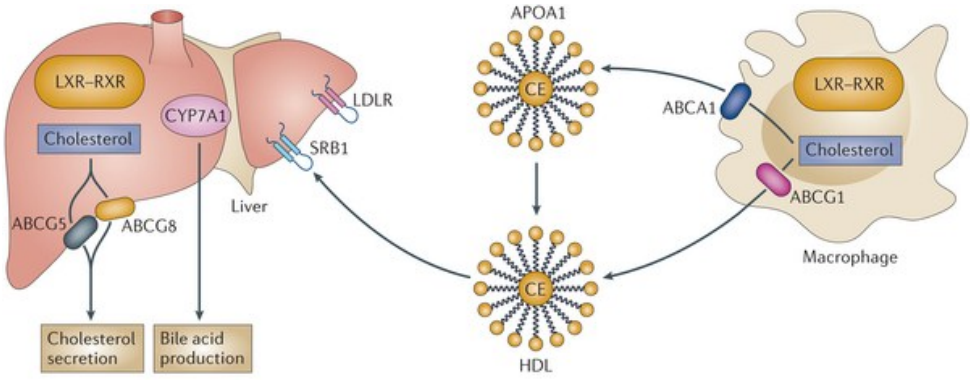

Figure 4. LXR functions

LXRs seem to be very appealing targets for the treatment of hypercholesterolemia. As reported in many papers,[40,41,42,43] LXR agonists are able to decrease cholesterol levels and inhibit the progression of atherosclerosis in murine models. In another murine model of diet inducted obesity, LXR synthetic agonists showed to be able to improve insulin resistance and glucose tolerance, thorough the regulation of genes involved in glucose metabolism.[44] Moreover, activation of LXR in macrophages inhibits the expression of inflammatory mediators.[45] LXR seems to have also an anti-proliferative effect as its activation suppresses the proliferation of breast and prostatic cancer.[46,47]

Unfortunately, the correlated induction of the expression of lipogenic genes leads to hyperglycaemia and liver steatosis; these two important side effects have

limited the therapeutic use of LXR agonists. The increase of lipogenesis could be attributed to the higher expression of SREBP-1c, the enzyme responsible of hepatic conversion of glucose into lipids.[48,49,50,51] For the potential use in treatment of pathologies linked to high levels of cholesterol, diabetes and treatment of cancer, it is fundamental to identify LXR agonists that show no effects on lipogenesis.

Both isoforms of LXR are activated by endogenous cholesterol metabolites (Figure 5) as 22(*R*)- and 24(*S*)-hydroxycholesterol and 24(*S*),25-epoxycholesterol;[52] in literature there are several natural compounds able to bind LXRs[15] and, noteworthy, berberine, an isoquinoline alkaloid component of *Rhizoma coptidis*, has been tested for its use as anti-inflammatory, antimicrobial, antihypertension, antiarrhythmias, antitumor and antidiabetic agent.[53,54,55]

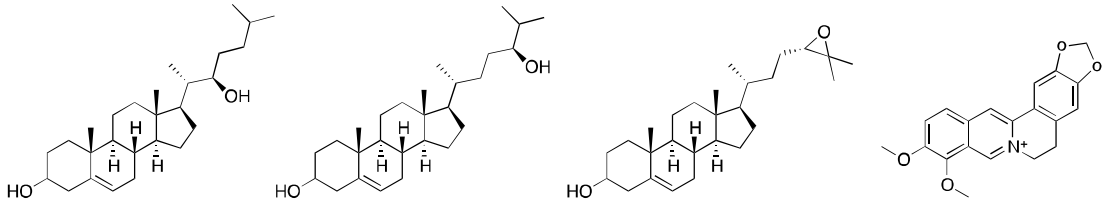

Figure 5. LXR natural ligands

As it will be discussed in Chapter 4, among bile acids, hyodeoxycholic acid (HDCA) is a weak LXRα agonist. In particular, the activation of LXRα by HDCA produces beneficial effects in metabolic disorders, cholesterol absorption and atherosclerotic plaque formation. These findings point out HDCA derivatives as possible lead compounds in the treatment of many metabolic disorders regulated by LXRα.

1.3. G-protein coupled receptors

G-protein coupled receptors (GPCRs), also called seven transmembrane domain receptors, are a huge class of proteins ubiquitously distributed in eukaryotes. These proteins are placed on the cell membrane surface and the interaction with an external ligand produces effects inside cytoplasm. Most of GPCRs are composed by seven transmembrane helices, with an N-terminal portion exposed outside the cell and responsible of the binding with the proper modulator, and a C-

terminal domain exposed into the cytoplasm. All GPCRs are associated to a guanine-binding class of proteins, called G proteins, composed by three subunits namely α, β and γ, with the last two linked together to form a βγ complex, and acting as molecular switches inside cells. The binding of a ligand to GPCR induces a conformational change responsible of the exchange of GDP for GTP (Figure 6). Then, depending on which type of G protein (G_s, G_q or G_i) the receptor is associated, different types of activity are triggered. In case of G_s, the binding with GTP allows the release of the inhibitory $G_{\beta\gamma s}$ subunit and the dissociation from the receptor itself. The activated G_α subunit stimulates the membrane enzyme adenylate cyclase, responsible of the conversion of ATP into cAMP, a second messenger able to interact with PKA, a protein kinase that phosphorylates a large number of targets, producing various effects. Regarding G_q related receptors, GTP binding leads to the activation of phospholipase C (PLC). This enzyme catalyses the cleavage of phosphatidylinositol 4,5-biphosphate (PIP2) into the second messenger inositol (1,4,5) trisphosphate (IP3) and diacylglycerol (DAG), both responsible for an increase of intracellular Ca^{2+} levels. Finally, the G_i protein, differently from G_s, hampers adenylate cyclase activity. Among this class of receptors, a part of my research activity was focused on the modulation of the G protein-coupled bile acid receptor 1 GPBAR1 (or TGR5), which is the first known GPCR able to bind bile acids.

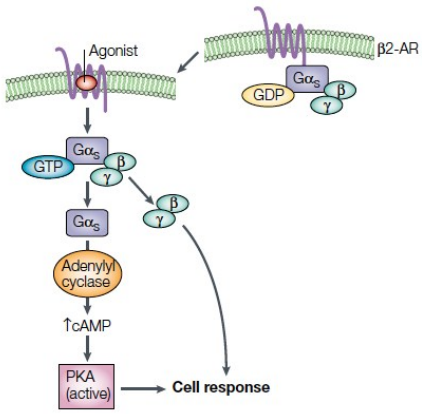

Figure 6. General activation mechanism of GPCRs

1.3.1 G protein-coupled bile acids receptor 1(GPBAR1)

GPBAR1, a G_s protein-coupled receptor, also known as Takeda G receptor 5 (TGR5), is the membrane bile acid receptor.

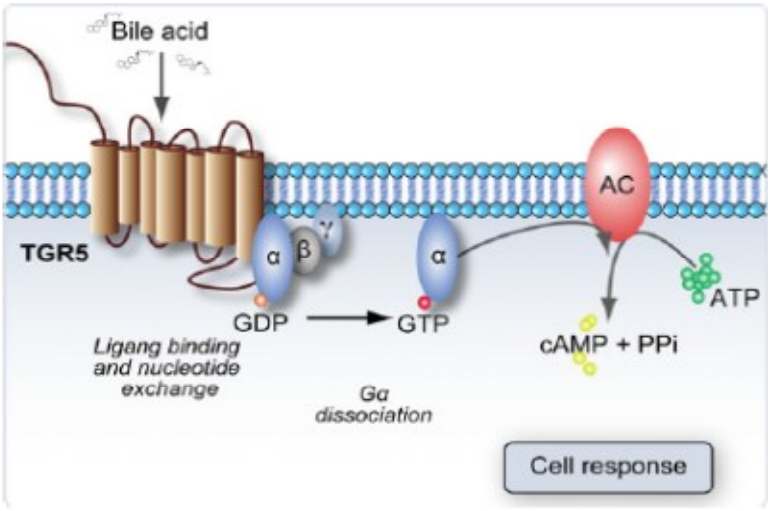

Figure 7. GPBAR1 activation effects

Discovered in 2002, the three-dimensional structure of GPBAR1 remains still unknown, but in 2014 a 3D homology model was proposed.[56]

GPBAR1 is mainly expressed in the cell surface of liver, bowel, skeletal muscle cells, adipose tissue and in macrophages/monocytes,[57] and depending on its tissue expression, it could produce different effects (Figure 7).

In liver sinusoidal endothelial cells, as well as in biliary tree, gallbladder epithelia, apical membranes and primary cilium of cholangiocytes,[58,59,60] activation of GPBAR1 by endogenous bile acids results in the inhibition of *de novo* bile acids synthesis and their re-uptake from enterohepatic circuit as reported also for FXR. Consequently, GPBAR1 could be a potential target for the treatment of obstructive cholestasis.

GPBAR1 is also involved in several metabolic processes. In brown adipose tissue and in skeletal muscle, it enhances energy expenditure and increase basal metabolic rate through the induction of iodothyrosine deiodinase (D2), an enzyme responsible of the conversion of inactive thyroid hormone T4 into the active thyroid hormone T3.[61] Since T3 is also involved in the increasing of glucose

consumption and the increase of LDL receptors, these findings point GPBAR1 as potential anti-obesity target.[62]

One of the most promising effects of GPBAR1 activation is on diabetes. Indeed, the receptor is expressed on enteroendocrine cells, ad its activation leads to the release of the glucagon-like peptide 1 (GLP-1).[63] This hormone acts on β-pancreatic cells, stimulating the release of insulin and the inhibition of hepatic gluconeogenesis, two actions that result in regulating hematic glucose levels, gastrointestinal motility and sense of appetite. Experimental data, performed on both mice and humans, demonstrated that the activation of GPBAR1 in enteroendocrine cells leads to an increasing of GLP-1 hematic levels.[64,65,66] Furthermore, other studies demonstrated that GPBAR1 agonists prevent obesity in mice fed with a high fat diet showing lower levels of plasma glucose.[67]

The expression of GPBAR1 in macrophages and monocytes points out the role of GPBAR1 agonists as potential leads in inflammatory diseases. The activation of GPBAR1 negatively regulates the expression of several NF-κB pro-inflammatory targeted genes such as inducible NOS, interferon-inducible protein, and interleukin IL-1α.[68] GPBAR1 is also expressed in Kupffer cells, and its activation induces the inhibition of the pro-inflammatory cytokines IL-1α, IL-1β, IL-6 and tumour necrosis factor-α (TNF-α).[69] Several applications of potential GPBAR1 agonists in the treatment of inflammatory diseases have been proposed. GPBAR1 has been recently demonstrated overexpressed in patients affected by Crohn's disease and in animal model of colitis.[7071] Furthermore, the anti-inflammatory properties of GPBAR1 could be useful for the treatment of the inflammatory bowel disease (IBD) and, as consequence, also in the treatment of primary sclerosis cholangitis (PSC), that often results from chronic IBD.[72,73]

Collectively, these effects affirm GPBAR1 as an appealing target in the pharmacological treatment of liver disorders, especially in the metabolic syndrome. As reported in literature, all these effects are mediated by the binding of GPBAR1 with bile acids, pointing out their role in modulation of metabolic syndrome.

1.4. Bile acids (BAs)

Bile acids (Figure 8) are the major components of bile, and their canonical function is to participate in lipid and vitamins absorption.

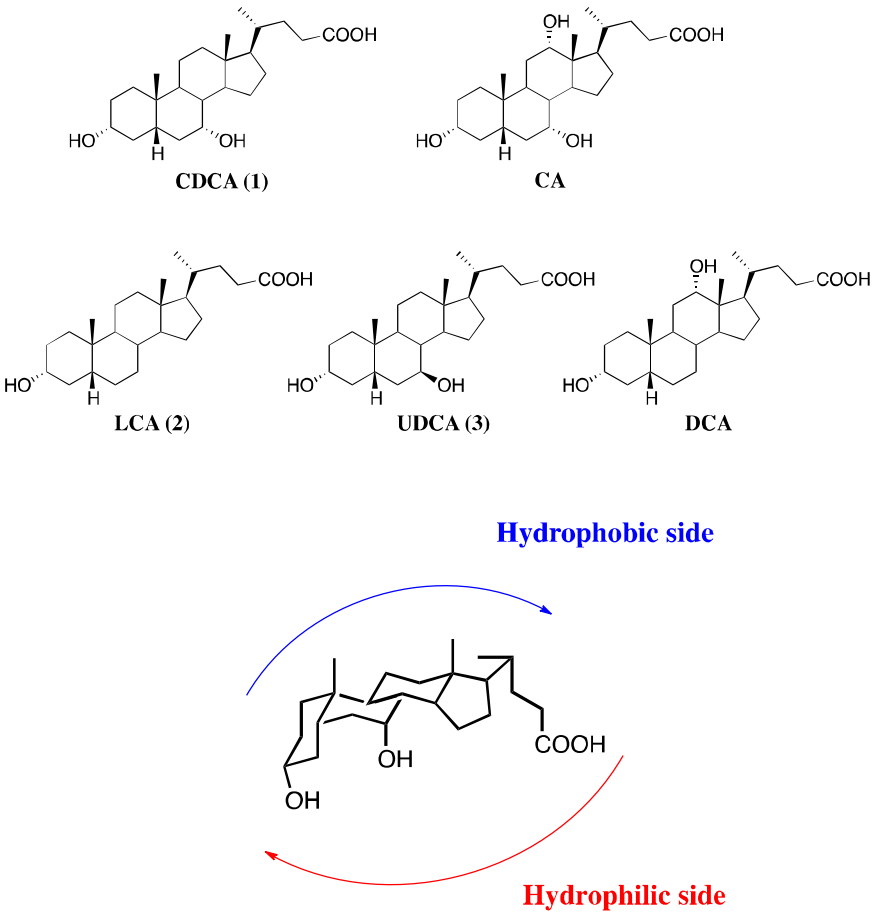

Figure 8. Endogenous bile acids and hydrophobic/hydrophilic character

From a chemical point of view, BAs are truncated derivatives of cholesterol,[74] with a five-carbon side chain placed in position 17 ending with a carboxylic acid moiety, and an hydroxyl function in position 3. Other –OH groups could be found at position 7 (as in CDCA and UDCA) and at position 12 (CA). The distinctive structural feature of bile acids is the *cis* junction between A/B rings producing two areas with different polarity (Figure 8). An hydrophilic side, composed by the carboxylic moiety in side chain and the –OH in position 3, and a hydrophobic area, resulting from the tetracyclic carbon scaffold.

Thanks to this structural organization, bile acids can act as emulsifier molecules, explaining their canonical function in lipid and vitamin absorption.

Regarding their synthesis, bile acids represent cholesterol hepatic metabolism products. There are two different oxidative processes that involve different hepatic cytochromes, and both of them took to the synthesis of the so-called primary bile acids (Figure 9).

In the first pathway (the classic pathway), CYP7A1 and CYP8B1 are involved in the production of cholic acid (CA), whereas, in the second pathway (the alternative one), CYP27A1 and CYP7B1 are responsible of the synthesis of chenodeoxycholic acid (CDCA).[47]

Once synthesized, BAs reach the intestine, where are deoxidised by resident bacteria producing secondary bile acids (Figure 10) such as deoxycholic acid (DCA), lithocholic acid (LCA) and, in small amount, ursodeoxycholic acid (UDCA).

Primary and secondary BAs could be subjected to conjugation with glycine in humans and taurine in mice, respectively, at C-24 by an N-acyl transferase enzyme; the conjugation products are stored in gallbladder, waiting to be released during the digestion. Most of BAs (94-98%) are re-absorbed in bowel and come back to liver thanks to the entero-hepatic circulation; only a small amount is expelled through faeces.

Although BAs are cholesterol derivatives, they are not able to bind hormone receptors. The *cis* junction between A/B rings pushes the A ring outside the plane formed by B-C-D rings, and the loss of a so extended planar structure doesn't allow the oxygen in position 3 to bind its counterpart in hormone receptors, whereas that kind of structural organization perfectly fits in BAs receptors previously mentioned.

Among BAs, CDCA is the most active physiological modulator of FXR. Differently, LCA (together with its tauro-conjugated form) is the best physiological modulator of GPBAR1, showing a high selectivity towards this receptor. Comparing the structure of these two molecules, it is clear that the –OH at C-7 represents the key pharmacophoric point in activating GPBAR1. Another key pharmacophoric portion is the side chain; differently from cholesterol, BAs bear a carboxylic acid moiety, responsible of the binding with a common polar pocket both in FXR and GPBAR1.[56]

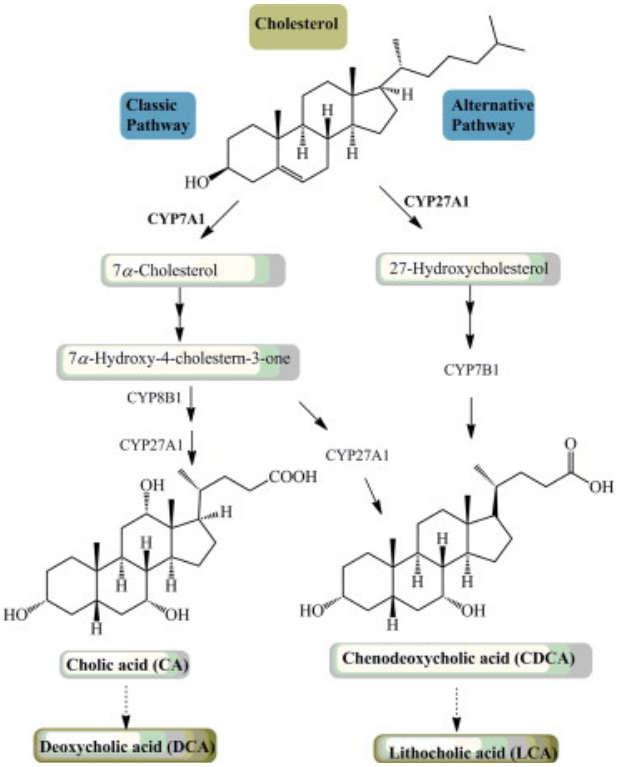

Figure 9. Primary BAs synthetic pathways

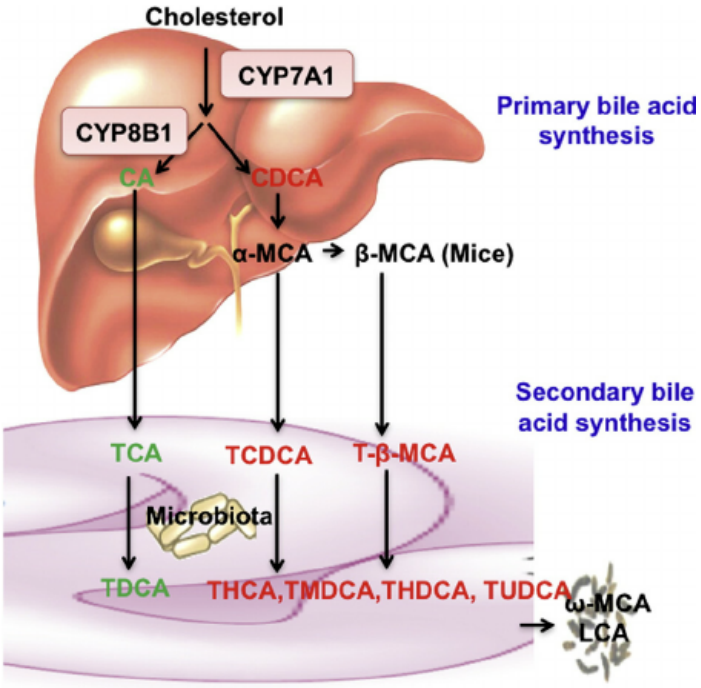

Figure 10. Secondary bile acid synthetic pathways

In this framework, my Ph.D. research work has been mainly focused on the speculation of different bile acid scaffolds to find novel lead compounds in the treatment of one or more components of the metabolic syndrome. Chemical modification at C-3 and/or C-7, the length and functionalization of side chain, as well as at the junction between rings A/B, generated new classes of selective/dual agonists of FXR, GPBAR1 and LXR. Thanks to the collaboration with the research group of Professor Stefano Fiorucci (University of Perugia), pharmacological assays were performed on the new synthesized compounds. In particular, to address the activity of the compounds towards one of the three receptors, transactivation assays were performed. Compounds showing the best pharmacologic profile *in vitro*, were also tested in different *ex vivo* and *in vivo* experiments, in order to understand their possible applications in the treatment of one or more aspect of the metabolic syndrome.

A more recent section of my work, regarded the synthesis of new synthetic nuclear receptor modulators. In particular, this work was focused on the synthesis of isoxazole derivatives as new SHP modulators, an orphan nuclear receptor whose activation could be useful in the treatment of liver fibrosis. Finally, the last part of my Ph.D. was spent in the laboratories of organic synthesis group of the Department of Chemistry, University of Antwerp, under the supervision of Professor Kourosch Abbaspour Tehrani, where my research activity was focused on the synthesis and the functionalization of quinone-compounds endowed with antiplasmodium activity.

CHAPTER 2:
URSODEOXYCHOLIC ACID DERIVATIVES

Among the endogenous bile acids, Ursodeoxycholic acid (UDCA) is a very interesting molecule. Generated from CDCA by a simple configuration inversion of the –OH at C-7, UDCA represents 3% of the total endogenous BAs. Despite its low concentration in human bile, today UDCA represents the only bile acid used in therapy. In fact, UDCA is the first choice in the pharmacological treatment of primary biliary cirrhosis (PBC), primary sclerosing cholangitis (PSC), intrahepatic cholestasis of pregnancy (ICP), as well as other uncommon adult and pediatric cholestatic conditions.[75] In addition, UDCA plays a neuroprotective role and chemopreventive action in colon cancer.[76,77,78] Although the mechanism of action of UDCA is still unknown, UDCA is a very safe molecule, with minimal side effects also when administered in high doses.

Although UCDA and CDCA exhibit a quite common chemical structure (Figure 11), the inversion of configuration at C-7 hydroxyl group (β in UDCA, α in CDCA) results in a loss of activity of UDCA towards FXR. Indeed, the 7β configuration pushes the –OH far from one of the most important site of interaction in FXR, resulting in the loss of activity.

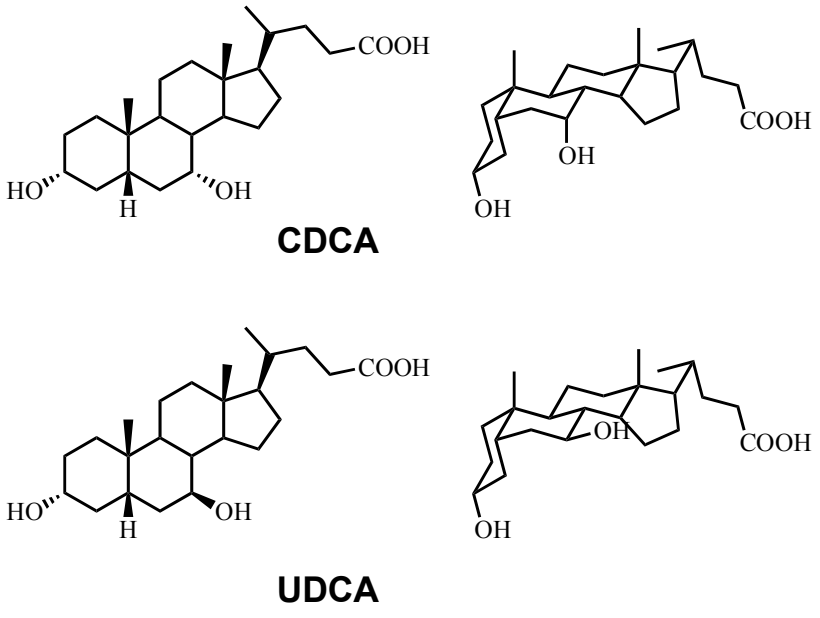

Figure 11. Structural differences between CDCA and UDCA

Considering its safe pharmacological profile, a first set of UDCA derivatives was synthetized. In particular, in this frame, the influence of the side chain in receptor selectivity was analysed, with modifications regarding both its length and functionalization type.

This modification led to a new class of GPBAR1 modulators (Figure 12), as demonstrated from transactivation assays. Computational studies on four compounds of the series have been performed to understand the binding pose in GPBAR1 binding pocket. Finally, a deep pharmacological evaluation was carried out on the best derivative of the group in order to characterize its pharmacological activity.

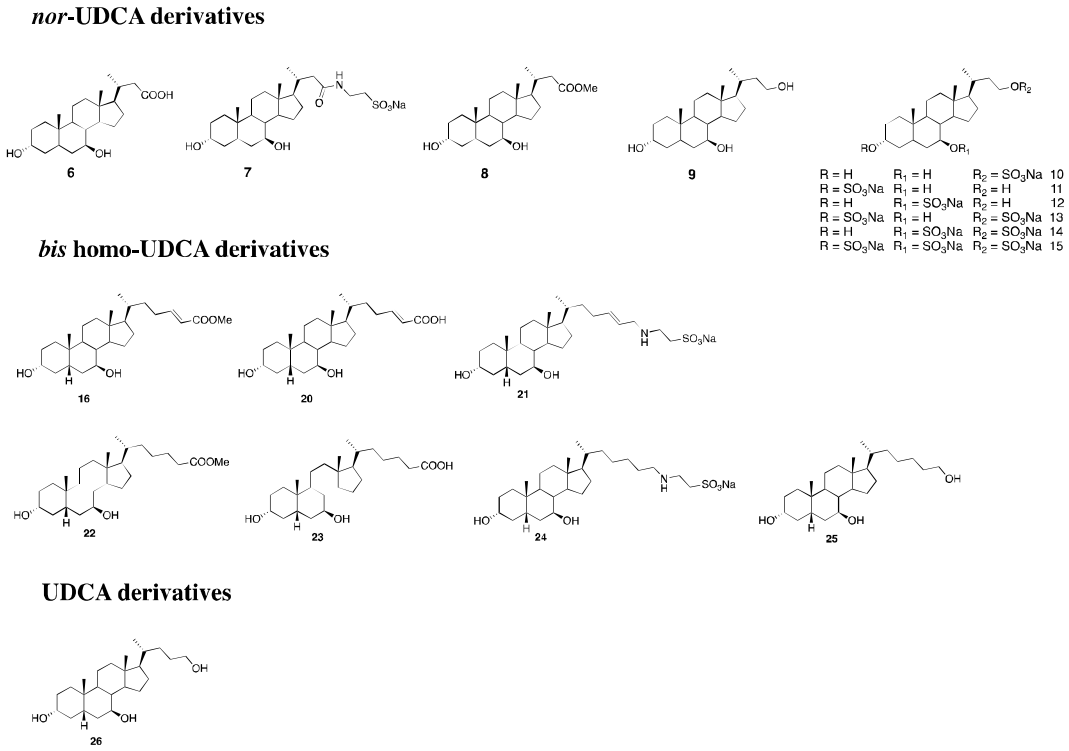

Figure 12. UDCA derivatives synthetized in this study

2.1. Synthesis of nor-UDCA derivatives

The preparation of *nor*-UDCA derivatives (Scheme 1) started from protection of hydroxyl groups at position 3 and 7 through Fisher's esterification with formic acid and perchloric acid on UDCA. Then, Beckmann one carbon degradation was performed treating compound **4** with sodium nitrite, trifluoroacetic acid (TFA) and trifluoroacetic anhydride (TFAA) to give the corresponding *nor*-nitrile **5** in high yield (96%). The temperature was set between 35-40 °C, preserving the two

formyl group from hydrolysis in the reaction mixture. The reaction proceeds with a concertize mechanism as shown in Figure 13. First, the reaction between the carboxylic acid moiety in side chain and TFA give the corresponding mixed anhydride, an instrumental step necessary to activate the α position at COOH (Figure 13, panel A).

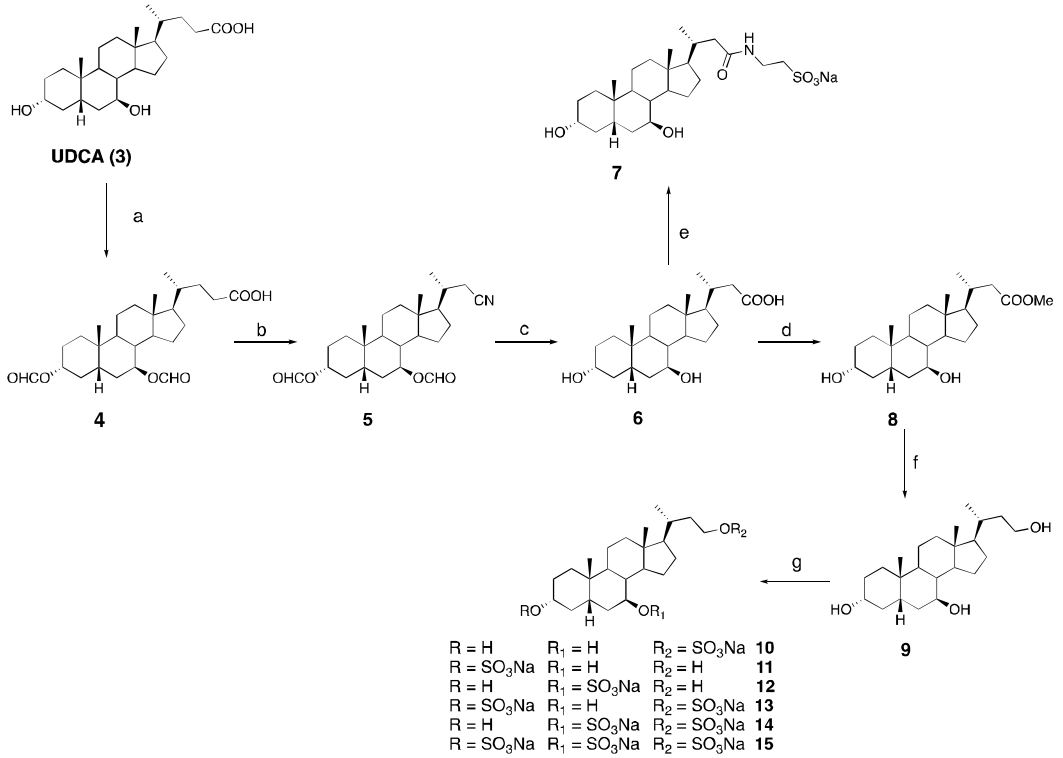

Scheme 1. *Reagents and Conditions.* a) HCOOH, $HClO_4$; b) TFA, trifluoroacetic anhydride, $NaNO_2$; c) KOH 30% in MeOH/H_2O 1:1 v/v; d) *p*-TsOH, MeOH dry; e) DMT-MM, Et_3N, taurine, DMF dry; f) $LiBH_4$, MeOH dry, THF, 0 °C; g) $Et_3N{\cdot}SO_3$, DMF, 95 °C

In the meantime, TFAA reacts with $NaNO_2$ in the acid catalytic environment to give the trifluoroacetic nitrite (Figure 13, panel B). The trifluoroacetic nitrite reacted with the activated α position of the BA derivative side chain to give the corresponding α-nitrose anhydride (Figure 13, panel C).

This product tautomerizes to the corresponding oxime that reacts immediately with TFAA. Then, the heating step induces the reaction between the two trifluoroacetate groups, the following electron shift forming the triple bond of nitrile with the elimination of CO_2 (Figure 13, panel D). Treatment of **5** with potassium hydroxide in MeOH/H_2O 1:1 gave the simultaneous hydrolysis of

nitrile and the de-protection at C-3 and C-7 furnishing compound **6**. A first aliquot of **6** was treated with taurine in the presence of a coupling agent, 4-(4,6-dimethoxy-1,3,5-triazin-2-yl)-4-methylmorpholinium chloride (DMT-MM), giving the amide derivative as ammonium sulphate salt. Purification on RP-18 column followed by HPLC furnished pure **7** as sodium salt. A second aliquot of **6** was subjected to Fisher's esterification in side chain with MeOH and p-toluensulfonic acid to give the corresponding methyl ester **8** that was transformed without purification in its corresponding alcohol **9** by treatment with $LiBH_4$ and MeOH in THF. Treatment of **9** with sulfur trioxide triethylamine complex ($Et_3N{\cdot}SO_3$) furnished a mixture of sulphate derivatives. HPLC purification gave three monosulphate (compounds **10**, **11**, **12**), two disulphate (compounds **13** and **14**) and a trisulphate (**15**) derivatives.

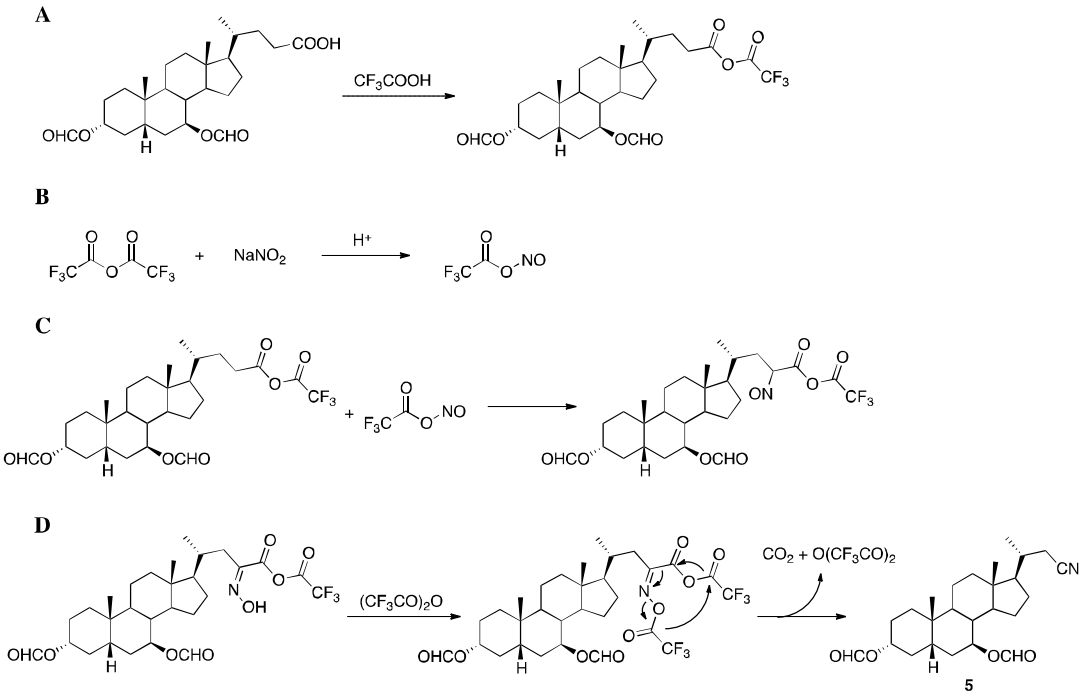

Figure 13. Reaction mechanism of Beckmann's one carbon degradation

2.2. Synthesis of bis homo-UDCA derivatives

Key step in C-2 homologation of the side chain on UDCA was the one-pot Swern's oxidation-Horner homologation. The synthetic protocol includes first the alcoholic protection at C-3 and C-7 with tert-butyldimethylsilyl

trifluoromethanesulfonate (TBSOTf) and 2,6-lutidine. Then, $LiBH_4$ treatment furnished the corresponding C-24 alcohol (**17**) that in turn was subjected to the one pot Swern's oxidation- Horner homologation.

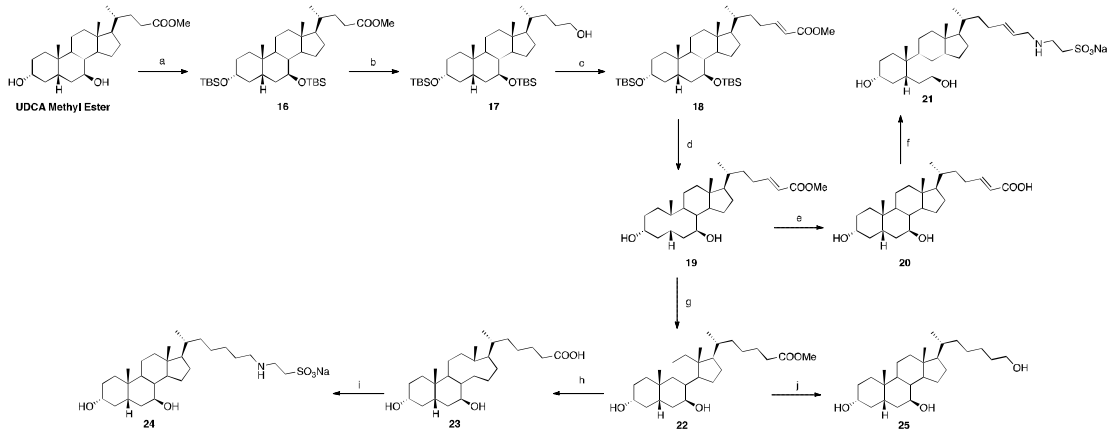

Scheme 2. *Reagents and Conditions*. a) 2,6-lutidine, *t*-butyldimethylsilyl trifluoromethanesulfonate, CH_2Cl_2, 0 °C; b) $LiBH_4$, MeOH dry, THF, 0 °C; c) DMSO, oxalyl chloride, TEA dry, CH_2Cl_2, -78 °C, then methyl(triphenylphosphoranylidene)acetate; d) HCl 37%, MeOH; e) NaOH 5% in MeOH/H_2O 1:1 v/v; f) DMT-MM, Et_3N, taurine, DMF dry; g) H_2, $Pd(OH)_2$/C degussa type, THF/MeOH 1:1; h) NaOH 5% in MeOH/H_2O 1:1 v/v; i) DMT-MM, Et_3N, taurine, DMF dry; j) $LiBH_4$, MeOH dry, THF, 0 °C.

From a mechanistic point of view, the reaction proceeds first with the activation of dimethylsulfoxide (DMSO) by oxalyl chloride [$(COCl)_2$] through the nucleophilic attach of the oxygen of DMSO to one of the acyl moiety of $(COCl)_2$ forming an intermediate positively charged on sulphur atom (Figure 14).

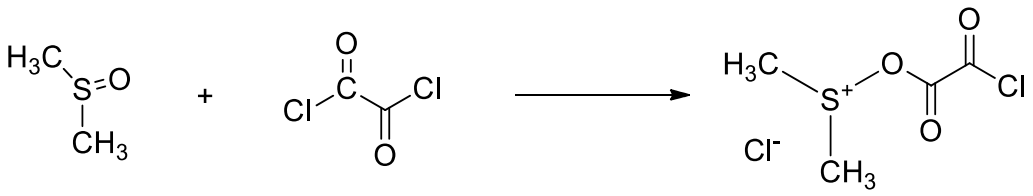

Figure 14. DMSO activation

Then, the nucleophilic attach of the alcohol (added subsequently at the reaction mixture) give the sulfonium ion depicted in Figure 15.

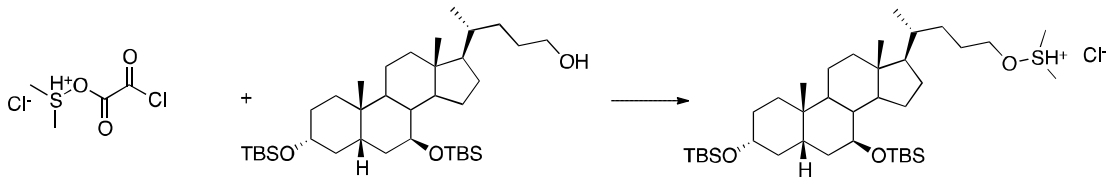

Figure 15. Nucleophilic attack to alcohol

Finally, the addition of triethylamine (TEA) produces the de-protonation and the subsequent intramolecular re-arrangement affording the formation of the aldehyde as shown in Figure 16.

The aldehyde was then subjected to Horner reaction with methyl (triphenylphosphoranylidene) acetate. The reaction was highly stereoselective, with the exclusive formation of *E* isomer **18**.

De-protection at the C-3 and C-7 carbinols by treatment with HCl 37% in MeOH, gave compound **19**.

A first aliquot was subjected to basic hydrolysis by treatment with NaOH 5% in MeOH/H_2O 1:1 to give compound **20**, that was treated with taurine in the same condition described for compound **7** furnishing the corresponding tauro-conjugate **21**.

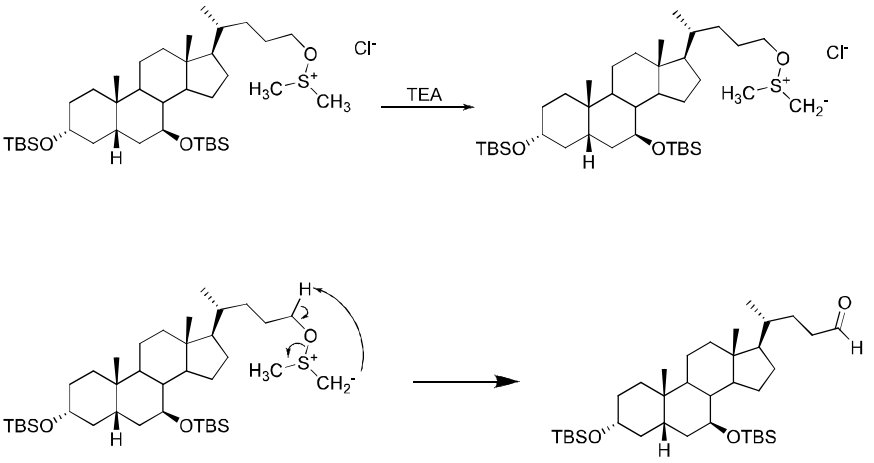

Figure 16. Deprotonation and re-arrangement

A second aliquot of **19** was subjected to catalytic reduction at the side chain double bond by treatment with H_2 and palladium hydroxide on carbon as catalyst to give compound **22**. Following the same reaction protocols described for compounds **19** and **21**, starting from an aliquot of **22**, compounds **23** and **24** were

obtained. Vice versa, $LiBH_4$ reduction of another part of **22** fournished the alcohol **25**.

The structure-activity relationship studies were completed with the synthesis of UDC-OH (compound **26**, scheme 3), obtained from the reduction with $LiBH_4$ and MeOH of UDCA methyl ester.

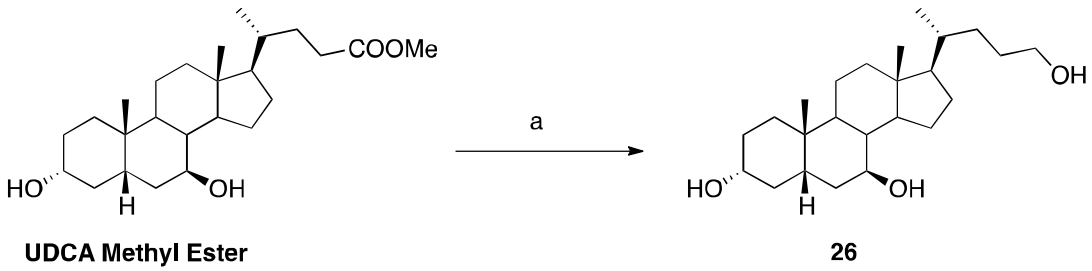

UDCA Methyl Ester **26**

Scheme 3. *Reagent and conditions*. a) $LiBH_4$, MeOH, THF.

2.3. Pharmacological evaluations

All the synthetized compounds were tested in transactivation assays using the luciferase reporter assays on HepG2 cells transfected with FXR. The results reported in Figure 17 indicated that none of the synthetized compounds was able to activate FXR, showing that independently from the length and functionalization of the side chain, the β configuration of hydroxyl group at C-7 plays a fundamental role in FXR activation.

Of interest, transactivation assays of CREB-responsive elements in HEK-293 cells transiently transfected with GPBAR1, showed that all the alcohols synthetized were able to transactivate GPBAR1 independently from the length and flexibility of the side chain (see compounds **9**, **25** and **26**). Interestingly, bis-*homo*UDCA **23** and its unsaturated $\Delta^{24,25}$ analogue **20** transactivated GPBAR1, with compound **23** endowed with a potency comparable to taurolithocholic acid (TLCA), the most potent endogenous GPBAR1 agonist. Consequently, the elongation of the side chain on UDCA produced positive effects towards GPBAR1 activation but the selectivity decays with tauro-conjugation (compare **23** with **24**), proving that a further elongation on the side chain is detrimental in term of GPBAR1 activation. The analysis of transactivation assays suggested that compounds **9**, **20**, **23**, **25** and **26** acted as selective GPBAR1 agonists, with no residual activity on FXR. For compounds **9** and **23**, the dose–concentration

response curve (Figure 19) allowed the calculation of an EC_{50} of 24.4 and 17.2 μM, respectively.

For *bis* homo-UDCA **23**, the most potent GPBAR1 agonist generated in this study, *ex-vivo* and *in vivo* experiments were also performed. In particular, the ability of compound **23** to stimulate the expression of FXR and GPBAR1 target genes in liver and intestine was evaluated by real time polymerase chain reaction (RT-PCR).

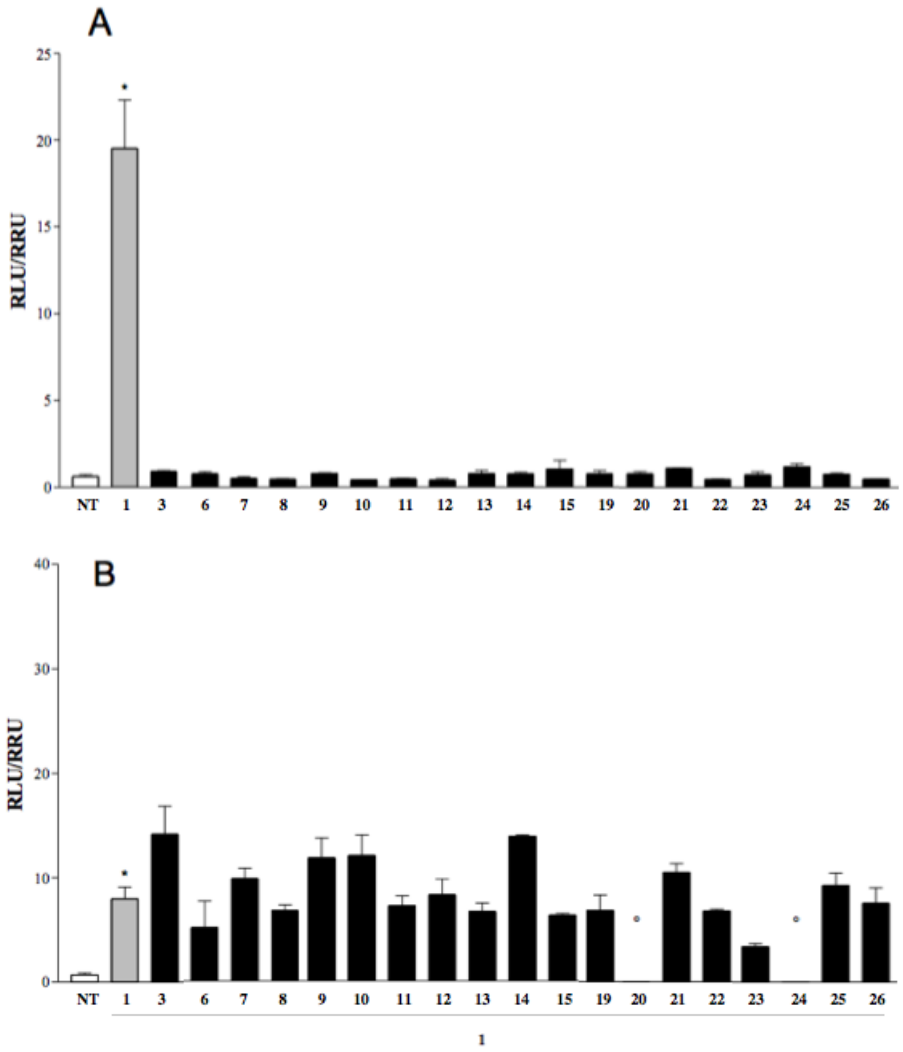

Figure 17. Transactivation assays on FXR. (A) HepG2 cells were transfected with pSG5-FXR, pSG5-RXR, pCMV-βgal, and p(hsp27)TKLUC vectors. Cells were stimulated with compounds **3-16** and **20-26** (10 μM). CDCA (**1**, 10 μM) was used as a positive control, UDCA (**2**, 10 μM) as negative control. Results are expressed as mean ± standard error; *p <0.05 *vs* not treated cells (NT). (B) HepG2 cells were transfected with pSG5-FXR, pSG5-RXR, pCMV-βgal, and p(hsp27)TKLUC vectors. Cells were stimulated with CDCA (**1**) 10 μM in combination with **3-15** and **19-26**, 50 μM. Results are expressed as mean ± standard error; *p <0.05 *vs* NT. #p<0.05 *vs* CDCA. °Cytotoxic at 50 μM

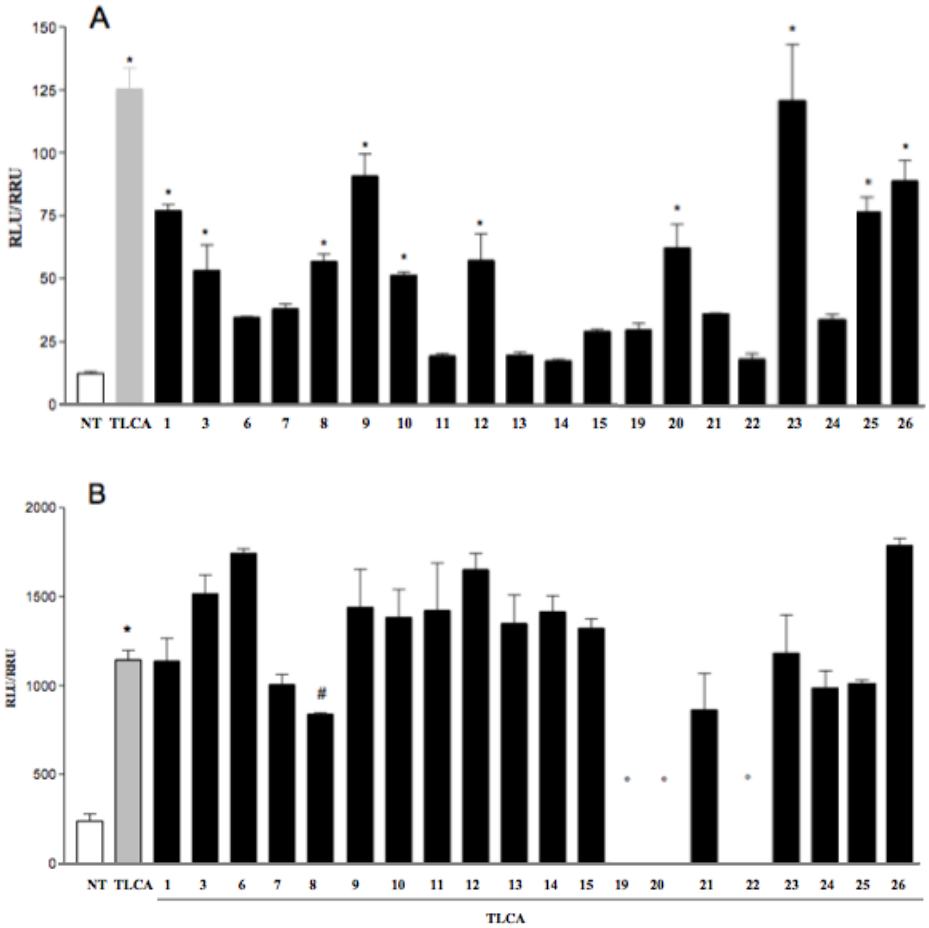

Figure 18. Transactivation assays on GPBAR1. (A) HEK293 cells were co-transfected with GPBAR1 and a reporter gene containing a cAMP responsive element in front of the luciferase gene. Twenty-four hour post transfection cells were stimulated with **1-26** (10 μM). Luciferase activity served as a measure of the rise in intracellular cAMP following activation of GPBAR1. TLCA (**T**, 10 μM) was used as a positive control. Results are expressed as mean ± standard error. *p<0.05 *vs* NT cells. (B) Antagonistic activity of compounds **1-26** on transactivation of cAMP responsive element induced by TLCA in HEK293 cells transfected with GP-BAR. Experimental conditions were the same described in panel A. None of the compound had an antagonistic activity. Concentrations used were: TLCA 10 μM while all the other compounds were tested at the concentration of 50 μM. Results are expressed as mean ± standard error. *p<0.05 *vs* NT cells. °Cytotoxic at 50 μM.

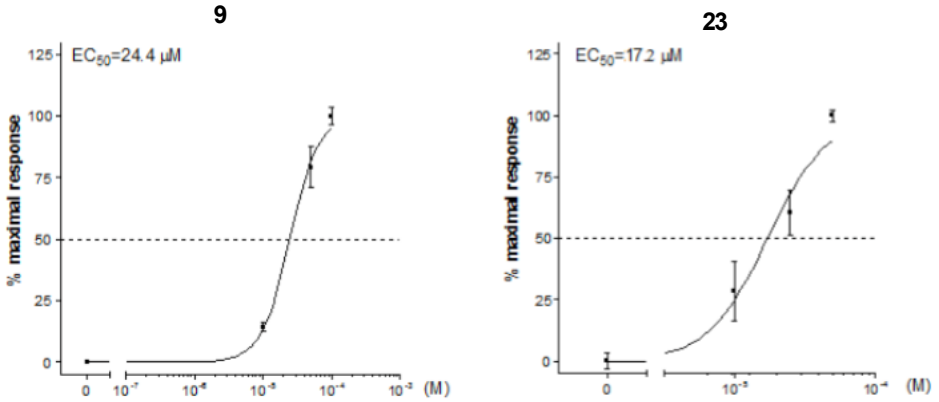

Figure 19. Concentration response-curves on GPBAR1 activation by compounds 9 and 23. HEK293T were transfected with GPBAR1 and stimulated with increasing concentration of **9** and **23** (0.1, 1 and 10 μM). Results are mean ± standard error of at least 3 determination in duplicate.

Compound **23** (64 mg/kg) or UDCA (60 mg/kg) were administrated to 11 weeks old male mice, and liver, intestine and blood were collected after 3, 6 and 24 hours. The results reported in Figure 20 indicated that compound **23** was not able to induce the expression of OSTα and BSEP mRNAs, two target genes for FXR in liver cells. Differently, compound **23** increased by two folds the expression of pro-glucagon-1, a classic GPBAR1 gene target.

The activities of bis-*homo* UDCA (**23**) and its parent compound UDCA (**3**) were tested in *in vivo* model of cholestasis inducted by α-naphthylisothiocyanate (ANIT).

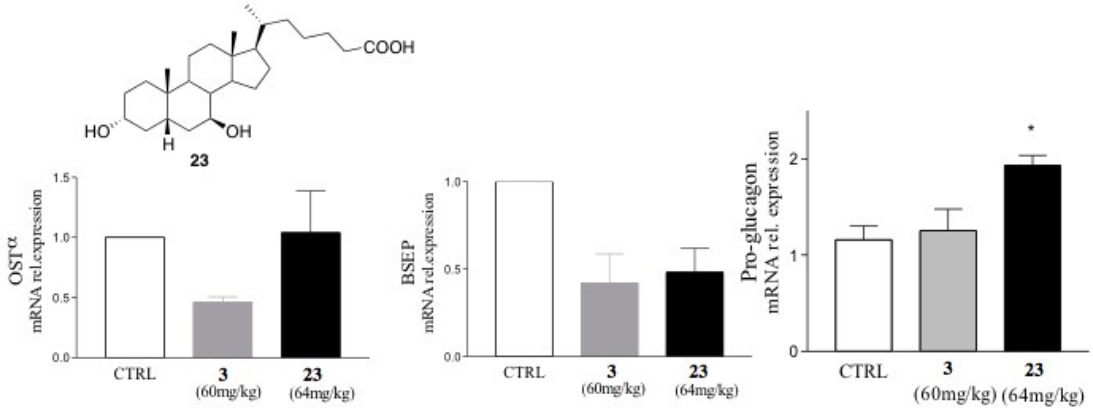

Figure 20. In vivo administration of **23** has no effect on expression of FXR target genes in the liver but increases the expression of pro-glucagon 1, a GPBAR1 regulated gene.

In rodent, ANIT is a widely used chemical that simulates human intrahepatic cholestasis. ANIT selectively damages the intrahepatic bile ducts, causing first cholangitis and, subsequently, cholestasis.

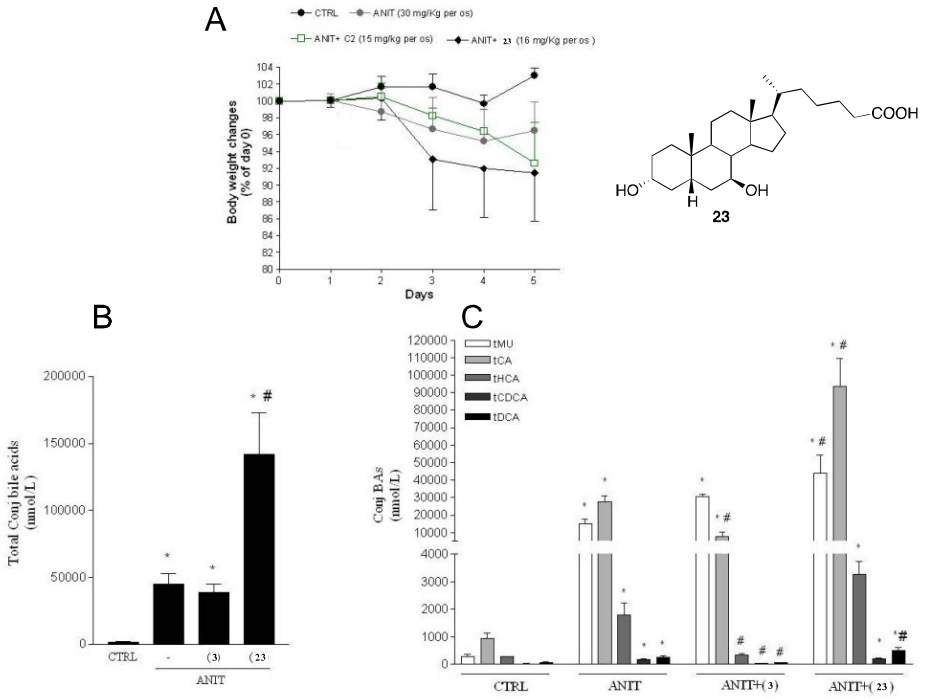

Figure 21. In vivo administration of UDCA (**3**) and **23** alters the bile acid pool in a rodent model of cholestasis. Cholestasis was induced by feeding mice with ANIT alone or in combination with **3**, 15 mg/kg, or **23**, 16 mg/kg, for 7 days. Blood was collected at the end of experiments and bile acids concentrations measured as described in the Experimental Section. (A) Analysis of body weight loss in control mice, mice administered ANIT, mice administered ANIT plus UDCA and mice administered ANIT plus **23**. (B) Blood concentrations of total conjugated bile acids. (C) Administration of **23** caused a robust increase in tauro-muricholic acid (tMU) and tauro-cholic acid (tCA).

Administration of ANIT induced cholestasis as confirmed by the analysis of plasma bile acids concentration; in particular, an increase in the total conjugated bile acids in comparison with not treated animals was observed (Figure 21, panel B and C). Furthermore, a significant weight loss was recorded in ANIT treated animals in comparison with not treated group (Figure 21, panel A). Regarding the administration of UDCA in ANIT treated animals, no significant differences in weight loss and bile acids concentration were observed between ANIT treated mice group and ANIT+UDCA treated group. In contrast, a significant increase of BAs concentration was observed when compound **23** was administered. In

particular, the amount of the tauro conjugated form of muriocholic acid, cholic acid and deoxycholic acid was increased in mice administered with compound **23** ($p<0.05$ versus ANIT treated mice). These results demonstrated the ability of compound **23** in reshaping the bile acid pool in a model of ANIT inducted cholestasis, pointing out the use of bis-*homo* UDCA for the treatment of enterohepatic and metabolic disorders.

2.4. Docking Studies

To elucidate the structural requisites involved in the activity of the UDCA derivatives on GPBAR1, docking simulations have been performed on the most active compounds of the series (**9**, **23**, **25** and **26**), using the tridimensional model of GPBAR1 recently reported by the research group in which my work was carried out.[57] The best score was obtained for compound **23**, for which H-bonding with the Glu169 and Asn93 side chains through the 3α- and 7β-hydroxyl groups, respectively was found; furthermore, the C-26 side chain pointed towards the transmembrane helices 1, 2 and 7, interacting with the side chains of Ser21 and Ser270. In addition, the binding was stabilized by hydrophobic interactions between the steroidal scaffold and several hydrophobic residues, such as Leu71, Phe83, Leu174 and Trp237 (Figure 22, panel A).

The substitution of –COOH group with an alcoholic moiety in the side chain does not perturb the ligand binding mode. Indeed, compound **25** (Figure 22, panel B) showed a comparable binding pose to that of compound **23**, with the steroidal scaffold engaging the same H-bonds, and the hydroxyl group on the side chain H-bonds with Ser270. Thus, the above in silico predictions are in full agreement with the pharmacological results, demonstrating that GPBAR1 activation resulted from the presence of a polar or a negatively charged group in side chain.

In order to better understand the binding mechanism of UDCA derivatives, docking calculations were performed also on the alcohols **26** (Figure 22 panel C) and **9** (Figure 22, panel D), bearing shorter side chains (C-24 and C-23 respectively). The results of these simulation confirmed that shorter side chains are allowed only if a polar end-group, able to bind Ser270 directly or through a water H-bond, is present on the side chain of the ligand. Another important

feature of the side chain is its flexibility. As confirmed by the pharmacological assays, compounds **19** and **20**, bearing a more rigid side chain, showed a reduced GPBAR1activation, as well as compounds **21** and **24**, where the presence of the amide group decreases the conformational flexibility of the ligand side chain. Another detrimental feature in GPBAR1 activation by UDCA derivatives is the presence of large groups on A and B rings. Indeed, compounds **10-15**, bearing one or more sulfate groups, showed a loss in the activity due to the non-proper orientation of the ligand in the binding site.

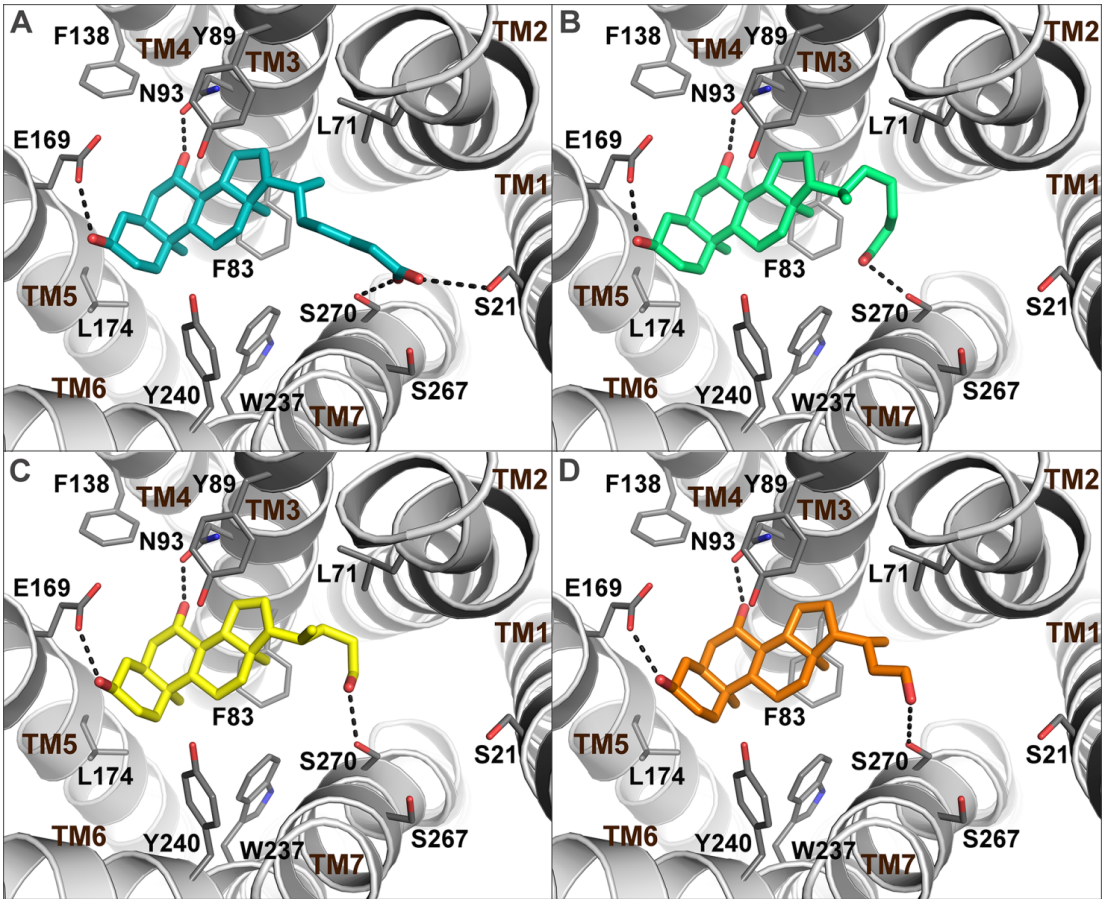

Figure 22. Proposed binding mode of **23** (A), **25** (B), **26** (C) and **9** (D) in the GPBAR1 homology model.[22] Ligands are represented as cyan (**23**), green (**25**) orange (**26**) and yellow (**9**) sticks. The receptor is shown as grey cartoons and sticks. Hydrogens are omitted for clarity.

CHAPTER 3:
CHOLANOIC ACID DERIVATIVES

As pointed before, the exogenous regulation of GPBAR1 represents an attractive strategy to treat metabolic disorders such as hypercholesterolemia, hypertriglyceridemia, and type 2 diabetes mellitus. However, activation of GPBAR1 associates with potential side effects, including itching,[79] cholesterol gallstone formation and gallbladder overfilling.[80,81] Considering the overlapping between FXR and GPBAR1 in their signalling pathways, selective FXR ligands are currently claimed as new therapeutic options in a wide range of diseases related to metabolic, inflammatory and immune-modulated disorders including type II diabetes, primary biliary cirrhosis (PBC), nonalcoholic fatty liver disease (NAFLD) and nonalcoholic steatohepatitis (NASH).

The activity of bile acids toward their receptor counterparts is structure dependent, with chenodeoxycholic acid (CDCA) and tauro-lithocholic acid (TLCA), being the most potent endogenus activators of FXR and GPBAR1, respectively.

In recent years, the chemical manipulation on CDCA scaffold afforded several hit compounds with promising pharmacological profiles.[82,83]

In detail, the introduction of an ethyl group at C-6 on the CDCA afforded to the disclosure of 6-ECDCA/OCA endowed with high potency toward FXR.[84] 6-ECDCA has been widely investigated *in vitro* and *in vivo* and in a phase III clinical trial in patients with non-alcoholic steatohepatitis (NASH),[85] 6-ECDCA improved several features of NASH, including inflammation and fibrosis. However, the positive findings were tempered by the appearance of pruritus in 23% of patients and by an increase in total cholesterol and LDL. In addition, administration in PBC patients caused pruritus in approx. 50-60% that was severe enough to cause drug discontinuation in 40% of patients.[86] Indeed, 6-ECDCA is also a ligand for GPBAR1,[83] and therefore the above side effect might be associated to the activation of the membrane bile acid receptor, recently demonstrated *bona fide* to be the physiological mediator of itching in mice.[80]

On the other hand, the elimination/inversion of the hydroxyl group at C-3 represents a good strategy in shifting selectivity toward FXR.[83]

In this context, the manipulation of LCA chemical scaffold regarded the position 3, the stereochemistry of A/B rings junction, the length and the functionalization of the side chain, generating the small library showed in Figure 23.

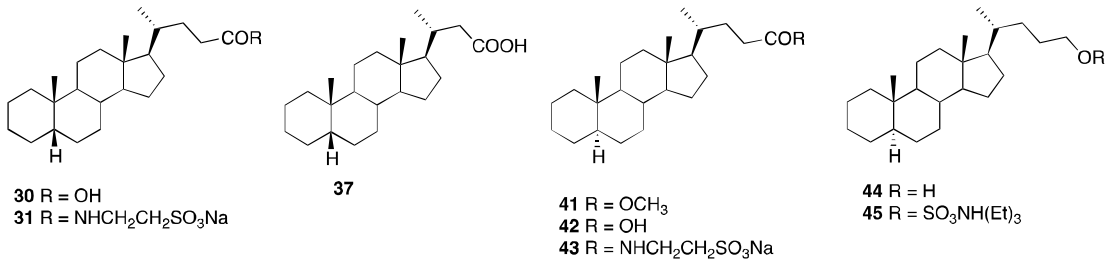

Figure 23. Cholane derivatives generated in this frame

As it will be discussed in the pharmacological section of this chapter, the elimination of 3α-OH from cholane scaffold generate a new class of BAs derivatives endowed with FXR agonistic/GPBAR1 antagonistic activity, that is, to the best of our knowledge, the first example reported in literature.

3.1. Synthesis of 5β-Cholane derivatives

In the following scheme the synthesis of 5β-cholanoic acid **30** and its tauro conjugated form **31,** is reported.

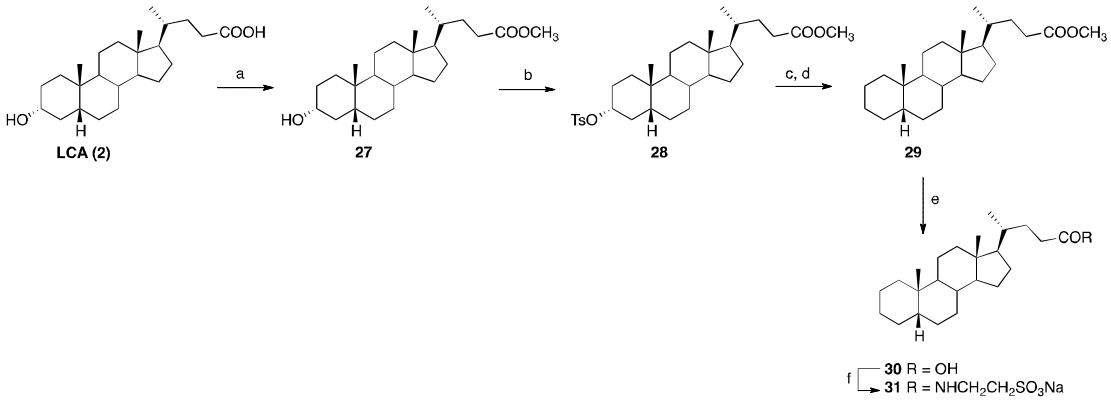

Scheme 4. *Reagents and Conditions*. a) *p*-TsOH, MeOH dry; b) *p*-TsCl, pyridine; c) LiBr, Li_2CO_3, DMF, reflux; d) H_2 3 atm, $Pd(OH)_2$/C degussa type, THF/MeOH 1:1; e) NaOH, MeOH:H_2O 1:1 v/v; f) DMT-MM, Et_3N, taurine, DMF dry.

LCA was subjected to Fisher's esterification of the carboxylic acid moiety in side chain and tosylation (tosyl chloride in pyridine) at C-3 hydroxyl group to give intermediate **28**. Elimination by treatment with $LiBr/LiCO_3$ in DMF dry, furnished a mixture of $\Delta^{2,3}$ and $\Delta^{3,4}$ derivatives that was hydrogenated with H_2, $Pd(OH)_2$ in THF/MeOH producing compound **29**. Finally, basic hydrolysis (NaOH, $MeOH/H_2O$) at the methyl ester on the side chain gave 5β-cholanoic acid **30** in quantitative yield. A small aliquot of compound **30** was treated with taurine in the presence of DMT-MM, 4-(4,6-dimethoxy-1,3,5-triazin-2-yl)-4-methylmorpholinium chloride to give the amide derivative as ammonium sulfate salt. Purification on RP-18 column followed by HPLC furnished pure **31** as sodium salt.

For the synthesis of *nor*-5β-cholanoic acid **37**, key step was the Beckmann's one carbon degradation (Scheme 5). Starting from LCA, following the same three-step synthetic protocol described in the scheme **1** for compounds **4**-**6**, compound **34** was obtained in high chemical yield. The subsequent Fisher's esterification followed by tosylation, furnished intermediate **35**. Elimination with $LiBr/LiCO_3$ and subsequent hydrogenation as detailed for compound **29**, furnished compound **36**. Finally, alkaline hydrolysis of the methyl ester moiety in side chain gave *nor*-5β-cholanoic acid **37**.

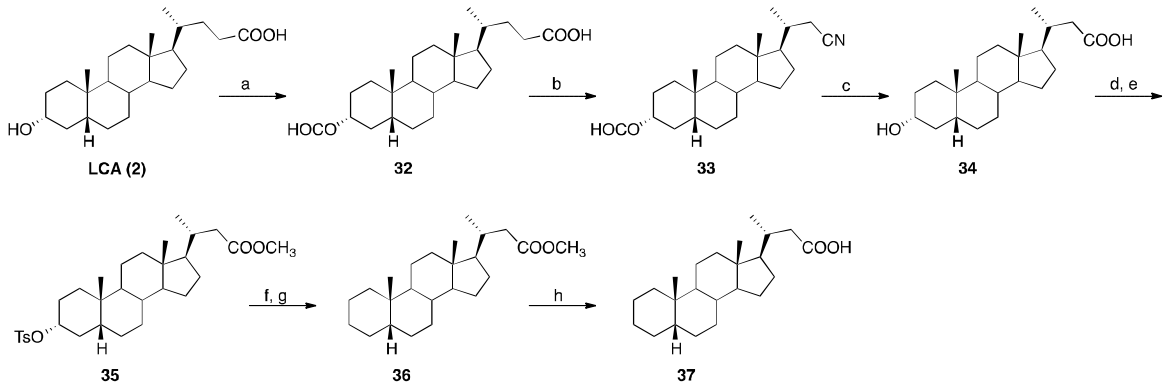

Scheme 5. *Reagents and Conditions*. a) HCOOH, $HClO_4$; b) TFA, trifluoroacetic anhydride, $NaNO_2$; c) KOH 30% in MeOH/H2O 1:1 v/v; d) *p*-TsOH, MeOH dry; e) *p*-TsCl, pyridine; f) LiBr, Li_2CO_3, DMF, reflux; g) H_2 3 atm, $Pd(OH)_2$/C degussa type, THF/MeOH 1:1; h) NaOH, $MeOH:H_2O$ 1:1 v/v.

3.2. Synthesis of 5α-Cholane derivatives

For the synthesis of 5α-cholane derivatives, the methyl ester of Hyodeoxycholic acid, obtained by Fisher's esterification of HDCA, was used as starting material (Scheme 6).

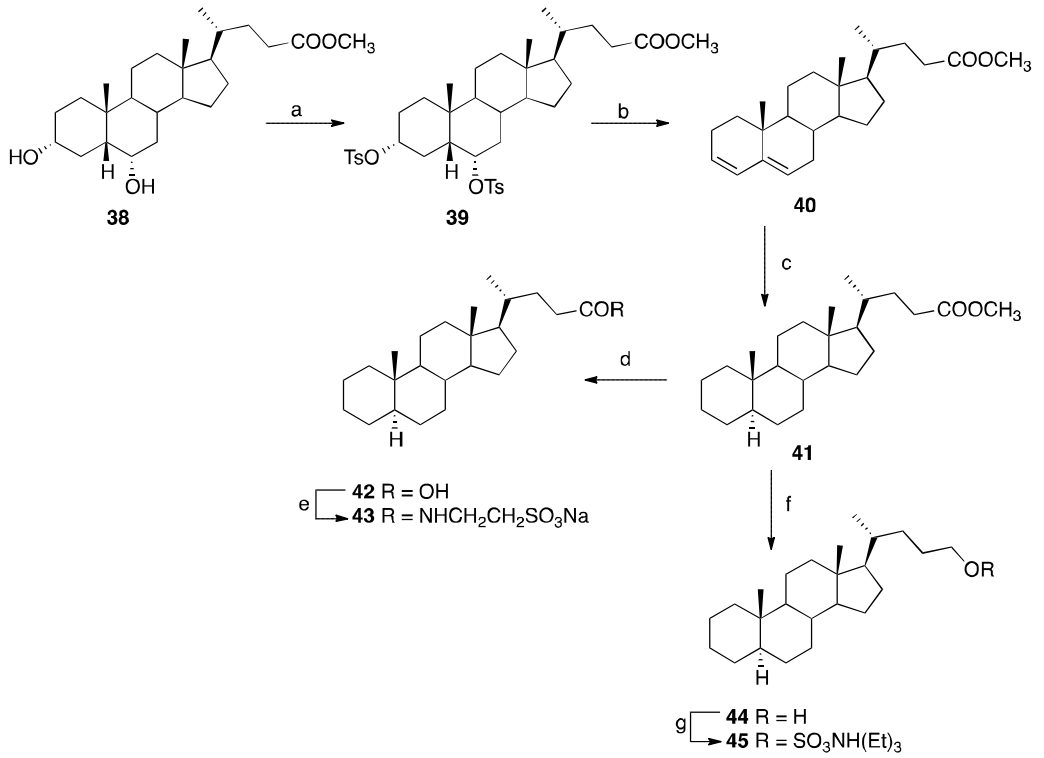

Scheme 6. *Reagents and Conditions*. a) *p*-TsCl, pyridine; b) CH_3COOK, DMF/H_2O 9:1, reflux; (c) H_2, Pd/C, THF/MeOH 1:1, room temperature; d) NaOH 5% in MeOH/H_2O 5:1 v/v%; e) DMT-MM, Et_3N, taurine, DMF dry; f) $LiBH_4$, MeOH dry, THF, 0 °C; g) $Et_3N{\cdot}SO_3$, DMF, 95 °C

Tosylation at position 3 and 6 was followed by double elimination with CH_3COOK in DMF/H_2O. The obtained diene **40** was then subjected to hydrogenation in the same operative condition described for compound **29** furnishing compound **41**. Due to the steric hindrance of the methyl-19, the attack of H_2 proceeds to the α face of the plane formed by A and B rings, affording the required A/B *trans* ring junction, exclusively. A portion of compound **41** was then subjected to alkaline hydrolysis furnishing 5α-cholanoic acid **42** that in turn was conjugated with taurine in the same condition described for compound **31**, giving compound **42**. Treatment of another aliquot of compound **41** with $LiBH_4$ in MeOH/THF produced the reduction of the methyl ester on the side chain

furnishing 5α-cholan-23-ol **44**. A small aliquot of **44** was then sulphated in side chain, giving compound **45**.

3.3. Pharmacological evaluations

The activity of the synthesized compounds was tested in a luciferase reporter assay using HepG2 and HEK-293T cells transfected with FXR and GPBAR1, respectively. Among this small library, the activity of 5β-cholanoic acid **30** is comparable to that of CDCA, the most potent endogenous FXR agonist (Figure 24).

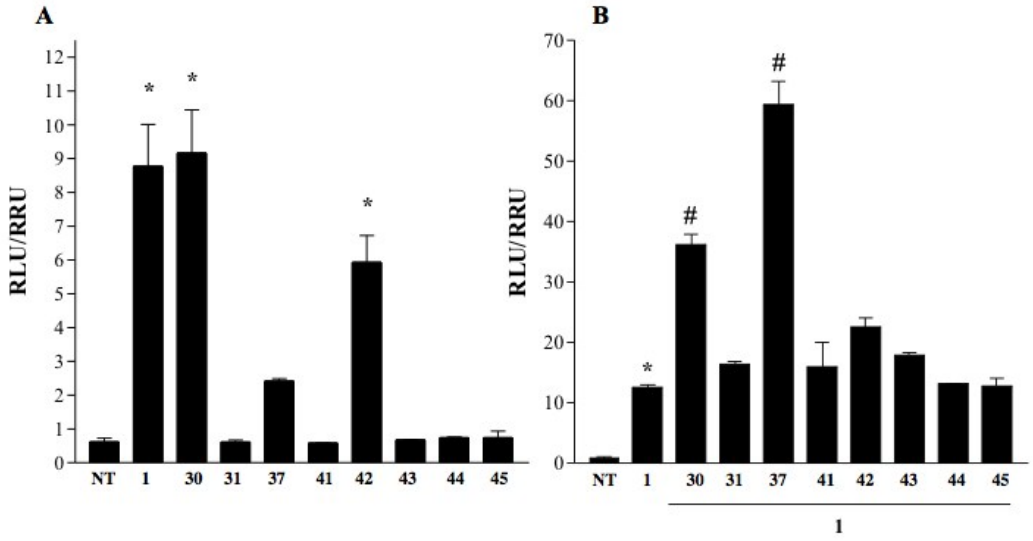

Figure 24. **Transactivation assays on FXR**. **A**, HepG2 cells were transfected with pSG5-FXR, pSG5-RXR, pCMV-βgal, and p(hsp27)TKLUC vectors. 24 hours post transfection cells were stimulated with compounds **30-45** (10 μM). CDCA (**1**, 10 μM) was used as a positive control. Results are expressed as mean ± standard error; *p <0.05 *versus* not treated cells (NT). **B**, HepG2 cells were transfected as described in A. 24 hours post transfection cells were stimulated with 10 μM CDCA alone or in combination with 50 μM compounds **30-45**. *p <0.05 *versus* not treated cells (NT). #p<0.05 *versus* CDCA stimulated cells.

Interestingly, also its 5-epimer, 5α-cholanoic acid **42**, showed a considerable activity towards FXR, indicating that in absence of the hydroxyl groups at C-3 and C-7, a flat BA scaffold is able to activate FXR. *Nor*-5β-cholanoic acid **37** was inactive at 10 μM but, at 50 μM and in presence of CDCA, it showed a four-fold

higher activity compared to that of compound **1**, indicating that also compound **37** could be an FXR modulator.

Transactivation assay on HEK-293T cells transiently transfected with the membrane bile acid receptor GPBAR1 (Figure 25), showed that, except compound **45,** none of the synthesized compound acted as GPBAR1 agonist, indicating that the elimination of the hydroxyl group at C-3 position on LCA is detrimental in terms of GPBAR1 activation and therefore represents a good strategy in shifting the activity of bile acid derivatives towards FXR.

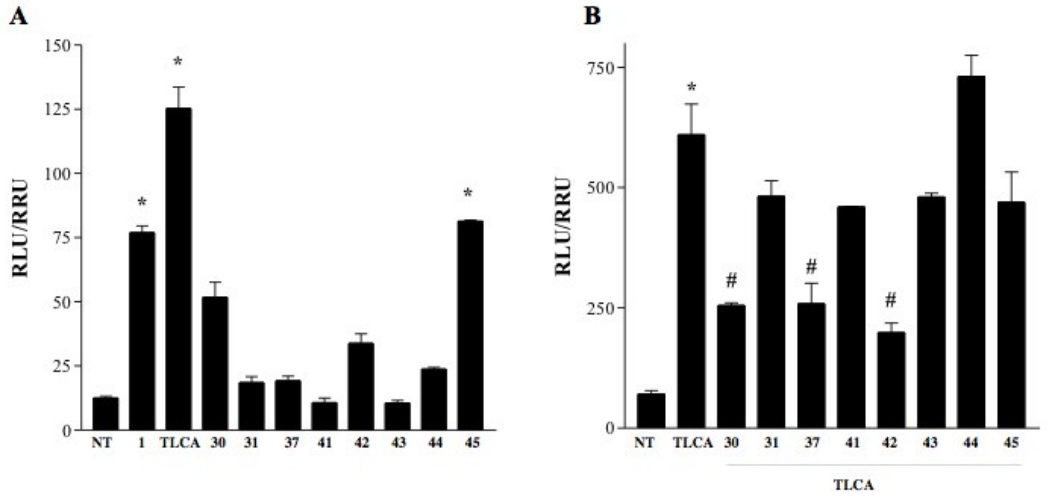

Figure 25. Transactivation assays on GPBAR-1. **A**, HEK-293T cells were co-transfected with GPBAR-1 and a reporter gene containing a cAMP responsive element in front of the luciferase gene. 24 hours post transfection, cells were stimulated with compounds **30-45** (10 μM). TLCA (**2**, 10 μM) was used as a positive control. Results are expressed as mean ± standard error. *$p < 0.05$ *versus* not treated cells (NT). **B**, HEK-293T cells were transfected as described in A. 24 hours post transfection cells were stimulated with 10 μM TLCA (**2**) alone or in combination with 50 μM compounds **30-45**. *$p < 0.05$ *versus* not treated cells (NT). #$p<0.05$ *versus* TLCA stimulated cells.

Of interest are the data showed in Figure **25,** panel B. When administrated in presence of TLCA, 5β-cholanoic acid **30**, *nor* 5β-cholanoic acid **37** or 5α-cholanoic acid **42** inhibited GPBAR1 activation caused by its endogenous ligand. These three compounds represented the first example of dual FXR agonists/GPBAR1 antagonistic. To further confirm the antagonistic profile of 5β-cholanoic acid **30** and 5α-cholanoic acid **42**, their concentration-response curve on GPBAR1 was analyzed. As shown in Figure 26, both compounds inhibited

TLCA-transactivation of GPBAR1 in a dose dependent fashion with IC_{50} values of 28 and 22 μM, respectively.

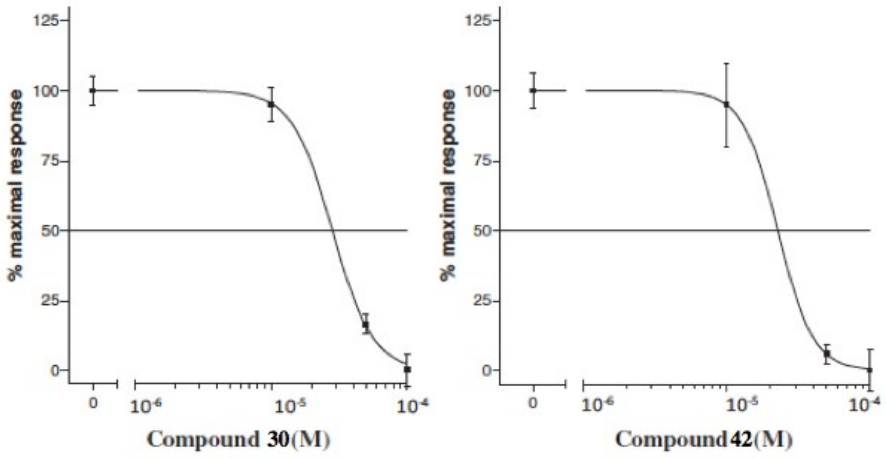

Figure 26. Concentration-response curve of **30** and **42** on GPBAR1. GPBAR1 activity was measured in HEK-293T cells cotransfected with GPBAR1 and a reporter gene containing a cAMP responsive element in front of the luciferase gene (CRE). Twenty-four h post transfection, cells were stimulated with increasing concentrations of each compound: range from 1 to 50 μM. Results are expressed as mean ± standard error.

Compound **30**, the most active molecule synthesized in this study, was evaluated in the recruitment of FXR and GPBAR1 target genes. RT-PCR results confirmed that it was able to induce the expression of FXR target genes SHP, OSTα and BSEP (Figure 27). At the same time, the expression of pro-glucagon mRNA resulted inhibited when compound **30** was administrated to GLUTAg cells, confirming again the FXR agonist/GPBAR1 antagonist profile of compound **30**.

Very recently, the effect of compound **30** has been evaluated on human gastric adenocarcinomas cells in which GPBAR1 is expressed in several adenocarcinomas and its activation by secondary bile acids increases intestinal cell proliferation. Activation of GPBAR1 in gastric cancer cells triggers the EMT (epithelial-mesenchymal transition, a process involved in metastasis) and acquisition of aggressive phenotype.[87]

These effects were inhibited by the administration of 5β-cholanoic acid **30**,[87] and these results highlight the potential beneficial effects of GPBAR1 antagonism in the management of advanced gastric cancer. Furthermore, these outcomes could shed light on the complex biological pathways under GPBAR1 control.

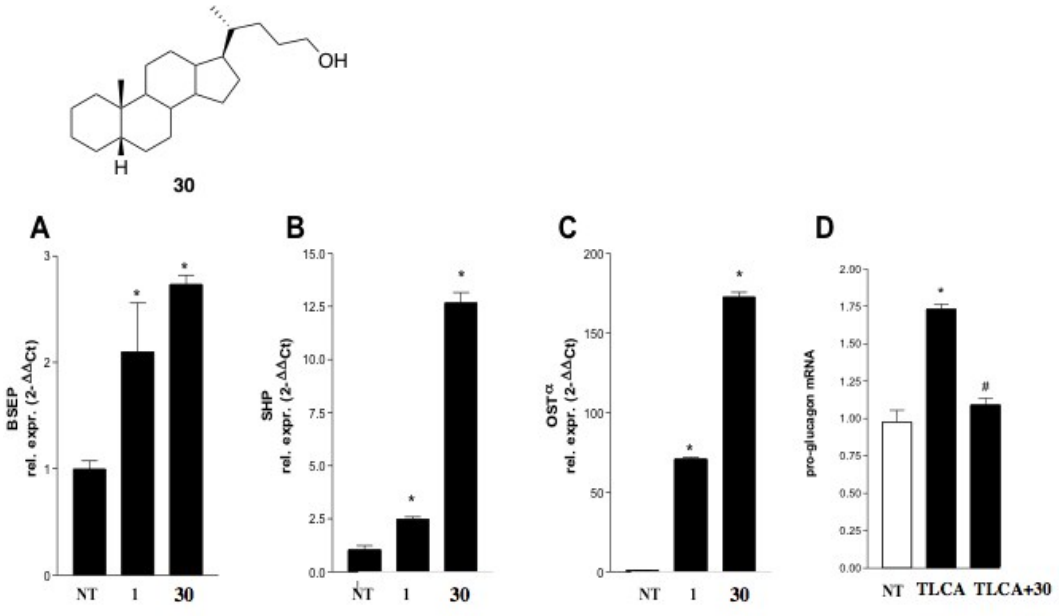

Figure 27. In vitro pharmacological evaluation of compound **30** effect on FXR and GPBAR1 target genes. (A-C) Real-time PCR analysis of mRNA expression of FXR target genes BSEP (A), SHP (B), and OSTα (C) in HepG2 cells primed with 10 μM compound **30**. CDCA (**1**) was used as positive control (10 μM). (D) Real-time PCR analysis of mRNA expression of GPBAR1 target gene pro-glucagon in Glutag cells stimulated with 10 μM TLCA alone or in combination with 50 μM compound **30**. Values are normalized relative to GAPDH mRNA and are expressed relative to those of not treated cells (NT), which are arbitrarily set to 1: *p < 0.05 vs NT. #p<0.05 vs TLCA stimulated cells

CHAPTER 4:
HYODEOXYCHOLIC ACID DERIVATIVES

As mentioned in the Introduction section, the activation of LXRα could be a promising therapeutic strategy for the treatment of hypercholesterolemia, inflammation and the regulation of glycaemia. Unluckily, synthetic LXRα agonists cause the activation of lipogenic enzymes with consequent accumulation of triglycerides, hampering their potential use in cardiovascular diseases. Despite their side effects, extensive efforts have been made in the investigation of new synthetic LXRα modulators.

Beside some oxysterols [22(*R*)- and 24(*S*)-hydroxycholesterol and 24(*S*),25-epoxycholesterol], only few examples of BAs capable of activate LXRα, are reported; among them, one of the most interesting molecule is the hyodeoxycholic acid (HDCA, **46**).[88]

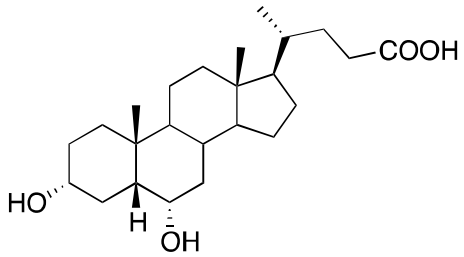

HDCA (**46**)

HDCA is a secondary bile acid generated by the C-6 hydroxylation of LCA.[89] It is present only in traces in human bile but it is the main component of hog bile.[90] HDCA is a weak LXRα agonist,[91] showing favourable outcomes in the treatment of metabolic disorders in rodent models.[92,] In addition, as reported by Shih et al.,[93] a diet enriched in HDCA reduced the absorption of cholesterol and increases the HDL-mediated outgoing of cholesterol from macrophages and foam cells, in LDL receptor-knockout mice. As consequence, a protective effect against atherosclerotic plaques formation is achieved. Furthermore, the administration of HDCA in mice produced hypolipidemic effects as confirmed by the inhibition of the expression of sterol regulatory element binding protein 1c (SREPB1c), acetyl-CoA carboxylase (ACoA synthase), fatty acid synthase (FAS), and stearoyl-CoA desaturase (S-CoA Des) genes in liver.[94]

HDCA also exhibits a weak but interesting activity on GPBAR1 with an EC_{50} of 31.6 μM.[95] The LXRα/GPBAR1 activity of HDCA could trace new roads towards the synthesis of a novel class of potential dual agonists. Considering that both receptors regulate the same physiological processes, a potential dual agonist could be a promising molecule for the treatment of metabolic/inflammatory disorders with a novel mechanism of action.

The key step for the synthesis of potential HDCA dual agonists was the analysis of the ligand-binding site of both LXRα and GPBAR1. LXRα binding pocket is rather amphipathic, allowing the accommodation of both polar and non-polar moieties,[96] while GPBAR1 exhibits a small lipophilic cavity that could represent a target for small hydrophobic side chains (Figure 28).

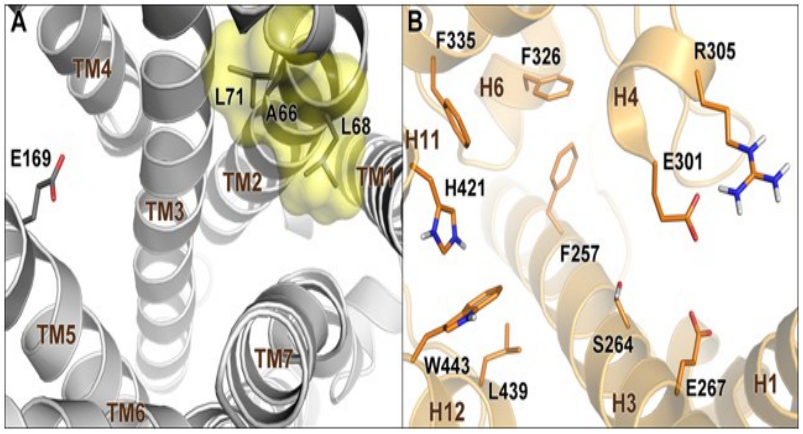

Figure 28. Binding pockets of LXRα (panel A) and GPBAR1 (panel B)

For this reason, hydrophobic side chains, differing for length, flexibility and ramification, have been introduced on HDCA scaffold as showed in Figure 29.

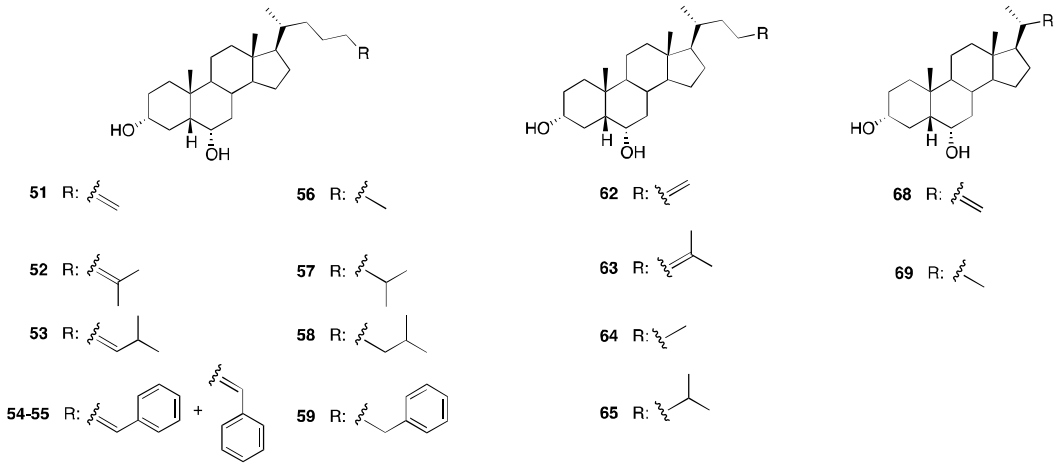

Figure 29. HDCA side chain derivatives

A second set of modification (Figure 30) regarded HDCA steroidal scaffold; in particular, the role of A/B rings junction and the hydroxyl group at C-6, as well as the configuration at C-3 in the selectivity towards LXRα and/or GPBAR1 receptors were investigated. Pharmacological evaluations showed several compounds endowed with LXRα or GPBAR1 agonist activity. Noteworthy, compound **65** represents the first example of dual LXRα/GPBAR1 agonist.

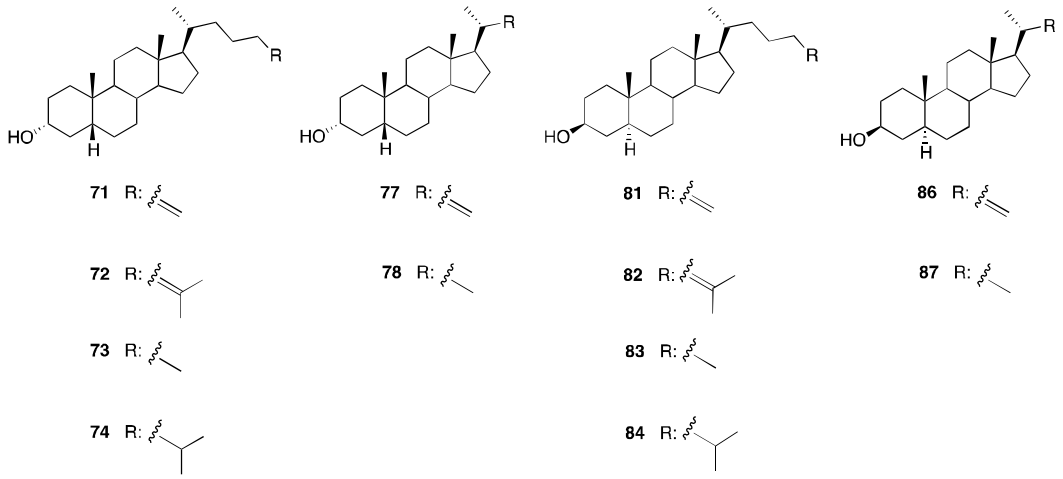

Figure 30. Cholane scaffold and side chain modifications

Furthermore, a deep pharmacological evaluation on this compound has been performed in order to evaluate the effects of the dual LXRα/GPBAR1 activation on mice metabolism.

4.1. Side chain modifications

In the preparation of the first class of HDCA derivatives (Figure 29), two sets of reactions were performed. First, Wittig reaction on protected aldehydes **50** and **61**, using various phosphorus ylides, allowed the elongation of the side chain, both on HDCA and on *nor*-HDCA. On the other hand, shorter side chains were prepared through an oxidative decarboxylation reaction, furnishing C-22 derivatives.
The starting material for the synthesis of aldehyde **50** was HDCA (**46**) and the synthetic scheme is reported below (Scheme 7)

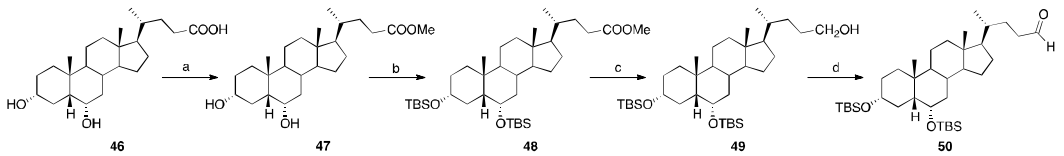

Scheme 7. *Reagents and conditions*: a) p-TsOH, MeOH dry, quantitative yield; b) 2,6-lutidine, t-butyldimethylsilyltrifluoromethanesulfonate, CH_2Cl_2, 0 °C, quantitative yield; c) $LiBH_4$, MeOH dry, THF, 0 °C, 56%; d) DMSO, oxalyl chloride, TEA dry, CH_2Cl_2, -78 °C, quantitative yield.

The carboxylic acid moiety was subjected to Fisher's esterification, furnishing the corresponding methyl ester **47**. Then, hydroxyls protection with TBS, followed by reduction of the ester in side chain, afforded the alcohol **49**. After purification, compound **49** was oxidised by Swern procedure to the corresponding aldehyde **50**. On this intermediate, Wittig reactions were performed using several type of phosphorus ylides, as methyl triphenylphosphonium iodide, isopropyl triphenylphosponium iodide, isobutyl triphenylphosponium iodide and benzyl triphenylphosphonium iodide, followed by –OH deprotection, producing compounds **51**, **52**, **53**, **54** and **55**, respectively (Scheme 8). Using isobutyl triphenylphosponium iodide and benzyl triphenylphosphonium iodide, a diasteromeric mixture of *cis/trans* isomers was obtained, but, differently from compounds **54** and **55**, the mixture of *cis/trans* **53** was tested as such.

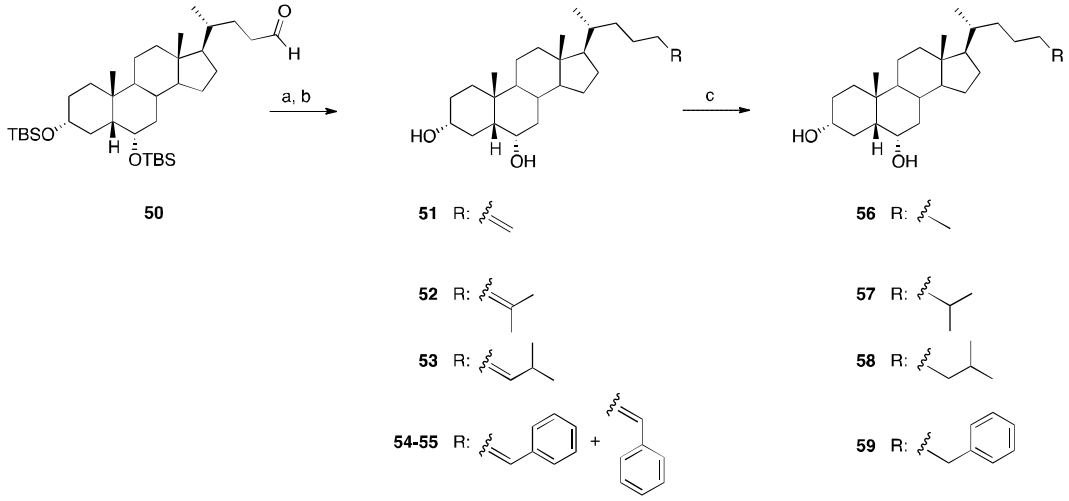

Scheme 8. *Reagents and conditions.* a) *n*-BuLi, methyl/isopropyl/isobutyl/phenyl triphenylphosponium iodide, THF dry, r.t.; b) HCl 37%, MeOH; c) H_2, $Pd(OH)_2$ degussa type, THF:MeOH dry 1:1.

Aiming at the synthesis of more flexible derivatives, $\Delta^{24,25}$ unsaturation in side chain was hydrogenated in catalytic conditions, furnishing compound **56** (from **51)**, **57** (from **52)**, **58** (from **53)** and **59** from the mixture of **54** and **55**.

For the synthesis of shorten side chains, HDCA was subjected to Beckmann's one carbon degradation (Scheme 9). Following the same operative condition reported in Scheme 1, steps a-d, HDCA was converted in the corresponding truncated methyl ester. Then, as reported for the methyl ester **47**, compound **60** was converted into its corresponding protected aldehyde **61**.

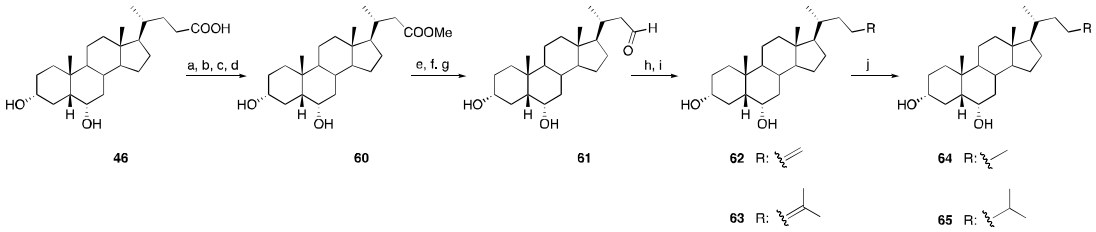

Scheme 9. *Reagents and conditions*: a) HCOOH, $HClO_4$; b) TFA, trifluoroacetic anhydride, $NaNO_2$; c) KOH 30% in MeOH/H_2O 1:1 v/v; d) *p*-TsOH, MeOH dry; e) 2,6-lutidine, t-butyldimethylsilyltrifluoromethanesulfonate, CH_2Cl_2, 0 °C; f) $LiBH_4$, MeOH dry in THF dry; g) DMSO, oxalyl chloride, TEA dry, CH_2Cl_2, -78 °C; h) *n*-BuLi, methyl/isopropyl triphenylphosphonium iodide, THF dry, r.t.; i) HCl 37%, MeOH; j) H_2, $Pd(OH)_2$ degussa type, THF/MeOH 1:1.

Again, two Wittig reactions, using methyl triphenylphosphonium iodide and isopropyl triphenylphosponium iodide, followed by acid deprotection, furnished $\Delta^{23,24}$ unsaturated derivatives **62** and **63**. Hydrogenation in catalytic condition of an aliquot of compounds **62** and **63** afforded derivatives **64** and **65**, respectively.

Bis-*nor*HDCA derivatives were obtained starting from HDCA by an oxidative decarboxylation procedure (Scheme 10). The first step was the protection of hydroxyl groups through a simple acetylation. Then, the oxidative decarboxylation was performed using $Cu(OAc)_2$ and $Pb(OAc)_4$ with a free radical mechanism.

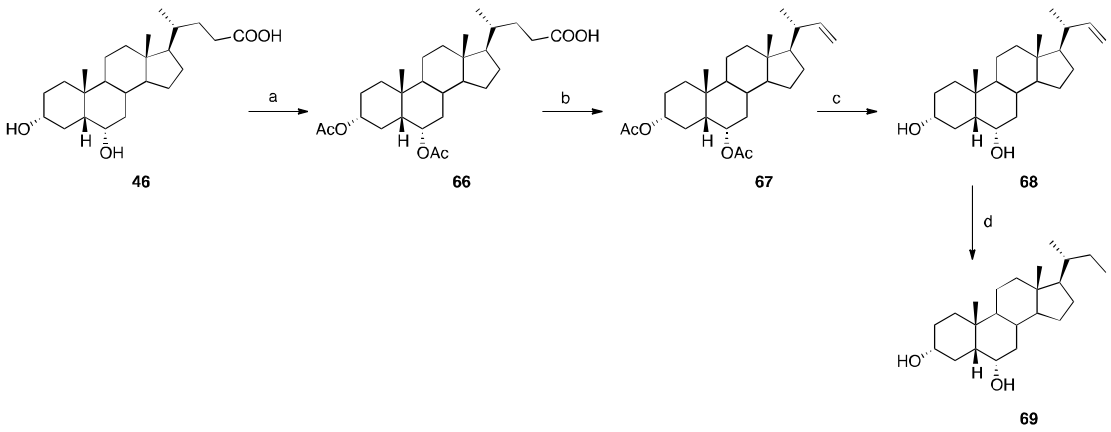

Scheme 10. *Reagents and conditions*: a) Ac_2O, pyridine; b) $Cu(OAc)_2\ H_2O$, $Pb(OAc)_4$ in toluene dry/pyridine dry; c) CH_3ONa, $CHCl_3$ dry/MeOH dry 5:3 v/v; d) H_2, $Pd(OH)_2$ degussa type, THF dry/MeOH dry 1:1 v/v.

The reaction of compound **66** with $Pb(OAC)_4$ furnished an interchange of ester groups as reported in the following Figure 31.

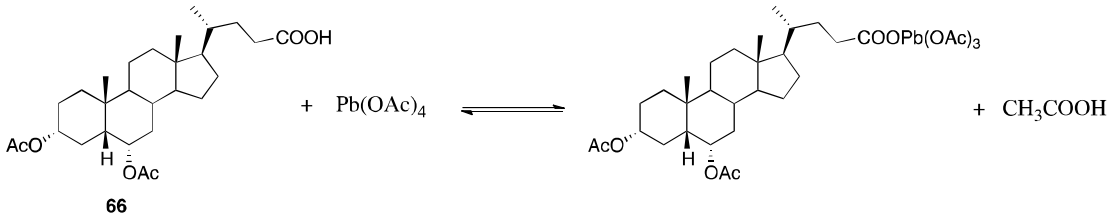

Figure 31. Insertion of $Pb(OAc)_4$

Then, a free radical mechanism started with the formation of the intermediate radical R• (Figure 32)

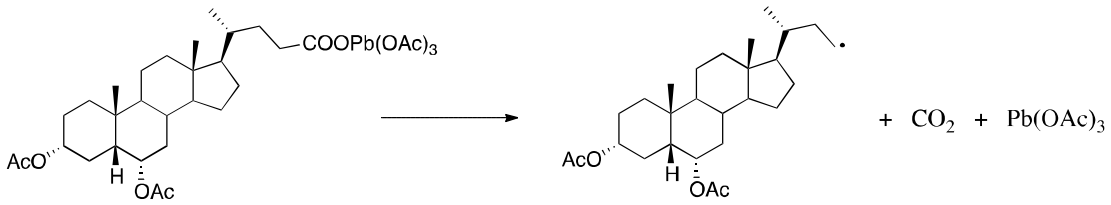

Figure 32. Radical R• formation

The following reaction step was then catalyzed by $Cu(OAc)_2$, allowing the oxidation of the intermediate radical to carbocation; in this condition, the loss of a proton furnished the corresponding alkene **67**.

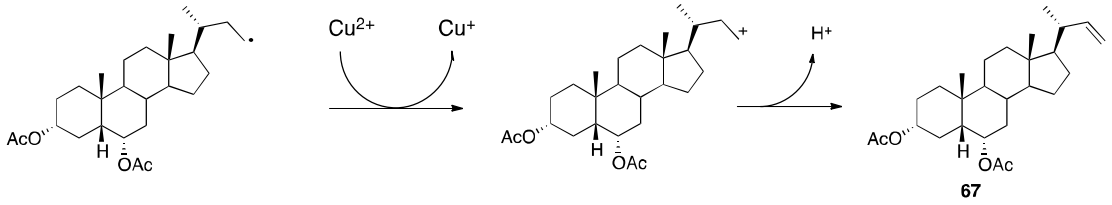

Figure 33. Carbocation and alkene formation

Deprotection at C-3 and C-6 with CH_3ONa furnished compound **68**; then, the reduction of the side chain double bond on an aliquot of **68** afforded derivative **69**.

4.2. Steroidal scaffold modifications

The analysis of the structural requirement for the synthesis of potential dual LXRα/GPBAR1 agonists was extended to the steroidical scaffold.

The effects of the 6-OH removal were analysed through the synthesis of novel lithocholic acid derivatives, introducing several apolar side chains on LCA, the corresponding 6-deoxy HDCA analogue, using a synthetic procedure reported in Scheme 11.

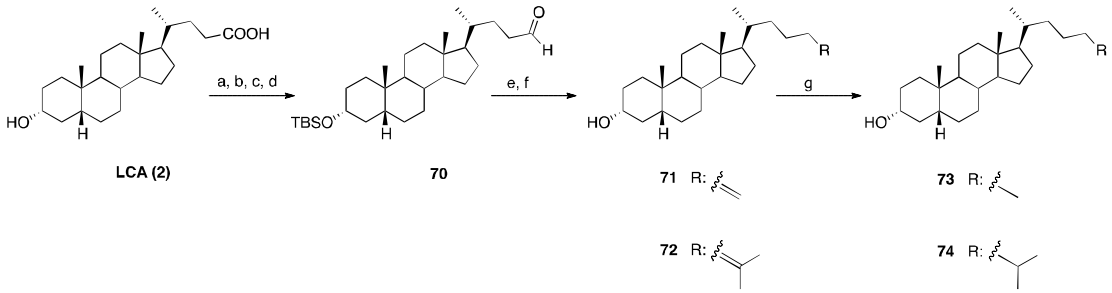

Scheme 11. *Reagents and conditions*: a) *p*-TsOH, MeOH dry; b) 2,6-lutidine, t-butyldimethylsilyltrifluoromethanesulfonate, CH_2Cl_2, 0 °C; c) $LiBH_4$, MeOH dry, THF, 0 °C; d) DMSO, oxalyl chloride, TEA dry, CH_2Cl_2, -78 °C; e) *n*-BuLi, methyl/isopropyl triphenylphosponium iodide, THF dry, r.t.; f) HCl 37%, MeOH; g) H_2, $Pd(OH)_2$ degussa type, THF:MeOH dry 1:1.

Aldehyde **70** was synthesized as reported for compound **50** (Scheme 7). Two Wittig reactions, using methyl triphenylphosphonium iodide and isopropyl triphenylphosponium iodide, followed by –OH deprotection, furnished the unsaturated compounds **71** and **72**, respectively. An aliquot of both compounds **71** and **72** was then subjected to catalytic double bond reduction, affording

compounds **73** and **74**, respectively. The LCA analogues of compounds **68** and **69** were obtained following the same protocol described in Scheme 10 starting from LCA (Scheme 12).

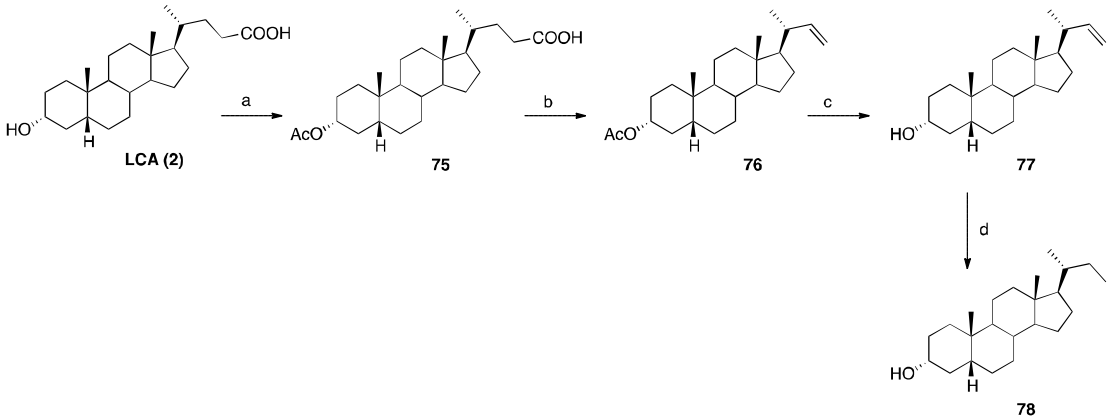

Scheme 12. *Reagents and conditions*: a) Ac_2O, Pyr; b) $Cu(OAc)_2$ H_2O, $Pb(OAc)_4$ in toluene dry/pyridine dry; c) CH_3ONa, $CHCl_3$ dry/MeOH dry 5:3 v/v; d) H_2, $Pd(OH)_2$ degussa type, THF dry/MeOH dry 1:1 v/v.

LCA was first subjected to acetylation at the 3-OH then, the oxidative decarboxylation produced compound **76**. The following deprotection furnished compound **77** that was in turn hydrogenated, giving compound **78**.

The synthesis of 3β, 5α-LCA derivatives started from HDCA and is showed in Scheme 13.

Applying the same set of four reactions described in a previous work,[97] a first aliquot of HDCA was converted into the methyl ester of 3β, 5α-LCA (compound **79**).

In detail, the inversion of configuration at C-3 and C-5 was realized through a double tosylation on the methyl ester of HDCA, and subsequent inversion/elimination with CH_3COOK in refluxing DMF. The so obtained $\Delta^{5,6}$ intermediate was hydrogenated in catalytic condition to give compound **79**. Following the same synthetic procedure described in Scheme 11 for LCA, compound **79** was converted into the corresponding protected aldehyde **80**, that was then subjected to Wittig reactions (with methyl triphenylphosphonium iodide and isopropyl triphenylphosponium iodide); the following deprotection furnished

compounds **81** and **82**. These compounds were subjected to catalytic hydrogenation to give compounds **83** and **84**, respectively.

A second aliquot of **79** was instead subjected to the shortening protocol as described in Scheme 12 for LCA. Thus, the methyl-3β-hydroxy-5α-cholanoate **79** was first subjected to basic hydrolysis of the side chain methyl ester. Then, acetylation at C-3 followed by oxidative decarboxylation furnished compound **85**. Deprotection afforded compound **86**, that was subjected to double bond hydrogenation, giving compound **87**.

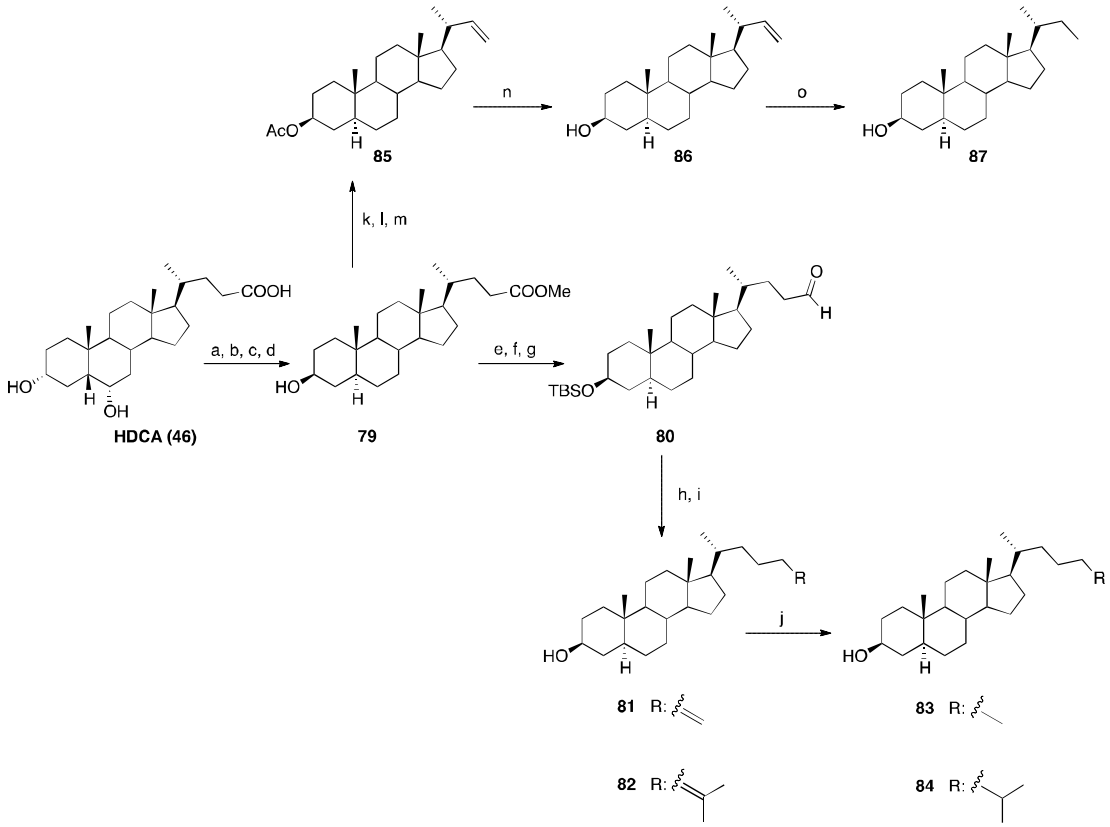

Scheme 13. *Reagents and conditions*: a) *p*-TsOH, MeOH dry; b) *p*-TsCl, pyridine; c) CH_3COOK, DMF/H_2O 9:1, reflux; c) H_2, Pd/C, THF/MeOH 1:1, room temperature; e) 2,6-lutidine, t-butyldimethylsilyltrifluoromethanesulfonate, CH_2Cl_2, 0 °C; f) $LiBH_4$, MeOH dry, THF, 0 °C; g) DMSO, oxalyl chloride, TEA dry, CH_2Cl_2, -78 °C; h) *n*-BuLi, methyl/isopropyl triphenylphosponium iodide, THF dry, r.t.; i) HCl 37%, MeOH; j) H_2, $Pd(OH)_2$ degussa type, THF:MeOH dry 1:1; k) NaOH, MeOH/H_2O 1:1 v/v, reflux; l) Ac_2O,pyridine; m) $Cu(OAc)_2$ H_2O, $Pb(OAc)_4$ in toluene dry/pyridine dry; n) CH_3ONa, $CHCl_3$ dry/MeOH dry 5:3 v/v; o) H_2, $Pd(OH)_2$ degussa type, THF dry/MeOH dry 1:1 v/v.

4.3. Pharmacological evaluations

Luciferase reporter assay on HepG2 and HEK-293T cells transfected with LXRα, β and GPBAR1 receptors, respectively, was used to evaluate the activity of the synthesized compounds. The well-known agonists GW3965[98] and TLCA (Figure 34) were used as positive controls for LXRα, β and GPBAR1, respectively.

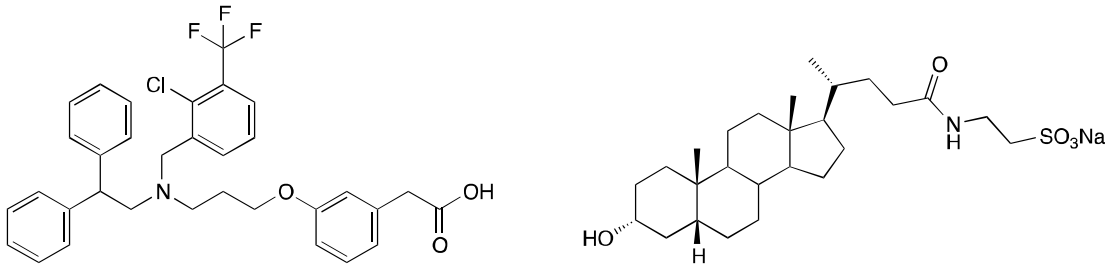

GW3965 **TLCA**

Figure 34. Chemical structures of GW3965 and TLCA

As reported in Figure 35, the introduction of a hydrophobic side chain on the hyodeoxycholane scaffold produces beneficial effects on the activation of LXRα receptor.

The analysis of the biological activity of compounds **51-69** suggested that pharmacological profile of these HDCA derivatives was strictly depended on the length and the flexibility of the side chain. Although there is no linear correlation between the size of the side chain and the activity towards LXRα, it is possible to affirm that too long (compounds **54** and **55**) or too short (compounds **62**, **64**, **68** and **69**) side chains produced detrimental effects in LXRα activation. Concerning the flexibility, compounds with a less rigid side chain showed a better activity compared to their unsaturated analogues. On the contrary, the elimination of the hydroxyl group at C-6, the inversion of configuration of 3-OH and *trans* A/B ring junction, produced detrimental effects on LXRα activation (see derivatives **71-87**), suggesting that these features are necessary for the receptor activation.

Consequently, compounds endowed with the best activity were **57**, **59** and **65**, with an efficacy of 73%, 63% and 109%, respectively.

Regarding GPBAR1 activation, their behaviour was the opposite of what described for LXRα (Figure 36).

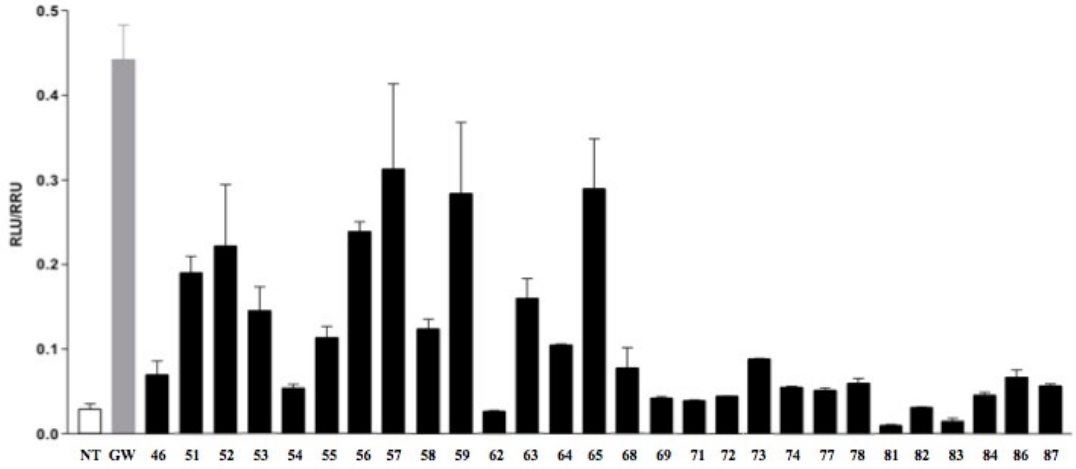

Figure 35. **Transactivation assays on LXRα.** Activity toward LXRα in a reporter assay was assessed in HepG2 cells transfected with an LXRα responsive element (LRE) cloned upstream to the luciferase gene. For calculation of efficacy data, maximal transactivation of LRE caused by each compound (10 μM) was compared to maximal transactivation caused by GW3965 (10 μM) and by HDCA (10 μM).

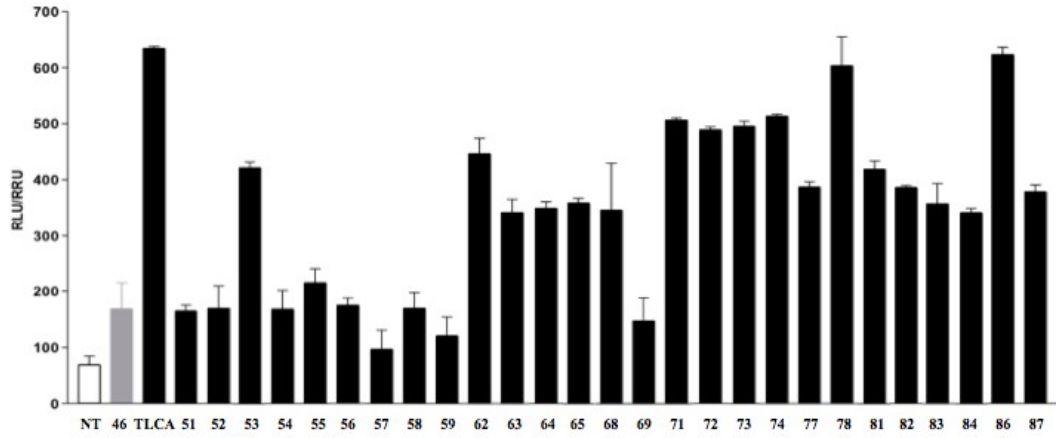

Figure 36. Transactivation assays on GPBAR1. Activity toward GPBAR1 in a reporter assay was assessed in HEK-293T cells transfected with a cAMP responsive element (CRE) cloned upstream to the luciferase gene. For calculation of efficacy data, maximal transactivation of CRE caused by each compound (10 μM) was compared to maximal transactivation caused by TLCA (10 μM) and by HDCA (10 μM).

The elimination of the hydroxyl group at C-6, as well as the inversion of configuration at C-3 and the *trans* A/B ring junction, produced beneficial effects on GPBAR1 activation, identifying compounds **78** and **86** as the best selective

GPBAR1 agonists generated in this study. Furthermore, compounds presenting a double bond in side chain showed a better activity compared to their saturated analogues, suggesting that, in presence of a *trans* A/B ring junction, a saturated side chain produces beneficial effects. HDCA scaffold derivatives did not show a significant activity towards GPBAR1, except compound **65**, the first and the only dual LXRα/GPBAR1 agonist generated in this study. Finally, transactivation assays on LXRβ (Figure 37) and FXR (not shown) indicated that none of synthesized compounds was a LXRβ/FXR agonist, confirming their selectivity towards LXRα and GPBAR1.

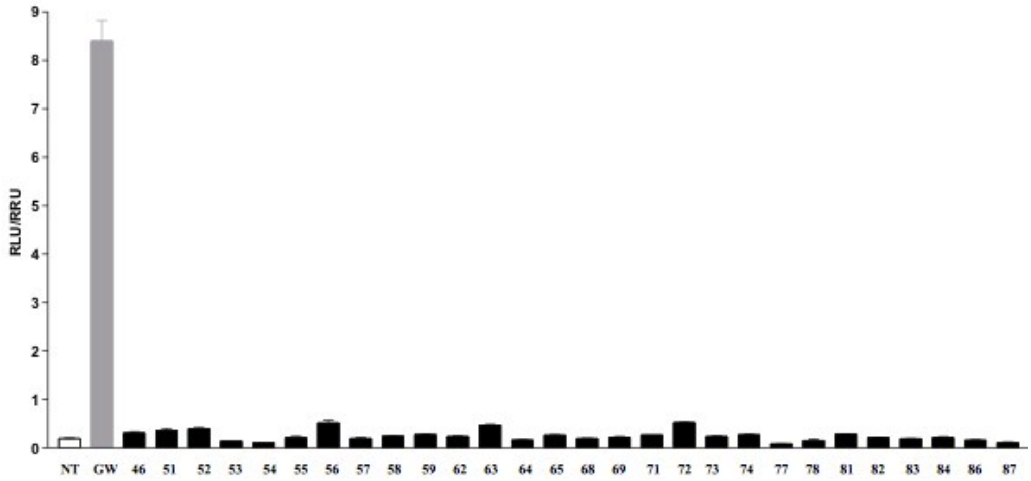

Figure 37. Transactivation assay on LXRβ. Activity towards LXRα in a reporter assay was assessed in HepG2 cells transfected with an LXRα responsive element (LRE) cloned upstream to the luciferase gene. For calculation of efficacy data, maximal transactivation of LRE caused by each compound (10 μM) was compared to maximal transactivation caused by GW3965 (10 μM) and by HDCA (10 μM).

For the most interesting compounds, dose response experiments were carried out (not shown) and the calculated EC_{50} are reported in Table 2.

The pharmacological analysis on compound **65** continued with the evaluation of the recruitment of LXRα and GPBAR1 target genes through RT-PCR. HepG2 and Glutag cells were stimulated with GW3965, TLCA and HDCA (10 μM) and with increasing concentration of compound **65** (1, 5, 10, 25, 50 μM). As expected, compound **65** was able to induce the expression of ABCA1 and SREBP1c, two target genes of LXRα, as well as pro-glucagon, a target gene of GPBAR1 (Figure

38). This behavior was a further confirmation of the crucial role exerted by compound **65** in both LXRα/GPBAR1 activity modulation.

Compound	GPBAR1	LXRα
	Affinity (μM)*	**Affinity (μM)**
Selective LXRα agonists		
51		2.7±0.65
52		5.1±0.43
53		6.99±0.31
54		8.2± 0.16
59		12.4±0.41
GPBAR1/LXRα dual agonists		
63	4.2±0.79	22.3±3.05
65	4.9±0.2	3.2±0.03
Selective GPBAR1 agonists		
62	3.7±0.38	
68	2.54±0.015	
72	5.9±0.055	
73	6.8±0.08	
78	0.91±0.092	
81	7.6±0.71	
82	1±0.062	
86	4.9±0.06	
87	1.98±0.145	

Table 2. EC_{50} of the most interesting compounds

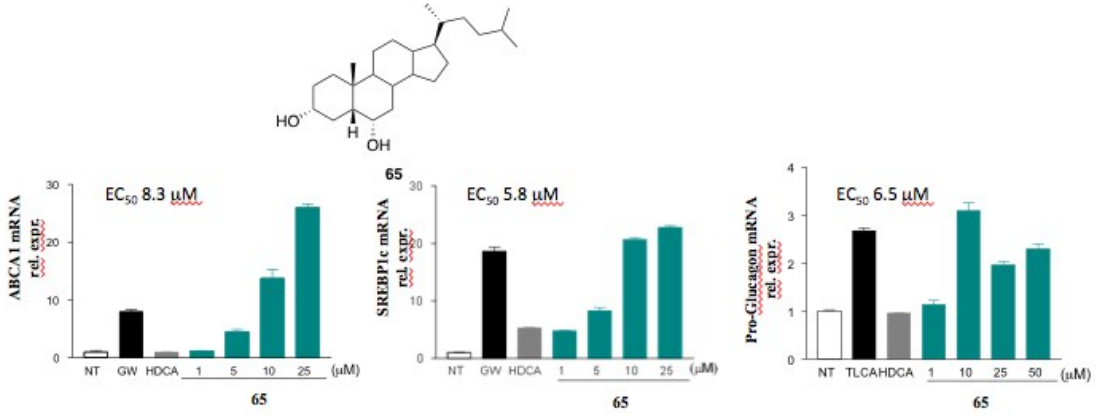

Figure 38. **Real-Time PCR analysis of mRNA expression on LXRα and GPBAR1 target genes**. ABCA1 (A) and SREBP1c (B) expression in HepG2 cells primed with increasing concentration of compound **65** (1, 5, 10 and 25 µM). GW3965 and HDCA were used as positive controls. C) Pro-glucagon expression in Glutag cells stimulated with increasing dose of compound **65** (1, 10, 25 and 50 µM). TLCA and HDCA were used as a positive control. Values are normalized to GAPDH and are expressed relative to those of not treated cells (NT) which are arbitrarily settled to 1. The relative mRNA expression is expressed as $2^{(-\Delta\Delta Ct)}$.

In vivo and *ex vivo* experiments were performed in order to evaluate whether the administration of compound **65** could lead to lipid accumulation in liver, the most common side effect shown by almost all LXRα synthetic agonists. As reported in Figure 39, panel A, administration of **65** (30 mg/kg) to C57BL6 mice for two weeks, did not produce any significant increase of plasmatic levels of AST, cholesterol and triglycerides. These results were confirmed by the analysis of liver histology, where no differences between the control group and mice treated with **65** in the hepatocytes shape were observed. In the Figure 39, panel B, the results of RT-PCR assayed on liver tissue after administration of **65**, were reported. As expected, administration of **65** did not affect the expression of steatosis markers genes such as FAS, SREBP1c, CD36 and PPARs. Finally, administration of **65** resulted in an expression increase of GPBAR1 target genes GLP1 and Fgf21 in terminal ileum, confirming the dual activity of this compound.

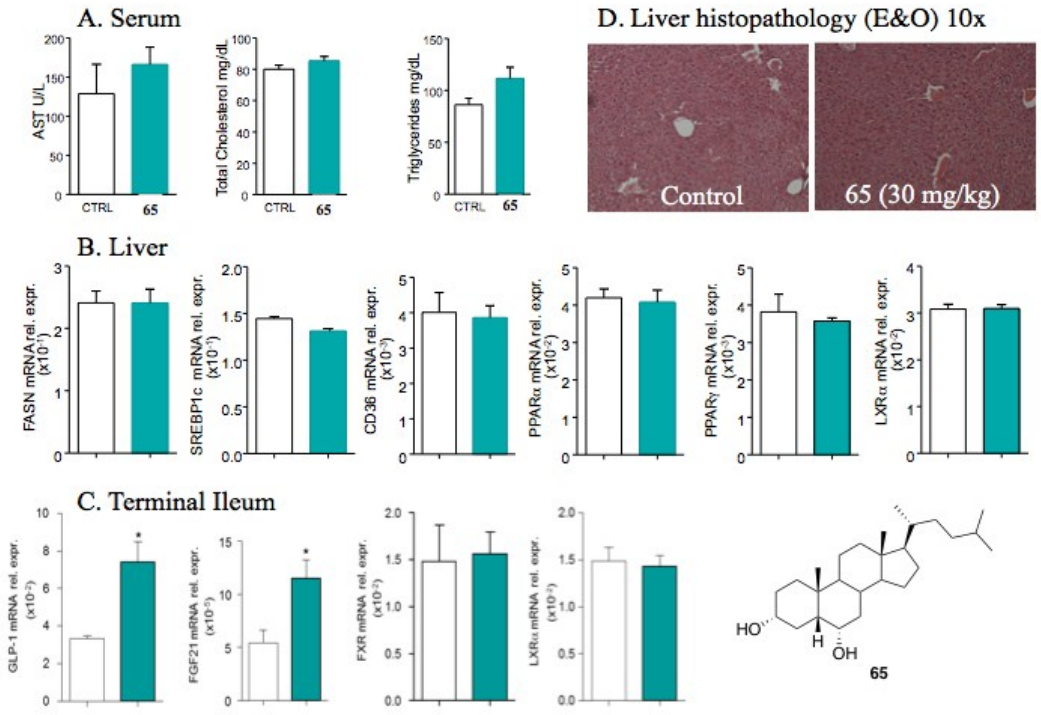

Figure 39. Effects of compound 65 on hepatic lipid metabolism and on terminal ileum after administration on intact mice. C57BL6 mice were treated with **65** (30 mg/Kg daily per os) for two weeks. Results are the mean ± SE of 3-5 mice per group; *p<0.05 versus control mice. A) Serum levels of AST, total cholesterol and triglycerides; B) Relative hepatic mRNA expression of GLP-1, FGF21, FXR and LXRα genes in terminal ileum; C) Relative hepatic mRNA expression of genes involved in fatty acids metabolism (FASN, SREBP1C, CD36) and genes for nuclear receptors (PPARα, PPARγ, LXR α); D) Hematoxilin and Eosin liver staining.

4.4. Molecular modelling.

Computational studies were then performed on compound **65**, in order to understand the structural features of its interaction with LXRα and GPBAR1 receptors.

Using the same GPBAR1 homology model that was used for compound **23** (see Chapter 2),[57] the docking pose of **65** in GPBAR1 binding pocket was modelled as reported in Figure 40. As shown in Figure 40, panel B, the best score model of compound **65**•GPBAR1 complex exibited similar structural feature as compound **23** (bis-*homo*UDCA, chapter 2) did. Despite this, some differences were found. In particular, the apolar side chain occupied a small lipophilic pocket formed by Ala66, Leu68 and Leu71 on TM2, a different site of interaction in comparison to

compounds bearing a polar side chain. This binding pose was further stabilized by the interaction of 3α-OH with Glu169 on TM5 and some hydrophobic interaction between bile acid scaffold and the side chains of Leu71, Phe96, Leu174 and Trp237.

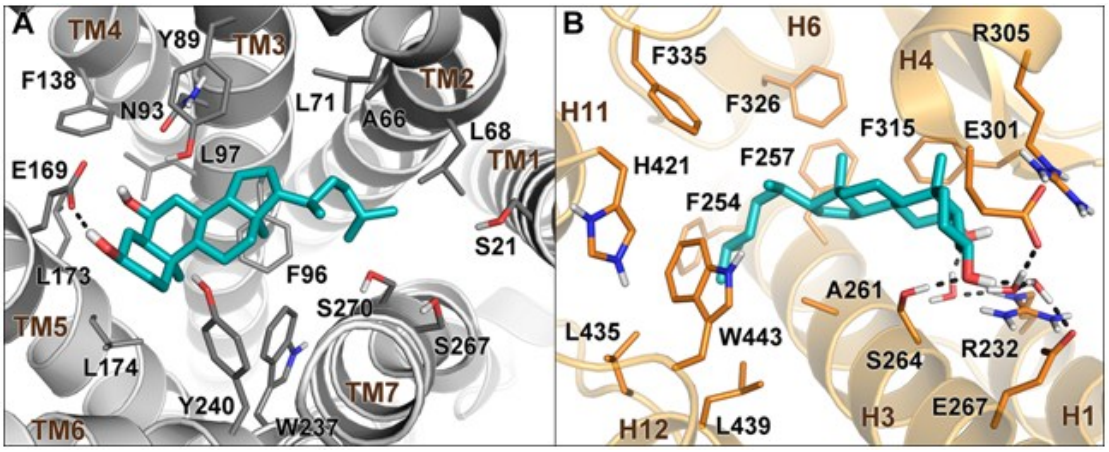

Figure 40. Proposed binding mode of 65 in GPBAR1 and in LXRα. (A) Docking pose in the homology model of GPBAR1. (B) Conformation obtained from MD simulations within the LXRα LBD (PDB code: 3IPU). Compound **65** is represented as cyan sticks. GPBAR1 and LXRα are shown as grey and orange cartoons, respectively. Amino acids important for ligand binding are depicted as sticks. Non-polar hydrogens are omitted for clarity.

Regarding the binding pose of **65** with LXRα, docking simulations have been performed using the crystal structure of the receptor ligand-binding domain (PDB code: 3IPU).[99] For this receptor, two possible binding poses, A and B, have been obtained. As reported in Figure 41, panel A, the hydrophobic chain of **65** is oriented towards the helices 11 and 12 of LXRα, whereas the 3α- and 6α-hydroxyl groups interact with the residues of the β-sheet close to H1. The binding mode B (Figure 41, panel B) showed that compound **65** is oriented in the opposite way in comparison to the binding mode A. In particular, the 3α-OH and 6α-OH groups are oriented towards His421 of helix 11, whereas the hydrophobic side chain extends towards the ligand binding pocket in the space between H4 and H1. In order to understand which of the two described binding pose was more stable, 100 ns molecular dynamics (MD) calculations were performed. The conservation of the interactions engaged by the ligand with the protein and the geometrical

stability of the ligand were evaluated through computing the root mean square displacement (rmsd) of its heavy atoms relative to their starting position.

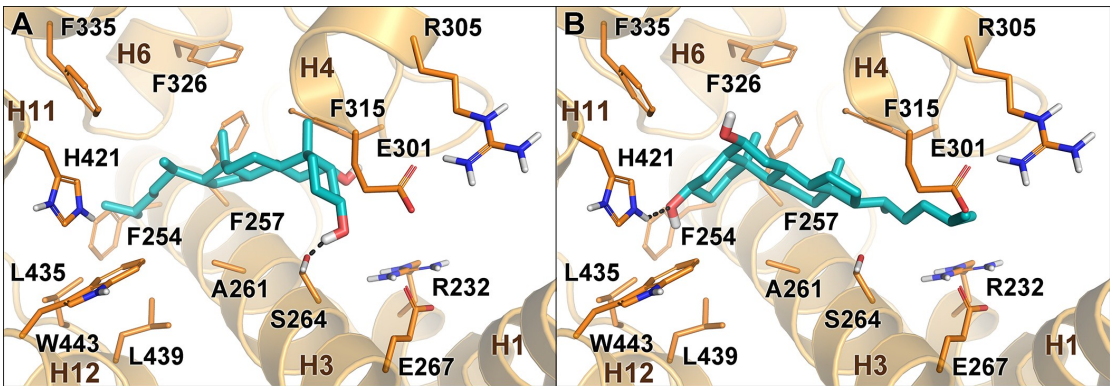

Figure 41. Binding poses A (A) and B (B) of **65** (cyan sticks) in the LXRα LDB (PDB code: 3IPU) as predicted by docking calculations. LXRα is shown as orange cartoons. Amino acids important for ligand binding are highlighted as sticks. Non-polar hydrogens are omitted for clarity

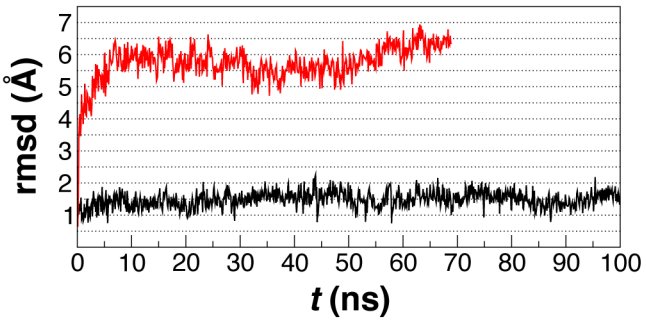

Figure 42. The rmsd plot of the heavy atoms of **65** during the MD simulations of binding modes A (black) and B (red) to LXRα. Prior to the rmsd calculations, trajectory frames were aligned using the coordinates of the Cα carbons of the receptor helices. Since binding mode B showed early to be unstable, its simulation was stopped at 70 ns.

The higher value of rmsd in binding mode B suggested that the complex between the binding pocket and compound **65** was not stable during the simulation. On the other hand, rmsd value for the binding mode A remained constant for all the simulation, suggesting that this kind of binding pose was more stable than the other one. In the binding pose A, as also shown in Figure 40, panel B, while the 3-OH moiety established H-bond interactions with the Ser264 side chain, the steroidal scaffold sets favourable contacts with lipophilic residues such as Phe257,

Phe315 and Phe326. Both 3-OH and 6-OH moieties are able to form water-mediated interactions with the side chains of Arg232, Glu267 and Glu301. Regarding the side chain of **65**, it pointed toward a deep lipophilic pocket defined by the helices 3, 4, 6, 11, and 12 forming hydrophobic interactions with Phe254, Phe335, Leu435, Leu439 and Trp443. These interactions allowed Trp443 to interact with His421 through a cation-π interplays. This receptor conformation is well recognized as fundamental for the activation of nuclear receptors, because it allowed the C-terminal helix to be in the right conformation for the binding of a co-activator, resulting in the activation of gene transcription.[101] Finally, the above described binding mode of **65** within LXR is comparable to the one reported for some oxysterols and with the mutagenesis data, suggesting a functional role of Glu267 in the binding of oxysterols to LXRs.[101]

CHAPTER 5:
SHP AGONISTS

In parallel to the synthesis of BAs derivatives as potential leads for the treatment of metabolic disease, a more recent part of my research activity was focused on the investigation of new synthetic chemical entities active in the treatment of liver fibrosis. In particular, the target of this study was the small (or short) heterodimer partner (SHP). SHP is an orphan nuclear receptor presenting a unique structure; differently from other NRs, SHP lacks the classical DNA binding domain (DBD), while seems to contain a putative ligand binding domain (LBD).[100] This structural deficiency does not allow SHP to directly bind DNA. Consequently, this receptor interacts with the LBD of other nuclear receptors and, in this way, SHP exerts its functions. SHP generally works as a negative regulatory co-factor, interacting both with NRs, like the farnesoid X receptor (FXR), estrogen receptor (ER), hepatocyte nuclear factor (HNF) 4, androgen receptor (AR), estrogen related receptor (ERR), liver receptor homolog-1 (LRH-1), liver X receptor (LXR), glucocorticoid receptor (GR), pregnane X receptor (PXR), retinoid X receptor (RXR), thyroid hormone receptor (THR), constitutive androstane receptor (CAR), and with other non nuclear transcriptional factors like NF-κB, c-Jun, SREBP-1c, and the forkhead transcription factor HNF3. [101,102]

Three mechanisms of inhibition have been hypothesized for SHP. The first, as in the case of the estrogen receptor, involves a competition with the co-activator for the binding with the C-terminal activation factor (AF-2) on the receptor.[102] A second mechanism of inhibition involves the recruitment of a co-repressor, as happens in the inhibition of cholesterol 7α-hydroxylase (CYP7A1).[103] The third involves the interaction of SHP with the surface of the NR or the transcriptional factor and in this way, the binding to DNA results hindered, like in the inhibition of RXR/RAR heterodimer complex formation.[102]

SHP mRNA is predominantly expressed in liver, but it is also present in heart, pancreas, spleen, small intestine of human adults, adrenal cortex and stomach.[102,103] The wide expression of SHP, together with the large number of its interacting partners, suggests that this receptor is involved in a number of physiological processes. Among them and in the context of metabolic pathologies,

one of the main SHP function is the regulation of bile acids homeostasis. Indeed, as mentioned in the Introduction, the activation of FXR induces an overexpression of SHP that negatively regulates the expression of CYP7A1 and sterol 12 hydroxylase (CYP8B1) through the inhibition of LRH-1 and HNF4α. [104] Furthermore, SHP has a role in cholesterol metabolism, glucose homeostasis and, interestingly, SHP seems to play an important role against hepatic carcinoma.[105] As discovered in 2014 from the research group of Professor Fiorucci, the activation of SHP seems to have beneficial effects in the reversion of liver fibrosis.[106] Fibrosis represents the natural consequence of a chronic liver injury. It is caused by a continuous remodelling of the extracellular matrix (ECM) due to an accumulation of type I collagen, proteoglycans, carbohydrates and other extracellular proteins. [107] With the persistence of this condition, the fibrosis develops into cirrhosis and, as final stage, could turn into hepatic carcinoma. A key role in the development of liver fibrosis is played by the activation of the hepatic stellate cells (HSC). Their activation, caused by a chronic liver injury, results into their trans-differentiation to myofibroblast-like cells, responsible of the overexpression of the ECM genes, as well as matrix-degrading enzymes and their respective inhibitors.[106] The nature of chronic liver injury could range from a persistent inflammation status, alcohol abuse, parasites, obesity, cholestasis, autoimmune attack and metabolic disorders. In the context so far described, it was shown that the activation of SHP results in the inhibition of the trans-differentiation of HSC into myofibroblast, with the reduction of 70% of type 1 collagen.[108] These data point out SHP as a potential pharmacological target for the treatment of liver fibrosis, one of the consequence of metabolic disease.

Actually, a specific endogenous ligand for SHP is not still found. Some retinoic acid related molecules (like all trans retinoic acid ATRA) bind SHP, while among synthetic compounds, (E)-4-[3-(1-Adamantyl)-4′-hydroxyphenyl]-3-chlorocinnamic acid (3-Cl-AHPC) is a weak SHP agonist, despite its anticancer activity (Figure 43).[108]

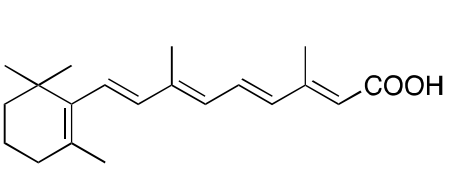

All trans retinoic acid (ATRA)

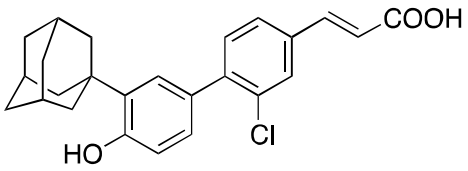

3-Cl-AHPC

Figure 43. SHP known agonists

Analysing these two structures, it is possible to highlight two common features: a carboxylic ending moiety and a cyclic portion on the opposite side of the molecule. The difference between these molecules lies in the spacer separating these two moieties. The same structural features are present in GW4064, a well-known FXR agonist (Figure 44).

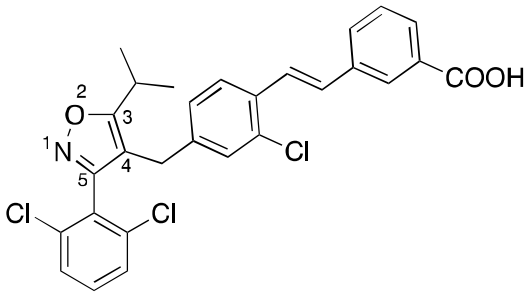

Figure 44. GW4064

In this molecule, the carboxylic moiety is separated from an isooxazole ring by an aromatic spacer, like in 3-Cl-AHPC.

Keeping in mind these considerations, it was thought that a structural simplification of GW4064 could produce new SHP agonists (Figure 45). Holding unchanged the 3-(2,6-chlorophenyl)-5-sopropyl-isooxazole, different side chains, ending with a polar moiety, were introduced in position 4. These modifications furnished the first set of specific SHP agonists, as demonstrated by the pharmacological assays. Among them, a deep pharmacological analysis was performed on compound **92**, demonstrating its potential application in the treatment of liver fibrosis, cholestasis and liver inflammation.

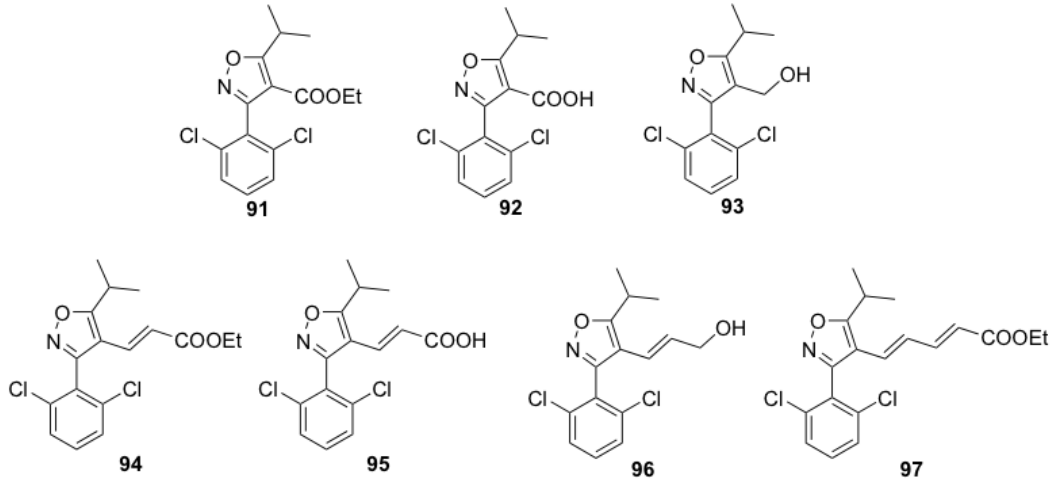

Figure 45. 3-(2,6-dichlorophenil)-5-isopropil isooxazole derivatives

5.1. Side chain modifications of 3-(2,6-dichlorophenil)-5-isopropil isooxazole.

Following a procedure reported in literature,[109] the synthesis of the 3-(2,6-dichlorophenyl)-5-isopropylisoxazole-4-carboxylate ethyl ester **91** started from 2,6-dichlorobenzaldehyde (Scheme 14)

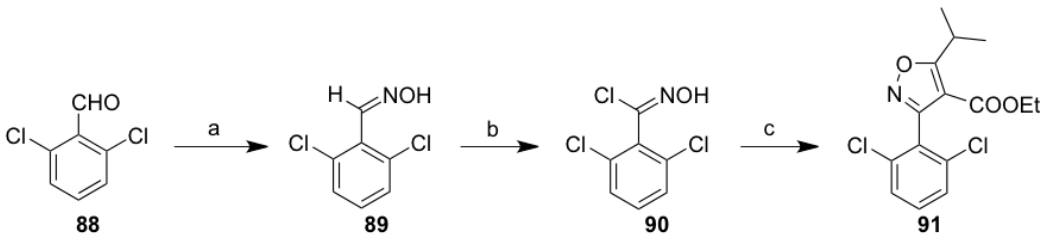

Scheme 14. *Reagents and conditions*: a) NH_2OH•HCl, NaOH in ethanole; b) N-chlorosuccinimmde in DMF dry; c) ethyl isobutyryl acetate, sodium ethoxide, in THF dry.

The starting material was converted into the corresponding hydroxylamine **89** by the treatment with NH_2OH•HCl in alkaline conditions. Then, the chlorination of intermediate **89** furnished the instrumental functional group for the reaction of cyclization with ethyl isobutyryl acetate, yielding 3-(2,6-dichlorophenyl)-5-isopropylisoxazole-4-carboxylate ethyl ester **91** in high chemical output. As reported in Scheme 15, an aliquot of **91** was hydrolyzed in alkaline condition to the corresponding carboxylic acid **92** (ISO-COOH), whereas another portion of **91** was subjected to reduction using diisobutyl aluminum hydride (DIBAL-H)

furnishing the alcohol **93**, a key intermediate for the synthesis of the elongated side chain analogues. Swern oxidation, followed by Horner C-2 homologation on compound **93** furnished the ethyl ester **94** that was in turn hydrolyzed to the corresponding carboxylic acid **95** by the treatment with LiOH. Finally, an aliquot of compound **94** was reduced with DIBAL-H furnishing the unsaturated alcohol **96**. With the aim to keep unchanged the unsaturation both in the ester hydrolysis and in the ester reduction, the use of two mild reagents, like LiOH and DIBAL-H respectively, was necessary. Stronger condition, like using NaOH or with $LiBH_4$, respectively, would have reduced also the double bond. Applying the same synthetic protocol described for compound **91**, an aliquot of **94** was hydrolyzed to the corresponding carboxylic acid **95**, while a second aliquot was reduced to yield the alcohol **96** that was in turn converted in ethyl ester **97** by Swern-Horner reaction.

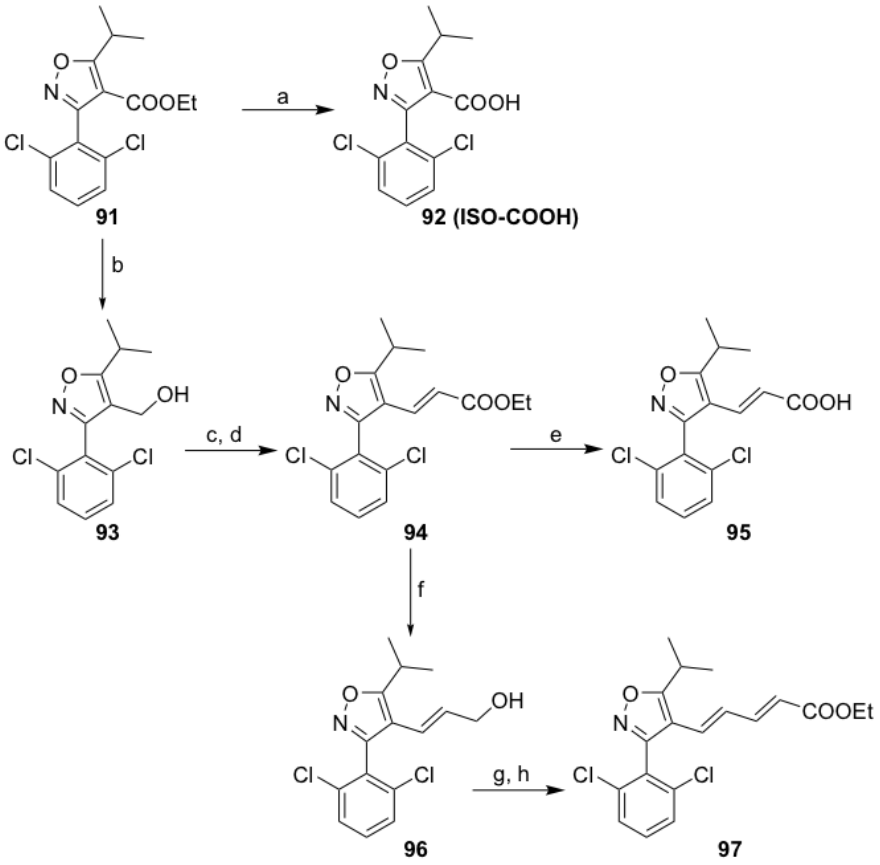

Scheme 15. *Reagents and conditions*: a) NaOH 5% in MeOH/H_2O 1:1 v/v; b) DIBAL-H in THF, Toluene; c) DMSO, oxalyl chloride, TEA dry, CH_2Cl_2, -78° C; d) LiOH, TEPA, THF dry; e) LiOH, THF: H_2O 1:1 v/v; f) DIBAL-H in THF, Toluene; g) DMSO, oxalyl chloride, TEA dry, CH_2Cl_2, -78° C; h) LiOH, TEPA, THF dry.

5.2. Pharmacological evaluations

To assess if the synthesized compounds were SHP agonists, transactivation assays were performed. HepG2 cells transfected with responsive elements of SHP were stimulated with compounds **91-97** (10 μM and 50 μM) and with ATRA, used as positive control. As shown in Figure 46, compounds **91**, **92** and **96** acted as SHP agonists, although their activity is lower than ATRA. Interestingly, the EC_{50} calculated for compounds **91** and **92** were similar to that of ATRA (9.6 μM, 8.9 μM and 8.6 μM, respectively). Further pharmacological analysis has been performed on ISO-COOH (**92**), the best derivative synthesized. First, the activity of ISO-COOH on HSC was evaluated and, in particular, the effects on αSMA and COL1α1 genes were assessed. Administration of ISO-COOH (**92**) to rat overexpressing SHP resulted into a decrease of α-Smooth muscle actin (αSMA) and Collagen Type I Alpha (COL1α) mRNAs, as assessed by RT-PCR (Figure 47, panels C and D). In wild type HSC, administration of ISO-COOH did not produce any significant effect, confirming that an overexpression of SHP was necessary to estimate the activity of **92** (Figure 47, panels A and B).

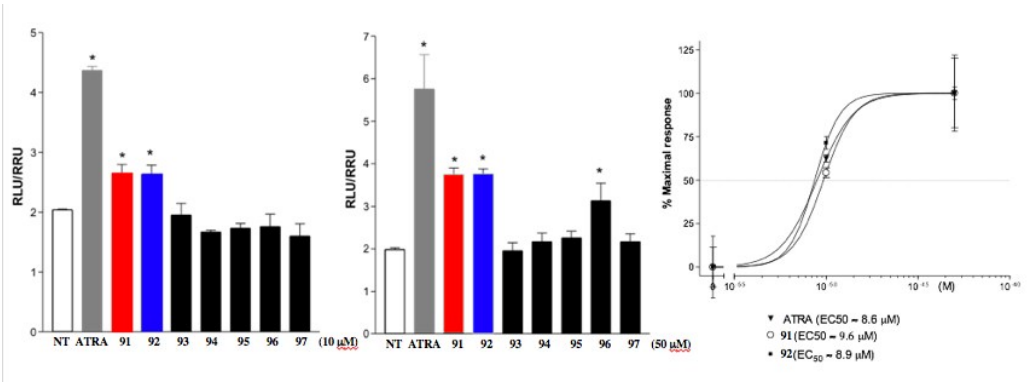

Figure 46. Transactivation assay on SHP ligand binding domain. HepG2 cells were transiently transfected with the fusion protein SHP/GAL4 and with the reporter vector pGL4.35. 24 hours post-transfection Cells were stimulated with 10 μM or 50 μM compounds **91**–**97** and with 10 or 50 μM all trans retinoic acid (ATRA), used as a positive control. Results are expressed as the mean Å} standard error (*p < 0.05 vs not treated cells (NT). Concentration−response curves for compounds **91** and **92** (ISO-COOH). HepG2 cells transiently transfected with the fusion protein SHP/GAL4 and with the reporter vector pGL4.35 were stimulated with increasing concentrations of compounds **91** and **92** (1, 10 and 50 μM). ATRA (1, 10 and 50 μM) was used as a positive control to evaluate the SHP ligand binding domain activity.

Then, the same experiments were performed on human HSC (Figure 48). In human HSC-LX2, the administration of CDCA was necessary to overexpress SHP. Since the concentration of SHP in human HSC in physiological condition is low, its increased expression is achieved through the activation of FXR. Indeed, stimulation of FXR with an agonist, like CDCA, resulted into an overexpression of SHP.[108] Co-administration of **92** and CDCA resulted in a decrease of αSMA and COL1α genes levels both in LX2 wild type cells and LX2 overexpressing SHP cells.

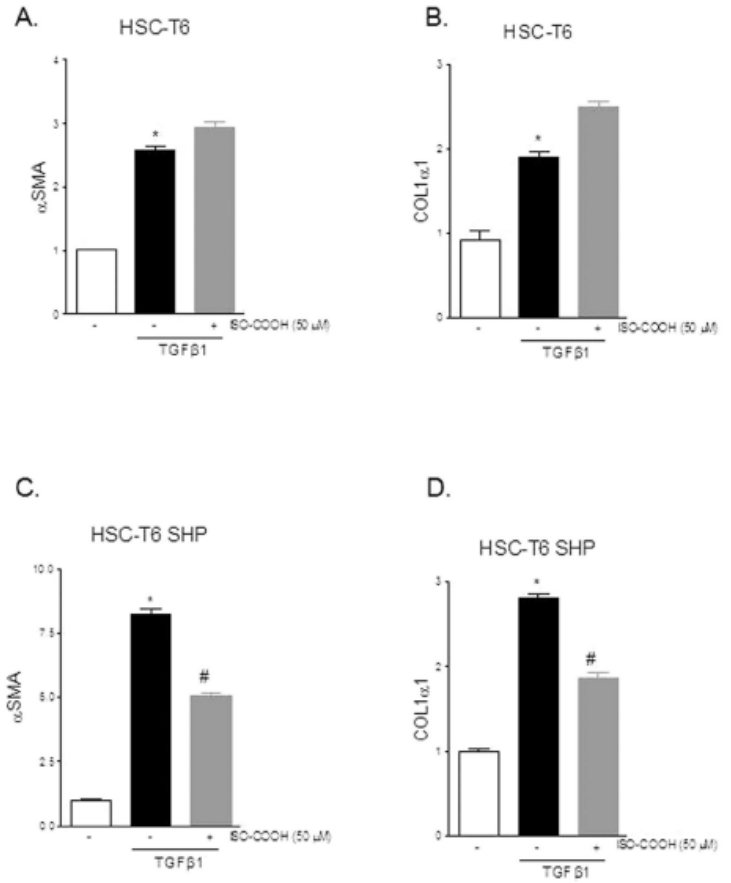

Figure 47. SHP agonism reverses the pro-fibrotic phenotype induces by TGFβ1 in rat HSC. Rat HSC-T6 and HSC-T6 overexpressing SHP were used. (A,B). Serum starved HSC-T6 were stimulated 18 hours with 10 ng/ml TGFβ1 alone or in combination with 50 μM ISO-COOH. At the end of stimulation the relative mRNA expression of αSMA and COL1α1 was assayed by Real-Time PCR. (C,D) Serum starved HSC-T6 overexpressing SHP were stimulated 18 hours with 10 ng/ml TGFβ1 alone or in combination with 50 μM ISOCOOH. At the end of stimulation the relative mRNA expression of αSMA and COL1α1 was assayed by Real-Time PCR. Values are normalized relative to GAPDH mRNA and are expressed relative to those of not treated cells (NT), which are arbitrarily set to 1. *$p < 0.05$ vs NT; #$p < 0.05$ vs TGFβ1.

The effects of compound **92** were also investigated *in vivo* in a model of liver fibrosis inducted in mice by two weeks treatment with CCl_4 (Figure 49). Again, the administration of CDCA was necessary to stimulate SHP expression. In particular, it has been reported that the administration of CDCA in CCl_4 treated mice results in an overexpression of SHP without reducing liver fibrosis.[110] Treatment with CCl_4 increased the levels of AST and bilirubin, and the treatment with CDCA worsened these conditions. On the other hand, co-administration of CDCA and **92** resulted in a decrease of these values. A morphometric analysis of liver sections confirmed these findings (Figure 50).

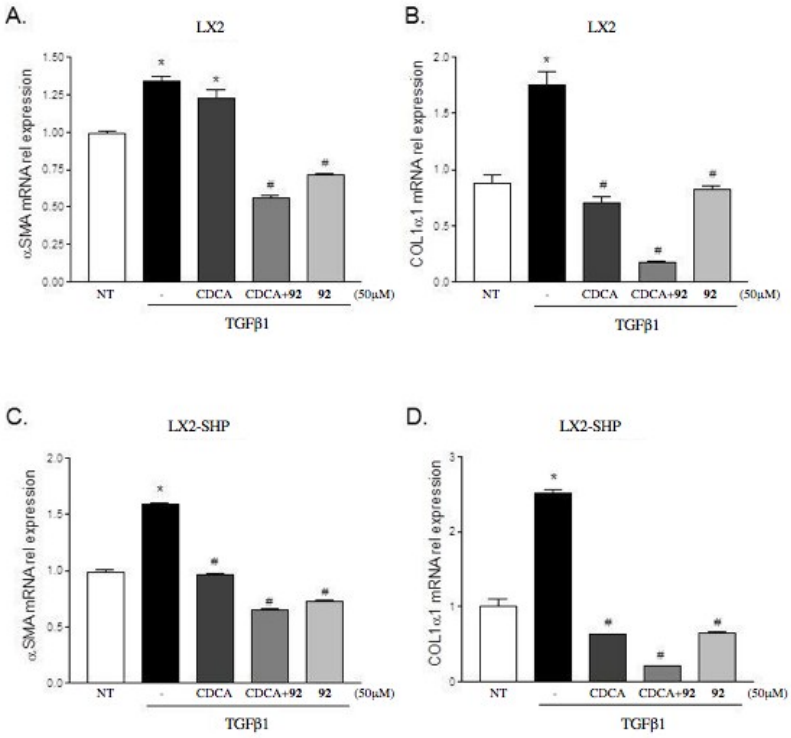

Figure 48. SHP agonism reverses the pro-fibrotic phenotype induced by TGFβ1 in human HSC. HSC-LX2 and HSC-LX2 overexpressing SHP were used. (A,B). Serum starved HSC-LX2 were activated with 10 ng/ml TGFβ1 and stimulated 18 hours with 50 μM CDCA and ISO-COOH 50 μM or with a combination of both agents. At the end of stimulation the relative mRNA expression of αSMA and COL1α1 was assayed by Real-Time PCR. (C,D) Serum starved HSC-LX2 overexpressing SHP were exposed to 10 ng/ml TGFβ1 for 18 h alone or in combination with 50 μM CDCA and 50 μM ISO-COOH or with a combination of both agents. At the end of the study cells were harvested and relative mRNA expression of αSMA and COL1α1 assayed by Real-Time PCR. Values were normalized relative to GAPDH mRNA and not treated cells (NT) were arbitrarily set to 1. *$p < 0.05$ vs NT; #$p < 0.05$ vs TGFβ1.

Imaging of liver sections coloured with two different techniques shows that while the treatment with CCl_4 increased the number of bridging fibrosis, co-treatment with CDCA and **92** almost restored the liver in physiological conditions. The same did not happen treating mice with CDCA alone. Furthermore, RT-PCR analysis showed that the treatment with CDCA alone aggravated the fibrotic condition (Figure 51). On the contrary, co-treatment of CDCA and ISO-COOH improved this condition, as demonstrated by the reduction of αSMA, COL1α1, TGFβ and IL1-β gene levels.

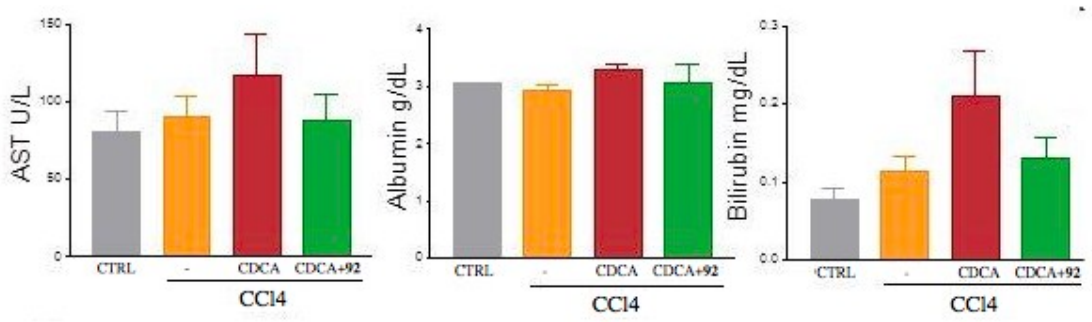

Figure 49. SHP activation protects against liver fibrosis in the CCl_4 model. Effect of compound **92** on AST, Albumin and Bilirubin in mice rendered cirrhotic by administration of CCl_4. Mice were administered CCl_4 for 3 weeks and after the first week of treatment randomized to receive CDCA, 5 mg/kg/day, alone or in combination with ISO-COOH, 30 mg/kg/day.

Since ISO-COOH seems to inhibit and to regress liver fibrosis only when administrated with CDCA, another model of liver fibrosis was set up using ANIT to demonstrate that the activity of compound **92** is independent from the presence of CDCA. Administration of ANIT induced an immune response that causes the injury of small intrahepatic bile ducts, bile duct regeneration and, finally, liver fibrosis and cholestasis, as described in Chapter 2. The hepatic injury was confirmed by morphometric analysis of a liver section (Figure 52, panels B and C), while cholestasis was confirmed by the evaluation of hematic levels of AST and alkaline phosphatase.

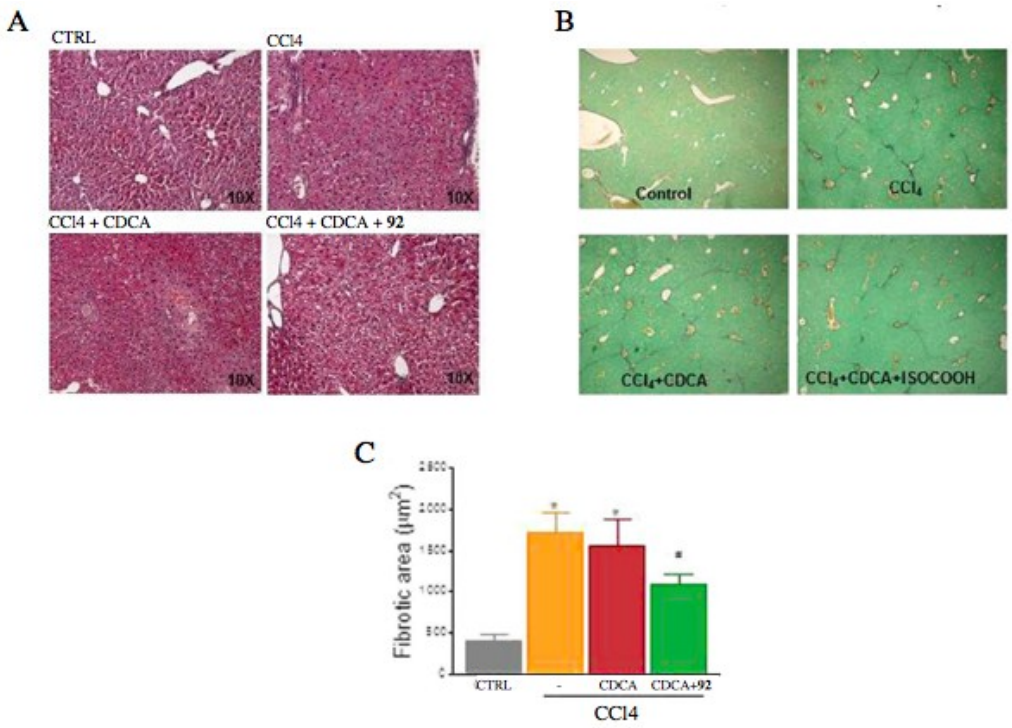

Figure 50. SHP activation protects against liver fibrosis in the CCl_4 model. (A) Hematoxylin and eosin (H&E) staining. (B) Syrius red staining. (C) Image J quantification of Syrius red staining.

While administration of CDCA alone did not reverse the fibrotic condition inducted by ANIT, compound **92**, alone or in combination with CDCA, enhanced the reversion of liver fibrosis. Then, the expression of various genes involved in liver fibrosis, cholestasis and liver inflammation was screened (Figure **53**). The data suggested that the administration of **92**, alone or in combination with CDCA, resulted in the reduction of αSMA and COL1α1 mRNAs expression, whereas administration of CDCA resulted in the increase their expression. Furthermore, compound **92** restored the physiological levels of OST-α, BSEP and NTCP, three canonical FXR target genes involved in bile acid uptakes and detoxification by hepatocytes. Finally, administration of **92**, alone or with CDCA, resulted in the reduction of the pro-inflammatory IL-1β and MCP-1 mRNAs, whereas CDCA alone did not produce any positive effects. All these data demonstrate that the administration of ISO-COOH results in a number of positive effects like preventing liver fibrosis, cholestasis and liver inflammation, pointing out SHP as an important physiological mediator of metabolic pathology.

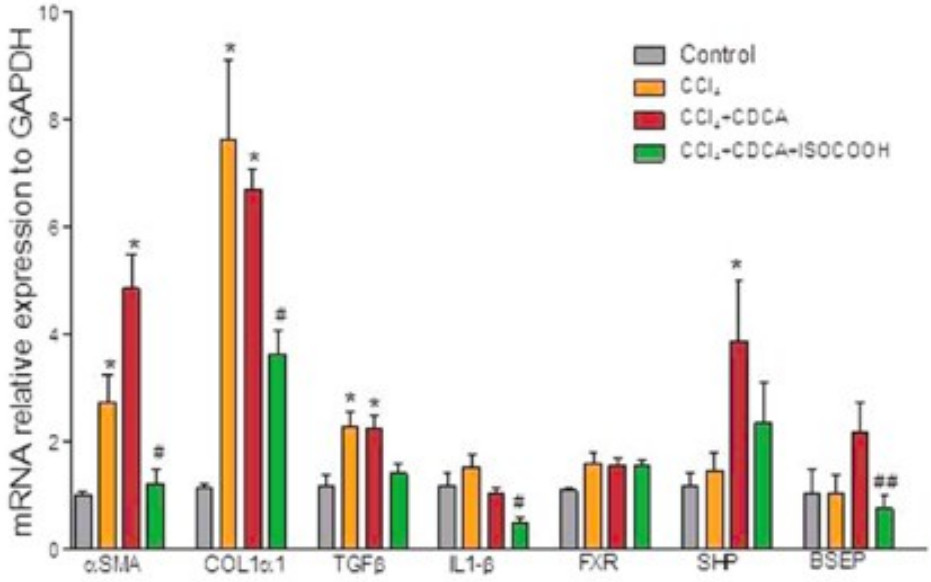

Figure 51. SHP activation protects against liver fibrosis in the CCL_4 model. Effect of CDCA (5 mg/kg) or ISO-COOH (30 mg/kg) on fibrotic genes in CCl4-treated mice. The relative hepatic mRNA expression of αSMA, COL1α1, TGFβ1, IL1β, FXR, SHP and BSEP was assayed by Real-Time PCR. Results are the mean Å} SE of 4–6 mice per group. *p < 0.05 versus naïve mice. #p < 0.05 versus CCl4 alone.

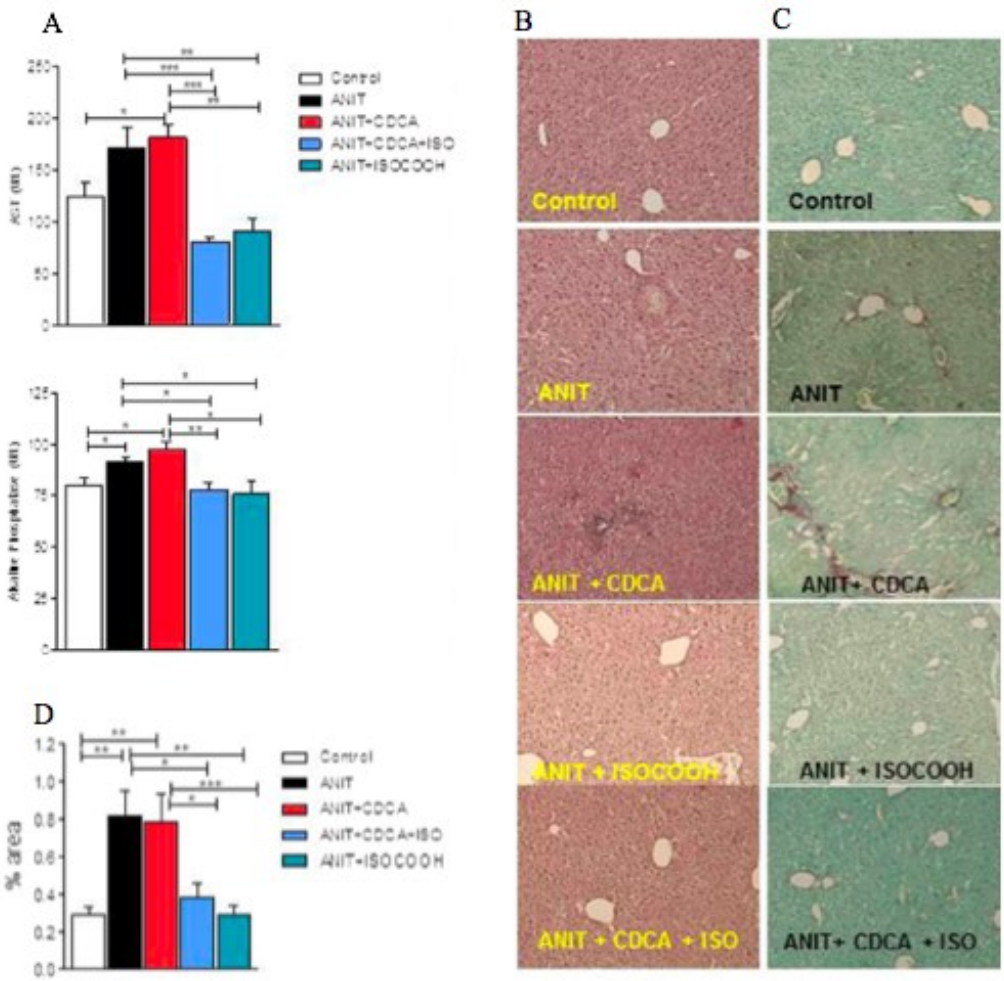

Figure 52. SHP agonism protects against liver fibrosis development in a mice model of cholestasis. (A) Effect of ISO-COOH on AST and Alkaline phosphatase in mice administered α-naphthyl-isothiocyanate (ANIT), 10 mg/kg per os for 4 weeks. Mice were randomized after 2 weeks to receive CDCA (5 mg/kg) alone or in combination with ISO-COOH (30 mg/Kg), or ISO-COOH alone (30 mg/Kg), for two additional weeks. Data shown are: (B) Hematoxylin and eosin (H&E) staining. (C) Syrius red staining. (D) Image J quantification of Syrius red staining. Results are the mean Å} SE of 6–9 mice per group. *p < 0.05, **p < 0.005, ***p < 0.0005.

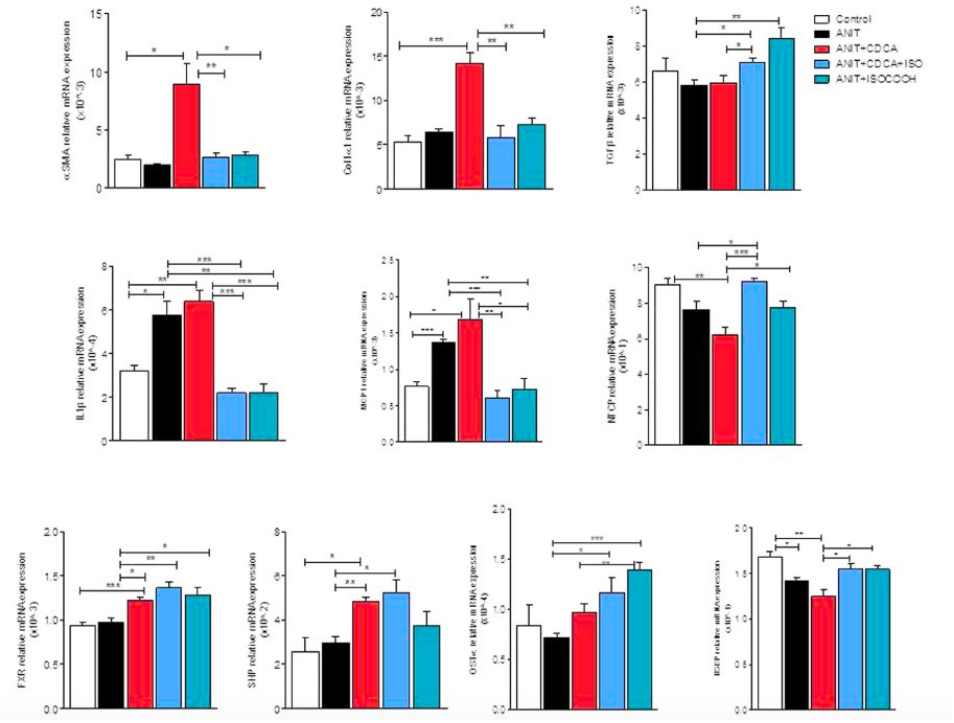

Figure 53. SHP activation protects against liver injury by modulating the expression of inflammatory genes. Effect of ISO-COOH on fibrosis, bile acid metabolism and inflammatory genes was assessed in mice administered α-naphthyl-isothiocyanate (ANIT), 10 mg/kg per os for 4 weeks. Mice were randomized after 2 weeks of ANIT to receive CDCA (5 mg/kg) alone or in combination with ISO-COOH (30 mg/Kg), or ISOCOOH alone (30 mg/Kg), for two additional weeks. The relative hepatic mRNA expression of αSMA, COL1α1, TGFβ1, IL1β, MCP1, NTCP, FXR, SHP, OSTα and BSEP was assayed by Real-Time PCR. Results are the mean Å} SE of 6–9 mice per group. *p < 0.05, **p < 0.005, ***p < 0.0005.

CHAPTER 6:
2-AZAANTHREAQUINONE: TOTAL SYNTHESIS AND FUNCTIONALIZATION

The last part of my Ph.D. was spent in the laboratories of Organic Synthesis of the Antwerp University, under the supervision of Professor Kourosch Abbaspour Tehrani, where the research activity was focused on the synthesis of the 2-azaanthraquinone, a benz[*g*]isoquinoline, and its direct functionalization.

Among natural compounds, the 2-aza-pyronaphtalenquinones are a very interesting class of molecules due to their different biological activities. Extracted from different kind of organism, and in spite of their pyranonaphthoquinones analogues, 2-azaanthraquinones (2-AAQs) have rarely been isolated.[111] Examples of 2-AAQs (Figure 54) are Bostrycoidin and 9-O-Methylbostrycoidin, both isolated from several fungi of the *Fusarium* species,[112] and both endowed with antibiotic activity, [113 , 114] Tolypocladin, isolated from the mycelium of *Tolypocladium inflatum,* showing metal-chelating properties,[115,116] and, finally, the benz[*g*]isoquinoline-5,10 dione itself, obtained from *Psychotria camponutans* and *Mitracarpus scaber*, endowed with biologic activity against *Plasmodium falciparum* and *Staphylococcus aureus*, two multidrug resistant pathogens.[117]

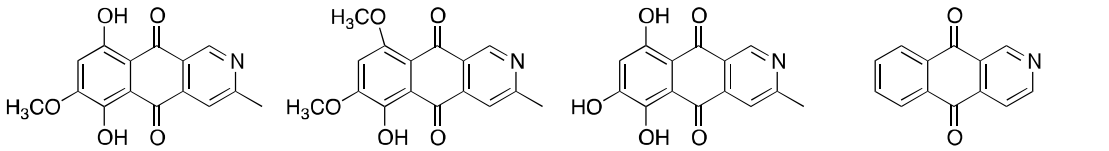

Figure 54. Naturally occurring 2-AAQs

Beside these antiplasmodial activities, 2-AAQs are intercalating DNA binding agents, attracting the researchers interest in cancer chemotherapy.[118] Under this respect, examples of synthetic 2-AAQs acting as DNA intercalating molecules are the pixantrone and the benzo-fused isoquinolinedione derivative BFI (Figure 55).[119,120] Studies on these molecules demonstrated that the planar aromatic ring is an essential feature for the intercalation, showing the highest activity with three or four conjugated cyclic systems. Finally, the presence of an N-heterocyclic moiety

seems to enhance the intercalation due to the formation of further H-bonds with DNA.[121] These features seems also to reduce the toxic effects related to other quinolone antitumor agents; indeed, while the mixantrone shows toxic dose-related side effects such as myelosuppresion and cardiotoxicity,[122] pixantrone, its N-heterocyclic analog, showed a reduced toxicity.[116]

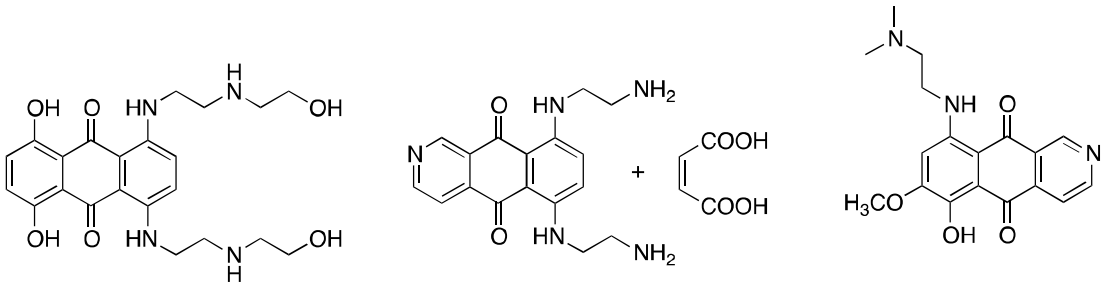

Mixantrone **Pixantrone** **BFI**

Figure 55. 2-AAQs with anticancer activity

These findings underline the importance of the 2-AAQs scaffold as potential lead for new anticancer molecules.

In this chapter, a new method for the functionalization of the benz[*g*]isoquinoline-5,10 dione N-heterocyclic ring with nucleophiles was investigated, leading to the synthesis of new 2-AAQ analogues .

6.1. Total synthesis of 2-AAQ

In literature, a number of methods for the synthesis of the 2-AAQ are reported;[111] one the most frequently used approach is the Diels Alder condensation between the isoquinoline-5,8-dione and a suitable substitute cyclohexa-1,3-diene, furnishing substitute 2-AAQs on the homocyclic moiety (Figure 56).[123]

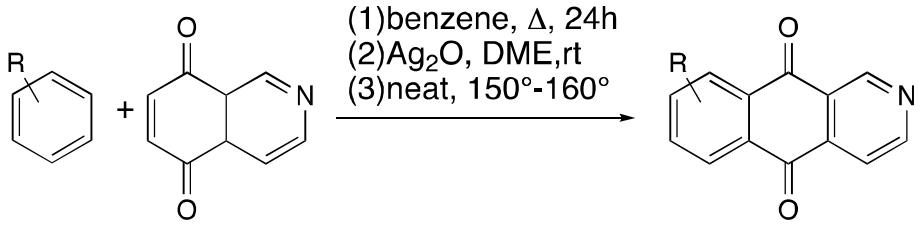

Figure 56. Diels-Alder condensation

Another classic approach to the synthesis of substitute 2-AAQs involves the use of a Fridel-Craft reaction between a substitute benzene and methylpyridine-4,5-dicarboxylic anhydride (Figure 57) .[124]

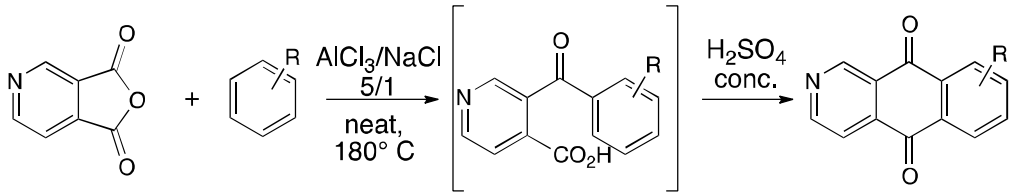

Figure 57. Fridel-Craft approach

Professor Tehrani research group developed a new synthetic strategy for the synthesis of the benz[*g*]isoquinoline through an intramolecular Hack reaction between a protected allylamino moiety and a bromine instrumental function (unpublished results). The synthetic procedure (Scheme 16) started from the commercially available Menadione (**98**); the first step was the conversion of the chetonic moieties in their alcoholic analogues **99**. In this way, the subsequent esterification with dimethyl sulphate and sodium methoxyde of that alcoholic moieties resulted in the protection of the two chetonic groups, limiting their reactivity in the next steps (Scheme 16, step b). Intermediate **100**, was then subjected to bromination in position 3 using molecular Bromine (intermediate **101**). A second bromination on benzylic position was performed using N-bromosuccinimide (NBS), furnishing intermediate **102**. The methyl bromine of **102** was then alkylated using a protected allylamine, furnishing compound **103** (Scheme 16, step e), a suitable substrate for a modified intramolecular Hack cyclization. In particular, the use of Cs_2CO_3 and tert-butyldicyclohexylphosphonium tetrafluoroborate represent the novelties proposed by professor Tehrani research group. This reaction furnished the N-protected intermediate **104**, that was in turn subjected to a one-step N-deprotection and aromatic oxidation furnishing intermediate **105**. Finally, the re-oxidation of the methyl ester moieties using cerium ammonium nitrate (CAN) provided the 2-AAQ **106**. Although the higher number of synthetic steps compared to the other methods reported in literature, this synthesis furnished the desired product in high chemical yields and with just one purification step.

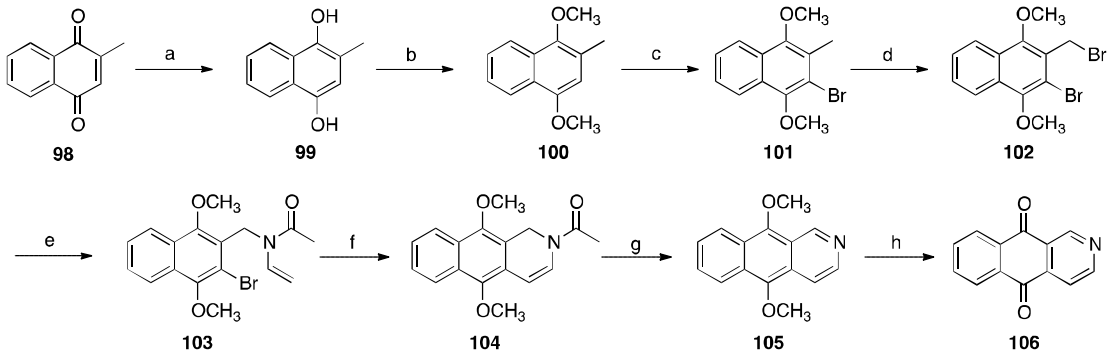

Scheme 16. *Reagents and conditions*. a) $Na_2S_2O_4$, H_2O, EtOAC; b) dimethyl sulphate, NaOMe, iPrOH, 63 °C; c) Br_2, DCM, 0 °C; d) NBS, (E)-Azobis(isobutyronitrile), EtOAc, reflux; e) NaH, N-Ethenylacetamide, DMSO, 2-bromo-3-(bromomethyl)-1,4-dimethoxynaphthalene; f) $Pd(OAc)_2$, tert-Butyldicyclohexylphosphonium tetrafluoroborate, Cs_2CO_3, DMF, 130 °C; g) NaOH, air, MeOH, reflux; h) CAN, CAN/H_2O 2:1 v/v, 0 °C.

6.2. 2-AAQ functionalization

Given the poor reactivity of 2-AAQ pyridine moiety, an intermediate reaction step was necessary to enhance the nucleophilic/electrophilc character of the heteroarene portion. One of the most used synthetic protocol for pyridine position-2 functionalization is the nucleophilic displacement of the corresponding 2-halopyridine; unfortunately, this strategy often gives low yields.[125] The use of Palladium as catalysts in a C2-metalated heteroarene cross-coupling improves the yields, but harsh condition or specific ligands are often required.[126] Another well-known strategy to enhance pyridine reactivity towards both nucleophiles and electrophilic agents involves its conversion in the corresponding N-oxide (Figure 58).[127] In the last decade, this activation method has drawn the attention of researchers for its versatility in the synthesis of the 2 and 4 substituted pyridine derivatives.

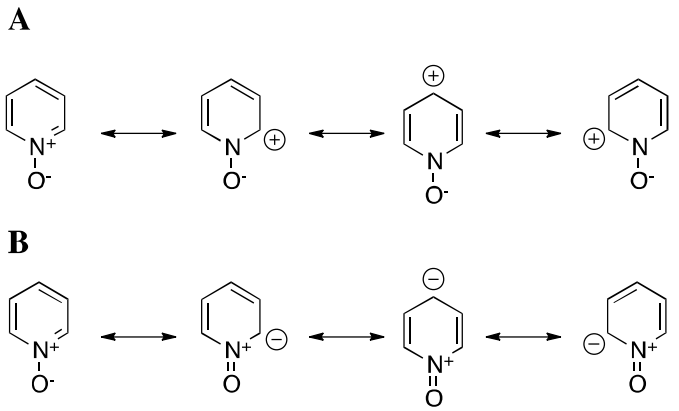

Figure 58. Electrophilic (A) and nucleophilic (B) behaviour of pyridine N-oxide

There are many different methods for the oxidation of pyridine, most of them require the use of peracids or peroxides as oxygen atom donors.[128] The products obtained are often stable, and this simple activation method offers a number of synthetic opportunities for the synthesis of 2 and 4 substitute pyridine derivatives. Consequently, using meta-chloroperbenzoic acid (mCPBA), the reaction with benz[*g*]isoquinoline-5,10-dione (**106**) furnished the stable N-oxide **107** (Scheme 18) that was used as substrate for the direct functionalization with nucleophiles.

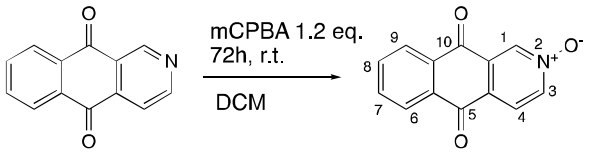

106 **107**

Scheme 18. *Reagent and conditions*. mCPBA 1.2 eq, DCM, 72 h , rt.

In order to further exalt the electrophilic character of positions 1 or 3 in benz[*g*]isoquinoline-5,10-dione N-oxide, the use of an activating agent became necessary. In this way, the addition of a generic nucleophilic agent under mild condition could be enhanced.

After a screening of the related literature, two methods of nucleophilic addition on compound **107**, were tested. In the first one, bromotripyrrolidinophosphonium hexafluorophosphate (PyBroP) as activating agent for the addition of primary and secondary amine, was used.[129] The second one was based on the work of Crisenza *et al*. which use a Brønsted acid (like p-toluensolfonic acic) as catalyst for the C-2 alkenylations on pyridine N-oxide scaffold. [130] Both methods have been investigated in order to achieve both the nucleophilic substitution and the de-

oxygenation in a single step. Unfortunately, both the reactions failed in the synthesis of the desired product, catalyzing only the de-oxygenation of 2-AAQ N-oxide. Although a further investigation about the reasons behind this failure was not performed, one possible explanation lays in the electron withdrawing effect played by the central quinone ring (Figure 59).

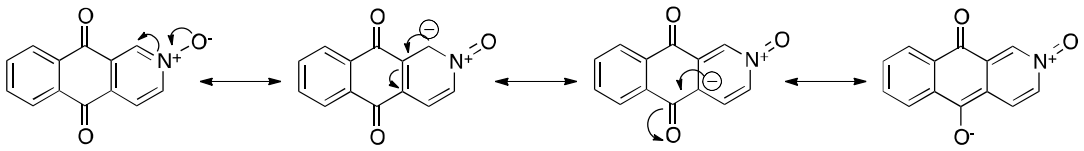

Figure 59. Resonance structures of 2-AAQ N-oxide

When the electrons shifted from the N-oxide oxygen to the ketone in position 5, the activating agent binds this moiety, resulting in a missed enhancement of the electrophilic properties of the heteroarene. Consequently, a new literature search about other N-oxide activation methods started. After analysing different procedures implicating the use of inorganic and organic metal catalysts, the work of Zhu *et al*. was considered appropriate for the purpose of a direct nucleophilic functionalization.[131] In this paper, copper iodide (CuI) was proposed as catalyst in a one-pot direct amination of quinoline and isoquinoline N-oxides by dehydrogenative C–N coupling. Copper ion worked as a Lewis acid in –CH activation of position 2 in quinoline N-oxide scaffold; finally, the presence of O_2 was necessary to re-oxidize the copper and complete the catalytic cycle. The mechanism of reaction reported in the paper suggested that the N-oxide oxygen was not involved in the process of amination, so this method have been applied for the nucleophilic substitution in position 1 or 3 of benz[*g*]isoquinoline-5,10-dione N-oxide scaffold. Using piperidine as nucleophilic agent, the same operative conditions described in Zhu's work were applied (Table 3). In 16 h, the reaction furnished 11.9% yield, with the 9% of the 3-monoaminated product (compound **108**) and the 2.9% of the 3,4-diaminated (compound **110)**, efficiently separated by silica gel chromatography. The substitution in position 3 was confirmed by the ^{1}H NMR spectrum, where the presence of two singlets at δ 8.88 and δ 7.60, instead of one singlet and two doublet (as in 2-AAQ N-oxide), suggesting that one proton was missing. The correlation in HMBC (Figure 60) between H-1 and H-4 with C-3, and between the α-N protons of piperidine (δ

3.52) and the carbon at δ 158.6 (C-3), established that the amination had to be necessary in position 3. Regarding compound **110**, the double substitution was confirmed by the presence of only one singlet at δ 8.6. Thanks to the HMBC correlations (Figure 60) between the proton at δ 3.34 with the carbons at δ 158, and the proton at δ 3.14 with the carbon at δ 148.3, it was possible to position the two piperidine moieties on carbons 3 and 4, respectively. The NOESY correlation between protons at δ 3.34 and δ 3.14 confirmed the adjacency of the two piperidine moieties, as suggested from HMBC.

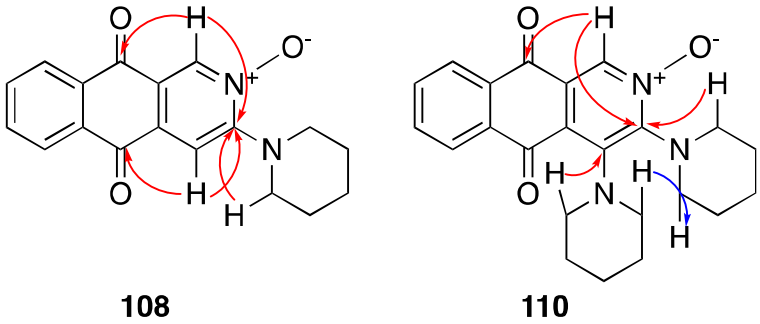

108 **110**

Figure 60. Principal HMBC (red) and NOESY (blue) correlations of compounds **108** and **110**

Interestingly, although the total yield was quite low, the presence of the expected 1-monoaminated product was not detected, probably because the reactivity of H-1 resulted limited for the steric hindrance given by the presence of the N-oxide oxygen and the ketone in position 10; on the other hand, the 3,4-diaminated product suggested that an amination in position 4 took place. Furthermore, the presence of both the de-oxygenated 3-monoaminated and 3,4-diaminated product was observed.

Several reaction conditions were then investigated, in order to improve the yields of the nucleophilic addition (table 3).

Using different type of solvents, the total yields were always constant (approximately 18%), with the exception of entry 3, where it raised to 55% (12% of compound **108** and 33% of compound **110**). After long time stirring (entry 5) or in case of piperidine excess (entry 6), beside the formation of compounds **108** and **110,** the presence of the 1,3,4-triaminated 2-AAQ (compound **114**, Figure 61), was observed.

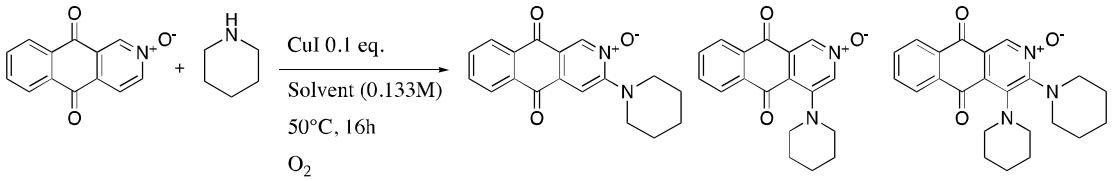

107 **108** **109** **110**

Entry	Solvent	Amine	Time	CuI	Additive	Yields of 108	Yields of 109	Yields of 110
1[a,b]	Toluene	8 eq.	16h	0.1 eq.	-	9%	-	2.9%
2[a]	DMSO	8 eq.	16h	0.1 eq.	-	15.7%	-	3.8%
3[c]	DMF	8 eq.	16 h	0.1 eq.	-	12.5%	-	33.6%
4	CH_3CN	8 eq.	16 h	0.1 eq.	-	9.5%	-	-
5[c,d]	Toluene	6 eq.	10 days	0.1 eq.	-	9.8%	-	5%
6[a,b,c]	Piperidine	Excess	16 h	0.1 eq.	-	-	-	4.4%
7	**Toluene**	**8 eq.**	**16 h**	**0.1 eq.**	**Cs_2CO_3 1 eq.**	**31.6%**	**-**	**60%**
8	Toluene	8 eq.	5 h	-	Cs_2CO_3 1 eq.	-	-	-
9	Toluene	2 eq.	16 h	-	Cs_2CO_3 1 eq.	-	-	-
10	Toluene	4 eq.	16 h	-	Cs_2CO_3 1 eq.	-	-	-
11	Toluene	8 eq.	72 h	-	Cs_2CO_3 1 eq.	5.2%	-	23%
12	Toluene	8 eq.	5 h	0.1 eq.	Cs_2CO_3 1 eq.	10.2%	13.6%	52.9%
13[e]	Toluene	1 eq.	4 h	0.1 eq.	Cs_2CO_3 1 eq.	8.5%	32%	26%

Table 3. Optimizing reaction parameters for the condensation of benz[*g*]isoquinoline-5,10-dione N-oxide with piperidine; [a] 3-monoaminated de-oxygenated side product; [b] 3,4-diaminated de-oxygenated side product; [c] 1,3,4-triaminated de-oxygenated side product; [d] 2-AAQ side product; [e] 2-AAQ N-oxide side product

This result suggested that also the substitution in position 1 could be obtained if harsh reaction condition (like a large excess of pyridine or the long reaction time) was set.

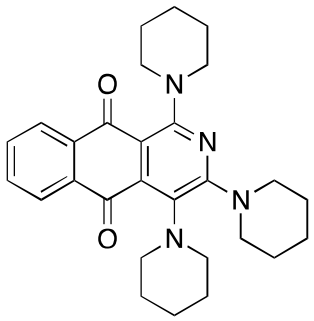

114

Figure 61. Structure of compound **114**

Trying to improve the yields, it was thought that the addition of a base, like caesium carbonate (Cs_2CO_3), could promote the removal of the proton in position 1, 3 or 4. The results obtained in entry 7 were surprising; adding Cs_2CO_3, the total yield increased to 92% (32% of **108** and 60% of **110**), without the presence of any side products. Considering the yields improvements by adding Cs_2CO_3, the effects of this additive were tested without CuI. Data reported in entries 8-11 show that Cs_2CO_3 alone did not produce any effect, unless it was let reacting for a longer time (entry 11). However, yields were not comparable with entry 7. With the scope of getting more insights about the mechanism of substitution, the reaction time and the amount of amine were evaluated in presence of CuI and Cs_2CO_3. Surprisingly, reducing the reaction time and/or working with stoichiometric amount of amine (entries 12 and 13), the 4-monosubstitute product **109** was obtained. The substitution in position 4 was confirmed by the analysis of mono and 2D NMR experiments (Figure 62). Two singlets at δ 8.48 and δ 8.18 in ^1H NMR were found, suggesting that these two protons should not be adjacent. HMBC experiment positioned the piperidine moiety on carbon 4 as a correlation between the protons at δ 3.18 with carbon at δ 150.36 was found; the couplings of H-1 (δ 8.48) with C-δ 181.5, C-δ 134.6, C-δ 132.9 and C-δ 118, and the couplings of H-3 (δ 8.18) with C-1 (δ 130), C-4 (δ 150.36) and the quaternary carbon at δ 118 confirmed the right placement of the piperidine moiety in position 4.

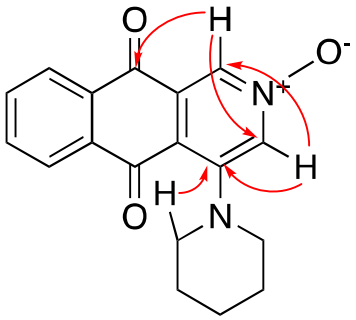

109

Figure 62. Principal HMBC correlation of compound **109**

Comparing the yields of compounds **109** and **110** with the reaction time in entries 7, 12 and 13, it was possible to get some insights about the mechanism of reaction of the different substitutions. Yields of compound **110** arise from 26% (entry 13) to 52% (entry 12) first, and finally to 60% (entry 7), whereas the amount of **109** decreases from 32% in entry 13 to 0% (entry 7); these results indicated that compound **109** was totally converted in compound **110** as long as the reaction proceeded. Regarding compound **108**, its presence could be justified by the attach of CuI to the position 3 of 2-AAQ N-oxide in parallel to the reaction in position 4. The substitution in position 4 could be explained considering the contribution of Mori-Quiroz *et al.* work;[132] in this paper, a direct coupling of primary and secondary amines with an alkylquinone was proposed for the synthesis of benzylic amines. The reaction mechanism hypothesized the alkylquinone tautomerization, with the formation of a methide intermediate that immediately reacted with the amine (Figure 63). The presence of a base (triethyl amine) was necessary for the formation of the methide intermediate.

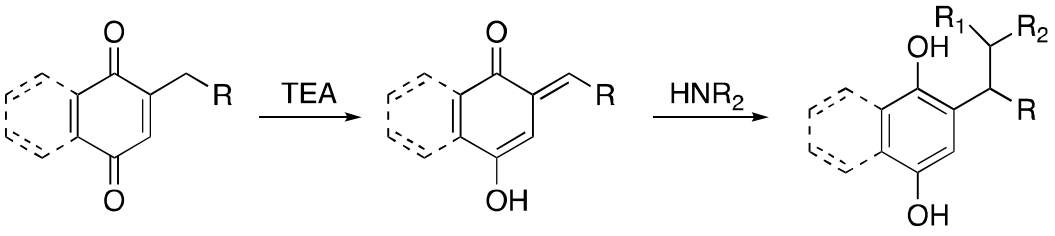

Figure 63. Amination by enolisation reported by Mori-Quiroz et al.

Treating benz[*g*]isoquinoline 5,10 dione N-oxide with CuI in presence of Cs_2CO_3, the tautomerization of the ketone in position 10 could enhance the dehydrogenative coupling in position 4. Interestingly, the use of Cs_2CO_3 alone

failed in the synthesis of mono and diaminated products (entries 8-10), indicating a pivotal role for the Cu^{+} in the mechanism of amination. On the other hand, without the addition of Cs_2CO_3, a small amount of compounds **108** and **110** was obtained, indicating that probably the counter ion $I^{(-)}$ could be involved in the dehydrogenative coupling in position 3 and 4, but with a lower efficiency compared to Cs_2CO_3.

Finally, the treatment of intermediate **108**, **109** and **110** with phosphorus threechloride (PCl_3) furnished their de-oxygenated analogues (compounds **111**, **112** and **113**, respectively) in quantitative yields (Scheme 19).

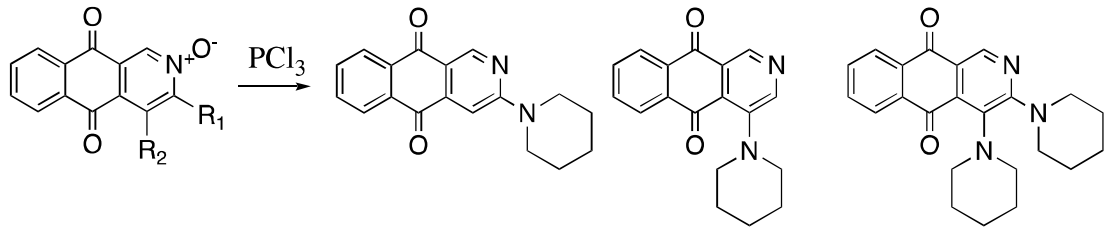

111 **112** **113**

Scheme 19. *Reagents and Conditions*. PCl_3 1.2 eq., DCM, r.t.

In conclusion, a new easy, cheap and versatile method for the direct functionalization of the 2-AAQ was developed. Although the reaction is not selective, the 3 and 4 monoaminated products (**108** and **109** respectively) could be obtained in decent yields, whereas the 3,4 diaminated product **110** could be synthetized in good chemical output. These reaction conditions could be applied for a screening of other secondary amines, and in other types of reaction like olefination, sulfonylation, alkylation, and acetoxylation, aiming at the synthesis of libraries of compounds that could be tested for their antiplasmodial and antitumoral activities.

CONCLUSIONS

During this Ph.D., my research activity was mainly focused on the synthesis of new potential lead compounds for the treatment of many factors composing the so-called metabolic syndrome. Among them, insulin resistance, visceral adiposity, atherogenic dyslipidaemia, endothelial dysfunction, genetic susceptibility, elevated blood pressure, and chronic stress play a critical role in metabolic syndrome. Although the clinical management of both short and long-term effects of metabolic syndrome yet exists, the necessity to find new pharmacological approaches to these syndromes lays in the side effects showed by the drugs used in the actual therapies. In this sense, the interaction between small molecules and metabolic nuclear and G-protein coupled receptors could represent a valid alternative. These receptors are involved in a number of metabolic physiological processes, and their activation or activity repression by a specific ligand accurately regulates the pathway in which receptor is involved in and, in many case, side effects are avoid.

Among nuclear and GPCR modulators, bile acids represent a very interesting class of molecules. Beside their role in lipid and vitamin absorption, in the last twenty years their ability to modulate the activity of both NR and GPCR, working as signalling molecules was shown. The main targets of BAs are FXR, LXRα (two NR) and GPBAR1 (a GPCR). These receptors are involved in the regulation of many physiological processes including BAs, lipid and glucose homeostasis, pointing out their modulation through BAs interaction as a new potential therapeutic approach in the treatment of some aspects composing the metabolic syndrome. As BAs are promiscuous molecules, interacting at the same time with more than one receptor, in this work, a deep speculation on BAs scaffold has performed in order to understand the structural features necessary for a specific modulation of one or more of the mentioned receptors.

The manipulation of UDCA side chain generated a first set of selective GPBAR1 agonists, with compound **23**, bis-*homo* UDCA, as the most active compound synthesized. Pharmacological evaluation on **23** showed that this compound could be a promising lead for the treatment of diabetes, as confirmed by the selective

increasing expression of proglucagon 1, a GPBAR1 target, in the small intestine, while it had no effect on FXR target genes in the liver. Furthermore, administration of compound **23** *in vivo* resulted in a significant reshaping of bile acid pool in a rodent model of cholestasis, thus demonstrating that compound **23** is a potential hit for the treatment of enterohepatic and metabolic disorders.

On the other hand, GPBAR1 is the physiological mediator of cholestatic itching, a very heavy side effect in patients affected by cholestasis. Considering that the elimination of the hydroxyl group at C-3 from CDCA resulted in a decrease of GPBAR1 activity, shifting the selectivity towards FXR, the activity of 5α and 5β-cholane derivatives was evaluated. Interestingly, the elimination of the hydroxyl group at C-3 from LCA resulted in the synthesis of the first class of dual FXR agonists/GPBAR1 antagonists. On the best of our knowledge, this result represents the first example of cholanoic acid derivatives able to antagonize GPBAR1, opening a new pharmacologic approach in the treatment of all the pathologies where GPBAR1 activation is associated with severe side effects.

As reported in literature, HDCA is an interesting molecule for its ability to weakly activate both LXRα and GPBAR1. Guided by the structural information on the binding site of the two mentioned targets, a rational lead optimization towards the synthesis of novel LXRα/GPBAR1 dual agonists was performed. These data suggested that the introduction of apolar side chains could be accepted in both receptors binding pockets. Consequently, a first set of HDCA apolar derivatives was synthesized. A second pattern of modification regarded the tetracyclic core of HDCA, where the influence of the elimination of the hydroxyl group at C-6 and the inversion in A/B rings junction on LXRα/GPBAR1 activation was evaluated. Among the library of HDCA derivatives obtained, compound **65** was the only LXRα/GPBAR1 dual agonist, as confirmed from pharmacologic evaluations. Interestingly, *in vivo* administration of **65** did not result in the expression of lipogenic enzymes, the most common side effect of LXRα agonists so far synthetized, probably for the contemporary activation of GPBAR1. These data point out on the double LXRα/GPBAR1 activation as a new potential therapeutic strategy for the treatment of metabolic disorders including diabetes, chronic inflammatory states and neurodegenerative diseases.

Beside the bile acids speculation, a more recent and small part of my Ph.D. research activity was focused on the synthesis of new SHP modulators as potential leads in the treatment of liver fibrosis. Modification of 3-(2,6-dichlorophenil)-5-isopropil isooxazole side chain afforded a small library of compounds, among which compound **92** showed the best activity. Deep pharmacologic analysis, both *in vitro* and *in vivo*, on compound **92** showed its potential application in the treatment of liver fibrosis.

Finally, the last part of my Ph.D. was spent in the laboratories of Organic Synthesis of the University of Antwerp, where my research activity was focused on the direct functionalization of the 2-AAQ through –CH catalytic activation. During that period, a new, cheap and easy method for the nucleophilic addition in position 3 and/or 4 of 2-AAQ was developed and optimized. These reaction conditions could be applied to a large number of nucleophiles, opening a new synthetic way to the functionalization of benz[*g*]isoquinoline without the use of halogen (for classic cross coupling reaction).

In conclusion, the results of this work underline that the interaction of small molecules and metabolic nuclear and G-protein coupled receptors could be a very promising strategy for the treatment of all the pathologies composing the metabolic syndrome. In this scenario, bile acids play a pivotal role, since their involvement in different metabolic physiologic processes. In this work, it was demonstrated that simple modifications to BAs scaffold could generate specific lead compounds for the treatment of one or more pathologies composing the metabolic disease.

EXPERIMENTAL SECTION

I. General procedures.

Chemistry

Specific rotations were measured on a Jasco P-2000 polarimeter. High-resolution ESI-MS spectra were performed with a Micromass Q-TOF mass spectrometer. NMR spectra were obtained on Varian Inova 400 and Varian Inova 500 NMR spectrometers (^{1}H at 400 MHz and 500 MHz, ^{13}C at 100MHz and 125 MHz) equipped with a Sun hardware and recorded in $CDCl_3$ (δ_H = 7.26 and δ_C = 77.0 ppm) and CD_3OD (δ_H = 3.30 and δ_C = 49.0 ppm). *J* are in hertz and chemical shifts (δ) are reported in ppm and referred to $CHCl_3$ and CHD_2OD as internal standards. HPLC was performed using a Waters Model 510 pump equipped with Waters Rheodine injector and a differential refractometer, model 401. Reaction progress was monitored via thin-layer chromatography (TLC) on Alugram® silica gel G/UV254 plates. Silica gel MN Kieselgel 60 (70-230 mesh) from Macherey-Nagel Company was used for column chromatography. All chemicals were obtained from Sigma-Aldrich, Inc. Solvents and reagents were used as supplied from commercial sources with the following exceptions. Tetrahydrofuran, dichloromethane, diisopropylamine and triethylamine were distilled from calcium hydride immediately prior to use. Methanol was dried from magnesium methoxide as follow. Magnesium turnings (5 g) and iodine (0.5 g) are refluxed in a small (50-100 mL) quantity of methanol until all of the magnesium has reacted. The mixture is diluted (up to 1 L) with reagent grade methanol, refluxed for 2-3 h then distilled under nitrogen. All reactions were carried out under argon atmosphere using flame-dried glassware.

The purity of all of the intermediates, checked by ^{1}H NMR, was greater than 95%.

II. Experimental section Ursodeoxycholic acid derivatives.

3α, 7β-diformyloxy-5β-cholan-24-oic acid (4). A solution of ursodeoxycholic acid **3** (550 mg, 1.3 mmol) in 10 mL of 90% formic acid containing 25 μL of 70% perchloric acid was stirred at 47-50 °C for 12 h. The temperature of the heating bath was lowered to 40 °C, then 5 mL of acetic anhydride was added over 10 min and the mixture was stirred for 10 min more. The solution was cooled to room temperature, poured into 50 mL of water and extracted with diethyl ether. The organic layers were washed with water to neutrality, dried over Na_2SO_4, and evaporated to give 570 mg of **4** (96%). An analytic sample was obtained by silica gel chromatography eluting with CH_2Cl_2:MeOH 9:1. Selected ^{1}H NMR (400 MHz CD_3OD): δ 8.03 (1H, s), 7.98 (1H, s), 4.89 (1H, m), 4.80 (1H, m), 0.98 (3H, s), 0.93 (3H, d, *J* = 6.5 Hz), 0.69 (3H, s); ^{13}C NMR (100 MHz CD_3OD): δ 178.1, 163.0, 162.5, 74.9, 74.8, 56.6, 56.4, 44.8, 43.5, 41.3, 41.2, 40.7, 36.6, 35.4 (2C), 35.1, 34.1, 34.0, 32.3, 32.0, 29.5, 27.6, 23.6, 22.3, 18.9, 12.5; HRMS-ESI *m/z* 449.2907 $[M+H]^+$, $C_{26}H_{41}O_6$ requires 449.2903.

3α, 7β-diformyloxy-24-*nor*-5β-cholan-23-nitrile (5). Crude **4** (500 mg, 1.1 mmol), 1.7 mL of cold trifluoroacetic acid, and 466 μL (3.3 mmol) of trifluoroacetic anhydride were stirred at 0-5 °C until dissolution. Sodium nitrite (83 mg, 1.2 mmol) was added in small portions. After the addition was complete, the reaction mixture was stirred first at 0-5 °C for 1 h, then at 38-40 °C for 8 h. On completion, the reaction was neutralized with NaOH 2 N, then the product was extracted with 50 mL of diethyl ether (3x50 mL), followed by washing with brine and dried over anhydrous Na_2SO_4. The ether was removed under reduced pressure to afford 440 mg of **5** (96%), that was subjected to next step without any purification. An analytic sample was obtained by silica gel chromatography eluting with *n*-hexane: ethyl acetate 8:2. Selected ^{1}H NMR (400 MHz CD_3OD): δ 8.04 (1H, s), 7.99 (1H, s), 4.87 (1H, m), 4.73 (1H, m), 1.12 (3H, d, *J* = 6.5 Hz), 0.98 (3H, s), 0.71 (3H, s); ^{13}C NMR (100 MHz CD_3OD): δ 163.1, 162.6, 120.3, 74.8 (2C), 56.4, 55.5, 44.8, 43.2, 41.2, 40.9,

40.6, 35.4, 35.1, 34.6, 34.1, 34.0, 30.9, 29.3, 27.6, 25.1, 23.6, 22.3, 19.8, 12.5; HRMS-ESI *m/z* 416.2807 $[M+H]^+$, $C_{25}H_{38}NO_4$ requires 416.2801.

24-*nor*-ursodeoxycholic acid (6). Crude compound **5** (400 mg, 1.0 mmol) was refluxed in *ca*. 50 mL of methanol-water 1:l with 30% KOH. After stirring for 48 h, the basic aqueous solution was neutralized with HCl 6 N. Then methanol was evaporated and the residue was extracted with AcOEt (3x50mL). The combined organic layers were washed with brine, dried and evaporated to dryness to give white solid residue, that was purified by silica gel chromatography, eluting with CH_2Cl_2:MeOH 9:1 (355 mg, 97%). $[\alpha]_{25}^{D}$=+11.0 (*c* 0.41, CH_3OH); selected ^1H NMR (400 MHz CD_3OD): δ 3.44 (2H, m), 0.98 (3H, d, *J* = 6.5 Hz), 0.93 (3H, s), 0.71 (3H, s). ^{13}C NMR (100 MHz CD_3OD): δ 177.3, 72.1, 71.9, 57.5, 56.6, 44.8, 44.5, 44.0, 42.5, 41.4, 40.7, 38.6, 38.0, 36.1, 35.2, 34.9, 31.0, 29.7, 27.9, 23.9, 22.4, 20.2, 12.7; HRMS-ESI *m/z* 379.2844 $[M+H]^+$, $C_{23}H_{39}O_4$ requires 379.2848.

3α, 7β-dihydroxy-24-*nor*-5β-cholan-23- oyl taurine sodium salt (**7**). Carboxylic acid **6** (20 mg, 0.1 mmol) in DMF dry (2 mL) was treated with DMT-MM (41 mg, 0.2 mmol) and triethylamine (174 μL, 1.3 mmol) and the mixture was stirred at room temperature for 10 min. Then to the mixture was added taurine (37 mg, 0.3 mmol). After 1h, the reaction mixture was concentrated under vacuo and dissolved in water (5 mL). The solution was poured over a C18 silica gel column. Fraction eluted with H_2O/MeOH 99:1 gave a mixture that was further purified by HPLC on a Nucleodur 100-5 C18 (5 μm; 4.6 mm i.d. x 250 mm) with MeOH/H_2O (60:40) as eluent (flow rate 1 mL/min), to give 7 mg (28%) of compound **7** (t_R=12.4 min); $[\alpha]_{25}^{D}$=-4.8 (*c* 0.15, CH_3OH); selected ^1H NMR (400 MHz CD_3OD): δ 3.58 (2H, t, *J* = 6.6 Hz), 3.48 (2H, m), 2.95 (2H, t, *J* = 6.6 Hz), 0.97 (3H, d, ovl), 0.96 (3H, s), 0.71 (3H, s); HR ESIMS *m/z* 484.2735 $[M-Na]^-$, $C_{25}H_{42}NO_6S$ requires 484.2732.

Methyl 3α,7β-dihydroxy-24-*nor*-5β-cholan-23-oate (8). The compound **6** (100 mg, 0.3 mmol) was dissolved in 30 mL of dry methanol and treated with *p*-toluenesulfonic acid (251 mg, 1.3 mmol). The solution was left to stand at room temperature for 5h. The mixture was quenched by addition until the neutrality of $NaHCO_3$ saturated solution. Most of the solvent was evaporated,

and the residue was extracted with EtOAc. The combined extract was washed with brine, dried with Na_2SO_4, and evaporated to give **8** as amorphous solid (100 mg, 97% yield). An analytic sample was obtained by silica gel chromatography eluting with CH_2Cl_2:MeOH 95:5. $[\alpha]_{25}^{D}$=+19.8 (*c* 0.22, $CHCl_3$); selected ^{1}H NMR (400 MHz $CDCl_3$): δ 3.60 (3H, s), 3.51 (2H, m), 0.92 (3H, d, *J* = 6.3 Hz), 0.88 (3H, s), 0.65 (3H, s). ^{13}C NMR (100 MHz $CDCl_3$): δ 173.8, 71.0, 70.9, 55.7, 54.9, 51.3, 43.6, 43.4, 42.4, 41.3, 39.9, 39.1, 37.1, 37.0, 34.8, 33.9, 33.6, 30.0, 28.6, 26.7, 23.3, 21.0, 19.5, 12.0; HRMS-ESI *m/z* 393.3009 $[M+H]^+$, $C_{24}H_{41}O_4$ requires 393.3005.

24-*nor*-5β-cholan-3α, 7β, 23- triol (9). To a solution of **8** (90 mg, 0.2 mmol) in dry THF (5 mL) at 0 °C under argon were added $LiBH_4$ (0.8 mL, 2 M in THF, 1.6 mmol) and dry methanol (65 µl, 1.6 mmol) and the resulting mixture was stirred for 3 h at 0 °C. The mixture was quenched by addition of NaOH (1 M, 1.4 mL) and then allowed to warm to room temperature. Ethyl acetate was added and the separated aqueous phase was extracted with ethyl acetate (3×30 mL). The combined organic phases were washed with water, dried (Na_2SO_4) and concentrated. Purification by silica gel (CH_2Cl_2:MeOH 97:3) gave compound **9** as a colorless oil (85 mg, quantitative yield). $[\alpha]_{25}^{D}$=+23.7 (*c* 0.18, CH_3OH); ^{1}H NMR (400 MHz CD_3OD): δ 3.60 (1H, m ovl), 3.51 (1H, m), 3.50 (2H, m), 0.97 (3H, d, ovl), 0.96 (3H, s), 0.72 (3H, s). ^{13}C NMR (100 MHz CD_3OD): δ 72.1, 71.9, 60.8, 57.5, 57.1, 44.8, 44.5, 44.0, 41.6, 40.7, 39.9, 38.6, 38.0, 36.1, 35.2, 34.1, 31.0, 29.8, 27.9, 23.9, 22.4, 19.5, 12.6; HRMS-ESI *m/z* 365.3053 $[M+H]^+$, $C_{23}H_{41}O_3$ requires 365.3056.

3α, 7β- dihydroxy-24-*nor*-5β-cholan-23-yl- 23-sodium sulfate (10), 7β,23-dihydroxy-24-*nor*-5β-cholan-3α-yl-3-sodium sulfate (11), 3α,23-dihydroxy-24-*nor*-5β-cholan-7β-yl-7-sodium sulphate (12), 7β-hydroxy-24-*nor*-5β-cholan-3α, 23-diyl- 3, 23-sodium disulfate (13), 3α-hydroxy-24-*nor*-5β-cholan-7β, 23-diyl- 7, 23-sodium disulfate (14) and 24-*nor*-5β-cholan-3α, 7β, 23-tryl-3, 7, 23-sodium trisulfate (15). The triethylamine-sulfur trioxide complex (253 mg, 1.4 mmol) was added to a solution of compound **9** (50 mg, 0.1 mmol) in DMF dry (5 mL) under an argon atmosphere, and the mixture was stirred at 95 °C for 24 h. The solution was then concentrated

under vacuum. To the solid dissolved in methanol (15 mL) was added three drops of HCl 37% v/v and the mixture was stirred for 3h at room temperature. At the end of reaction, silver carbonate was added to precipitate chloride. Then the reaction mixture was centrifuged and the supernatant was concentrated *in vacuo*. The residue was poured over a RP18 column. Fraction eluted with H_2O/MeOH 99:1 gave a mixture that was further purified by HPLC on a Nucleodur 100-5 C18 (5 µm; 4.6 mm i.d. x 250 mm) with MeOH/H_2O (35:65) as eluent (flow rate 1 mL/min), to give 3.7 mg (4%) of compound **15** (t_R = 5 min); fraction eluted with H_2O/MeOH 95:5 and with H_2O/MeOH 9:1 gave a mixture that was purified as previously to afford respectively 8.7 mg (11 %) of compound **13** (t_R = 15 min) and 7 mg (9%) of compound **14** (t_R = 14 min). Fraction eluted with H_2O/MeOH 75:25 gave a mixture that was further purified by HPLC on a Nucleodur 100-5 C18 (5 µm; 4.6 mm i.d. x 250 mm) with MeOH/H_2O (65:35) as eluent (flow rate 1 mL/min), to give 15 mg (23 %) of compound **12** (t_R = 7 min). Fraction eluted with H_2O/MeOH 7:3 gave a mixture that was further purified as previously to give 5 mg (8%) of compound **10** (t_R = 8.4 min) and 4 mg (6 %) of compound **11** (t_R = 6.4 min).

3α, 7β- dihydroxy-24-*nor*-5β-cholan-23-yl- 23-sodium sulfate (10): $[\alpha]_{25}^{D}$=+35.8 (*c* 0.69, CH_3OH); ^{1}H NMR (400 MHz CD_3OD): δ 4.04 (2H, m), 3.48 (2H, m), 1.00 (3H, d, *J* = 6.5 Hz), 0.97 (3H, s), 0.72 (3H, s). HR ESIMS *m/z* 443.2469 $[M\text{-}Na]^-$, $C_{23}H_{39}O_6S$ requires 443.2467. **7β,23- dihydroxy-24-*nor*-5β-cholan-3α-yl-3-sodium sulfate (11)**: $[\alpha]_{25}^{D}$=+11.4 (*c* 0.04, CH_3OH); ^{1}H NMR (400 MHz CD_3OD): δ 4.23 (1H, m), 3.48 (3H, m), 0.98 (3H, d, *J* = 6.4 Hz), 0.97 (3H, s), 0.72 (3H, s). HR ESIMS *m/z* 443.2462 $[M\text{-}Na]^-$, $C_{23}H_{39}O_6S$ requires 443.2467.

3α,23- dihydroxy-24-*nor*-5β-cholan-7β-yl-7-sodium sulfate (12): $[\alpha]_{25}^{D}$=+7.8 (*c* 0.19, CH_3OH); ^{1}H NMR (400 MHz CD_3OD): δ 4.29 (1H, m), 3.61 (1H, m), 3.51 (2H, m), 0.97 (3H, s), 0.96 (3H, d, ovl), 0.70 (3H, s). HR ESIMS *m/z* 443.2465 $[M\text{-}Na]^-$, $C_{23}H_{39}O_6S$ requires 443.2467.

7β-hydroxy-24-*nor*-5β-cholan-3α, 23-diyl- 3, 23-sodium disulfate (13): $[\alpha]_{25}^{D}$=+0.3 (*c* 0.23, CH_3OH); ^{1}H NMR (400 MHz CD_3OD): δ 4.23 (1H, m),

4.04 (2H, m), 3.48 (1H, m), 1.00 (3H, d, J = 6.6 Hz), 0.97 (3H, s), 0.72 (3H, s). HR ESIMS *m/z* 545.1859 $[M-Na]^-$, $C_{23}H_{38}NaO_9S_2$ requires 545.1855.

3α-hydroxy-24-*nor*-5β-cholan-7β, 23-diyl- 7, 23-sodium disulfate (14): $[\alpha]_{25}^{D}$=+0.5 (*c* 0.15, CH_3OH); ^1H NMR (400 MHz CD_3OD): δ 4.29 (1H, m), 4.05 (2H, m), 3.50 (1H, m), 0.99 (3H, d, J = 6.5 Hz), 0.97 (3H, s), 0.71 (3H, s). HR ESIMS *m/z* 545.1857 $[M-Na]^-$, $C_{23}H_{38}NaO_9S_2$ requires 545.1855.

24-*nor*-5β-cholan-3α, 7β, 23-tryl-3, 7, 23-sodium trisulfate (15): $[\alpha]_{25}^{D}$=+13.3 (*c* 0.03, CH_3OH); ^1H NMR (400 MHz CD_3OD): δ 4.31 (1H, m), 4.23 (1H, m), 4.04 (2H, m), 1.00 (3H, d, J = 6.4 Hz), 0.98 (3H, s), 0.71 (3H, s). HR ESIMS *m/z* 647.1247 [M-Na], $C_{23}H_{37}Na_2O_{12}S_3$ requires 647.1243.

5β-cholan-3α, 7β, 24-triol (16). At a solution of methyl 3α, 7β-dihydroxy-5β-cholan-24-oate (50 mg, 0.1 mmol) in THF dry (10 mL) were added at 0 °C dry methanol (51 µl, 1.3 mmol) and $LiBH_4$ (300 µL, 2M in THF, 1.3 mmol). After 1h, the mixture was quenched by addition of NaOH (1 M, 240 µL) and then allowed to warm to room temperature. Ethyl acetate was added and the separated aqueous phase was extracted with ethyl acetate (3×30 mL). The combined organic phases were washed with water, dried (Na_2SO_4) and concentrated. Purification by silica gel (CH_2Cl_2/MeOH 9:1) gave compound **16** as colourless oil (42 mg, 93%). $[\alpha]_{25}^{D}$=+54.7 (*c* 0.36, $CHCl_3$); selected ^1H NMR (400 MHz CD_3OD): δ 3.51 (4H, m), 0.97 (3H, d, ovl), 0.97 (3H, s), 0.72 (3H, s). ^{13}C NMR (100 MHz CD_3OD): δ 72.1, 71.9, 63.6, 57.6, 56.8, 44.8, 44.5, 44.0, 41.6, 40.7, 38.6, 38.0, 37.0, 36.1, 35.2, 33.3, 31.0, 30.3, 29.7, 27.9, 23.9, 22.4, 19.4, 12.6; HRMS-ESI *m/z* 379.3215 $[M+H]^+$, $C_{24}H_{43}O_3$ requires 379.3212.

3α, 7β-di(*tert*-butyldimethylsilyloxy)-5β-cholan-24-ol (18). 2,6-lutidine (2.8 mL, 20 mmol) and *tert*-butyldimethylsilyltrifluoromethanesulfonate (1.7 mL, 6 mmol) were added at 0 °C to a solution of methyl 3α, 7β-dihydroxy-5β-cholan-24-oate (800 mg, 2 mmol) in 30 mL of CH_2Cl_2. After 2 h stirring at 0 °C, the reaction was quenched by addition of aqueous $NaHSO_4$ (1M, 100 mL). The layers were separated and the aqueous phase was extracted with CH_2Cl_2 (3×100 mL). The combined organic layers were washed with $NaHSO_4$, water, saturated aqueous $NaHCO_3$, and brine and evaporated *in vacuo* to give 1.3 g of methyl 3α,

7β-di(*tert*-butyldimethylsilyloxy)-5β-cholan-24-oate in the form of colourless needles, that was subjected to next step without any purification. To a solution of methyl ester (1 g, 1.6 mmol) in dry THF (30 mL), at 0 °C dry methanol (453 μL, 11.2 mmol) and $LiBH_4$ (5.6 mL, 2M in THF, 11.2 mmol) was added. The resulting mixture was stirred for 2 h at 0 °C. The mixture was quenched by addition of 1M NaOH (3.2 mL) and then ethyl acetate. The organic phase was washed with water, dried (Na_2SO_4) and concentrated. Purification by silica gel (hexane/ethyl acetate 99:1 and 0.5% TEA) gave 3α, 7β-di(*tert*-butyldimethylsilyloxy)-5β-cholan-24-ol (**18**) as a white solid (1.2 g, quantitative yield over two steps).

Methyl 3α, 7β-di(tert-butyldimethylsilyloxy)-25, 26-bis-*homo*-5β-chol-24-en-26-oate (19). DMSO (2 mL, 28 mmol) was added dropwise for 15 min to a solution of oxalyl chloride (7 mL, 14 mmol) in dry dichloromethane (50 mL) at -78 °C under argon atmosphere. After 30 min a solution of alchol **23** (1.2 g, 2 mmol) in dry CH_2Cl_2 was added via cannula and the mixture was stirred at -78 °C for 30 min. Et_3N (2.8 mL, 20 mmol) was added dropwise. After 1 h, methyl(triphenylphosphoranylidene)acetate (2.1 g, 3 mmol) was added and the mixture was allowed to warm to room temperature. NaCl saturated solution was added and the aqueous phase was extracted with diethyl ether (3×100 mL). The combined organic phases were washed with water, dried (Na_2SO_4) and concentrated. Purification by silica gel (hexane-ethyl acetate 95:5 and 0.5% TEA) gave compound **19** as a colourless oil (1 g, 76%); $[\alpha]_{25}^{D}$=+45.0 (*c* 0.70, CH_3OH); ^{1}H NMR (400 MHz $CDCl_3$): δ 6.94 (1H, dt, *J* = 7.3, 15.5 Hz), 5.78 (1H, d, *J* = 15.5 Hz), 3.66 (3H, s), 3.64 (1H, m), 3.50 (1H, br s), 0.92 (3H, d, *J* = 6.5 Hz), 0.90 (3H, s), 0.86 (18H, s), 0.62 (3H, s), 0.04 (6H, s), 0.03 (6H, s). ^{13}C NMR (100 MHz $CDCl_3$): δ 167.0, 150.0, 120.9, 72.7, 72.5, 55.5, 54.9, 51.3, 43.9, 43.7, 42.8, 39.9, 38.8, 37.9, 37.8, 35.3 (2C), 35.1, 34.3, 34.1, 30.9 (2C), 30.8, 28.9, 27.3, 26.4 (3C), 25.9 (3C), 23.5, 21.2, 18.6, 12.1, -2.8, -3.4, -4.6 (2C); HRMS-ESI *m/z* 661.5050 $[M+H]^+$, $C_{39}H_{73}O_4Si_2$ requires 661.5047.

Methyl 3α, 7β-dihydroxy-25, 26-bis-*homo*-5β-cholan-26-oate (23). A solution of compound **24** (500 mg, 0.76 mmol) in THF dry/EtOH dry (5 mL/5 mL, v/v) was hydrogenated in presence of $Pd(OH)_2$ 5% wt on activated carbon Degussa type (5 mg). The flask was evacuated and flushed first with argon and then with

hydrogen. After 12 h, the reaction was complete. The catalyst was filtered through celite, and the recovered filtrate was concentrated under vacuum to give the methyl ester, which was dissolved in methanol (40 mL). At the solution was added 1 mL of HCl 37% v/v. After 1h, silver carbonate was added at the solution to precipitate chloride. Then the reaction mixture was centrifuged and the supernatant was concentrated *in vacuo* to give compound **23** as colourless amorphous solids (330 mg, quantitative yield). An analytic sample was purified by HPLC on a Nucleodur 100-5 C18 (5 μm; 4.6 mm i.d. x 250 mm) with MeOH/H_2O (92:8) as eluent (flow rate 1 mL/min), to give compound **23** (t_R=13 min). $[\alpha]_{25}^{D}$=+41.8 (*c* 0.15, CH_3OH); selected ^1H NMR (400 MHz $CDCl_3$): δ 3.67 (3H, s), 3.59 (2H, m), 2.30 (2H, dt, *J* = 2.5, 7.5 Hz), 0.95 (3H, s), 0.91 (3H, d, *J* = 6.5 Hz), 0.67 (3H, s). ^{13}C NMR (100 MHz $CDCl_3$): 167.1, 71.3 (2C), 55.7, 55.1, 51.4, 43.8, 43.7, 42.4, 40.1, 39.2, 37.3, 36.8, 35.5 (2C), 34.9, 34.2, 34.1, 30.4, 28.7, 26.9, 25.7, 25.4, 23.4, 21.2, 18.7, 12.1. HRMS-ESI *m/z* 435.3479 $[M+H]^+$, $C_{27}H_{47}O_4$ requires 435.3474.

3α, 7β-dihydroxy-25, 26-bis-*homo*-5β-cholan-26-oic acid (24). A portion of compound **23** (200 mg, 0.46 mmol) was hydrolyzed with NaOH (184 mg, 4.6 mmol) in a solution of MeOH: H_2O 1:1 v/v (20 mL). The mixture was stirred for 4 h at reflux. The resulting solution was then acidified with HCl 6N and extracted with ethyl acetate (3 x 50 mL). The collected organic phases were washed with brine, dried over Na_2SO_4 anhydrous and evaporated under reduced pressure to give compound **24** (115 mg, 60%). An analytic sample was purified by HPLC on a Nucleodur 100-5 C18 (5 μm; 4.6 mm i.d. x 250 mm) with MeOH/H_2O (95:5) as eluent (flow rate 1 mL/min), to give compound **24** (t_R = 5 min). $[\alpha]_{25}^{D}$=-9.0 (*c* 0.04, CH_3OH); selected ^1H NMR (500 MHz CD_3OD): δ 3.47 (2H, m), 2.27 (2H, dt, *J* = 3.4, 7.4 Hz), 0.96 (3H, s), 0.94 (3H, d, *J* = 6.5 Hz), 0.70 (3H, s). ^{13}C NMR (125 MHz CD_3OD): δ 178.2, 72.1, 71.9, 57.6, 56.7, 44.8, 44.5, 44.0, 41.6, 40.7, 38.6, 38.0, 36.9, 36.8, 36.1, 35.3, 35.2, 30.9, 29.8, 27.9, 26.7, 26.6, 23.9, 22.4, 19.3, 12.7; HRMS-ESI *m/z* 421.3315 $[M+H]^+$, $C_{26}H_{45}O_4$ requires 421.3318.

3α, 7β-dihydroxy-25, 26-bis-*homo*-5β-cholan -26-oyl taurine sodium salt (25). Carboxylic acid **24** (20 mg, 0.1 mmol) in DMF dry (5 mL) was treated with DMT-MM (39 mg, 0.1 mmol) and triethylamine (164 μL, 1.2 mmol) and the mixture

was stirred at room temperature for 10 min. Then to the mixture was added taurine (35 mg, 0.3 mmol). After 3h, the reaction mixture was concentrated under vacuo and dissolved in water (5 mL). The solution was poured over a C18 silica gel column. Fraction eluted with H_2O/MeOH 95:5 gave a mixture that was further purified by HPLC on a Nucleodur 100-5 C18 (5 μm; 4.6 mm i.d. x 250 mm) with MeOH/H_2O (45:55) as eluent (flow rate 1 mL/min), to give 12 mg (45%) of compound **25** (t_R=12.4 min); $[\alpha]_{25}^{D}$=+108.3 (*c* 0.06, CH_3OH); selected ^{1}H NMR (400 MHz CD_3OD): δ 3.59 (2H, t, *J* = 6.5 Hz), 3.47 (2H, m), 2.96 (3H, t, *J* = 6.5 Hz), 2.18 (2H, t, *J* = 7.4 Hz), 0.96 (3H, s), 0.94 (3H, d, *J* = 6.2 Hz), 0.71 (3H, s). HRMS-ESI *m/z* 526.3200 $[M-Na]^-$, $C_{28}H_{48}NO_6S$ requires 526.3202.

25, 26-bis-*homo*-5β-cholan-3α, 7β, 26-triol (26). To a solution of compound **23** (50 mg, 0.11 mmol) in THF dry (10 mL) were added at 0 °C dry methanol (31 μl, 0.8 mmol) and $LiBH_4$ (382 μL, 2 M in THF, 0.8 mmol). After 1h, the mixture was quenched by addition of NaOH (1M, 220 μL) and then allowed to warm to room temperature. Ethyl acetate was added and the separated aqueous phase was extracted with ethyl acetate (3×30 mL). The combined organic phases were washed with water, dried (Na_2SO_4) and concentrated. Purification by silica gel (CH_2Cl_2/MeOH 9:1) gave compound **26** as a colourless oil (35 mg, 77%); $[\alpha]_{25}^{D}$=+41.8 (*c* 0.21, CH_3OH); selected ^{1}H NMR (400 MHz CD_3OD): δ 3.53 (2H, t, *J* = 6.5 Hz), 3.48 (2H, m), 0.95 (3H, s), 0.94 (3H, d, ovl), 0.70 (3H, s). ^{13}C NMR (100 MHz CD_3OD): δ 72.1, 71.9, 63.0, 57.5, 56.7, 44.7, 44.4, 44.0, 41.6, 40.7, 38.5, 37.9, 37.2, 37.0, 36.1, 35.2, 33.7, 30.9, 29.8, 27.9, 27.4, 27.1, 23.9, 22.4, 19.4, 12.7; HRMS-ESI *m/z* 407.3520 $[M+H]^+$, $C_{26}H_{47}O_3$ requires 407.3525.

Methyl 3α, 7β-dihydroxy-25, 26-bis-*homo*-5β-chol-24-en-26-oate (20). To compound **19** (180 mg, 0.3 mmol), dissolved in methanol (30 mL), 1 mL of HCl 37% v/v was added and the mixture was stirred for 2 h at room temperature. At the end of reaction, silver carbonate was added to precipitate chloride. Then the reaction mixture was centrifuged and the supernatant was concentrated *in vacuo* to give 120 mg (quantitative yield) of the desired compound **20** as colourless amorphous solids. An analytic sample was purified by HPLC on a Nucleodur 100-5 C18 (5 μm; 4.6 mm i.d. x 250 mm) with MeOH/H_2O (92:8) as eluent (flow rate 1 mL/min), to give compound **20** (t_R=14 min). $[\alpha]_{25}^{D}$=+45.0 (*c* 0.70, CH_3OH); ^{1}H

NMR (400 MHz $CDCl_3$): δ 6.93 (1H, dt, *J* = 6.6, 15.7 Hz), 5.79 (1H, d, *J* = 15.7 Hz), 3.64 (3H, s), 3.58 (2H, m), 0.92 (3H, s), 0.91 (3H, d, *J* = 6.4 Hz), 0.65 (3H, s). ^{13}C NMR (100 MHz $CDCl_3$): δ 167.2, 150.1, 120.4, 71.1, 71.0, 55.9, 55.1, 51.4, 43.7, 43.6, 42.5, 40.2, 39.3, 37.3, 37.1, 35.4, 34.9, 34.3, 34.0, 30.2, 29.0, 28.7, 26.9, 23.4, 21.2, 18.5, 12.2; HRMS-ESI *m/z* 433.3323 $[M+H]^+$, $C_{27}H_{45}O_4$ requires 433.3318.

3α, 7β-dihydroxy-25, 26-bis-*homo*-5β-chol-24-en-26-oic acid (21). A portion of compound **20** (100 mg, 0.23 mmol) was hydrolyzed with NaOH (93 mg, 2.3 mmol) in a solution of MeOH: H_2O 1:1 v/v (20 mL). The mixture was stirred for 1h at reflux. The resulting solution was then acidified with HCl 6N and extracted with ethyl acetate (3 x 50 mL). The collected organic phases were washed with brine, dried over Na_2SO_4 anhydrous and evaporated under reduced pressure to give compound **21** (89 mg, 93% yield). An analytic sample was purified by HPLC on a Nucleodur 100-5 C18 (5 μm; 4.6 mm i.d. x 250 mm) with MeOH/H_2O (95:5) as eluent (flow rate 1 mL/min), to give compound **21** (t_R=5 min). $[\alpha]_{25}^{D}$= +203.0 (*c* 0.39, CH_3OH); selected ^1H NMR (400 MHz $CDCl_3$): δ 7.07 (1H, dt, *J* = 7.0, 15.0 Hz), 5.81 (1H, d, *J* = 15.0 Hz), 3.60 (2H, m), 0.94 (3H, s), 0.94 (3H, d, ovl), 0.67 (3H, s). ^{13}C NMR (100MHz CD_3OD): δ 170.7, 151.6, 122.7, 72.1, 71.9, 57.5, 56.6, 44.8, 44.5, 44.0, 41.6, 40.7, 38.6, 38.0, 36.8, 36.1, 35.6, 35.2, 31.0, 29.9, 29.7, 27.9, 23.9, 22.4, 19.1, 12.7. HRMS-ESI *m/z* 419.3163 $[M+H]^+$, $C_{26}H_{43}O_4$ requires 419.3161.

3α, 7β-dihydroxy-25, 26-bis-*homo*-5β-chol-24-en-26-oyl taurine sodium salt (22). Carboxylic acid **21** (10 mg, 0.024 mmol) in DMF dry (2 mL) was treated with DMT-MM (20 mg, 0.1 mmol) and triethylamine (87 μL, 0.6 mmol) and the mixture was stirred at room temperature for 10 min. Then to the mixture was added taurine (18 mg, 0.1 mmol). After 2 h, the reaction mixture was concentrated under vacuo and dissolved in water (5 mL). The solution was poured over a C18 silica gel column. Fraction eluted with H_2O/MeOH 95:5 gave a mixture that was further purified by HPLC on a Nucleodur 100-5 C18 (5 μm; 4.6 mm i.d. x 250 mm) with MeOH/H_2O (45:55) as eluent (flow rate 1 mL/min), to give 3.5 mg (26%) of compound **22** (t_R=15.8 min); $[\alpha]_{25}^{D}$=+52.1 (*c* 0.08, CH_3OH); selected ^1H NMR (400 MHz CD_3OD): δ 6.73 (1H, dt, *J* = 6.5, 14.0 Hz), 5.89 (1H, d, *J* = 14.0

Hz), 3.65 (2H, t, *J* = 7.0 Hz), 3.47 (2H, m), 2.98 (2H, t, *J* = 7.0 Hz), 0.97 (3H, d, ovl), 0.96 (3H, s), 0.71 (3H, s). HRMS-ESI *m/z* 524.3043 $[M-Na]^-$, $C_{28}H_{46}NO_6S$ requires 524.3046.

Animal studies. All studies were approved by the Animal Study Committee of the University of Perugia (Italy). Mice were maintained in a temperature controlled facility with a 12-hour light/dark cycle and were given free access to food and water. C57BL/6j mice were obtained from Charles River Breeding Laboratories (Monza-Italy). Mice (*n* = 5,6) were orally administered for seven days with 30 mg/kg dose of α-naphthylisothiocyanate (ANIT) in methylcellulose 1%, a chemical agent that cause a specific damage to biliary epithelial cells leading to bile duct injury and cell proliferation ultimately causing intrahepatic cholestasis. Animals were administered with C2 or C16 at the dose of 15 mg/kg. At the end of the experiment serum and liver samples were collected. During the experiment mice were daily weight.

In another experimental section C57BL/6j mice were treated 6 hours with C2 (60 mg/Kg, IP) or with C16 (64 mg/Kg, IP). At the end of the treatments mice were sacrificed and liver samples were collected to perform Real-Time PCR analysis.

Transactivation assay. For FXR mediated transactivation, HepG2 cells were plated in a 24 well-plate and transfected with 100 ng of pSG5-FXR, 100 ng of pSG5-RXR, 200 ng of the reporter vector p(hsp27)-TK-LUC containing the FXR response element IR1 cloned from the promoter of heat shock protein 27 (hsp27) and with 100 ng of pGL4.70 (Promega), a vector encoding the human Renilla gene. For GP-BAR1 mediated transactivation, HEK-293T cells were plated in a 24 well-plate and transfected with 200 ng of pGL4.29 (Promega), a reporter vector containing a cAMP response element (CRE) that drives the transcription of the luciferase reporter gene luc2P, with 100 ng of pCMVSPORT6-human GP-BAR1, and with 100 ng of pGL4.70. At 24 h post-transfection, cells were stimulated 18 h with 10 μM CDCA, TLCA and synthetized compounds. After treatments, cells were lysed in 100 μL of lysis buffer (25 mM Tris-phosphate, pH 7.8; 2 mM DTT; 10% glycerol; 1% Triton X-100), and 20 μL of cellular lysate was assayed for luciferase activity using the luciferase assay system (Promega). Luminescence was measured using Glomax 20/20 luminometer (Promega).

Real-Time PCR. Real-Time PCR was performed as previously described. Forward and reverse primer sequences were the following:

mouse GAPDH, ctgagtatgtcgtggagtctac and gttggtggtgcaggatgcattg;

mOSTα, cagtggacatagccctcacc and gaccaaagcagcagaacaca;

mBSEP, aaatcggatggtttgactgc and tgacagcgagaatcaccaag;

mPro-glucagon, tgaagacaaacgccactcac and caatgttgttccggttcctc.

Bile acids determination. Stock solutions of bile acids (tMu, tCA, tDCA, tCDCA, tHCA) were prepared separately in methanol at the concentration of 10 mmol/L, and stored at −20 °C. The appropriate amounts of each bile acid stock solution was added into pooled samples ranging a five-points calibration curve from 5 nM to 50 μM.

Aliquots of 100 μL of each cell lysate were deproteinized with 1 mL of cold acetonitrile with 5% of NH_4OH vortexing for 1 min. After centrifugation at 16000 g for 10 min, the clear supernatant was transferred to a new vial, snap frozen and lyophilized. The samples were then re-dissolved in methanol-water (2:1, v/v) for tauro-conjugated bile acids determination. A bile acids extraction yield of 95% has been measured using bile acids standards addition in blank samples before and after deproteinization procedure.

Liquid chromatography and mass spectrometry. For LC–MS/MS analysis, chromatographic separation was carried out on the HPLC–MS system LTQ XL ThermoScientific equipped with Accelera 600 Pump and Accelera AutoSampler system. The mixture was separated on a Jupiter 5u C18 column from Phenomenex (150X2.00 mm) and the column flow rate was set at 200 μl/min. Tauro-conjugated bile acids were separated using a methanol-aqueous ammonium acetate (NH_4OAc) gradient. Mobile phase A was 5% methanol in water containing 2mM ammonium acetate at pH 7, mobile phase B was methanol, containing ammonium acetate at 2mM. The gradient started at 30 % B and increased to 100% B in 20 min, kept at 100% B for 5 min then decreased to 30% B in 1 min and kept at 30% B for 10 min. ESI was performed in negative ion mode, the ion source temperature was set at 280 °C. The tune page parameters were automatically optimized injecting taurocholic acid at 1 μM as standard. The MS/MS detection was operated in MRM mode using a collision energy of 20 (arbitrary units), the observed transitions were: tauromuricholic acid (t-MCA) at 13.5 min MRM of 514.28 Th→514.28 Th,

taurohyocholic acid (t-HCA) at 15.6 min MRM of 498.29 Th→498.29 Th, taurocholic acid (t-CA) at 16.6 min MRM of 514.28 Th→514.28 Th, taurochenodeoxycholic acid (t-CDCA) at 18.5 min MRM of 498.29 Th→498.29 Th, and taurodeoxycholic acid (t-DCA) at 18.9 min MRM of 498.29 Th→498.29 Th.

Molecular Docking. The AutoDock4.2 software package was used to perform molecular docking calculations in the three-dimensional model of hGP-BAR1 and in the crystal structure of the FXR-LBD from Rattus Norvegicus (rFXR) in complex with 6-ethylchenodeoxycholic acid (6-ECDCA) and the GRIP-1 co-activator peptide, NID-3 (PDB code 1osv). rFXR-LBD shares the 95% of homology with that of the human FXR-LBD (hFXR-LBD), with all of the residues in the ligand binding pocket conserved among the two species. Ligands tridimensional structures were generated with the Maestro Build Panel. For each ligand, an extensive ring conformational sampling was performed with the OPLS-AA force field and a 2.0 Å rmsd cutoff using MacroModel (version 9.9) as implemented in Maestro 9.3. All conformers were then refined using LigPrep as implemented in Maestro 9.3. Protonation states at pH 7.0 were assigned using Epik. Protein structure was prepared through the Protein Preparation Wizard through the graphical user interface of Maestro 9.3. Water molecules were removed and hydrogen atoms were added and minimized using the OPLS-2005 force field. Ligands and receptor structures were converted to AD4 format files using ADT, and the Gesteiger-Marsili partial charges were then assigned. Grid points of 70 × 70 × 70 for FXR and of 65 × 80 × 55 for GP-BAR1 with a 0.375 Å spacing were calculated around the binding cavity using AutoGrid4.2. Thus, 100 separate docking calculations were performed for each run. Each docking run consisted of 10 million energy evaluations using the Lamarckian genetic algorithm local search (GALS) method. Otherwise default docking parameters were applied. Docking conformations were clustered on the basis of their rmsd (tolerance = 2.0 Å) and were ranked based on the AutoDock scoring function.

All the residue labels were taken from crystal structure of rFXR-LBD with PDB ID 1osv and the wild-type amino acidic sequence of human GP-BAR1.

All figures were rendered using PyMOL (http://www.pymol.org).

^{1}H NMR (400 MHz, CD_3OD) of compound **16**

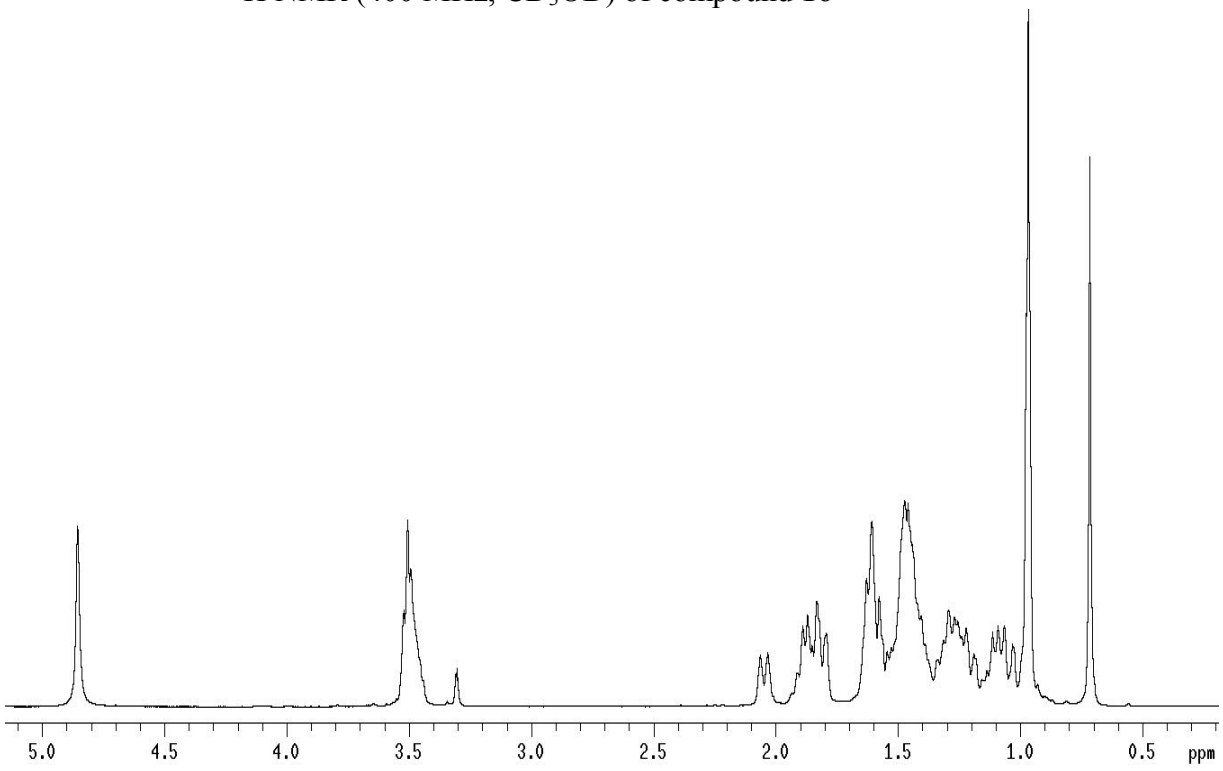

^{13}C NMR (100 MHz, CD_3OD) of compound **16**

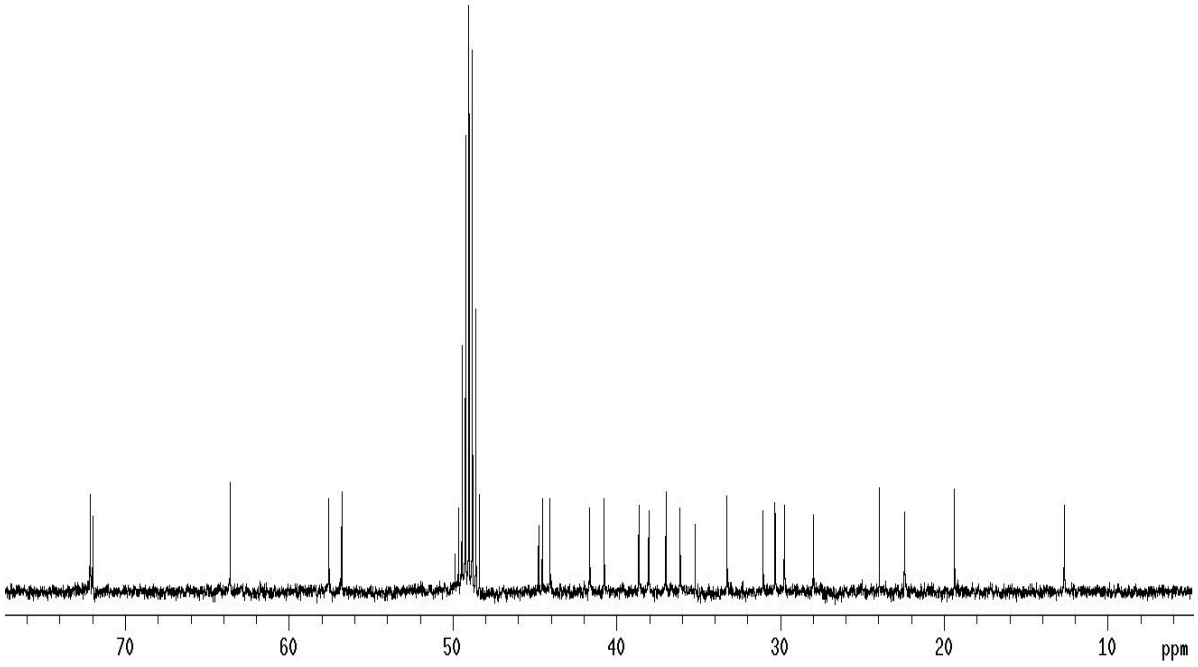

^{1}H NMR (400 MHz, CD_3OD) of compound **9**

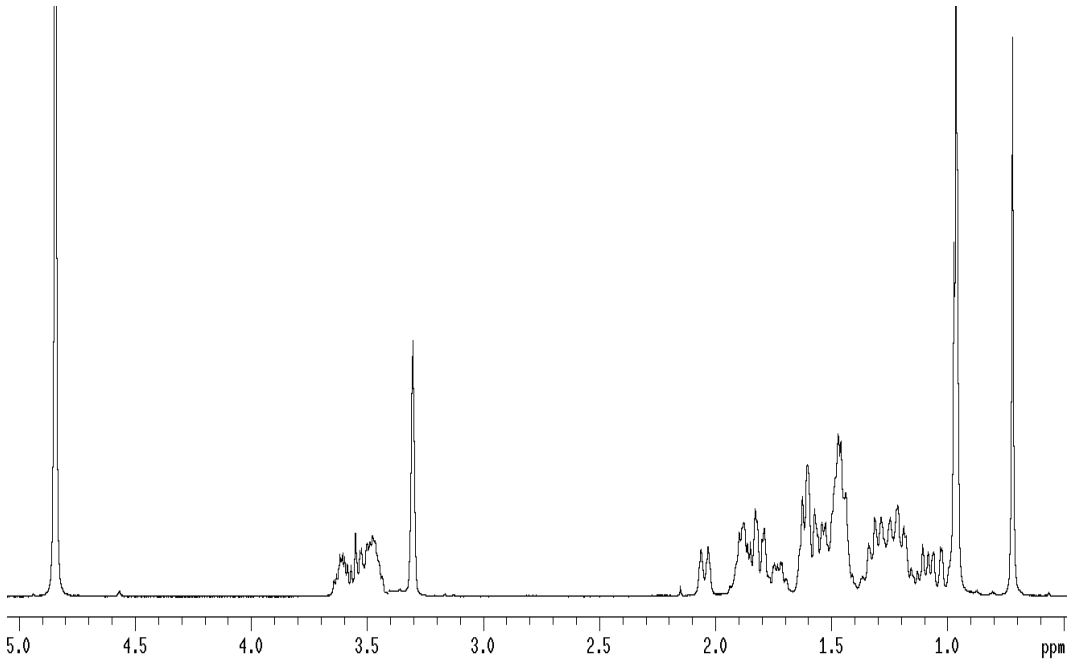

^{13}C NMR (100 MHz, CD_3OD) of compound **9**

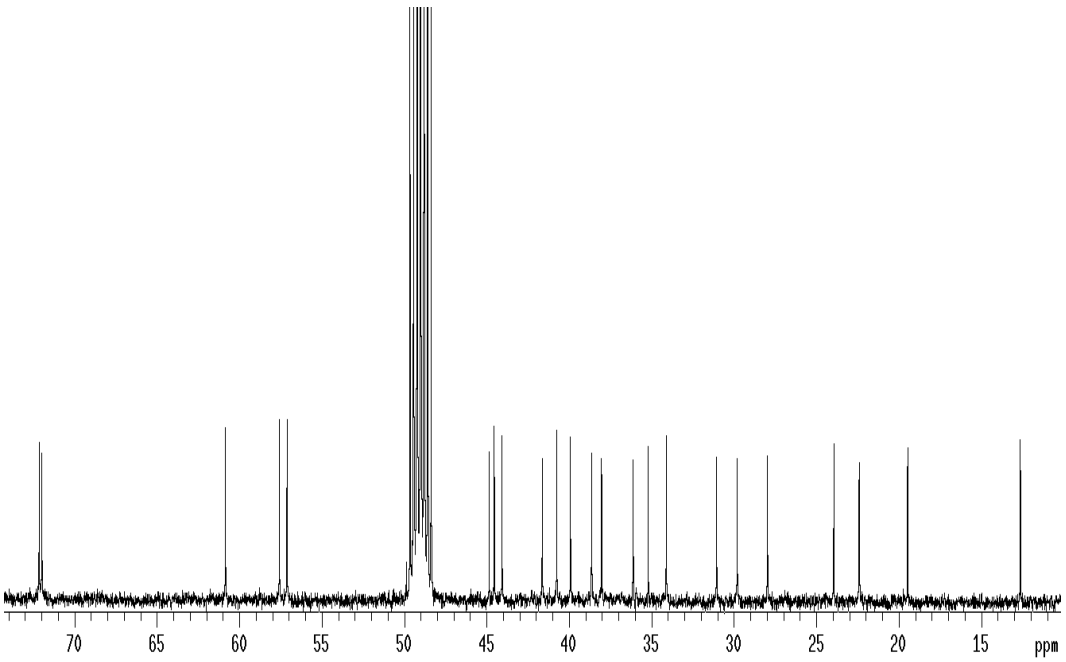

^{1}H NMR (400 MHz, CD_3OD) of compound **10**

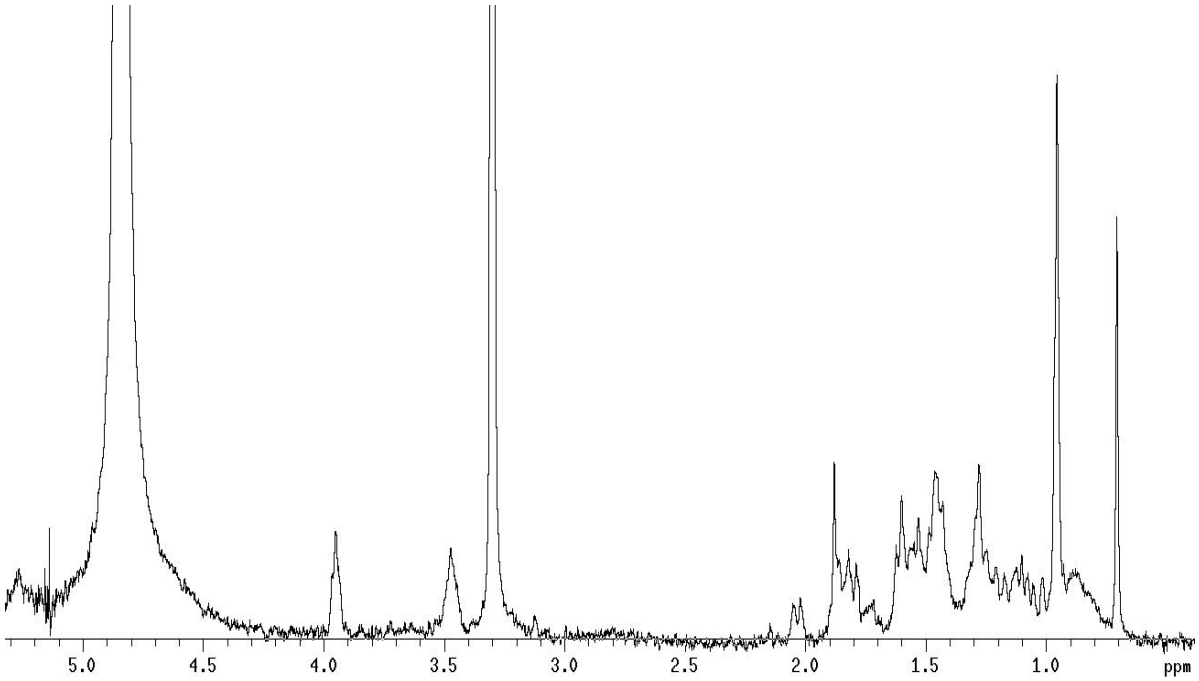

^{1}H NMR (400 MHz, CD_3OD) of compound **11**

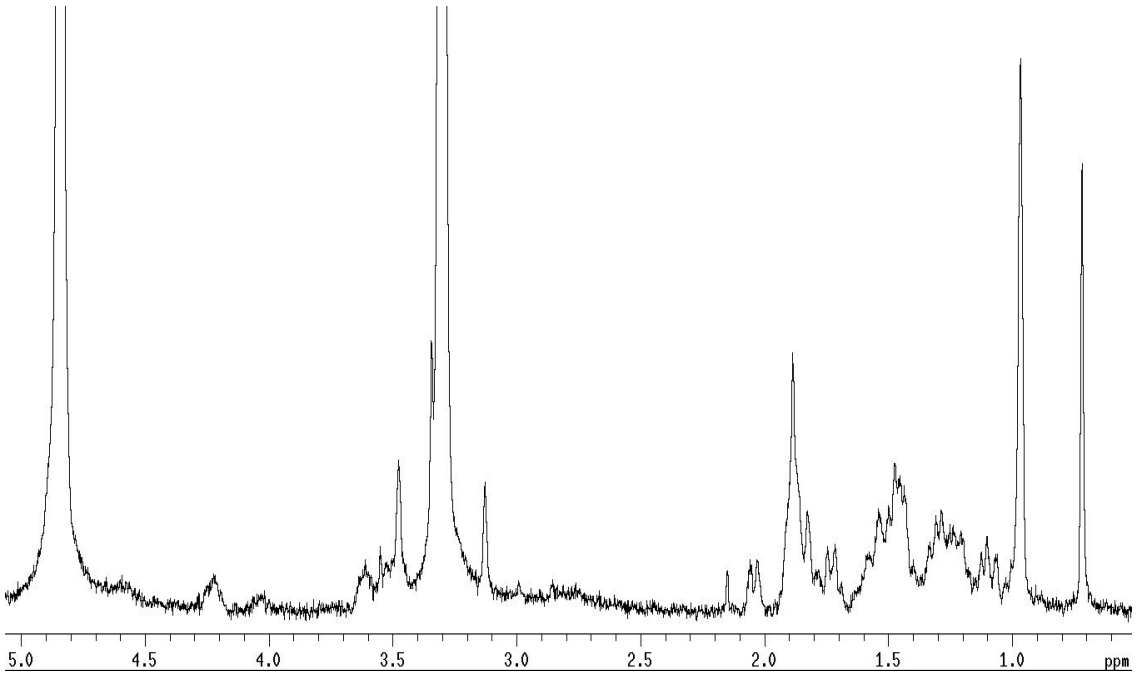

^{1}H NMR (400 MHz, CD_3OD) of compound **12**

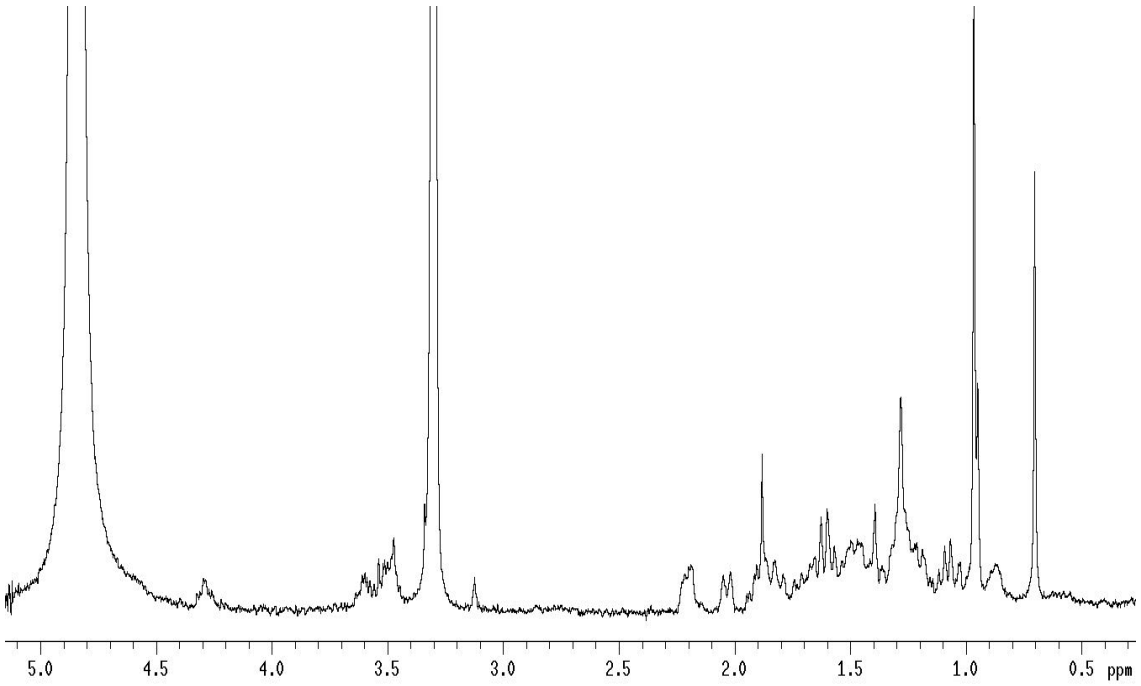

^{1}H NMR (400 MHz, CD_3OD) of compound **13**

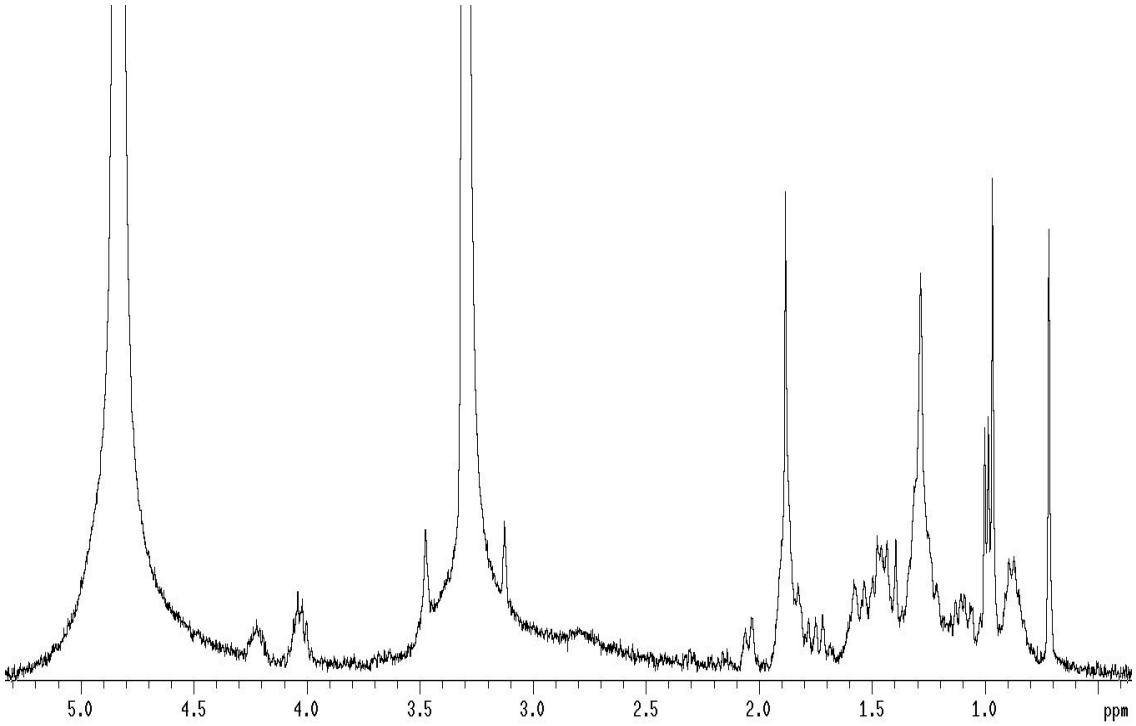

^{1}H NMR (400 MHz, CD_3OD) of compound **14**

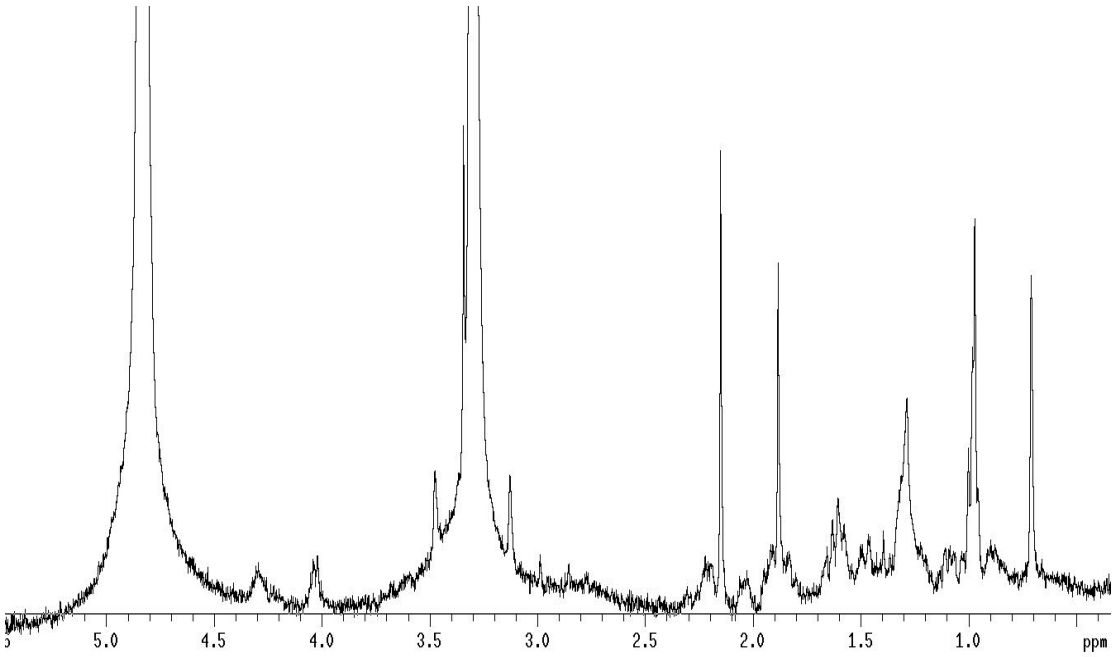

^{1}H NMR (400 MHz, CD_3OD) of compound **15**

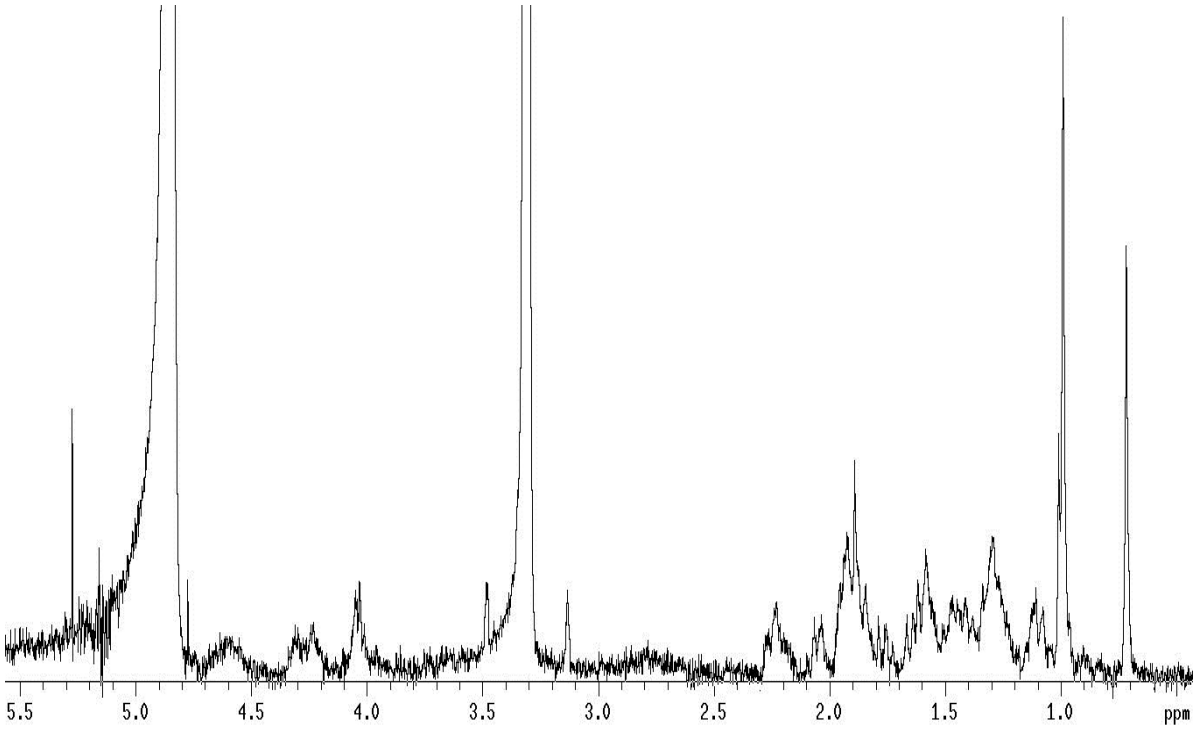

^{1}H NMR (400 MHz, CD_3OD) of compound **6**

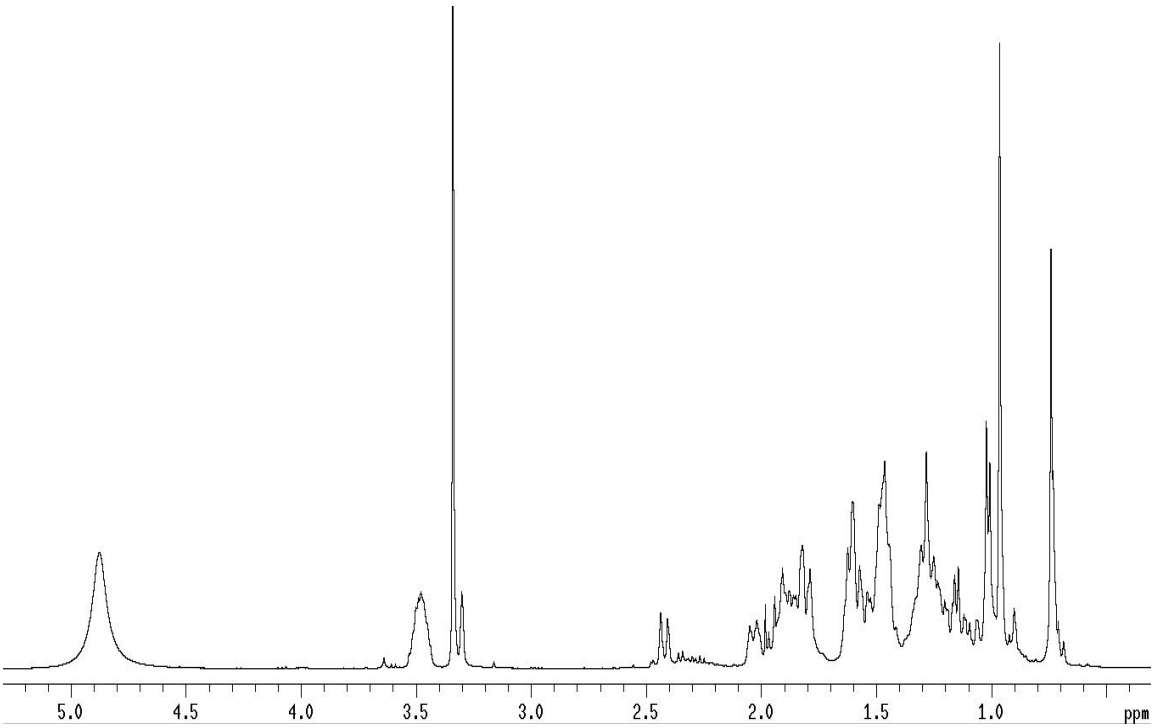

^{13}C NMR (100 MHz, CD_3OD) of compound **6**

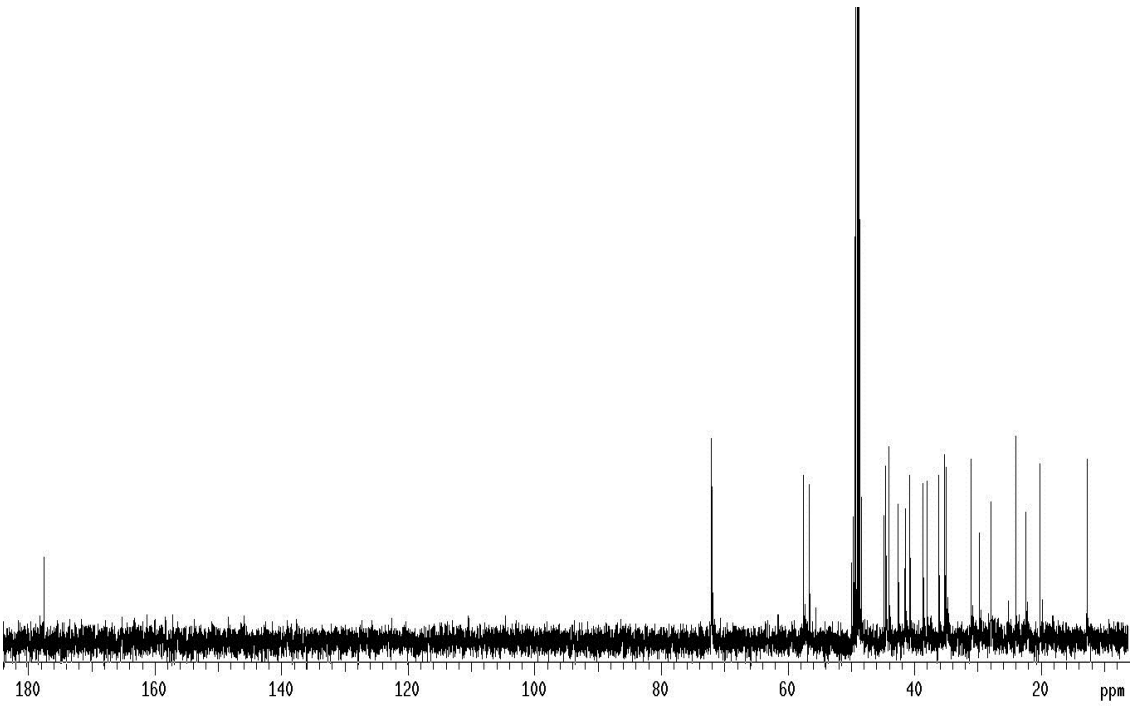

^{1}H NMR (400 MHz, CD_3OD) of compound **7**

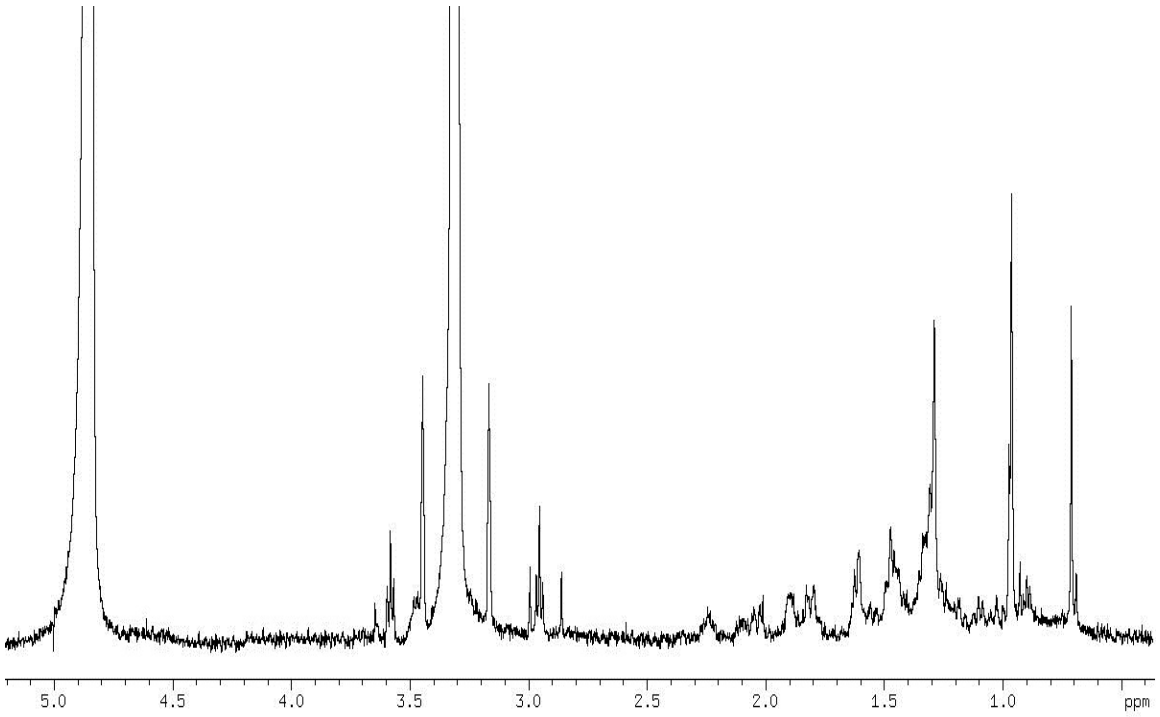

^{1}H NMR (400 MHz, $CDCl_3$) of compound **8**

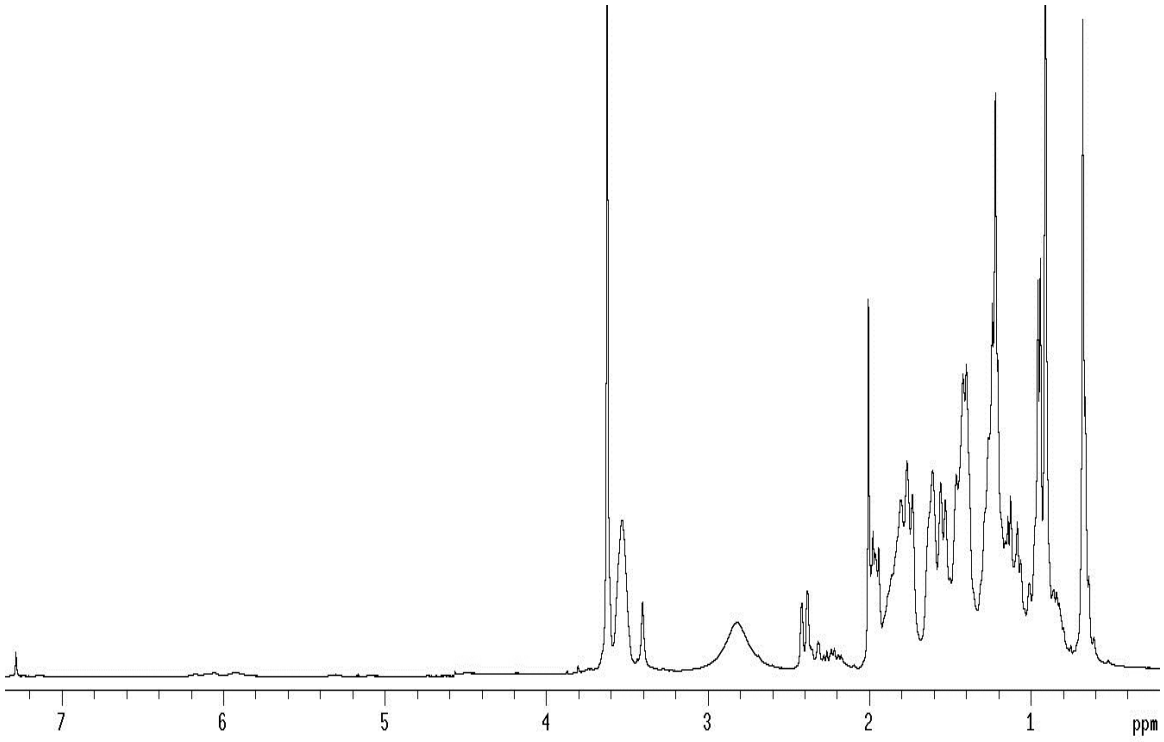

^{13}C NMR (100 MHz, $CDCl_3$) of compound **8**

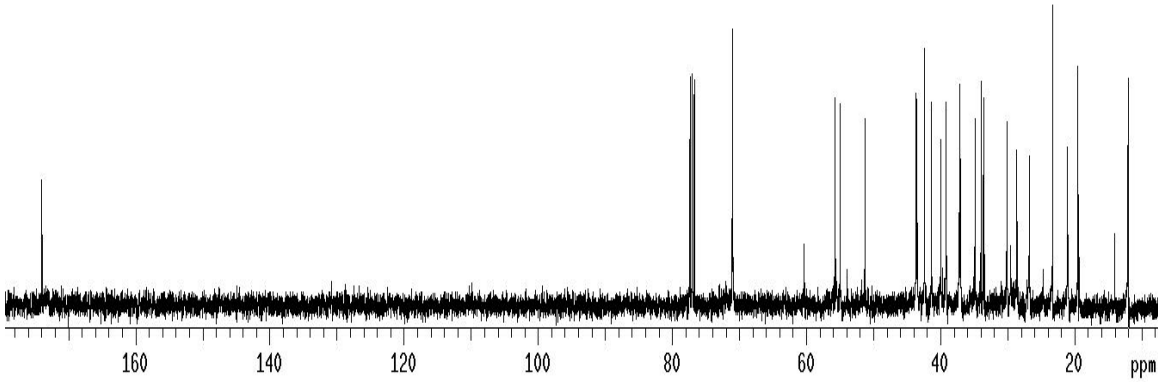

^{1}H NMR (400 MHz, CD_3OD) of compound **26**

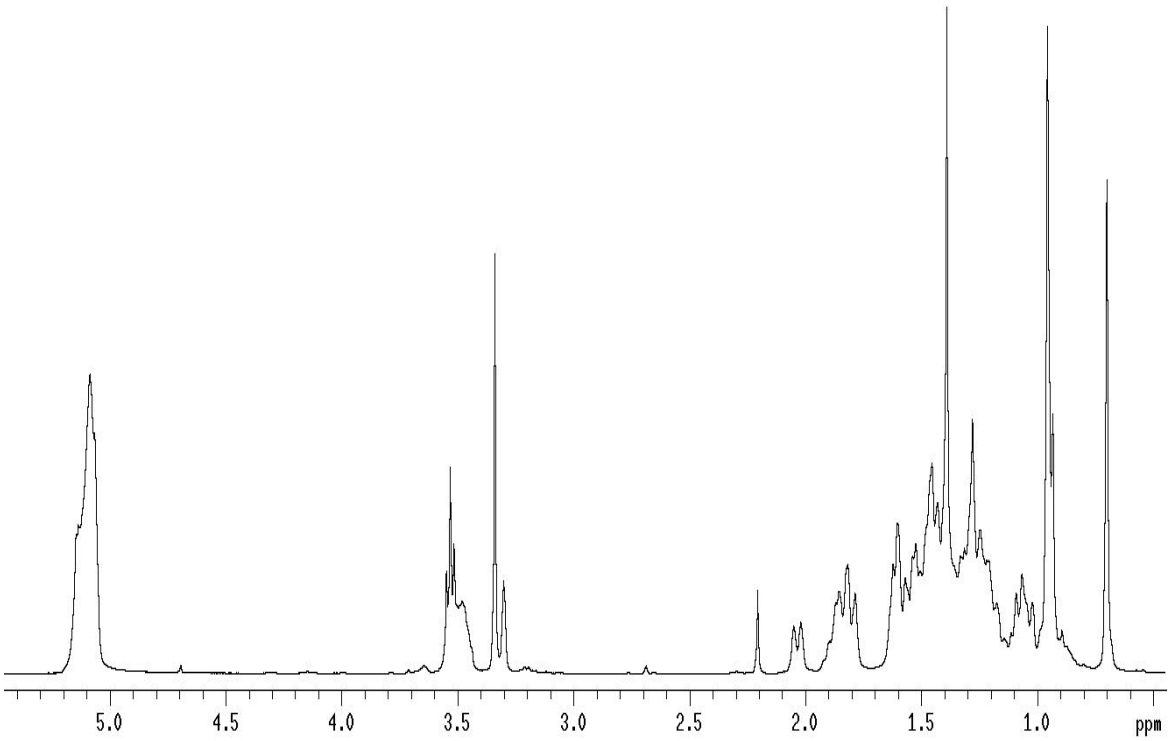

^{13}C NMR (100 MHz, CD_3OD) of compound **26**

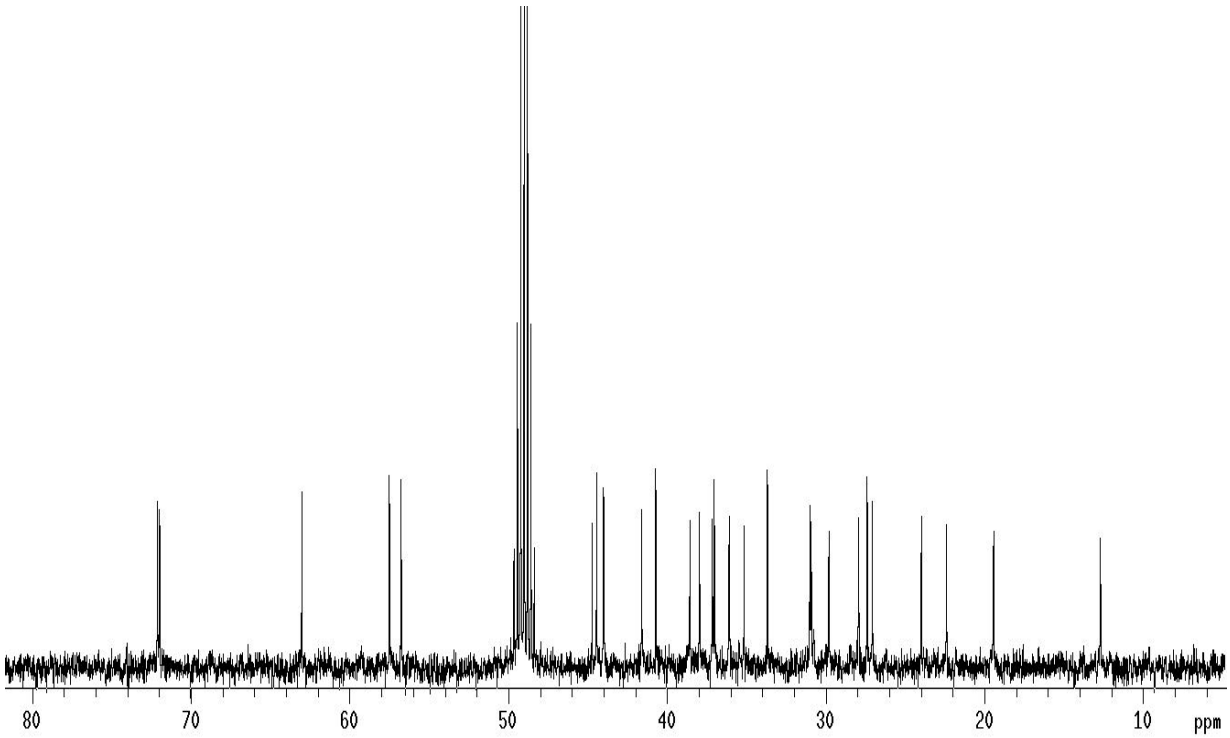

^{1}H NMR (400 MHz, $CDCl_3$) of compound **23**

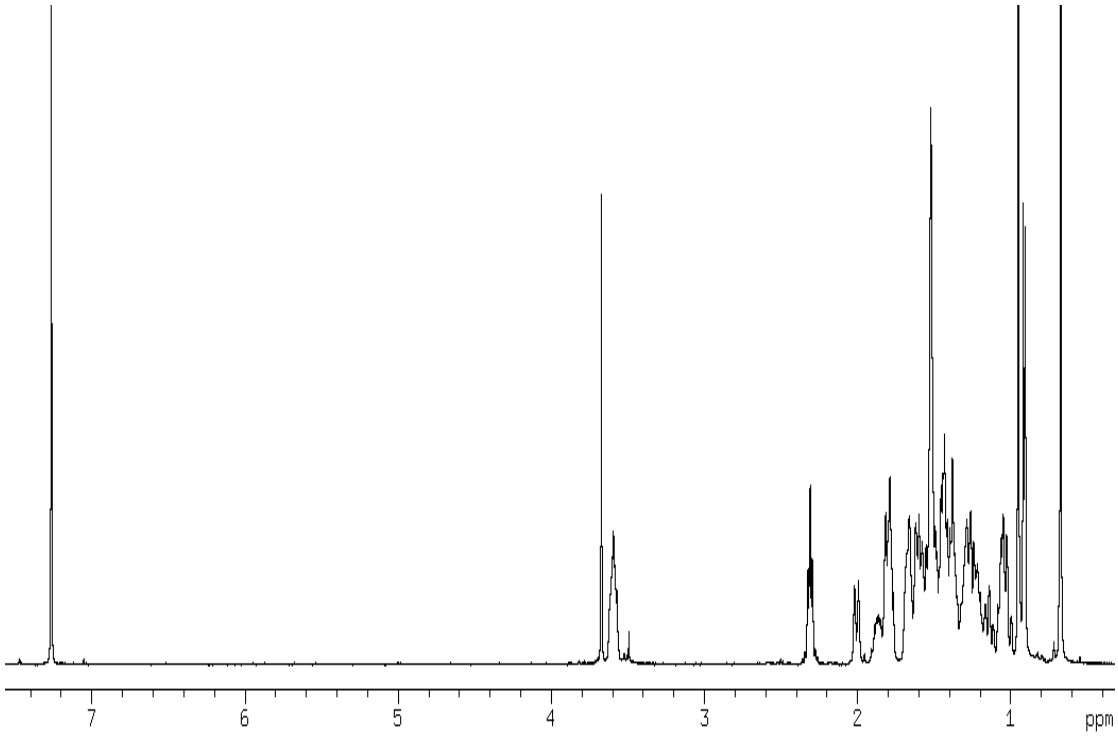

^{13}C NMR (100 MHz, $CDCl_3$) of compound **23**

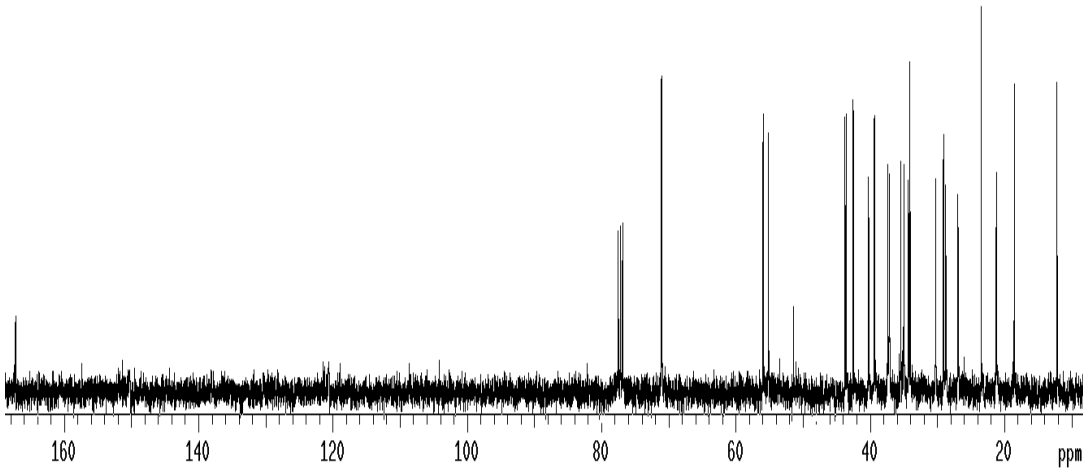

^{1}H NMR (500 MHz, CD_3OD) of compound **24**

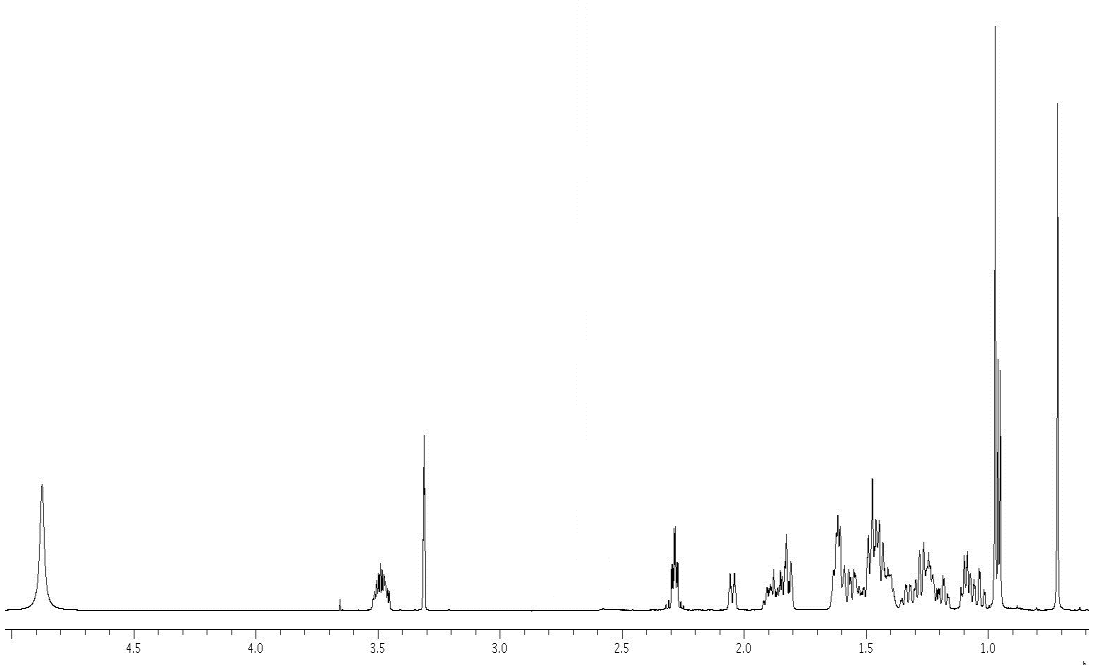

^{13}C NMR (125 MHz, CD_3OD) of compound **24**

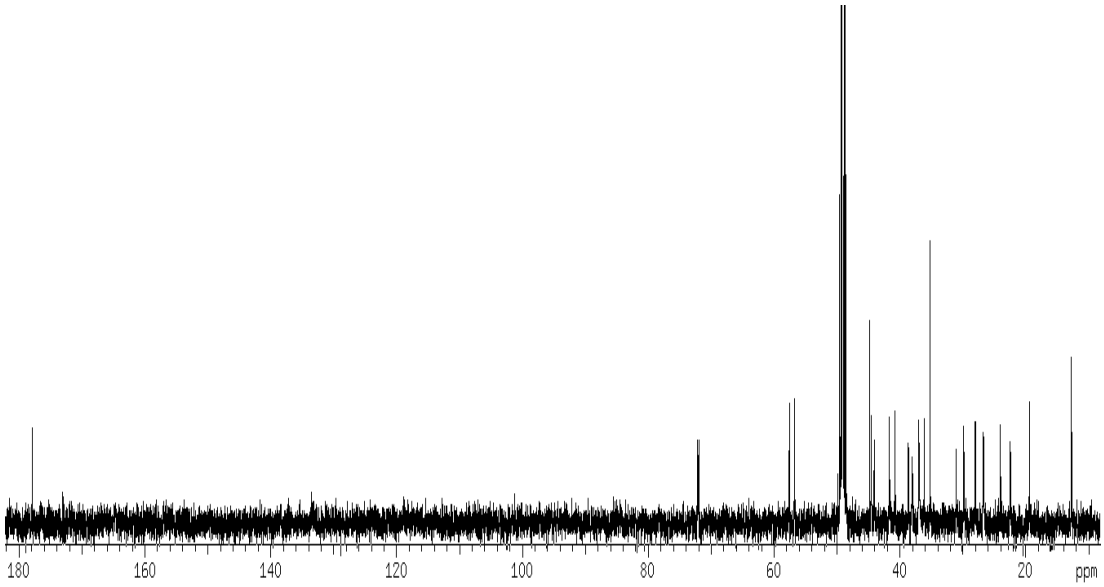

^{1}H NMR (400 MHz, CD_3OD) of compound **25**

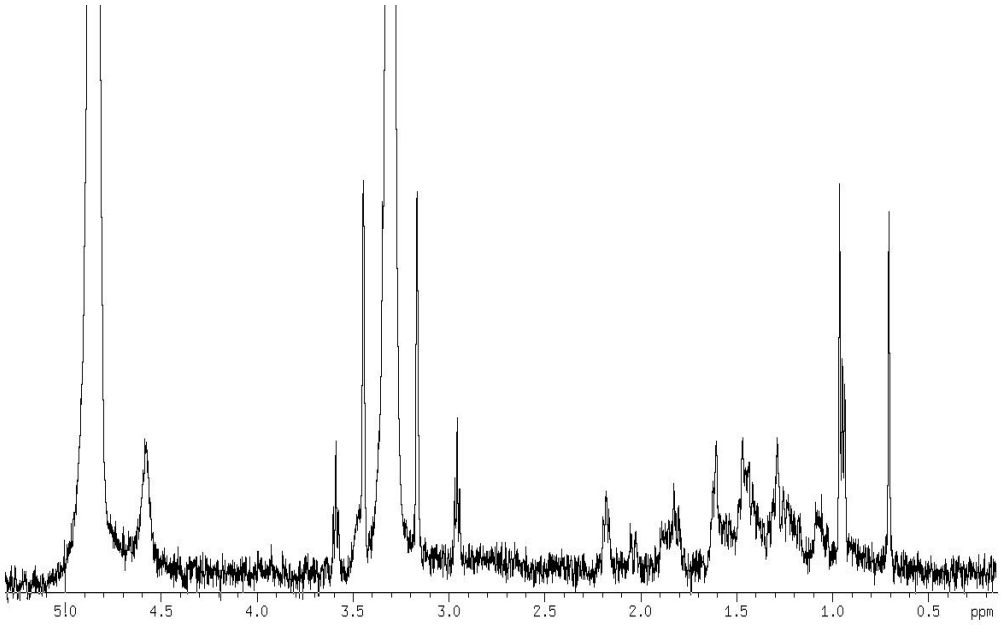

^{1}H NMR (400 MHz, $CDCl_3$) of compound **20**

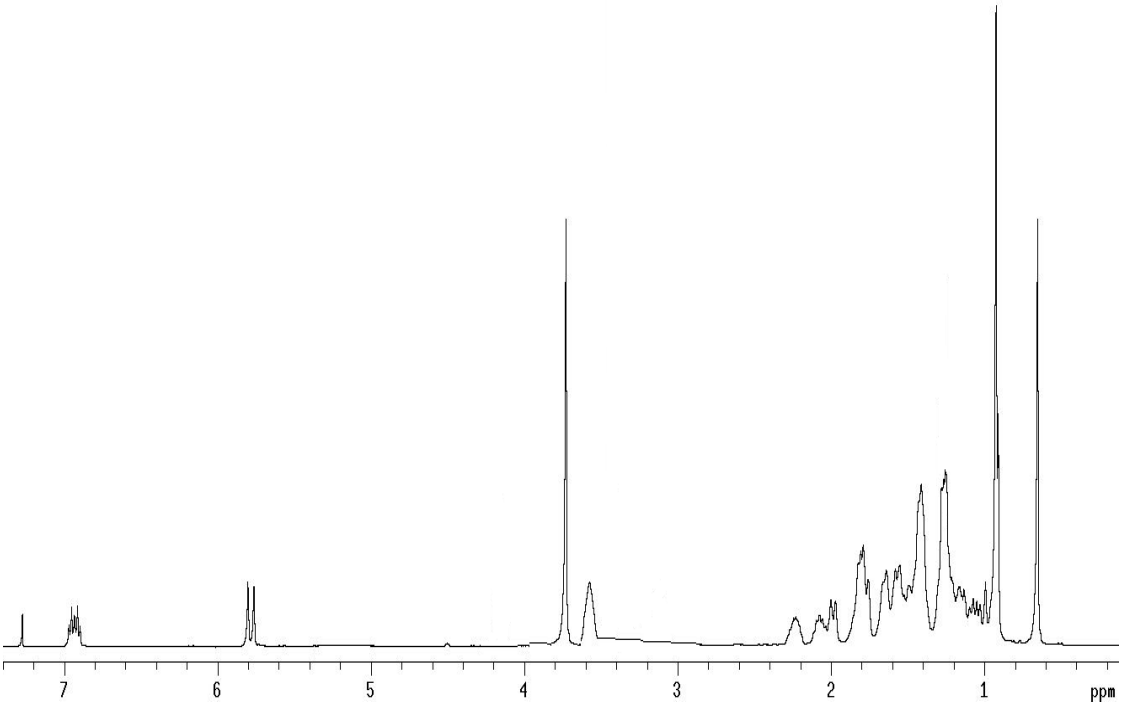

^{13}C NMR (100 MHz, $CDCl_3$) of compound **20**

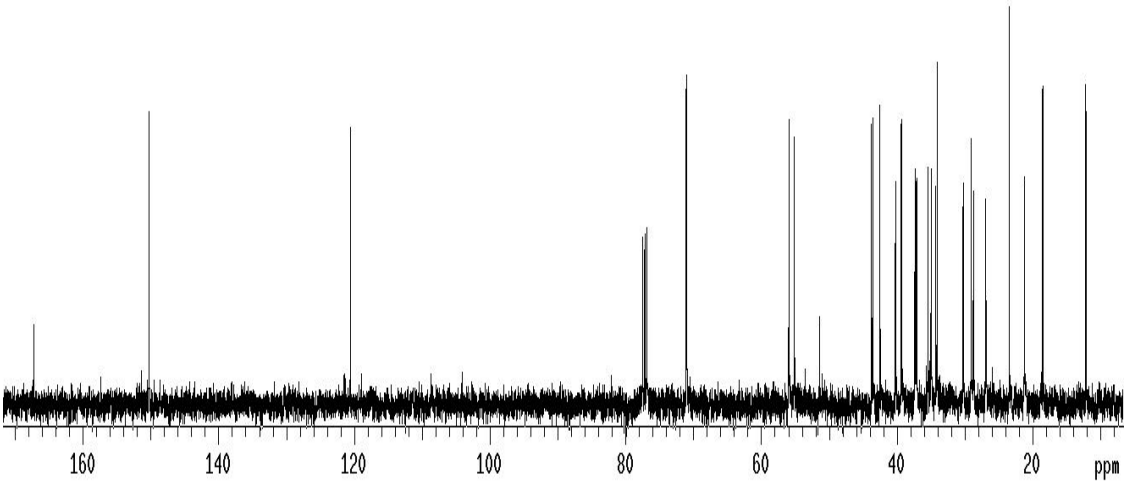

^{1}H NMR (400 MHz, $CDCl_3$) of compound **21**

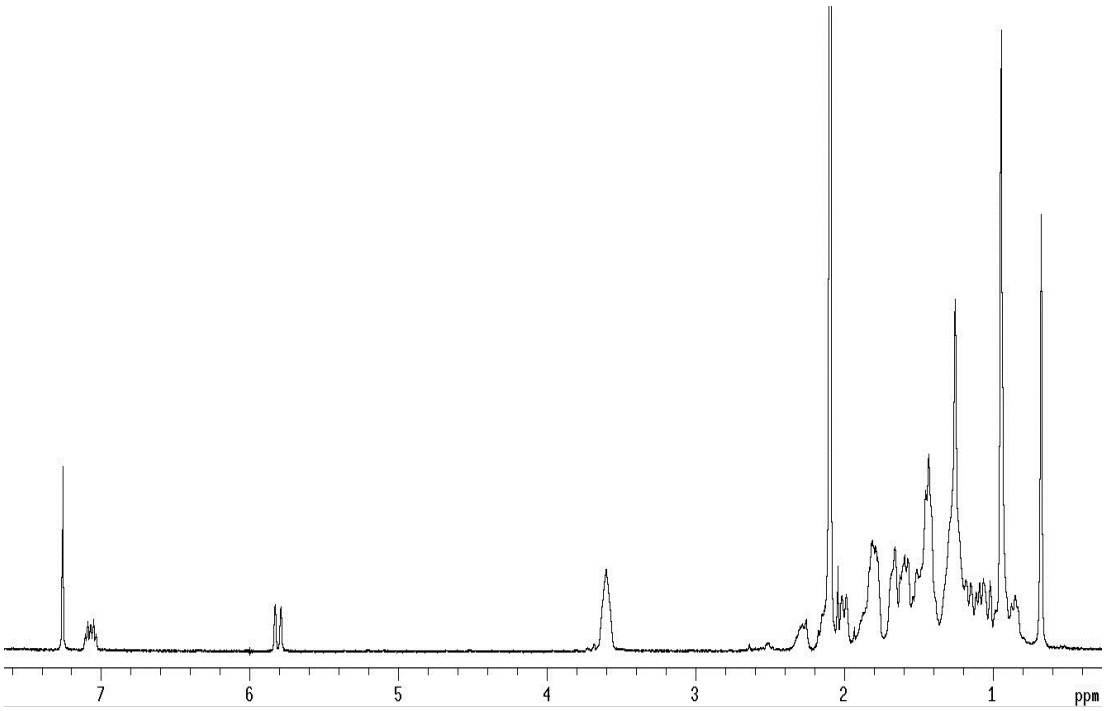

^{13}C NMR (100 MHz, CD_3OD) of compound **21**

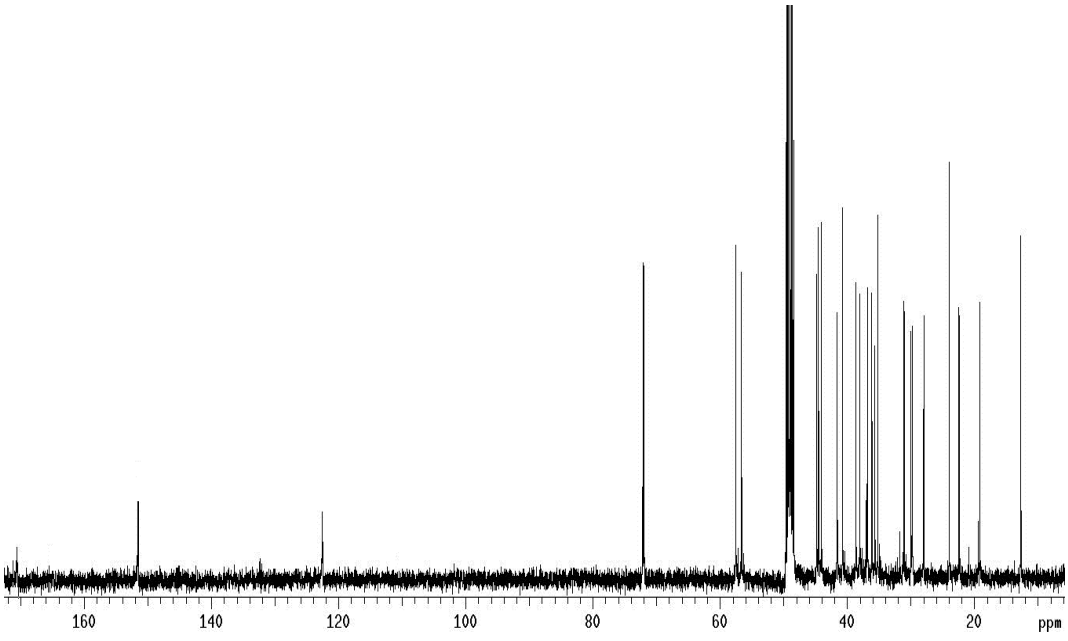

^{1}H NMR (400 MHz, CD_3OD) of compound **22**

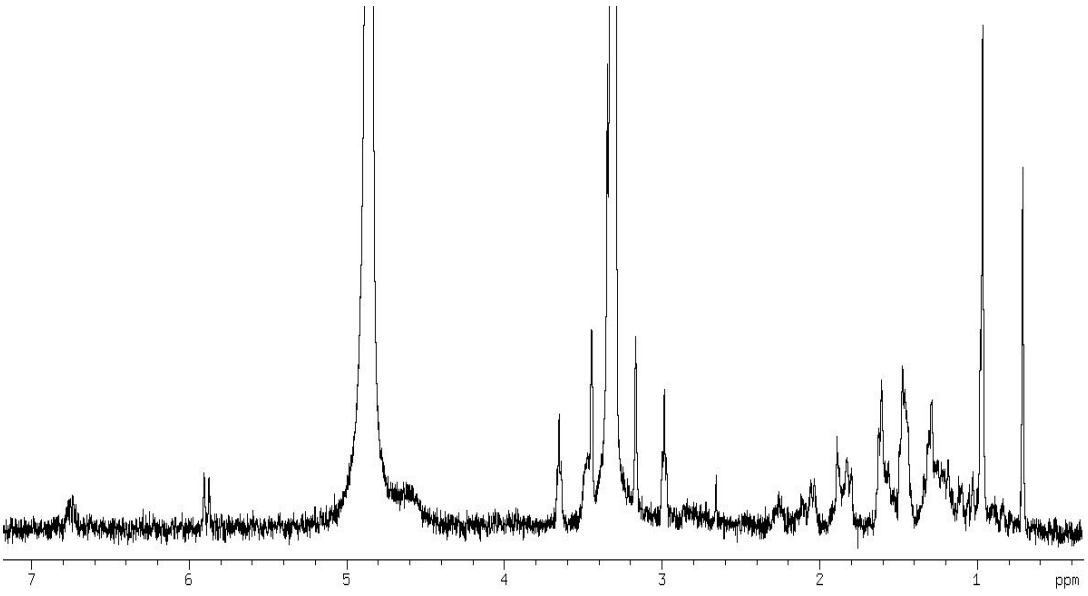

III. Experimental section Cholanoic acid derivatives.

Methyl 3α-tosiloxy-5β-cholan-24-oate (28). To a solution of lithocholic acid **2** (2 g, 5.3 mmol), dissolved in 50 mL of dry methanol was added *p*-toluenesulfonic acid (4.5 g, 26.5 mmol). The solution was left to stand at room temperature for 1 h. The mixture was quenched by addition until the neutrality of $NaHCO_3$ saturated solution. After the evaporation of the methanol, the residue was extracted with ethyl acetate. The combined extract was washed with brine, dried with Na_2SO_4, and evaporated to give the methyl ester **27** as amorphous solid (2.1 g, quantitative yield).

At the solution of the methyl ester **27** (2 g, 5.1 mmol) in dry pyridine (30 mL), tosyl chloride (4.9 g, 25.6 mmol) was added, and the mixture was stirred at room temperature for 8 h. It was poured into cold water (50 mL) and extracted with CH_2Cl_2 (3 × 50 mL). The combined organic phases were washed with saturated $NaHCO_3$ solution (50 mL) and water (50 mL), dried (Na_2SO_4) and concentrated to give 2.6 g of **28** as a white solid (92%). $[\alpha]_D^{25}$= +59.5 (*c* 0.02, CH_3OH); selected ^1H NMR (500 MHz, $CDCl_3$): δ 7.77 (2H, d, *J* = 8.2 Hz), 7.31 (2H, d, *J* = 8.2 Hz), 4.43 (1H, m), 3.64 (3H, s), 2.32 (1H, m), 2.19 (1H, m), 0.88 (3H, d, *J* = 6.6 Hz), 0.86 (3H, s), 0.60 (3H, s); HR ESIMS *m/z* 545.3309 $[M + H]^+$, $C_{32}H_{49}O_5S$ requires 545.3301.

Methyl 5β-cholan-24-oate (29). Lithium bromide (800 mg, 9.2 mmol) and lithium carbonate (680 mg, 9.2 mmol) were added to a solution of compound **28** (2.5 g, 4.6 mmol) in dry DMF (30 mL), and the mixture was refluxed for 2 h. After cooling to room temperature, the mixture was slowly poured into saturated $NaHCO_3$ solution (50 mL) and extracted with ethyl acetate (3 × 50 mL). The combined organic layer

was washed successively with water, and then dried over anhydrous $MgSO_4$ and evaporated to dryness to give 1.7 g of oily residue (quantitative yield), that was subjected to next step without any purification.

A solution of compound previously obtained (1.7 g, 4.6 mmol) in THF dry/MeOH dry (10 mL/10 mL, v/v) was hydrogenated in presence of $Pd(OH)_2$ 20% wt on activated carbon Degussa type (30 mg) in PARR apparatus. The flask was evacuated and flushed first with argon and then with hydrogen (about 5 atm). After 12 h, the reaction was complete. The mixture was filtered through celite, and the recovered filtrate was concentrated to give 1.7 g of crude product. Purification by silica gel (hexane/ethyl acetate 95:5) gave compound **29** as a colourless oil (1.27 g, 74%). $[\alpha]_{25}^{D}$=-3.0 (*c* 0.03, CH_3OH); selected ^{1}H NMR (400 MHz, $CDCl_3$): δ 3.68 (3H, s), 2.37 (1H, m), 2.24 (1H, m), 0.94 (3H, d, ovl), 0.93 (3H, s), 0.66 (3H, s).^{13}C NMR (100 MHz, $CDCl_3$): δ 175.2, 56.9, 56.3, 51.8, 44.0 (2C), 40.8, 40.6, 37.9, 36.2, 35.7, 31.4 (2C), 28.5, 27.8, 27.6, 27.4, 26.9 (2C), 24.6, 21.6, 21.2, 18.6, 12.4. HR ESIMS *m/z* 375.3267 $[M+H]^+$, $C_{25}H_{43}O_2$ requires 375.3263.

5β-cholan-24-oic acid (30). Compound **29** (500 mg, 1.3 mmol) was hydrolyzed with a methanol solution of sodium hydroxide (5%, 5 mL) in H_2O (5 mL) overnight under reflux. The resulting solution was then concentrated under vacuum, diluted with water, acidified with HCl 6 N and extracted with ethyl acetate (3x50 mL). The collected organic phases were washed with brine, dried over Na_2SO_4 anhydrous and evaporated under reduced pressure to give 480 mg of compound **30** (quantitative yield). An analytic sample was obtained by HPLC on a Nucleodur 100-5 C18 (5 μm; 10 mm i.d. x 250 mm) with MeOH/H_2O (999.5:0.5) as eluent (flow rate 3 mL/min, t_R=21 min);

$[\alpha]_{25}^{D}$=+13.3 (*c* 0.32, $CHCl_3$); selected ^{1}H NMR (400 MHz $CDCl_3$): δ 2.39 (1H, m), 2.26 (1H, m), 0.93 (3H, d, *J* = 6.6 Hz), 0.91 (3H, s), 0.66 (3H, s). ^{13}C NMR (100 MHz $CDCl_3$): δ 179.1, 56.8, 56.2, 50.6, 43.9, 43.0, 40.7, 40.5, 37.8, 36.1 (2C), 35.6 (2C), 31.1, 28.4, 27.7, 27.5, 27.3, 26.8, 24.5, 21.6, 21.0, 18.5, 12.3. HR ESIMS *m/z* 359.2956 $[M-H]^-$, $C_{24}H_{39}O_2$ requires 359.2950.

5β-cholan-24-oyl taurine sodium salt (31). Compound **30** (50 mg, 0.1 mmol) in DMF dry (3 mL) was treated with DMT-MM (77.5 mg, 0.3 mmol) and triethylamine (70 μL, 0.5 mmol) and the mixture was stirred at room temperature for 10 min. Then to the mixture was added taurine (15 mg, 0.2 mmol). After 24 h, the reaction mixture was concentrated under vacuo and dissolved in water (5 mL). The mixture was purified by HPLC on a Nucleodur 100-5 C18 (5 μm; 4.6 mm i.d. x 250 mm) with MeOH/H_2O (83:17) as eluent (flow rate 1 mL/min), to give 3.5 mg of compound **31** (t_R=11 min); $[\alpha]_{25}^{D}$=+22.5 (*c* 0.05, CH_3OH); selected ^{1}H NMR (400 MHz, CD_3OD): δ 3.58 (2H, t, *J* = 7.0 Hz), 2.95 (2H, t, *J* = 7.0 Hz), 2.24 (1H, m), 2.08 (1H, m), 0.95 (3H, d, ovl), 0.94 (3H, s), 0.68 (3H, s). HR ESIMS *m/z* 480.3150 $[M-Na]^-$, $C_{27}H_{46}NO_4S$ requires 480.3153.

3α-formyloxy-5β-cholan-24-oic acid (32). A solution of lithocholic acid **2** (500 mg, 1.3 mmol) in 10 mL of 90 % formic acid containing 25 μL of 70% perchloric acid was stirred at 47-50 °C for 12 h. The temperature of the heating bath was lowered to 40 °C, then 5 mL of acetic anhydride was added and the mixture was stirred for 15 min. The solution was cooled to room temperature, poured into 50 mL of water and extracted with diethyl ether. The organic layers were washed with saturated $NaHCO_3$ solution (50 mL) and water to neutrality, dried over Na_2SO_4, and evaporated to give 540 mg of **32** (quantitative yield). An analytic

sample was obtained by silica gel chromatography eluting with CH_2Cl_2:MeOH 9:1. Selected ^{1}H NMR (400 MHz CD_3OD): δ 8.04 (1H, s), 4.85 (1H, m), 2.39 (1H, m), 2.25 (1H, m), 0.93 (3H, s), 0.92 (3H, d, *J* = 6.7 Hz), 0.65 (3H, s); ^{13}C NMR (100 MHz CD_3OD): δ 178.1, 160.8, 74.4, 56.5, 55.9, 41.9, 40.5, 40.2, 40.1, 35.8 (3C), 35.4 (2C), 32.3, 30.8, 30.7, 28.2, 27.0, 26.3, 24.2, 23.4, 20.8, 18.2, 12.1; HRMS-ESI *m/z* 405.2997 $[M+H]^+$, $C_{25}H_{41}O_4$ requires 405.2999.

3α- formyloxy-24-*nor*-5β-cholan-23-nitrile (33). Crude **32** (500 mg, 1.2 mmol), 3.8 mL of cold trifluoroacetic acid, and 1 mL (7.2 mmol) of trifluoroacetic anhydride were stirred at 0 °C until dissolution. Sodium nitrite (248 mg, 3.6 mmol) was added at the solution. The reaction mixture was stirred first at 0-5 °C for 1 h, then at 45-50 °C for 3 h. When the reaction was completed, it was neutralized with NaOH 2 N, then the product was extracted with 50 mL of diethyl ether (3 x 50 mL), followed by washing with brine and dried over anhydrous Na_2SO_4. The ether was removed under reduced pressure to afford 380 mg of **33** (85%), that was subjected to next step without any purification.

24-*nor*-lithodeoxycholic acid (34). Compound **33** (350 mg, 0.94 mmol) was refluxed in *ca*. 50 mL of methanol-water 1:1 with 30% KOH. After 2 h, the basic aqueous solution was neutralized with HCl 6 N. Then methanol was evaporated and the residue was extracted with ethyl acetate (3 x 50mL) and then with CH_2Cl_2 (3 x 50 mL). The organic layers were washed with brine, dried and evaporated to dryness to give white solid residue, that was purified by silica gel chromatography, eluting with CH_2Cl_2:MeOH 9:1 (340 mg, quantitative yield). An analytic sample was purified by HPLC on a Nucleodur 100-5 C18 (5 μm; 4.6 mm i.d. x 250 mm) with MeOH/H_2O (95:5) as eluent (flow rate 1 mL/min), to give compound **34** (t_R=10.5 min). $[\alpha]_{25}^{D}$=+21.9 (*c* 0.58, CH_3OH); selected ^{1}H NMR

(400 MHz CD_3OD): δ 3.54 (1H, m), 2.41 (2H, m), 1.00 (3H, d, *J* = 7.0 Hz), 0.94 (3H, s), 0.71 (3H, s). ^{13}C NMR (100 MHz CD_3OD): δ 178.0, 72.5, 57.9, 57.5, 43.6, 42.5, 41.9, 41.4, 37.2, 37.1, 36.5, 35.7, 34.9, 31.1, 29.3, 28.3, 27.6, 25.2, 23.9, 21.9, 19.9, 12.5; HRMS-ESI *m/z* 363.2895 $[M+H]^+$, $C_{23}H_{39}O_3$ requires 363.2899.

24-*nor*-5β-cholanoic acid (37). Compound **37** (210 mg, 75% over five steps) was synthesized, starting from compound **34** (300 mg, 0.8 mmol) as described in Scheme 2, by an analogous procedure to that detailed above for compound **30**. An analytic sample was obtained by HPLC on a Nucleodur 100-5 C18 (5 μm; 10 mm i.d. x 250 mm) with MeOH/H_2O (999.5:0.5) as eluent (flow rate 3 mL/min, t_R=20 min); $[\alpha]_D^{25}$= +24.6 (*c* 0.03, CH_3OH); selected ^1H NMR (400 MHz CD_3OD): δ 2.41 (1H, m), 1.00 (3H, d, *J* = 6.0 Hz), 0.95 (3H, s), 0.72 (3H, s); ^{13}C NMR (100 MHz CD_3OD): δ 178.0, 58.0, 57.6, 45.2, 44.0, 42.8, 41.9, 41.5, 38.7, 37.3, 36.5, 35.0, 29.3, 28.6, 28.4, 28.2, 27.7, 25.3, 24.8, 22.4, 21.9, 20.0, 12.5; HR ESIMS *m/z* 347.2947 $[M + H]^+$, $C_{23}H_{39}O_2$ requires 347.2950.

Methyl cholan-3,5-dien-24-oate (40). To a solution of the ditosylate **39** (500 mg, 0.7 mmol) in water (3 ml) and *N*,*N*'-dimethylformamide (DMF; 27 ml) was added CH_3COOK (206 mg, 2.1 mmol) and the mixture was refluxed for 36 h. The solution was cooled at room temperature, then water and ethyl acetate were added and the separated aqueous phase was extracted with ethyl acetate (3 × 20 mL). The combined organic phases were washed with water, dried (Na_2SO_4) and concentrated. Purification by silica gel eluting with hexane-ethyl acetate (99:1) gave the diene **40** (200 mg, 78%). selected ^1H NMR (400 MHz CD_3OD): δ 5.92 (1H, d, *J* = 9.7 Hz), 5.58 (1H, d, *J* = 11.3 Hz), 5.38 (1H, m), 3.66 (3H, s), 2.34

(1H, m), 2.22 (1H, m), 0.94 (3H, d, J = 5.8 Hz), 0.92 (3H, s), 0.70 (3H, s); ^{13}C NMR (100 MHz CD_3OD): δ 174.8, 141.5, 129.1, 125.2, 123.2, 57.0, 55.8, 51.5, 48.4, 43.4, 39.8, 35.4, 33.8, 31.9, 31.8, 31.7, 31.0, 30.9, 28.1, 24.2, 23.9, 23.0, 20.9, 18.8, 12.0. HR ESIMS *m/z* 371.2947 $[M + H]^+$, $C_{25}H_{39}O_2$ requires 371.2950.

Methyl 5α-cholan-24-oate (41). A solution of compound **40** (150 mg, 0.4 mmol) in methanol (5 mL) and dry THF (5 mL) was added in an oven-dried 50 mL flask, that was charged with 10% palladium on carbon (10 mg). The flask was evacuated and flushed first with argon and then with hydrogen. The reaction was stirred at room temperature under H_2 (1 atm) for 1 h. The mixture was filtered through celite, and the recovered filtrate was concentrated to give 147 mg of compound **41** (quantitative yield). $[\alpha]_{25}^{D}$=-2.9 (*c* 2.54, CH_3OH); selected ^{1}H NMR (400 MHz $CDCl_3$): δ 3.66 (3H, s), 2.34 (1H, m), 2.21 (1H, m), 0.91 (3H, d, J = 6.4 Hz), 0.77 (3H, s), 0.64 (3H, s); ^{13}C NMR (100 MHz $CDCl_3$): δ 176.0, 56.9, 56.2, 55.0, 51.6, 47.3, 40.4, 39.0 (2C), 35.7 (3C), 32.5, 31.4, 31.3, 29.4, 29.3, 28.4, 27.2, 24.5, 22.6, 21.2, 18.6, 12.5, 12.4; HR ESIMS *m/z* 375.3269 $[M+H]^+$, $C_{25}H_{43}O_2$ requires 375.3263.

5α-cholan-24-oic acid (42). Compound **41** (50 mg, 0.1 mmol) was hydrolyzed with a methanol solution of sodium hydroxide (5%, 5 mL) in H_2O (1 mL) overnight under reflux. The resulting solution was then concentrated under vacuum, diluted with water, acidified with HCl 6 N and extracted with ethyl acetate (3 x 30 mL). The collected organic phases were washed with brine, dried over Na_2SO_4 anhydrous and evaporated under reduced pressure to give compound **42** (40 mg, 87%). An analytic sample was obtained by HPLC on a Nucleodur

100-5 C18 (5 μm; 4.6 mm i.d. x 250 mm) with MeOH/H_2O (92:8) as eluent (flow rate 1 mL/min, t_R=12 min);

$[\alpha]_{25}^{D}$=+17.7 (*c* 0.14, CH_3OH); selected ^1H NMR (400 MHz, CD_3OD): δ 2.31 (1H, m), 2.20 (1H, m), 0.94 (3H, d, *J* = 6.2 Hz), 0.81 (3H, s), 0.69 (3H, s). HR ESIMS *m/z* 359.2953 $[M-H]^-$, $C_{24}H_{39}O_2$ requires 359.2950.

5α-cholan-24-oyl-taurine sodium salt (43). Compound **42** (10 mg, 27.8 x 10^{-3} mmol) in DMF dry (3 mL) was treated with DMT-MM (16 mg, 58.2 x 10^{-3} mmol) and triethylamine (70 μL, 0.5 mmol) and the mixture was stirred at room temperature for 10 min. Then to the mixture was added taurine (15 mg, 0.2 mmol). After 24 h, the reaction mixture was concentrated under *vacuo* and dissolved in water (5 mL). The mixture was purified by HPLC on a Nucleodur 100-5 C18 (5 μm; 4.6 mm i.d. x 250 mm) with MeOH/H_2O (83:17) as eluent (flow rate 1 mL/min), to give 3.5 mg (27 %) of compound **43** (t_R=10.4 min); $[\alpha]_{25}^{D}$=+37. (*c* 0.03, CH_3OH); selected ^1H NMR (400 MHz, CD_3OD): δ 3.58 (2H, t, *J* = 7.0 Hz), 2.96 (2H, t, *J* = 7.0 Hz), 2.24 (1H, m), 2.09 (1H, m), 0.95 (3H, d, *J* = 6.2 Hz), 0.82 (3H, s), 0.69 (3H, s). HR ESIMS *m/z* 452.2840 $[M-Na]^-$, $C_{25}H_{42}NO_4S$ requires 452.2835.

5α-cholan-24-ol (44). Dry methanol (40 μL, 0.9 mmol) and $LiBH_4$ (470 μL, 2 M in THF, 0.9 mmol) were added to a solution of the compound **43** (50 mg, 0.11 mmol) in dry THF (10 mL) at 0 °C under argon and the resulting mixture was stirred for 2 h at 0 °C. The mixture was quenched by addition of NaOH (1 M, 260 μL) and then allowed to warm to room temperature. Ethyl acetate was added and the separated aqueous phase was extracted with ethyl acetate (3×15 mL). The combined organic phases were washed with water, dried (Na_2SO_4) and

concentrated. Purification by silica gel eluting with CH_2Cl_2:MeOH (85:15) gave the alcohol **44** as a white solid (45 mg, quantitative yield). An analytic sample was obtained by HPLC on a Nucleodur 100-5 C18 (5 μm; 4.6 mm i.d. x 250 mm) with MeOH/H_2O (92:8) as eluent (flow rate 1 mL/min, t_R=17.6 min); $[\alpha]_{25}^{D}$=+5.5 (*c* 1.14, CH_3OH); selected ^{1}H NMR (400 MHz $CDCl_3$): δ 3.51 (2H, m), 0.87 (3H, d, *J* = 6.3 Hz), 0.72 (3H, s), 0.60 (3H, s).^{13}C NMR (100 MHz $CDCl_3$): δ 63.6, 56.6, 56.1, 54.7, 47.0, 42.6, 40.1, 38.6, 35.6, 35.5 (2C), 32.2, 31.8, 29.3, 29.0 (2C), 28.2, 26.8, 24.2, 22.2, 20.8, 18.6, 12.2, 12.1; HR ESIMS *m/z* 347.3318 $[M+H]^+$, $C_{24}H_{43}O$ requires 347.3314.

5α-cholan-24-yl-24-triethylammonium solfate (45). At a solution of compound **44** (10 mg, 0.1 mmol) in DMF dry (3 mL) was added triethylamine-sulfur trioxide complex (26 mg, 0.1 mmol) under an argon atmosphere, and the mixture was stirred at 95 °C for 12 h. Most of the solvent was evaporated and the residue was poured over a RP18 column to remove excess $SO_3 \cdot NEt_3$. Fraction eluted with MeOH:H_2O 1:1 gave a mixture that was further purified by HPLC on a Nucleodur 100-5 C18 (5 μm; 4.6 mm i.d. x 250 mm) with MeOH:H_2O (90:10) as eluent (flow rate 1 mL/min), to give 1.4 mg of compound **10** (18%, t_R= 5 min). $[\alpha]_{25}^{D}$=-26.7 (*c* 0.02, CH_3OH); selected ^{1}H NMR (400 MHz, CD_3OD): δ 3.95 (2H, t, J = 6.7 Hz), 0.94 (3H, d, J = 6.5 Hz), 0.81 (3H, s), 0.69 (3H, s). HR ESIMS *m/z* 425.2730 $[M-Na]^-$, $C_{24}H_{41}O_4S$ requires 425.2726.

Luciferase reporter gene assay. To evaluate FXR mediated transactivation, HepG2 cells were transfected with 100 ng of pSG5-FXR, 100 ng of pSG5-RXR, 200 ng of the reporter vector p(hsp27)-TK-LUC containing the FXR response element IR1 cloned from the promoter of heat shock protein 27 (hsp27) and with

100 ng of pGL4.70 (Promega), a vector encoding the human Renilla gene. To evaluate GPBAR1 mediated transactivation, HEK-293T cells were transfected with 200 ng of pGL4.29 (Promega), a reporter vector containing a cAMP response element (CRE) that drives the transcription of the luciferase reporter gene luc2P, with 100 ng of pCMVSPORT6-human GPBAR1, and with 100 ng of pGL4.70. At 24 h post-transfection, cells were stimulated 18 h with 10 μM CDCA, TLCA and the synthetized compounds. In another experimental setting, at 24 hours post-transfection cells were stimulated with 50 μM of synthetized in combination with 10 μM CDCA (**1**) or TLCA (**2**). To calculate the IC_{50} versus GPBAR1, a dose response curve was performed in HEK-293T transfected as described above and stimulated 18 h with 1, 5, 25 and 50 μM compounds **30** and **42**. After treatments, 10 μL of cellular lysates were read using Dual Luciferase Reporter Assay System (Promega Italia srl, Milan, Italy) according manufacturer specifications using the Glomax20/20 luminometer (Promega Italia srl, Milan, Italy). Luciferase activities were assayed and normalized with Renilla activities.

Real-Time PCR. Total RNA was isolated from HepG2 or Glutag cells using the TRIzol reagent according to the manufacturer's specifications (Invitrogen). One microgram of purified RNA was treated with DNase-I and reverse transcribed with Superscript II (Invitrogen). For Real Time PCR, 10 ng template was dissolved in 25 μL containing 200 nmol/L of each primer and 12.5 μL of 2X SYBR FAST Universal ready mix (Invitrogen). All reactions were performed in triplicate, and the thermal cycling conditions were as follows: 2 min at 95 °C, followed by 40 cycles of 95 °C for 20 s and 60 °C for 30 s in iCycler iQ instrument (Biorad). The relative mRNA expression was calculated and expressed

as 2−(ΔΔCt). Forward and reverse primer sequences were the following, respectively:

human GAPDH, gaaggtgaaggtcggagt and catgggtggaatcatattggaa;

human OSTα, tgttgggccctttccaatac and ggctcccatgttctgctcac;

human BSEP, gggccattgtacgagatcctaa and tgcaccgtcttttcactttctg;

human SHP, gctgtctggagtccttctgg and ccaatgatagggcgaaagaagag;

mouse GAPDH, ctgagtatgtcgtggagtctac and gttggtggtgcaggatgcattg;

mouse Pro-glucagon, tgaagacaaacgccactcac and caatgttgttccggttcctc.

^{1}H NMR (400 MHz, $CDCl_3$) of compound **30**

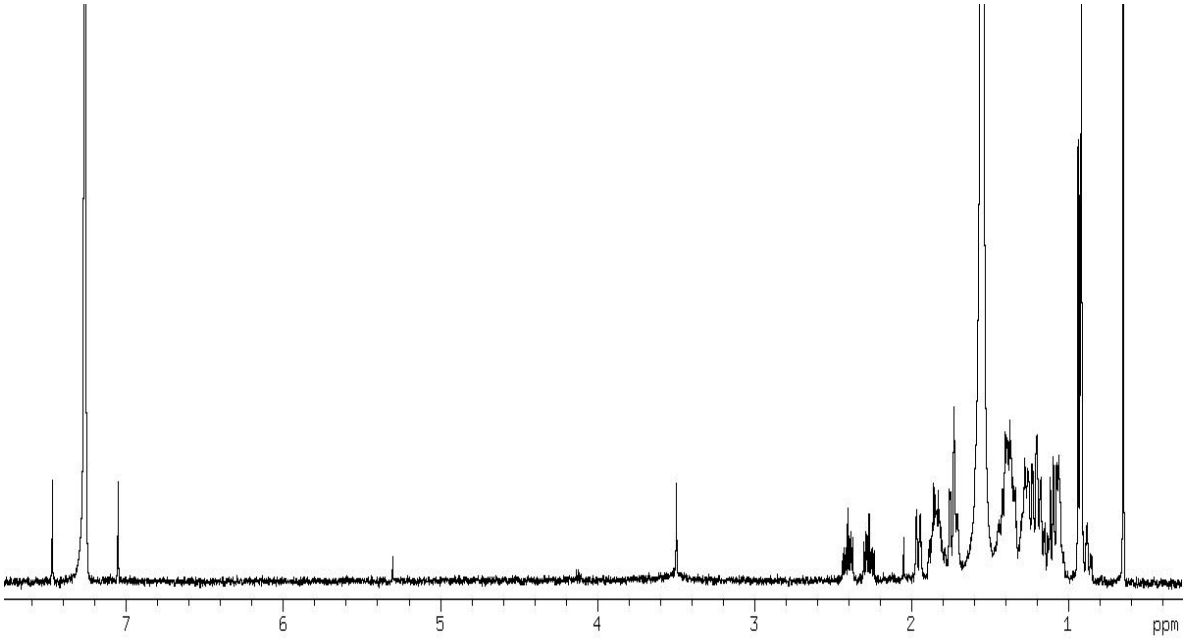

^{1}H NMR (400 MHz, CD_3OD) of compound **31**

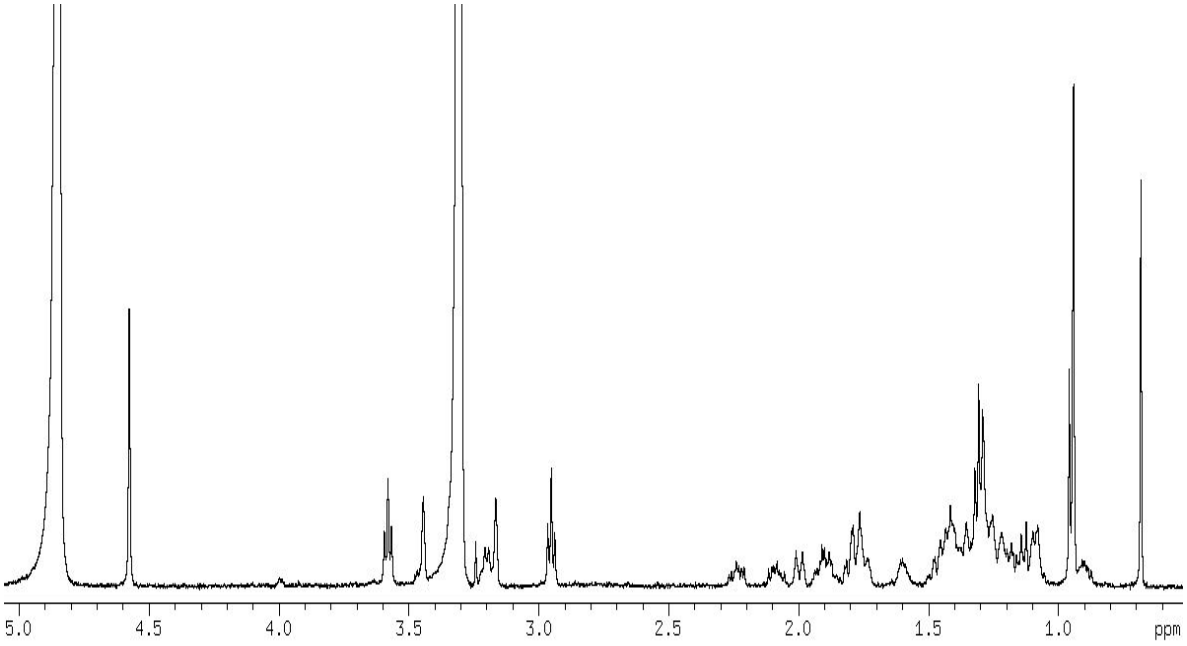

^{1}H NMR (400 MHz, CD_3OD) of compound **37**

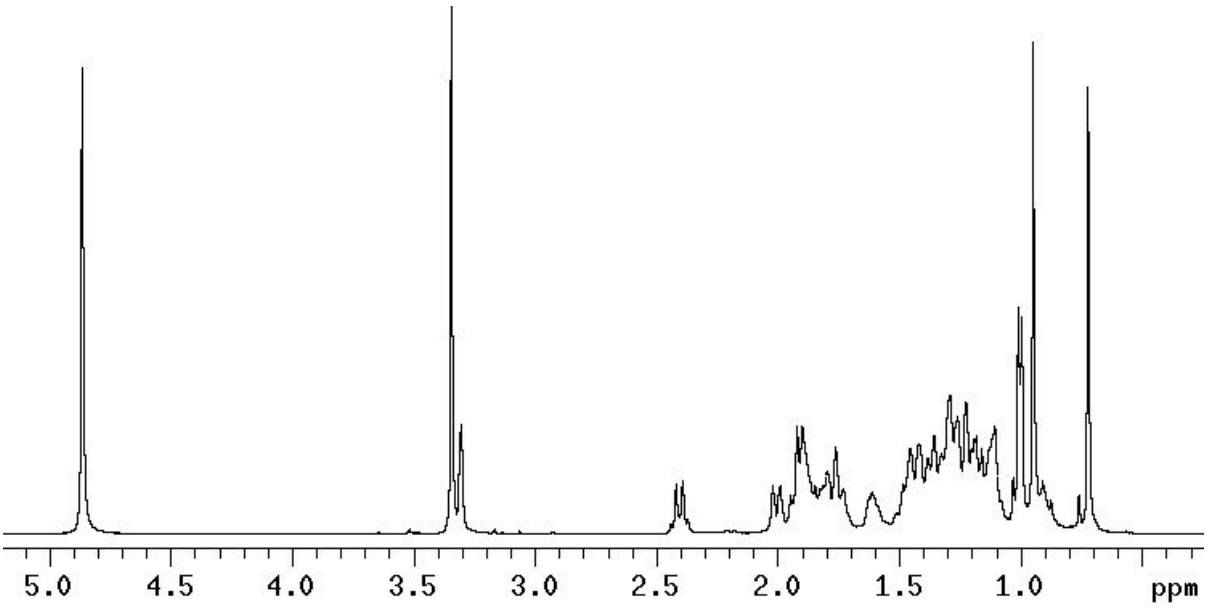

^{1}H NMR (400 MHz, CD_3OD) of compound **41**

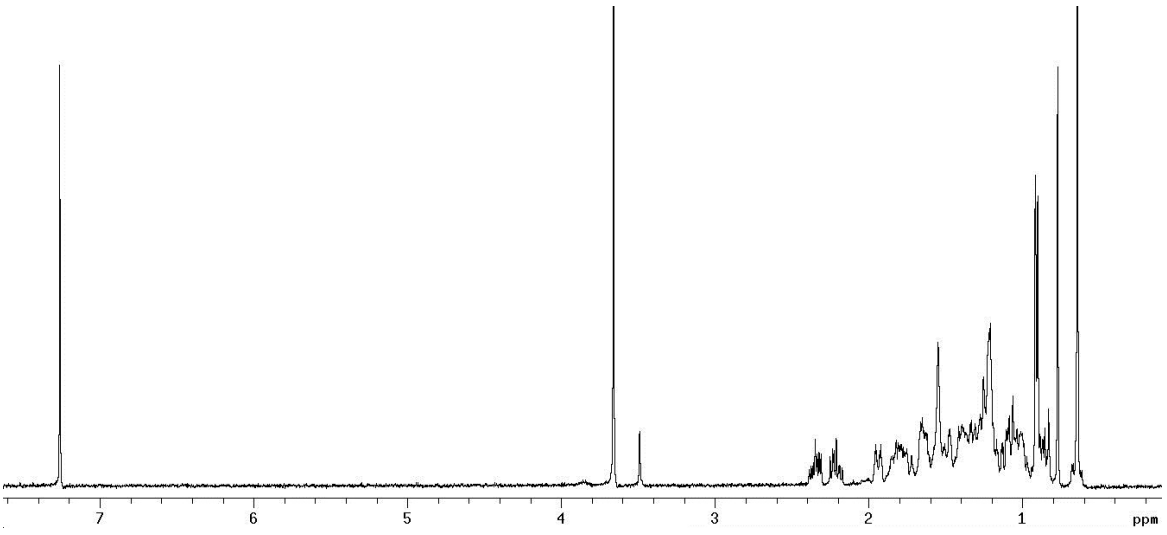

^{1}H NMR (400 MHz, CD_3OD) of compound **42**

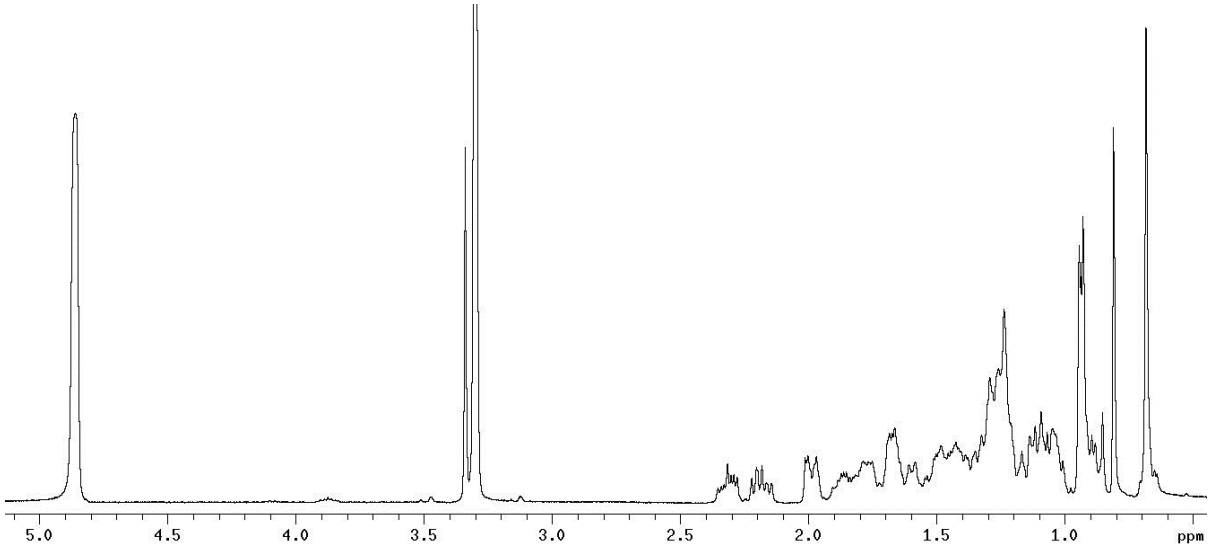

^{1}H NMR (500 MHz, CD_3OD) of compound **43**

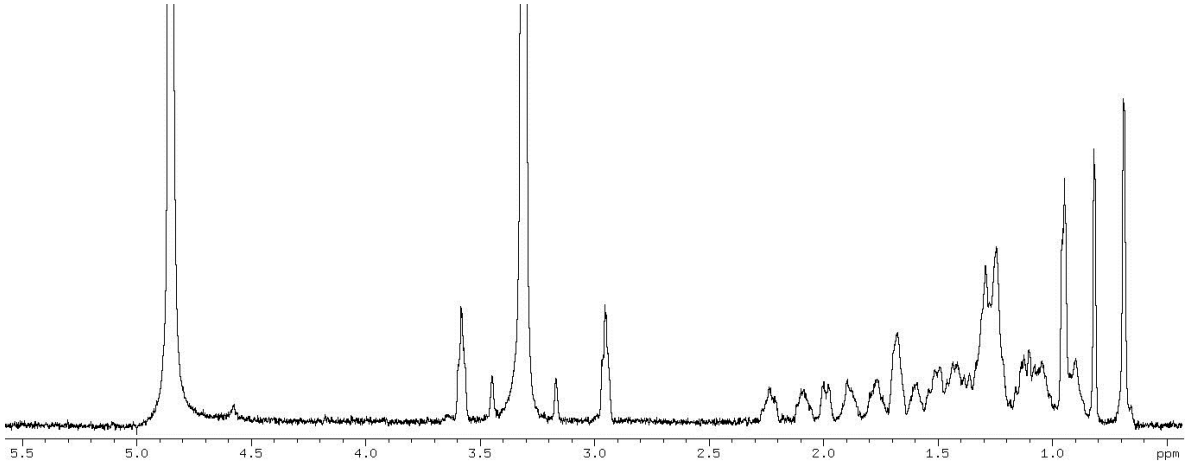

^{1}H NMR (400 MHz, $CDCl_3$) of compound **44**

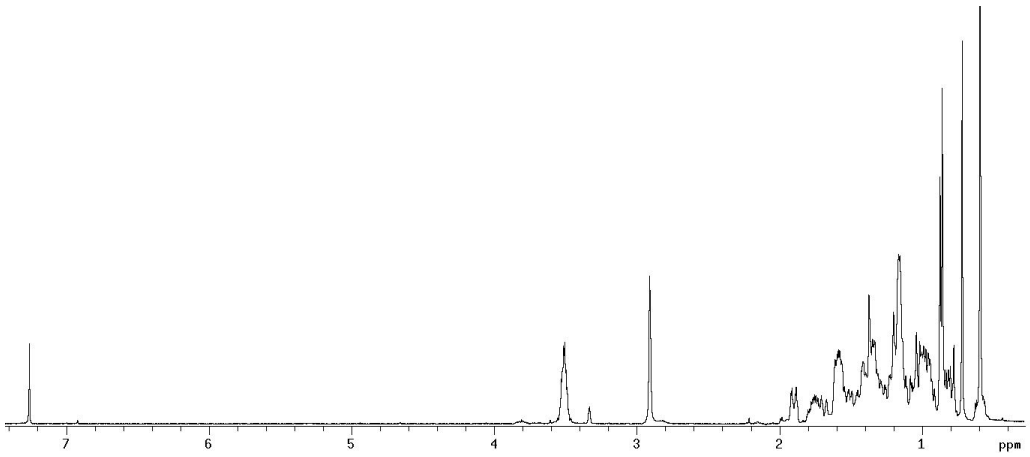

^{1}H NMR (400 MHz, CD_3OD) of compound **45**

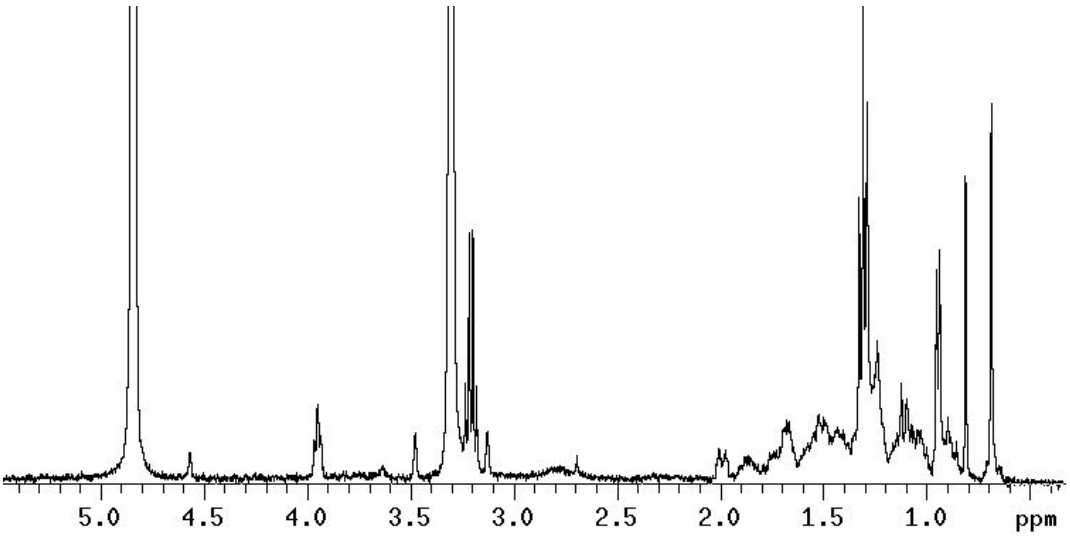

IV. Experimental section Hyodeoxycholic acid derivatives.

Compound 50. To a solution of HDCA (6 g, 15.3 mmol) in 50 mL of dry methanol, *p*-toluenesulfonic acid (10 g, 58.1 mmol) was added at room temperature. After 1h, the mixture was quenched by addition of $NaHCO_3$ saturated solution until the neutrality and, after evaporation, the residue was extracted with EtOAc (3×100 mL). The combined extracts were washed with brine, dried on Na_2SO_4, and evaporated to give the methyl ester **47** in quantitative yield.

2,6-Lutidine (17.4 mL, 150 mmol) and *tert*-butyldimethylsilyltrifluoromethanesulfonate (10.3 mL, 45 mmol) were added at 0 °C to a solution of **47** (6.1 g, 15 mmol) in 50 mL of CH_2Cl_2. After 2 h stirring at 0 °C, the reaction was quenched by addition of aqueous $NaHSO_4$ (1M, 100 mL). The layers were separated and the aqueous phase was extracted with CH_2Cl_2 (3×100 mL). The combined organic layers were washed with $NaHSO_4$, water, saturated aqueous $NaHCO_3$, brine and evaporated *in vacuo* to give protected methyl ester **48** in quantitative yield. To a solution of **48** (9.5 g, 15 mmol) in dry THF (50 mL) and dry methanol (1.82 mL, 45 mmol), $LiBH_4$ (22.5 mL, 2M in THF, 45 mmol) was added at 0 °C. After stirring for 2 h at 0 °C, the mixture was quenched by addition of NaOH 1M and then EtOAc. The organic phase was washed with water, dried (Na_2SO_4) and concentrated. Purification on silica gel (hexane/EtOAc 9:1 and 0.5% TEA) gave alcohol **49** in 56% yield (5 g, 8.3 mmol). DMSO (6.6 mL, 92 mmol) was added dropwise for 15 min to a solution of oxalyl chloride (23 mL, 46 mmol) in dry CH_2Cl_2 (50 mL) at -78 °C under argon atmosphere. After 30 min, a solution of alcohol **49** (4 g, 6.6 mmol) in dry CH_2Cl_2

was added via cannula and the mixture was stirred at -78 °C for 30 min. Et_3N (13.8 mL, 99 mmol) was added dropwise followed by NaCl saturated solution. The aqueous phase was extracted with Et_2O (3×100 mL). The combined organic phase was washed with water, dried (Na_2SO_4) and concentrated to give aldehyde **50** (4 g) as a colourless oil in quantitative yield.

Compound 52. To a solution of isopropyl triphenylphosphonium iodide (5.4 g, 12.5 mmol) in THF (2 mL), *n*-BuLi (5 mL, 12.5 mmol) was added dropwise at room temperature until the solution reached a red colour. After 30 min, a solution of aldehyde **50** (1.5 g, 2.5 mmol) in THF (5 mL) was added. After 1h, the mixture was quenched by addition of saturated aqueous $NaHCO_3$ (50 mL) and extracted with EtOAc (3x50 mL). The organic phase was dried (Na_2SO_4) and concentrated. Purification on silica gel (hexane) gave the protected intermediate in 84% yield.

To a solution of the protected intermediate (1.3 g, 2.1 mmol) in MeOH, 1 mL of HCl 37% v/v was added. After 1h, silver carbonate was added, the reaction mixture was centrifuged, and the supernatant was concentrated *in vacuo* to give compound **52** as a colourless amorphous solid (850 mg, quantitative yield). An analytic sample was purified by HPLC on a Nucleodur 100-5 C18 (5μm; 10 mm i.d. x 250 mm) with MeOH/H_2O (96:4) as eluent (flow rate 3 mL/min, t_R= 12 min). Selected ^{1}H NMR (400 MHz, $CDCl_3$): δ 5.10 (1H, t, *J* = 6.7 Hz, H-24), 4.08 (1H, dt, *J* = 11.9, 4.6 Hz, H-6β), 3.64 (1H, m, H-3β), 1.68 (3H, s, Me-26), 1.60 (3H, s, Me-27), 0.92 (3H, d, *J* = 7.0 Hz, Me-21), 0.91 (3H, s, Me-19), 0.65 (3H, s, Me-18); ^{13}C NMR (100 MHz, $CDCl_3$): δ 130.9, 125.3, 71.6, 68.2, 56.2 (x 2), 48.4, 42.9, 40.0, 39.9, 36.4, 36.2, 35.6, 35.3, 35.0, 34.9, 30.3, 29.3, 28.4, 25.7, 24.7, 24.3, 23.3, 20.9, 18.4, 17.7, 12.1. HR ESIMS *m/z* 403.3576 $[M+H]^+$, $C_{27}H_{46}O_2$ requires 403.3578.

Compound 57. A solution of **52** (350 mg, 0.9 mmol) in THF dry/MeOH dry (5 mL/5 mL, v/v) was hydrogenated in presence of $Pd(OH)_2$ 5% wt on activated carbon. After 12 h, the catalyst was filtered through Celite, and the recovered filtrate was concentrated under vacuum to give a colourless amorphous solid (350 mg, quantitative yield). An analytic sample was purified by HPLC on a Nucleodur 100-5 C18 (5μm; 10 mm i.d. x 250 mm) with MeOH/H_2O (95:5) as eluent (flow rate 3 mL/min, t_R= 8 min). Selected ^{1}H NMR (400 MHz, $CDCl_3$): δ 4.06 (1H, dt, *J* = 11.9, 4.6 Hz, H-6β), 3.62 (1H, m, H-3β), 0.91 (3H, s, Me-19), 0.90 (3H, d, *J* = 7.0 Hz, Me-21), 0.87 (3H, d, *J*= 6.6 Hz, Me-26), 0.86 (3H, d, *J*= 6.6 Hz, Me-27), 0.64 (3H, s, Me-18).^{13}C NMR (100 MHz, $CDCl_3$): δ 71.6, 68.2, 56.3, 56.2, 48.4, 42.9, 40.0, 39.9, 39.4, 36.4, 36.0, 35.9, 35.6, 35.5, 34.9, 30.4, 29.3, 28.4, 28.2, 22.7 (x 2), 24.4, 23.9, 23.3, 20.9, 18.8, 12.1. HR ESIMS *m/z* 405.3733 $[M+H]^+$, $C_{27}H_{49}O_2$ requires 405.3735.

Compound 53. Compound **53** (141 mg, 0.3 mmol, 20%) was prepared from **50** (1 g, 1.7 mmol) by an analogous procedure to that detailed above for **52**. An analytic sample was purified by HPLC on a Nucleodur 100-5 C18 (5μm; 4.6 mm i.d. x 250 mm) with MeOH/H_2O (96:4) as eluent (flow rate 3 mL/min) gave compound **53** (t_R= 17.2 min).

Compound 58. Hydrogenation on **53** gave **58**. An analytic sample was purified by HPLC purification on a Nucleodur 100-5 C18 (5μm; 4.6 mm i.d. x 250 mm) with MeOH/H_2O (96:4) as eluent (flow rate 1 mL/min) gave compound **58** (t_R= 16 min). Selected ^{1}H NMR (400 MHz, CD_3OD): δ 4.01 (1H, dt, *J* = 11.9, 4.5 Hz, H-6β), 3.50 (1H, m, H-3β), 0.93 (3H, d, *J* = 6.6 Hz, Me-21), 0.92 (3H, s, Me-19), 0.87 (6H, d, *J* = 6.7 Hz, Me-27 and Me-28), 0.68 (3H, s, Me-18).^{13}C NMR (100

MHz, $CDCl_3$): δ 71.6, 68.1, 56.2 (x 2), 48.4, 42.8, 39.9, 39.8, 39.1, 36.0, 35.9, 35.7, 35.5, 35.1, 34.8, 30.3, 29.1, 28.2, 28.0, 27.9, 26.3, 24.2, 23.7, 23.6, 23.5, 20.7, 18.6, 12.0. HR ESIMS *m/z* 419.3889 $[M+H]^+$, $C_{28}H_{51}O_2$ requires 419.3892.

Compound 51. Compound **51** (370 mg, 1.0 mmol, 60%) was obtained from **50** (1 g, 1.7 mmol) by an analogous procedure to that detailed above for **52**. An analytic sample was purified by HPLC on a Nucleodur 100-5 C18 (5μm; 10 mm i.d. x 250 mm) with MeOH/H_2O (96:4) as eluent (flow rate 3 mL/min) giving pure compound **51** (t_R=5 min). Selected ^{1}H NMR (400 MHz, $CDCl_3$): δ 5.80 (1H, m, H-24), 4.99 (1H, d, *J* = 17.1 Hz, H-25), 4.91 (1H, d, *J* = 9.8 Hz, H-25), 4.05 (1H, dt, *J* = 12.0, 4.5 Hz, H-6β), 3.62 (1H, m, H-3β), 0.91 (3H, s, Me-19), 0.92 (3H, d, *J* = 7.0 Hz, Me-21), 0.64 (3H, s, Me-18).^{13}C NMR (100 MHz, $CDCl_3$): δ 139.6, 113.9, 71.6, 68.1, 56.2, 56.1, 48.4, 42.8, 39.9, 39.8, 36.0, 35.5, 35.3, 35.2, 35.1, 34.8, 30.5, 30.2, 29.2, 28.2, 24.2, 23.5, 20.7, 18.4, 12.0.

HR ESIMS *m/z* 375.3263 $[M+H]^+$, $C_{25}H_{43}O_2$ requires 375.3266.

Compound 56. Reduction of **51** (125 mg, 0.3 mmol) in the same procedure to that detailed above for **57**, gave 87 mg of compound **56** (70%). Purification by HPLC on a Nucleodur 100-5 C18 (5μm; 4.6 mm i.d. x 250 mm) with MeOH/H_2O (9:1) as eluent (flow rate 1 mL/min), (t_R=18.6 min) furnished pure compound **56**. Selected ^{1}H NMR (400 MHz, CD_3OD): δ 3.99 (1H, dt, *J* = 12.2, 4.6 Hz, H-6β), 3.50 (1H, m, H-3β), 0.92 (3H, s, Me-19), 0.93 (3H, d, *J* = 6.8 Hz, Me-21), 0.90 (3H, t, *J* = 6.8 Hz, Me-25), 0.68 (3H, s, Me-18). ^{13}C NMR (100 MHz, $CDCl_3$): δ 71.6, 68.1, 56.2, 56.1, 48.4, 42.8, 39.9, 39.8, 35.9, 35.7, 35.5, 35.2, 35.0, 34.8, 30.2, 29.2, 28.3, 28.2, 24.2, 23.5, 23.1, 20.7, 18.6, 14.2, 12.0. HR ESIMS *m/z* 377.3420 $[M+H]^+$, $C_{25}H_{45}O_2$ requires 377.3422.

Compounds 54 and **55.** The mixture of diasteroisomers at the side chain double bond (125 mg, 0.3 mmol, 67% over two steps) was prepared from **50** (250 mg, 0.4 mmol) by an analogous procedure to that detailed above for **52**. A small portion of the mixture was purified by HPLC on a Nucleodur 100-5 C18 (5 μm; 10 mm i.d. x 250 mm) with MeOH/H_2O (96:4) as eluent (flow rate 3 mL/min) to give pure compounds **54** (t_R= 13.6 min) and **55** (t_R=16.2 min).

Compound 54. Selected ^{1}H NMR (400 MHz, $CDCl_3$): δ 7.33-7.18(5H, Ph), 6.38 (1H, d, *J* = 15.7 Hz, H-25), 6.20 (1H, dt, *J* = 15.7, 6.8 Hz, H-24), 4.05 (1H, dt, *J* = 12.1, 4.5 Hz, H-6β), 3.62 (1H, m, H-3β), 2.28 (1H, m, H-23), 2.10 (1H, m, H-23), 0.96 (3H, d, *J* = 6.4 Hz, Me-21), 0.91 (3H, s, Me-19), 0.65 (3H, s, Me-18).^{13}C NMR (100 MHz, $CDCl_3$): δ 138.0, 131.5, 129.3, 128.4, 126.8, 125.9, 71.6, 68.2, 56.2 (x 2), 48.4, 42.9, 40.0, 39.9, 36.4, 35.8, 35.6, 35.5, 35.2, 35.1, 30.4, 29.8, 29.3, 28.4, 24.4, 23.4, 20.9, 18.6, 12.1. HR ESIMS *m/z* 451.3576 $[M+H]^+$, $C_{31}H_{47}O_2$ requires 451.3580.

Compound 55. Selected ^{1}H NMR (400 MHz, $CDCl_3$): δ 7.33-7.21 (5H, Ph),6.39 (1H, d, *J* = 11.7 Hz, H-25), 5.64 (1H, dt, *J* = 11.7, 7.3 Hz, H-24), 4.05 (1H, dt, *J* = 12.0, 4.5 Hz, H-6β), 3.62 (1H, m, H-3β), 2.38 (1H, m, H-23), 2.22 (1H, m, H-23), 0.91(3H, s, Me-19), 0.89 (3H, d, *J* = 6.8 Hz, Me-21), 0.64 (3H, s, Me-18).^{13}C NMR (100 MHz, $CDCl_3$): δ 137.8, 133.6, 128.7, 128.6, 128.2, 126.4, 71.6, 68.2, 56.2 (x 2), 48.4, 42.9, 40.0, 39.9, 36.4, 36.2, 35.6, 35.5, 35.1 (x2), 30.4, 29.3, 28.4, 25.5, 24.4, 23.3, 20.9, 18.5, 12.1. HR ESIMS *m/z* 451.3576 $[M+H]^+$, $C_{31}H_{47}O_2$ requires 451.3579.

Compound 59. Hydrogenation on the mixture of **54** and **55** (40 mg, 0.1 mmol) gave compound **59** (quantitative yield). An analytic sample was purified by HPLC

on a Nucleodur 100-5 C18 (5 μm; 4.6 mm i.d. x 250 mm) with MeOH/H_2O (96:4) as eluent (flow rate 1 mL/min, t_R= 7.6 min). Selected ^{1}H NMR (400 MHz, $CDCl_3$): δ 7.27-7.16 (5H, Ph), 4.05 (1H, dt, *J* = 11.9, 4.5 Hz, H-6β), 3.62 (1H, m, H-3β), 2.60 (2H, m, H_2-25), 0.90 (3H, s, Me-19), 0.89 (3H, d, *J* = 6.8Hz, Me-21), 0.64 (3H, s, Me-18).^{13}C NMR (100 MHz, $CDCl_3$): δ 143.0, 128.4, 128.3, 125.6, 71.6, 68.2, 56.2 (x 2), 48.4, 42.9, 40.0, 39.9, 36.3, 36.1, 35.7, 35.6, 35.5, 35.2 (x 2), 32.0, 30.4, 29.3, 28.4, 26.0, 24.4, 23.4, 20.9, 18.6, 12.1. HR ESIMS *m/z* 453.3733 $[M+H]^+$, $C_{31}H_{49}O_2$ requires 453.3735.

Compound 60. Compound **60 (**1.9 g, 4.8 mmol) was prepared as previously reported[133]

Compound 61. Aldehyde **61** (1 g, 1.7 mmol, 94%) was prepared from **60** (1.9 g, 4.8 mmol) by an analogous procedure to that detailed above for **50**.

Compound 63. Compound **63** (264 mg, 0.7 mmol, 80% over two steps) was prepared from **61** (500 mg, 0.9 mmol) by the same procedure described for **52**. An analytic sample was purified by HPLC on a Nucleodur 100-5 C18 (5 μm; 10 mm i.d. x 250 mm) with MeOH/H_2O (96:4) as eluent (flow rate 3mL/min, t_R=16 min) giving pure compound **63**. Selected ^{1}H NMR (400 MHz, CD_3OD): δ 5.12 (1H, brt, *J* = 6.8 Hz, H-23), 4.01 (1H, dt, *J* = 11.9, 4.6 Hz, H-6β), 3.50 (1H, m, H-3β), 1.70 (3H, s, Me-26), 1.59 (3H, s, Me-25), 0.93 (3H, s, Me-19), 0.90 (3H, d, *J* = 6.7 Hz, Me-21), 0.69 (3H, s, Me-18).^{13}C NMR (100 MHz, CD_3OD): δ 132.8, 124.2, 72.4, 68.6, 57.6 (x 2), 49.9, 44.1, 41.3 (x 2), 38.2, 37.0, 36.8, 36.2, 35.6, 35.5, 31.1, 29.9, 29.5, 26.1, 25.5, 24.1, 21.9, 19.2, 18.0, 12.4. HR ESIMS *m/z* 389.3420 $[M+H]^+$, $C_{26}H_{45}O_2$ requires 389.3424.

Compound 65. Hydrogenation on **63** (100 mg, 0.3 mmol), in the same procedure detailed for **57**, gave **65** (90 mg, 0.2 mmol, 90%). An analytic sample was purified by HPLC on a Nucleodur 100-5 C18 (5 μm; 10 mm i.d. x 250 mm) with MeOH/H_2O (96:4) as eluent (flow rate 3mL/min) giving pure compound **65** (t_R=18.4 min). Selected ^{1}H NMR (400 MHz, CD_3OD): δ 4.01 (1H, dt, *J* = 12.1, 4.6 Hz, H-6β), 3.51 (1H, m, H-3β), 0.94 (3H, s, Me-19), 0.93(3H, d, *J* = 6.5 Hz, Me-21), 0.89 (3H, d, *J* = 6.0 Hz, Me-25), 0.87 (3H, d, *J* = 6.0 Hz, Me-26), 0.68 (3H, s, Me-18).^{13}C NMR was recorded on Varian Inova100 MHz, using $CDCl_3$ as solvent: δ 71.6, 68.1, 56.2 (x 2), 48.4, 42.8, 39.9, 39.8, 35.9, 35.8, 35.5, 35.3, 35.1, 34.8, 33.5, 30.3, 29.2, 28.4, 28.2, 24.2, 23.5, 23.0, 22.4, 20.7, 18.7, 12.0. HR ESIMS *m/z* 391.3576 $[M+H]^+$, $C_{26}H_{47}O_2$ requires 391.3579.

Compound 62. Wittig olefination on aldehyde **61** (500 mg, 0.9 mmol), as described for compound **52**, gave **62** (290 mg, 0.8 mmol, 95% over two steps). An analytic sample was purified by HPLC on a Nucleodur100-5 C18 (5 μm; 10 mm i.d. x 250 mm) with MeOH/H_2O (96:4) as eluent (flow rate 3mL/min), giving pure compound **62** (t_R=11.0 min). Selected ^{1}H NMR (400 MHz, $CDCl_3$): δ 5.77 (1H, m, H-23), 5.01 (1H, ovl, H-24), 4.99 (1H, ovl, H-24), 4.06 (1H, dt, *J* = 12.1, 4.6 Hz, H-6β), 3.63(1H, m, H-3β), 0.92 (3H, d, *J* = 6.6 Hz, Me-21), 0.91 (3H, s, Me-19), 0.66 (3H, s, Me-18). ^{13}C NMR (100 MHz, $CDCl_3$): δ 137.3, 115.7, 71.6, 68.1, 56.1, 55.8, 48.4, 42.8, 40.5, 39.9, 39.8, 35.9, 35.8, 35.5, 35.1, 34.8, 30.3, 29.2, 28.2, 24.2, 23.5, 20.7, 18.6, 12.0. HR ESIMS *m/z* 361.3107 $[M+H]^+$, $C_{24}H_{41}O_2$ requires 361.3109.

Compound 64. Hydrogenation on **61** (100 mg, 0.3 mmol), in the same procedure detailed for **57**, gave **64** (88 mg, 0.2 mmol, 88%). Purification by HPLC on a

Nucleodur100-5 C18 (5 μm; 4.6 mm i.d. x 250 mm) with MeOH/H_2O (96:4) as eluent (flow rate 1 mL/min), gave pure compound **64** (t_R=8.0 min). Selected ^{1}H NMR (400 MHz, $CDCl_3$): δ 4.06 (1H, dt, *J* = 12.1, 4.6 Hz, H-6β), 3.62 (1H, m, H-3β), 0.91 (3H, s, Me-19), 0.89 (3H, d, *J* = 7.0 Hz, Me-21), 0.86 (3H, t, *J* = 7.6 Hz, Me-23), 0.64 (3H, s, Me-18).^{13}C NMR (100 MHz, $CDCl_3$): δ 71.6, 68.2, 56.0, 55.9, 48.4, 42.7, 39.9, 39.8, 38.2,36.4, 35.5, 35.4, 35.1, 34.8, 30.2, 29.3,28.2, 24.3, 23.5, 20.8, 19.2, 18.6, 12.0, 14.5. HR ESIMS *m/z* 363.3263 $[M+H]^+$, $C_{24}H_{43}O_2$ requires 363.3266.

Compound 66. To a solution of HDCA (2 g, 5.1 mmol) in dry pyridine (100 mL), an excess of acetic anhydride was added. Pyridine was concentrated under vacuum and the residue was poured into cold water (100 mL) and extracted with EtOAc (3×50 mL). The combined organic phases were dried (Na_2SO_4) and concentrated. Flash chromatography on silica gel using CH_2Cl_2/MeOH 98:2 as eluent gave **66** (2.35 g, quantitative yield).

Compound 67. Compound **66** (2.35 g, 4.9 mmol) was dissolved in toluene dry/pyridine dry (10 mL:100 μL, 10:1 v/v) and $Cu(OAc)_2$ H_2O (2.9 g, 14.7 mmol) was added in dark. After 30 min, $Pb(OAc)_4$ (11 g, 24.5 mmol) was added. After 3 h, the solution was heated to reflux for 1 h (no longer in the dark). The mixture was then cooled, and aqueous ethylene glycol was added. The resulting mixture was extracted with ether (3x50 mL) and the combined organic phases were washed with saturated solution of $NaHCO_3$, water and brine. After drying over Na_2SO_4, the residue was evaporated under vacuum to give **67**. Purification by flash chromatography on silica gel (Hexane/EtOAc 95:5 with 0.5% of TEA) gave pure **67** (360 mg, 0.8 mmol).

Compound 68. Compound **67** (360 mg, 0.8 mmol) was treated with CH_3ONa (224 mg, 4.15 mmol) in $CHCl_3$ dry/MeOH dry (10 mL:6mL, 5:3 v/v). After stirring for 12 h, water was added and methanol was evaporated. The residue was extracted with EtOAc (3x50mL). The combined organic layers were washed with brine, dried and evaporated to dryness to give 259 mg (90%) of **68**. An analytic sample was purified by HPLC on a Nucleodur 100-5 C18 (5 μm; 4.6 mm i.d. x 250 mm) with MeOH/H_2O (93:7) as eluent (flow rate 1 mL/min, t_R= 6 min). Selected ^{1}H NMR (400 MHz, $CDCl_3$): δ 5.68 (1H, m, H-22), 4.89 (1H, d, *J* = 17.3 Hz, H-23), 4.81 (1H, d, *J* = 10.1 Hz, H-23), 4.06 (1H, dt, *J* = 11.8, 4.4 Hz, H-6β), 3.62 (1H, m, H-3β), 1.02 (3H, d, *J* = 6.5 Hz, Me-21), 0.91 (3H, s, Me-19), 0.66 (3H, s, Me-18).^{13}C NMR (100 MHz, $CDCl_3$): δ 145.3, 111.5, 71.6, 68.2, 56.3, 55.5, 48.5, 42.7, 41.2, 40.0, 39.8, 36.4, 35.6, 35.5, 34.9, 30.4, 29.3, 28.5, 24.2, 23.3, 20.9, 20.2, 12.1. HR ESIMS *m/z* 347.2950 $[M+H]^+$, $C_{23}H_{39}O_2$ requires 347.2953.

Compound 69. Hydrogenation on **68** (100 mg, 0.3 mmol) furnished **69** (99 mg, 0.3 mmol, quantitative yield). An analytic sample was purified by HPLC on a Nucleodur 100-5 C18 (5μm; 4.6 mm i.d. x 250 mm) with MeOH/H_2O (90:10) as eluent (flow rate 1 mL/min, t_R=9.4 min). Selected ^{1}H NMR (400 MHz, $CDCl_3$): δ 4.07 (1H, dt, *J* = 12.1, 4.6 Hz, H-6β), 3.63 (1H, m, H-3β), 0.91 (3H, s, Me-19), 0.89 (3H, d, *J* = 7.0 Hz, Me-21), 0.82 (3H, t, *J* = 7.4 Hz, Me-23), 0.64 (3H, s, Me-18). ^{13}C NMR (100 MHz, $CDCl_3$): δ 71.6, 68.1, 56.1, 55.7, 48.4, 42.7, 39.9, 39.8, 37.2, 36.4, 35.5, 35.4, 35.1, 30.4, 29.3, 28.5, 28.4, 24.5, 23.5, 21.0, 18.0, 12.0, 10.4. HR ESIMS *m/z* 349.3107 $[M+H]^+$, $C_{23}H_{41}O_2$ requires 349.3110.

Compound 70. Aldehyde **70** (1.8 g, 3.8 mmol, 72%) was prepared starting from LCA (2 g, 5.3 mmol), as reported for aldehyde **34**.

Compound 71. Compound **71** (653 mg, 1.8 mmol, quantitative yield over two steps) was obtained from **70** (900 mg, 1.9mmol) as described for **52**. An analytic sample was purified by HPLC on a Nucleodur 100-5 C18 (5 μm; 4.6 mm i.d. x 250 mm) with MeOH/H_2O (99:1) as eluent (flow rate 1 mL/min, t_R=10 min). Selected^{1}H NMR (400 MHz, $CDCl_3$): δ 5.80 (1H, m, H-24), 4.99 (1H, d, *J* = 17.1 Hz, H-25), 4.91 (1H, d, *J* = 9.8 Hz, H-25), 4.05 (1H, dt, *J* = 12.0, 4.5 Hz, H-6β), 3.62 (1H, m, H-3β), 0.91 (3H, s, Me-19), 0.92 (3H, d, *J* = 7.0 Hz, Me-21), 0.64 (3H, s, Me-18).^{13}C NMR (100 MHz, $CDCl_3$): δ 139.6, 113.9, 71.6, 56.5, 56.2, 42.7, 42.2, 40.5, 40.2, 36.5, 35.8, 35.3, 35.2, 34.8, 34.6, 30.5, 30.2, 28.3, 27.2, 26.4, 24.2, 23.5, 20.8, 18.4, 12.0. HR ESIMS *m/z* 359.3314 $[M+H]^+$, $C_{25}H_{43}O$requires 359.3317.

Compound 73. Hydrogenation on **71** (400 mg, 1.1 mmol) gave **73** (338 mg, 0.9 mmol, 86%). An analytic sample was purified by HPLC on a Nucleodur 100-5 C18 (5μm; 4.6 mm i.d. x 250 mm) with MeOH/H_2O (99:1) as eluent (flow rate 1 mL/min, t_R=13.4 min). Selected ^{1}H NMR (400 MHz, $CDCl_3$): δ 3.63 (1H, m, H-3β), 0.93 (3H, s, Me-19), 0.92 (3H, ovl,Me-21), 0.89 (3H, t, *J*= 7.3 Hz, Me-25).^{13}C NMR (100 MHz, $CDCl_3$): δ 71.9, 56.5, 56.3, 42.7, 42.1, 40.5, 40.2, 36.5, 35.9, 35.7, 35.6, 35.3, 34.6, 30.6, 28.3 (x2), 27.2, 26.4, 24.2, 23.4, 23.1, 20.8, 18.6, 14.2, 12.0. HR ESIMS *m/z* 361.3470 $[M+H]^+$, $C_{25}H_{45}O$ requires 361.3472.

Compound 72. Compound **72** (367 mg, 1.0 mmol, 40% over two steps) was prepared from **70** (900 mg, 1.9 mmol) as detailed for **52**. An analytic sample was purified by HPLC on a Nucleodur 100-5 C18 (5 μm; 4.6 mm i.d. x 250 mm) with

MeOH/H_2O (99:1) as eluent (flow rate 1 mL/min, t_R=12.4 min). Selected ^{1}H NMR (400 MHz, $CDCl_3$): δ 5.08 (1H, t, *J* = 6.6 Hz, H-24), 3.62 (1H, m, H-3β), 1.68 (3H, s, Me-26), 1.60 (3H, s, Me-27), 0.92 (3H, ovl, Me-21), 0.92 (3H, s, Me-19), 0.64 (3H, s, Me-18).^{13}C NMR (100 MHz, $CDCl_3$): δ 130.9, 125.2, 71.9, 56.5, 56.2, 42.7, 42.1, 40.4, 40.2, 36.5, 36.1, 35.8, 35.6, 35.3, 34.6, 30.6, 28.3, 27.2, 26.4, 25.7, 24.7, 24.2, 23.4, 20.8, 18.6, 17.6, 12.0. HR ESIMS *m/z* 387.3620 $[M+H]^+$, $C_{27}H_{47}O$ requires 387.3623.

Compound 74. Hydrogenation on **72** (100 mg, 0.3 mmol) gave **74** (98 mg, quantitative yield). An analytic sample was purified by HPLC on a Nucleodur 100-5 C18 (5 μm; 4.6 mm i.d. x 250 mm) with MeOH/H_2O (99:1) as eluent (flow rate 1 mL/min, t_R=16.6 min). Selected ^{1}H NMR (400 MHz, $CDCl_3$): δ 3.63 (1H, m, H-3β), 0.93 (3H, s, Me-19), 0.91 (3H, d, *J*= 6.6 Hz, Me-21), 0.87 (6H, d, *J*= 6.7 Hz, Me-26 and Me-27), 0.65 (3H, s, Me-18).^{13}C NMR (100 MHz, $CDCl_3$): δ 71.9, 56.5, 56.3, 42.6, 42.0, 40.5, 40.2, 39.5, 36.5, 36.2, 35.9, 35.8, 35.3, 34.7, 30.6, 28.3 (x 2), 27.2, 26.4, 24.2, 23.8, 23.3, 22.5 (x 2), 20.8, 18.7, 12.1. HR ESIMS *m/z* 389.3783 $[M+H]^+$, $C_{27}H_{49}O$ requires 389.3786.

Compound 76. Compound **76** (954 mg, 2.6 mmol, quantitative yield over two steps) was obtained from LCA (1 g, 2.7 mmol) as reported for compound **67**.

Compound 77. Compound **77** was obtained from **76** (954 mg, 2.6 mmol)as reported for **68**. Purification on silica gel (hexane/EtOAc 97:3 and 0.5% TEA) gave pure **77** (228 mg, 0.7 mmol, 27% yield). Selected ^{1}H NMR (400 MHz, $CDCl_3$): δ 5.68 (1H, m, H-22), 4.90 (1H, d, *J*= 17.2 Hz, H-23), 4.82 (1H, d, *J*= 10.0 Hz, H-23), 3.63 (1H, m, H-3β), 1.03 (3H, d, J= 6.2 Hz, Me-21), 0.93 (3H, s, Me-19), 0.68 (3H, s, Me-18).^{13}C NMR (100 MHz, $CDCl_3$): δ 145.3, 111.5, 71.9,

56.4, 55.6, 42.7, 42.1, 41.2, 40.5, 40.1, 36.4, 35.9, 35.3, 34.6, 30.5, 28.5, 27.2, 26.4, 24.3, 23.4, 20.8, 20.2, 12.3. HR ESIMS *m/z* 331.3001 $[M+H]^+$, $C_{23}H_{39}O$ requires 331.3004.

Compound 78. Hydrogenation on **77** (100 mg, 0.3 mmol) gave **78** (22 mg, 0.1 mmol, 22%). HPLC purification on a Nucleodur 100-5 C18 (5 μm; 4.6 mm i.d. x 250 mm) with MeOH/H_2O (92:8) as eluent (flow rate 1 mL/min,) gave pure compound **78** (t_R=26 min). Selected ^{1}H NMR (400 MHz, $CDCl_3$): δ 3.62 (1H, m, H-3β), 0.92 (3H, s, Me-19), 0.89 (3H, d, *J* = 6.6 Hz, Me-21), 0.83 (3H, t, J = 7.5 Hz, Me-23), 0.65 (3H, s, Me-18).^{13}C NMR (100 MHz, $CDCl_3$): δ 71.8, 56.4, 56.2, 42.6, 42.0, 40.5, 40.2, 37.2, 36.5, 35.7, 35.3, 35.0, 30.6, 28.4, 28.3, 27.1, 26.4,24.2, 23.3, 20.8, 18.2, 12.1, 10.4.HR ESIMS *m/z* 333.3157 $[M+H]^+$, $C_{23}H_{41}O$ requires 333.3159.

Compound 79. Compound **79** was prepared as previously described.[95]

Compound 80. Compound **80** (820 mg, 1.7 mmol, 34%) was prepared from **79** (2 g, 5.1 mmol) in the same operative conditions reported for aldehyde **50**.

Compound 82. Compound **82** (110 mg, 0.3 mmol, 34%) was prepared from **80** (400 mg, 0.8 mmol) in the same operative conditions reported for **52.** An analytic sample was purified by HPLC on a Nucleodur 100-5 C18 (5 μm; 4.6 mm i.d. x 250 mm) with MeOH/H_2O (99:1) as eluent (flow rate 1 mL/min), giving pure compound **82** (t_R=20.4 min). Selected ^{1}H NMR (400 MHz, $CDCl_3$): δ 5.10 (1H, brt, *J* = 6.9 Hz, H-24), 3.63 (1H, m, H-3α), 1.69 (3H, s, Me-26), 1.61 (3H, s, Me-27), 0.94 (3H, d, *J* = 6.6 Hz, Me-21), 0.93 (3H, s, Me-19), 0.65 (3H, s, Me-18).^{13}C NMR (100 MHz, $CDCl_3$): δ 130.9, 125.2, 71.4, 56.5, 56.2, 54.4, 44.8, 42.6, 40.0, 38.2, 37.0, 36.1, 35.6, 35.5, 35.4, 32.0, 31.5, 28.7, 28.2, 25.7, 24.7, 24.2, 21.3,

18.6, 17.6, 12.3, 12.1. HR ESIMS *m/z* 387.3627 $[M+H]^+$, $C_{27}H_{47}O$ requires 387.3630.

Compound 84. Hydrogenation on **82** (90 mg, 0.2 mmol) afforded **84** (86 mg, 0.2 mmol, quantitative yield). Purification by HPLC on a Nucleodur 100-5 C18 (5 μm; 4.6 mm i.d. x 250 mm) with MeOH/H_2O (99:1) as eluent (flow rate 1 mL/min) gave pure compound **84** (t_R= 25.2 min). Selected ^{1}H NMR (400 MHz, $CDCl_3$): δ 3.61(1H, m, H-3α), 0.91 (3H, d, *J*= 6.5 Hz,Me-21), 0.87 (3H, d, *J*= 6.6 Hz, Me-26), 0.86 (3H, d, *J*= 6.6 Hz, Me-27), 0.81 (3H, s, Me-19), 0.66 (3H, s, Me-18).^{13}C NMR (100 MHz, $CDCl_3$): δ 71.4, 56.5, 56.3, 54.4, 44.9, 42.7, 40.0, 39.4, 38.2, 37.0, 36.4, 36.0, 35.7, 35.6, 32.1, 31.5, 28.7, 28.4, 28.2, 22.5 (x 2), 24.2, 23.9, 21.3, 18.6, 12.3, 12.1. HR ESIMS *m/z* 389.3783 $[M+H]^+$, $C_{27}H_{49}O$ requires 389.3785.

Compound 81. Compound **81** (114 mg, 0.3 mmol, 38%) was obtained from **80** (400 mg, 0.8 mmol) in the same operative conditions reported for **52**. An analytic sample was purified by HPLC on a Nucleodur 100-5 C18 (5 μm; 4.6 mm i.d. x 250 mm) with MeOH/H_2O (99:1) as eluent (flow rate 1 mL/min), giving pure compound **81** (t_R=15.4 min). Selected ^{1}H NMR (400 MHz, $CDCl_3$): δ 5.80 (1H, m, H-24), 4.98 (1H, d, *J* = 17.0Hz, H-25), 4.90 (1H, d, *J* = 9.8 Hz, H-25), 3.60(1H, m, H-3α), 0.92 (3H, d, *J* = 7.0 Hz, Me-21), 0.80 (3H, s, Me-19), 0.65 (3H, s, Me-18).^{13}C NMR (100 MHz, $CDCl_3$): δ 139.6, 113.9, 71.5, 56.5, 56.3, 54.3, 44.8, 42.8, 39.9, 38.2, 36.9, 35.7, 35.6, 35.2, 34.8, 32.1, 31.5, 30.2, 28.7, 28.2, 24.1, 21.3, 18.6, 12.3, 12.1. HR ESIMS *m/z* 359.3314 $[M+H]^+$, $C_{25}H_{43}O$ requires 359.3317.

Compound 83. Hydrogenation on **81** (100 mg, 0.3 mmol) gave **83** (98 mg, 0.3 mmol, quantitative yield). Purification by HPLC on a Nucleodur 100-5 C18 (5 μm; 4.6 mm i.d. x 250 mm) with MeOH/H_2O (99:1) as eluent (flow rate 1 mL/min), gave pure compound **83** (t_R= 19.4 min). Selected ^{1}H NMR (400 MHz, $CDCl_3$): δ 3.63 (1H, m, H-3α), 0.88 (3H, ovl, Me-21), 0.88 (3H, ovl, Me-25),0.80 (3H, s, Me-19), 0.65 (3H, s, Me-18).^{13}C NMR (100 MHz, $CDCl_3$): δ 71.6, 56.4, 56.2, 54.3, 45.0, 42.7, 39.9, 38.3, 36.9, 35.9, 35.7, 35.6, 35.3, 32.1, 31.5, 28.6, 28.4, 28.2, 24.2, 23.1, 21.2, 18.6, 14.2, 12.3, 12.0. HR ESIMS *m/z* 361.3470 $[M+H]^+$, $C_{25}H_{45}O$ requires 361.3473.

Compound 85. Compound **79** (1 g, 2.6 mmol) was hydrolyzed with NaOH (96 mg, 2.4 mmol) in a solution of MeOH:H_2O 1:1 v/v (10 mL). The mixture was stirred for 4 h at reflux. The resulting solution was then acidified with HCl 6N and extracted with ethyl acetate (3x50 mL). The collected organic phases were washed with brine, dried over Na_2SO_4 anhydrous and evaporated under reduced pressure to give the carboxylic acid. The intermediate was treated in the same operative conditions reported for **67** furnishing compound **85** (755 mg, 2.0 mmol, 78% over three steps).

Compound 86. Compound **86** (413 mg, 1.3 mmol, 62%) was obtained from **85** (755 mg, 2.0 mmol) in the same operative conditions reported for **68**. An analytic sample was purified by HPLC on a Nucleodur 100-5 C18 (5 μm; 4.6 mm i.d. x 250 mm) with MeOH/H_2O (96:4) as eluent (flow rate 1 mL/min), giving pure compound **86** (t_R=17.4 min). Selected ^{1}H NMR (400 MHz, CD_3OD): δ 5.66 (1H, m, H-22), 4.89 (1H, d, *J* = 17.4 Hz, H-23), 4.81 (1H, ovl with solvent signal, H-23), 3.50 (1H, m, H-3α), 1.02 (3H, d, *J* = 6.5 Hz, Me-21), 0.83 (3H, s, Me-19),

0.71 (3H, s, Me-18).^{13}C NMR (100 MHz, $CDCl_3$): δ 145.3, 111.6, 71.4, 56.4, 55.5, 54.4, 45.0, 42.7, 41.2, 39.9, 38.2, 36.9, 35.6, 35.5, 32.1, 31.5, 28.7, 28.3, 24.2, 21.3, 20.2, 12.3, 12.1. HR ESIMS *m/z* 331.3001 $[M+H]^+$, $C_{23}H_{39}O$ requires 331.3003.

Compound 87. Hydrogenation on **86** (300 mg, 0.9 mmol) gave **87** (287 mg, 0.9 mmol, quantitative yield). Purification by HPLC on a Nucleodur 100-5 C18 (5 μm; 4.6 mm i.d. x 250 mm) with MeOH/H_2O (99:1) as eluent (flow rate 1 mL/min), gave pure compound **87** (t_R=14.8 min). Selected ^{1}H NMR (400 MHz, $CDCl_3$): δ 3.63 (1H, m, H-3α), 0.93 (3H, s, Me-19), 0.90 (3H, d, *J* = 6.7 Hz, Me-21), 0.83 (3H, t, *J* = 7.5 Hz, Me-23), 0.65 (3H, s, Me-18).^{13}C NMR (100 MHz, $CDCl_3$): δ 71.4, 56.5, 56.0, 54.4, 44.9, 42.6, 40.2, 38.2, 37.2, 36.9, 35.8, 35.5, 32.0, 31.5, 28.7, 28.5, 28.3, 24.1, 21.3, 18.2, 12.2, 12.0, 10.4. HR ESIMS *m/z* 333.3157 $[M+H]^+$, $C_{23}H_{41}O$ requires 333.3159.

Cell culture. HepG2, an immortalized human hepatocarcinoma cell line, was cultured and maintained at 37 °C and 5% CO_2 in E-MEM added with 10% FBS, 1% glutamine and 1%penicillin/streptomycin. HEK-293T and Glutag cells were cultured and maintained at 37 °C and 5% CO_2 in D-MEM additioned with 10% FBS, 1% glutamine and 1% penicillin/streptomycin.

Luciferase reporter gene assay and dose-response curves. To evaluate LXRα mediated transactivation, HepG2 cells were transfected with 200 ng of the reporter vector p(UAS)5XTKLuc, 100 ng of a vector containing the ligand binding domain of LXRα cloned upstream of the GAL4-DNA binding domain (i.e. pSG5-LXRαLBD-GAL4DBD) and 100 of pGL4.70 (Promega), a vector encoding the human Renilla gene. To evaluate GPBAR1 mediated transactivation, HEK-293T cells were transfected with 200 ng of human pGL4.29 (Promega), a

reporter vector containing a cAMP response element (CRE) that drives the transcription of the luciferase reporter gene luc2P, with 100 ng of pCMVSPORT6-human GPBAR1, and with 100 ng of pGL4.70 Renilla. To evaluate FXR mediated transactivation, HepG2 cells were transfected with 100 ng of human pSG5-FXR, 100 ng of human pSG5-RXR, 200 ng of the reporter vector p(hsp27)-TK-LUC containing the FXR response element IR1 cloned from the promoter of heat shock protein 27 (hsp27) and with 100 ng of pGL4.70 Renilla. At 24 h post-transfection, cells were stimulated 18 h with 10 μM GW3965, TLCA, or CDCA and the synthetized compounds (10 μM). Luciferase activities were assayed and normalized with Renilla activities. Dose-response curves were performed in HepG2 and HEK-293T cells transfected as described above and then treated with increasing concentrations of compounds selected compounds (1, 5, 10, 25 and 50 μM). At 18 h post stimulations, cellular lysates were assayed for luciferase and Renilla activities using the Dual-Luciferase Reporter assay system (E1980, Promega). Luminescence was measured using Glomax 20/20 luminometer (Promega). Luciferase activities (RLU) were normalized with Renilla activities (RRU).

Animal model. C57BL6 mice were originally donated by Dr. Galya Vassileva (Schering-Plough Research Institute, Kenilworth). The colonies were maintained in the animal facility of University of Perugia. Mice were treated with compound **65** (30 mg/Kg daily by oral gavage) or vehicle (distilled water) for two weeks. Mice were housed under controlled temperatures (22 °C) and photoperiods (12:12-hour light/dark cycle), allowed unrestricted access to standard mouse chow and tap water and allowed to acclimate to these conditions for at least 5 days before inclusion in an experiment. The study was conducted in agreement with the

Italian law and the protocol was approved by a ethical committee of University of Perugia and by a National committee of Ministry of Health (permission n.42/2014-B). The health and body conditions of the animals were monitored daily by the Veterinarian in the animal facility. The study protocol caused minor suffering, however, animals that lost more than 25% of the initial body weight were euthanized. At the day of sacrifice mice were deeply anesthetised with a mixture of tiletamine hypochoride and zolazepam hypocloride/xylazine at a dose of 50/5 mg/Kg. Blood, liver and terminal ileum were collected for further analysis. Aspartate aminotransferase (AST), Total cholesterol and Tryglicerides were measured by routine biochemical clinical chemistry. For histological examination, portions of liver lobes were fixed in 10% formalin, embedded in paraffin, sectioned (5 μm thin) and stained with Hematoxylin/Eosin (H&E), for morphometric analysis.

RNA isolation and RT-PCR. HepG2 and Glutag cells were plated at $1x10^6$ cells/well in a 6 well plate. After an overnight incubation, cells were starved and then stimulated for 18 h with GW3965 or TLCA (10 μM), HDCA (10 μM), and with increasing concentrations of compound **65** (1, 5, 10, 25, 50 μM).

Total RNA was isolated from HepG2 or Glutag cells using the TRIzol reagent according to the manufacturer's specifications (Invitrogen). One microgram of purified RNA was treated with DNase-I and reverse transcribed with Superscript II (Invitrogen). For Real Time PCR, 25 ng template was dissolved in 25 μL containing 200 nmol/L of each primer and 12.5 μL of 2× SYBR FAST Universal ready mix (Invitrogen). All reactions were performed in triplicate, and the thermal cycling conditions were as follows: 2 min at 95 °C, followed by 40 cycles of 95 °C for 20 s and 60 °C for 30 s in StepOnePlus (Applied Biosystems). The relative

mRNA expression was calculated and expressed as $2^{-(\Delta\Delta Ct)}$. Forward and reverse primer sequences were the following, respectively:

human GAPDH, gaaggtgaaggtcggagt and catgggtggaatcatattggaa;

human ABCA1, gcttgggaagatttatgacagg and aggggatgattgaaagcagtaa;

human SREBP1c, gcaaggccatcgactacatt and ggtcagtgtgtcctccacct;

mouse GAPDH, ctgagtatgtcgtggagtctac and gttggtggtgcaggatgcattg;

mouse Pro-glucagon, tgaagacaaacgccactcac and caatgttgttccggttcctc.

Molecular docking. The Glide (version 7.1) software package was used to perform molecular docking calculations in the three-dimensional model of hGPBAR1 and in the crystal structure of LXRα-LBD bound to a synthetic benzisoxazole urea agonist (PDB code: 3IPU).

This structure was selected among the several available using the following criteria: i) the higher resolution of the electron density map; ii) the presence of all amino acids in helix 1, which is not fully resolved in all the LXRα crystal structures; iii) the presence of an agonist with bulkiness comparable to bile acid derivatives. Missing residues in the loop connecting H1 with H3 were added and refined using Prime. Ligand and receptors structures were prepared as described in a previous paper.

For both GPBAR1 and LXRα, a box of 30× 30× 30 Å centered on the ligand binding cavities was created. The standard precision (SP) mode of the GlideScore function was used to score the predicted binding poses.

Molecular dynamics. All the simulations were performed with NAMD 2.10 using the *ff14SB* and *gaff* Amber force field parameters for the protein and the ligand, respectively. Each complex was solvated in a 12.0 Å layer cubic water box using the TIP3P water model parameters. The addition of 2 Na^+ ions ensured

neutrality. Amber charges were applied to the proteins and water molecules, whereas the ligand charges were computed using the restrained electrostatic potential (RESP) fitting procedure. The ESP was first calculated by means of the Gaussian09 package using a 6-31G* basis set at Hartree-Fock level of theory, and then the RESP charges were obtained by a two-stages fitting procedure using Antechamber. A 10 Å cutoff (switched at 8.0 Å) was used for atom-pair interactions. The long-range electrostatic interactions were computed by means of the particle mesh Ewald (PME) method, using a 1.0 Å grid spacing in periodic boundary conditions. The SHAKE algorithm was applied to constraint bonds involving hydrogen atoms, and thus an integration time step of 2 fs could be used. Each complex was heated up to 300 K while putting harmonic constraints on the protein and the ligand, which were gradually released along the thermalization process. Production runs were then performed under NPT conditions at 1 atm and 300 K.

All figures were rendered using PyMOL (http://www.pymol.org).

^{1}H NMR (400 MHz, $CDCl_3$) of compound **52**

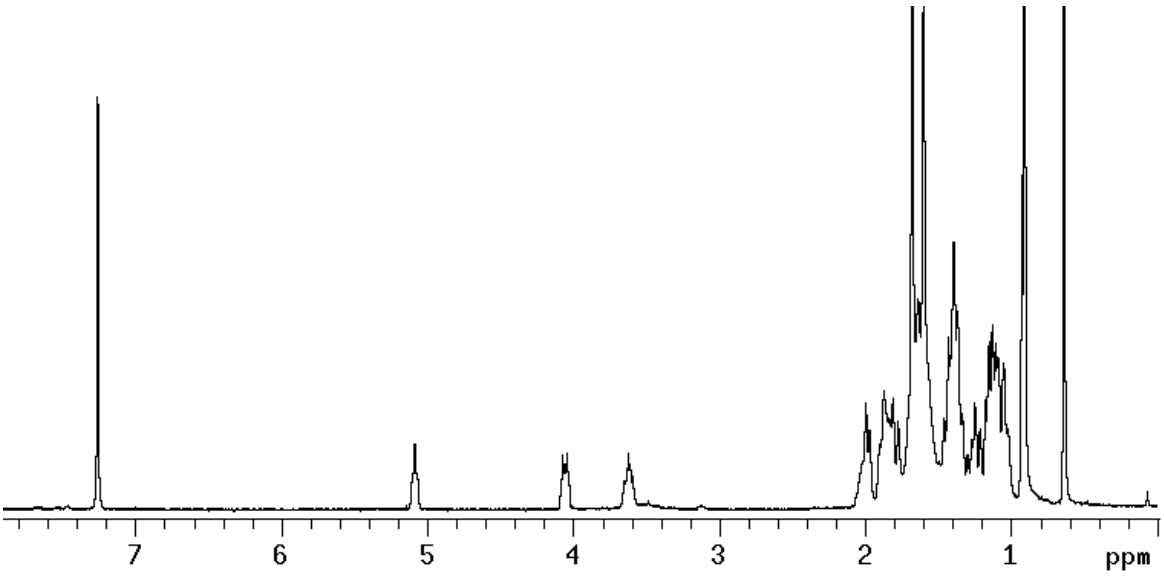

^{1}H NMR (400 MHz, $CDCl_3$) of compound **57**

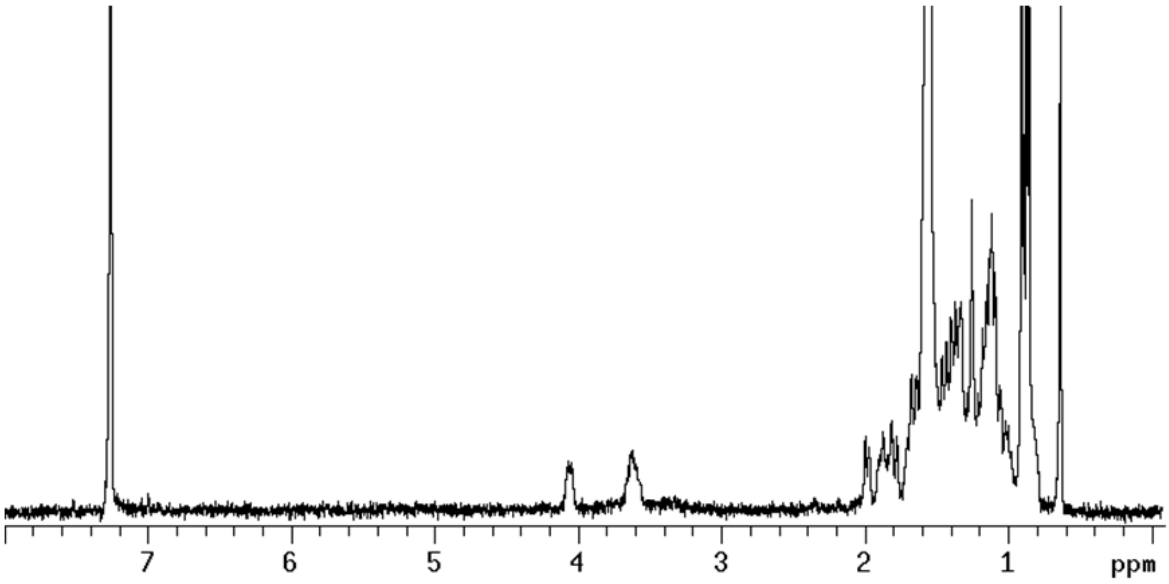

^{1}H NMR (400 MHz, $CDCl_3$) of compound **53**

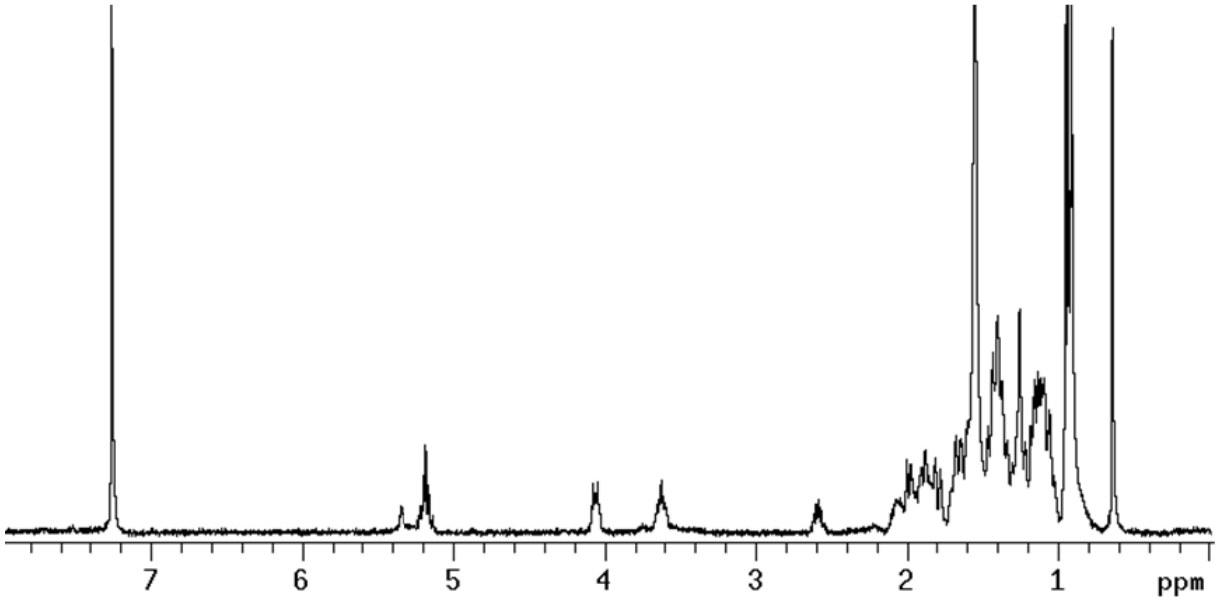

^{1}H NMR (400 MHz, CD_3OD) of compound **58**

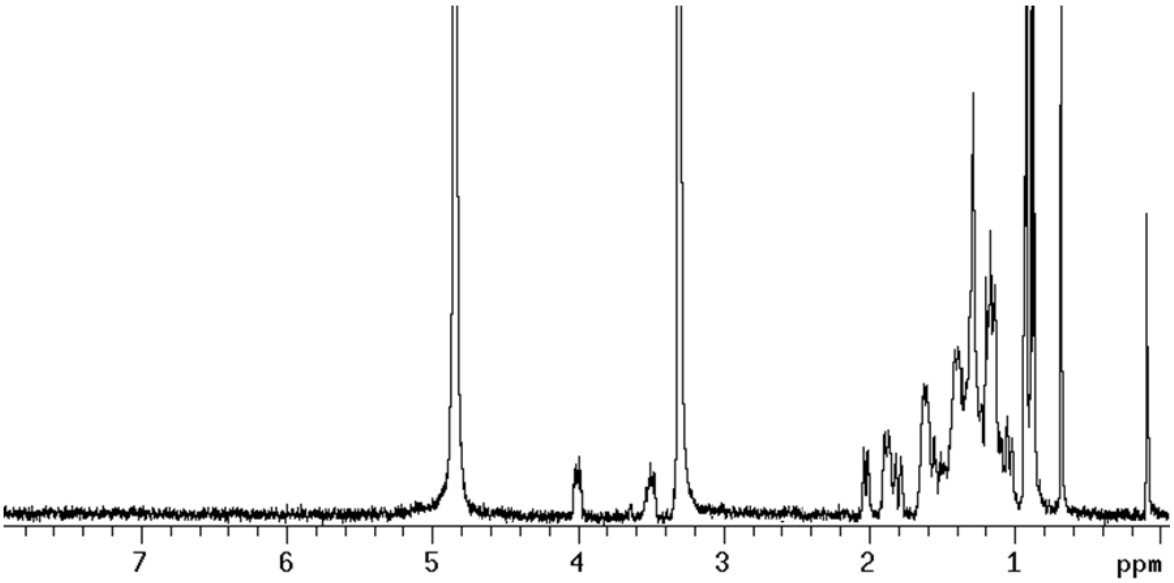

^{1}H NMR (400 MHz, $CDCl_3$) of compound **51**

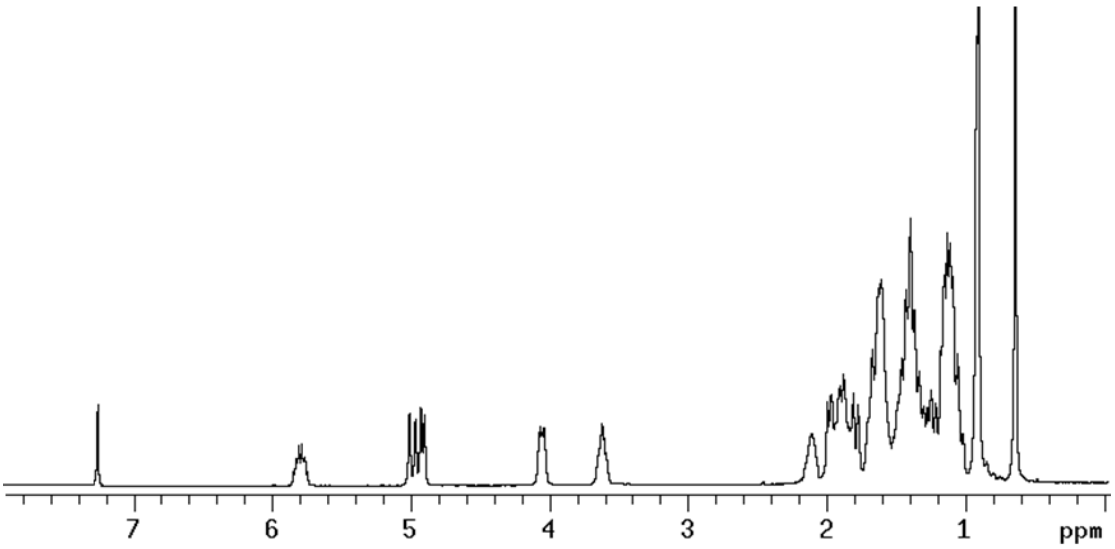

^{1}H NMR (400 MHz, CD_3OD) of compound **56**

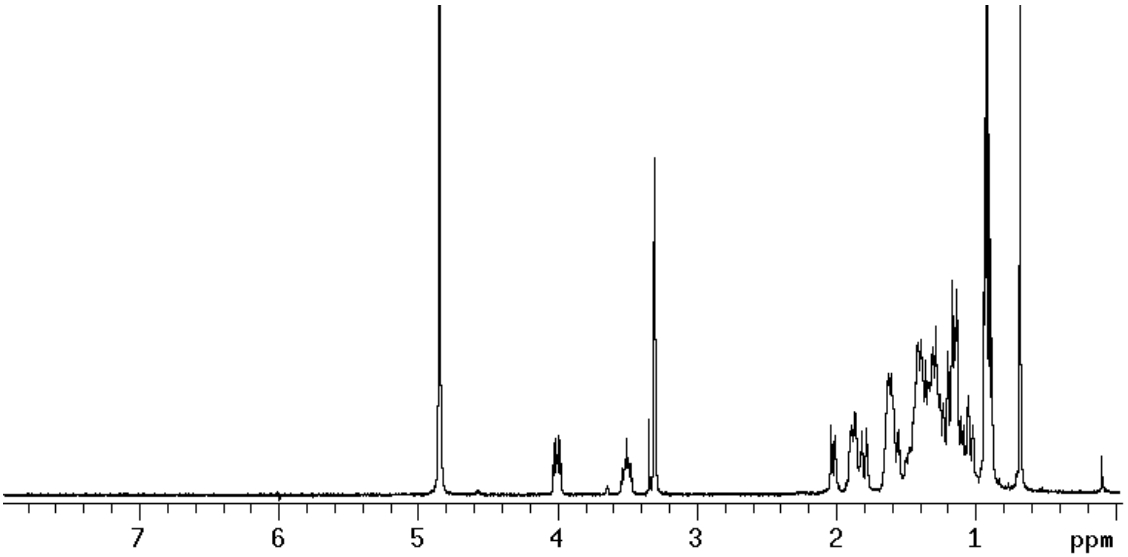

^{1}H NMR (400 MHz, $CDCl_3$) of compound **54**

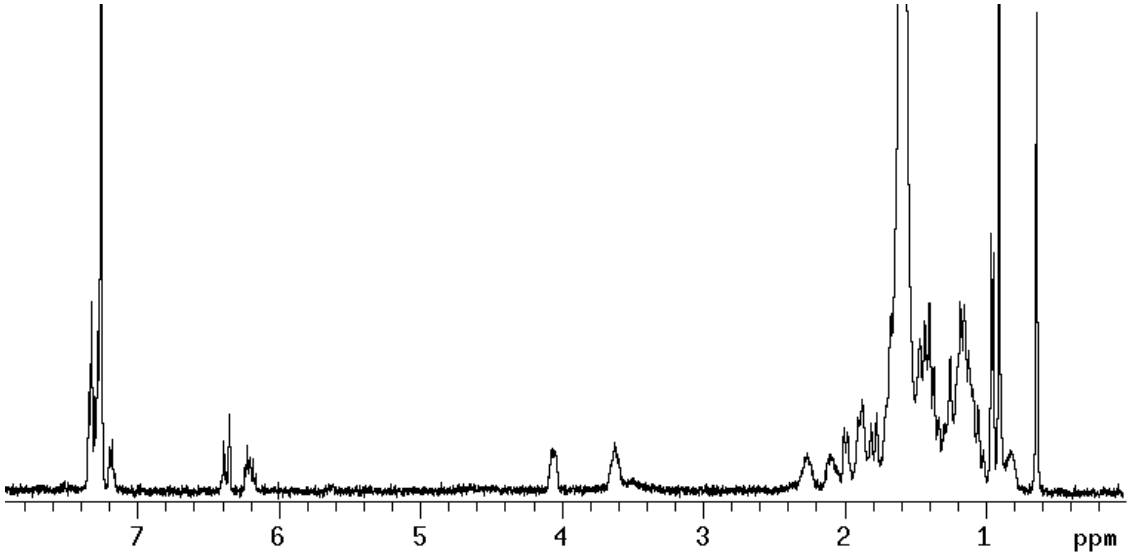

^{1}H NMR (400 MHz, $CDCl_3$) of compound **55**

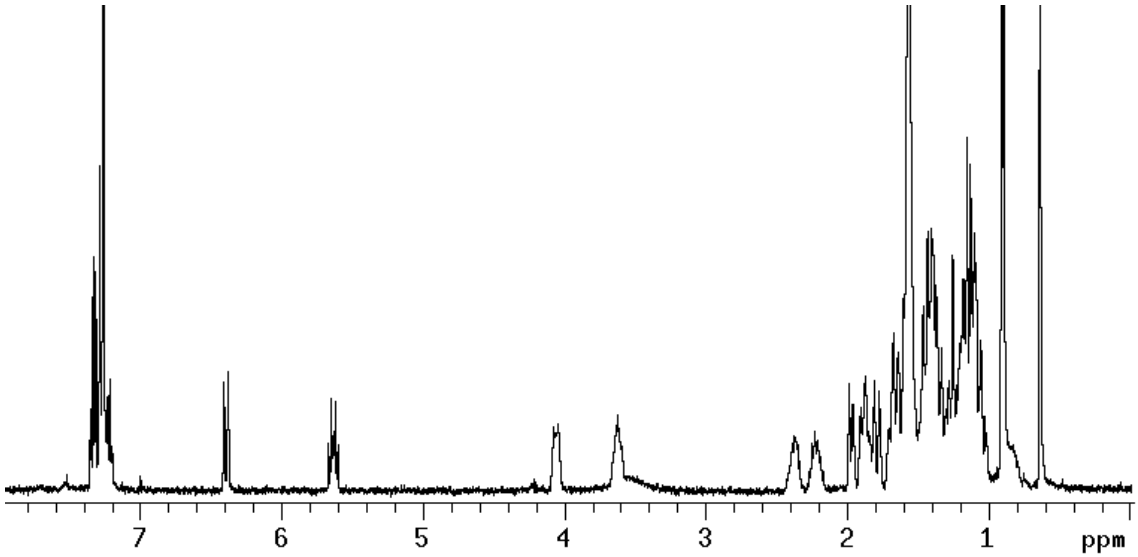

^{1}H NMR (400 MHz, $CDCl_3$) of compound **59**

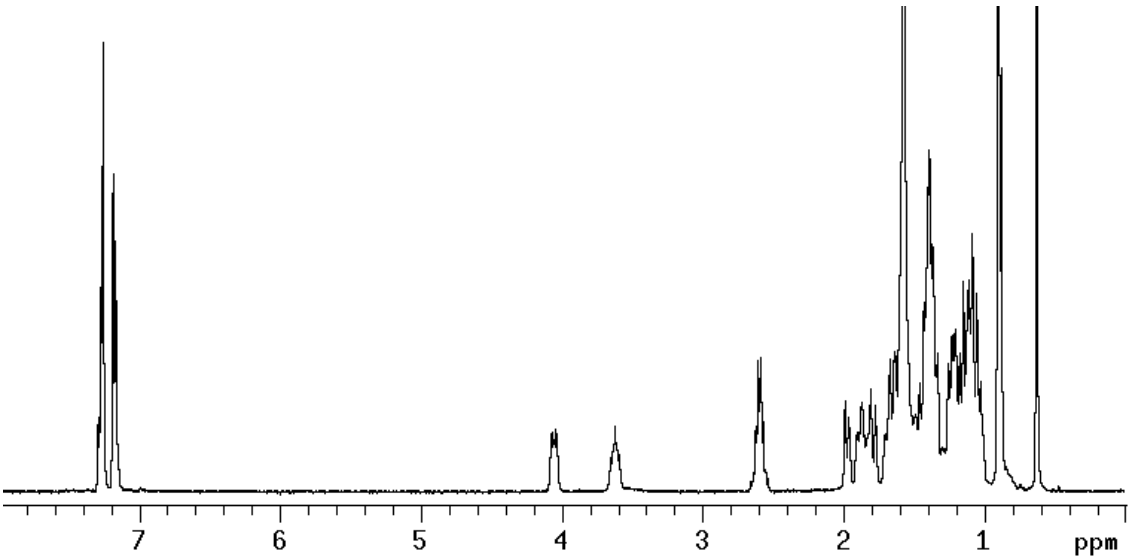

^{1}H NMR (400 MHz, CD_3OD) of compound **63**

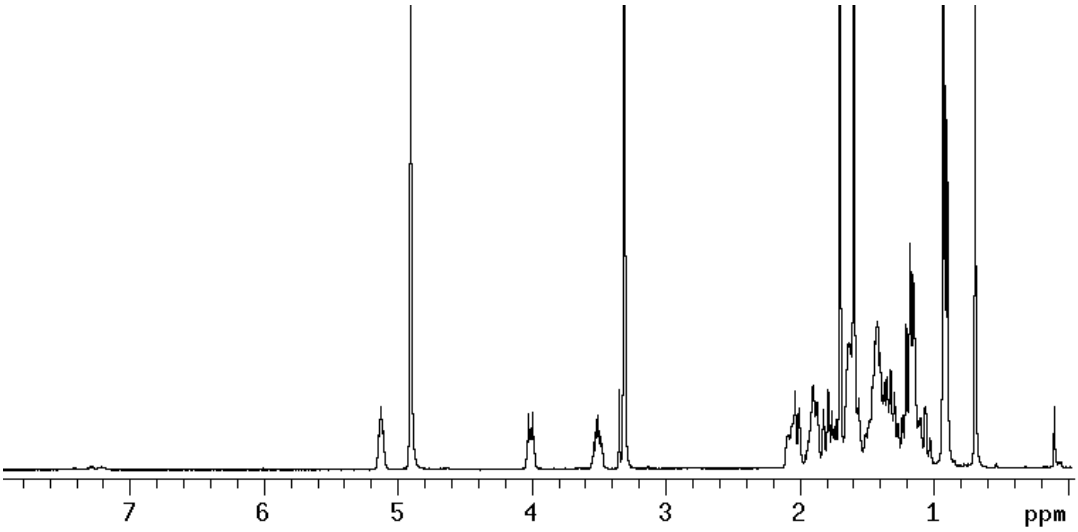

^{1}H NMR (400 MHz, CD_3OD) of compound **65**

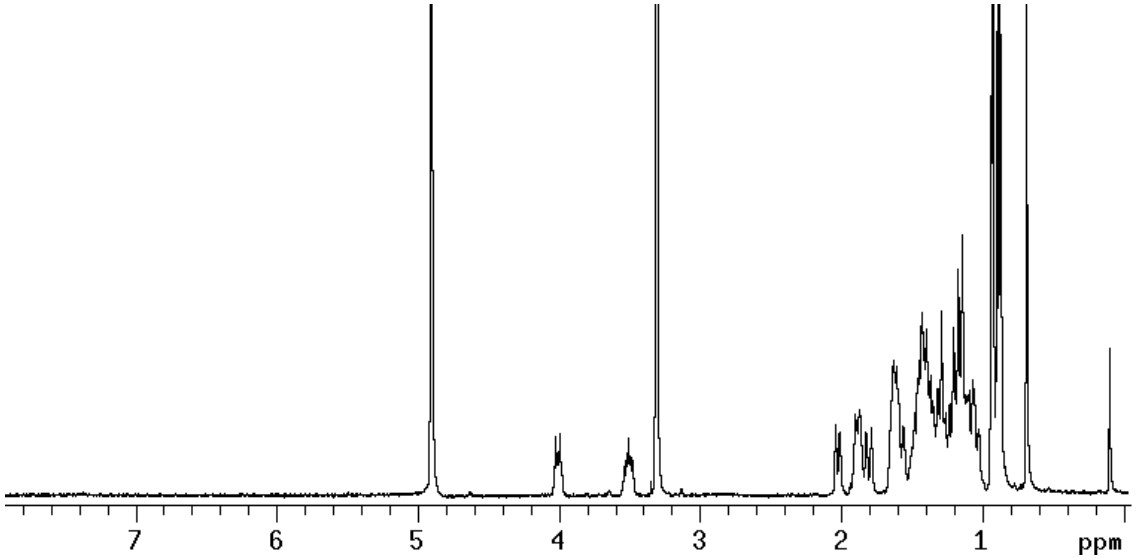

^{1}H NMR (400 MHz, $CDCl_3$) of compound **62**

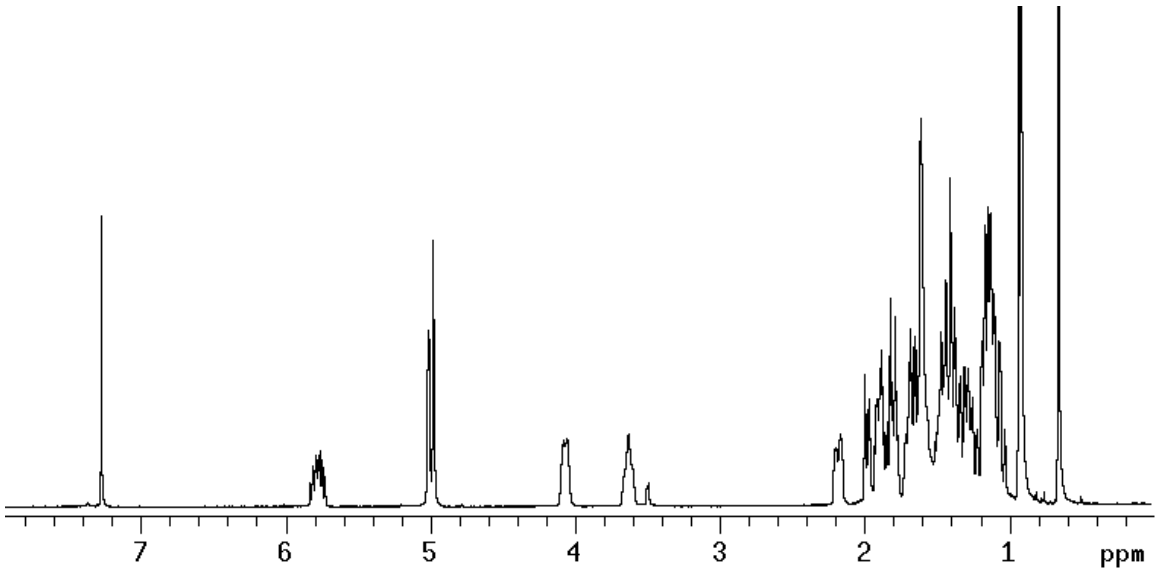

^{1}H NMR (400 MHz, $CDCl_3$) of compound **64**

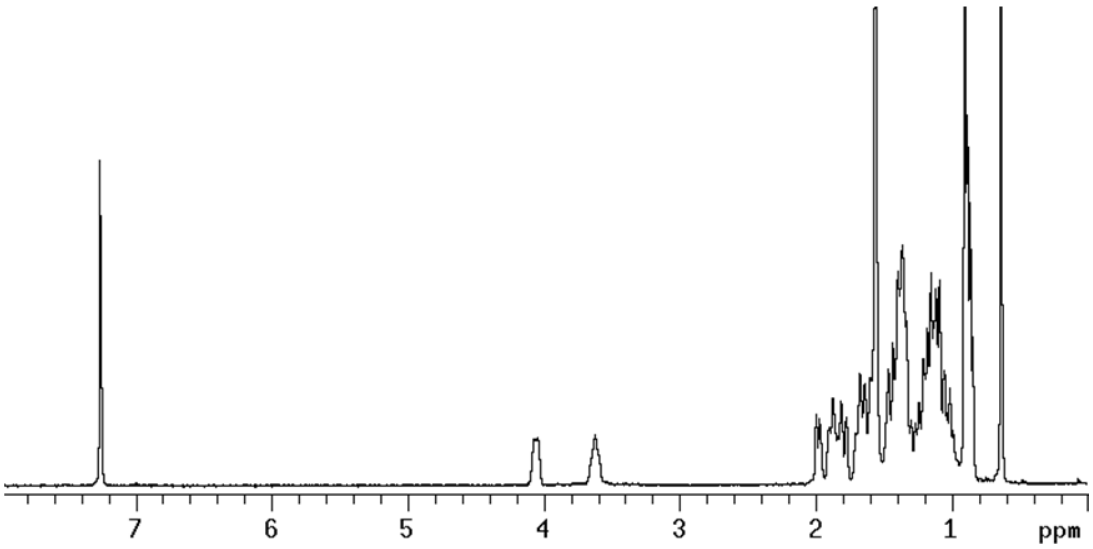

^{1}H NMR (400 MHz, $CDCl_3$) of compound **68**

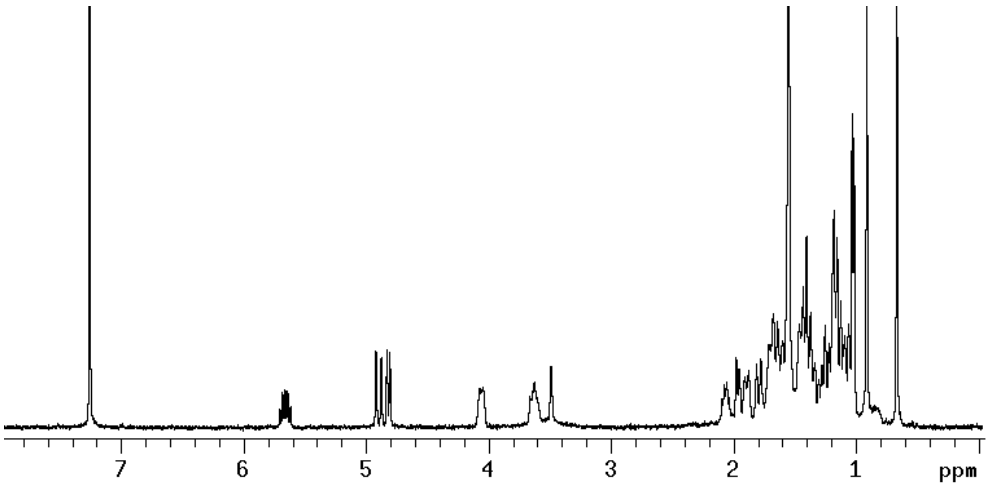

^{1}H NMR (400 MHz, $CDCl_3$) of compound **69**

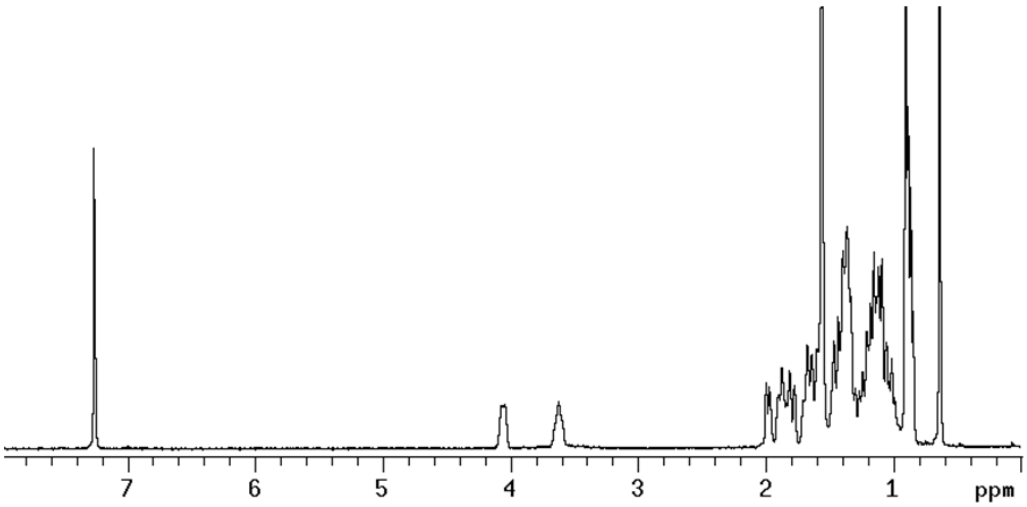

^{1}H NMR (400 MHz, $CDCl_3$) of compound **71**

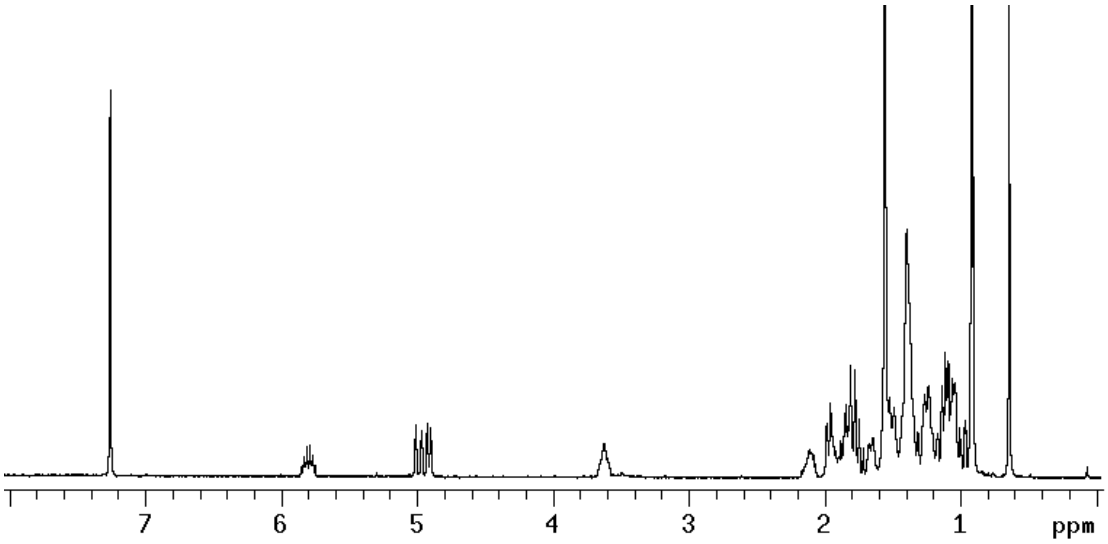

^{1}H NMR (400 MHz, $CDCl_3$) of compound **73**

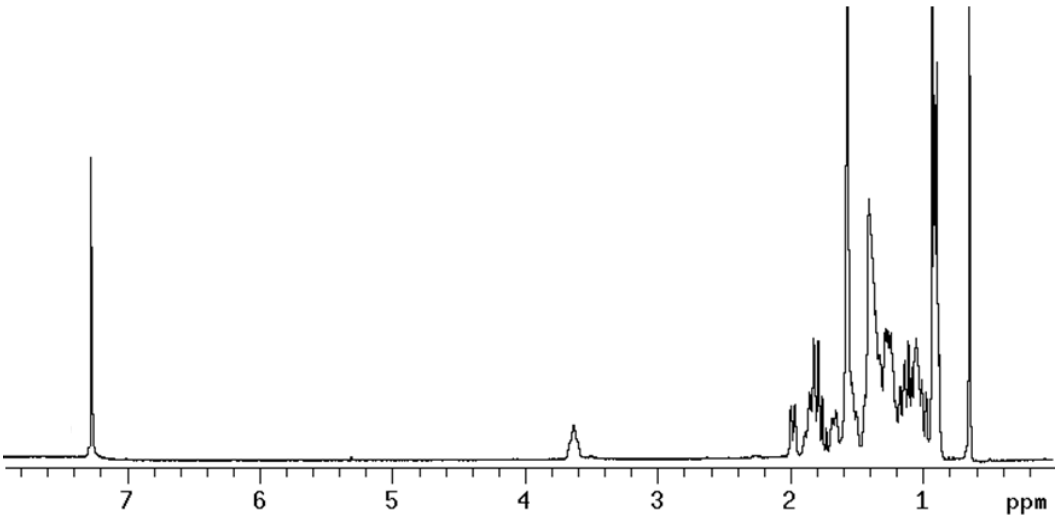

^{1}H NMR (400 MHz, $CDCl_3$) of compound **72**

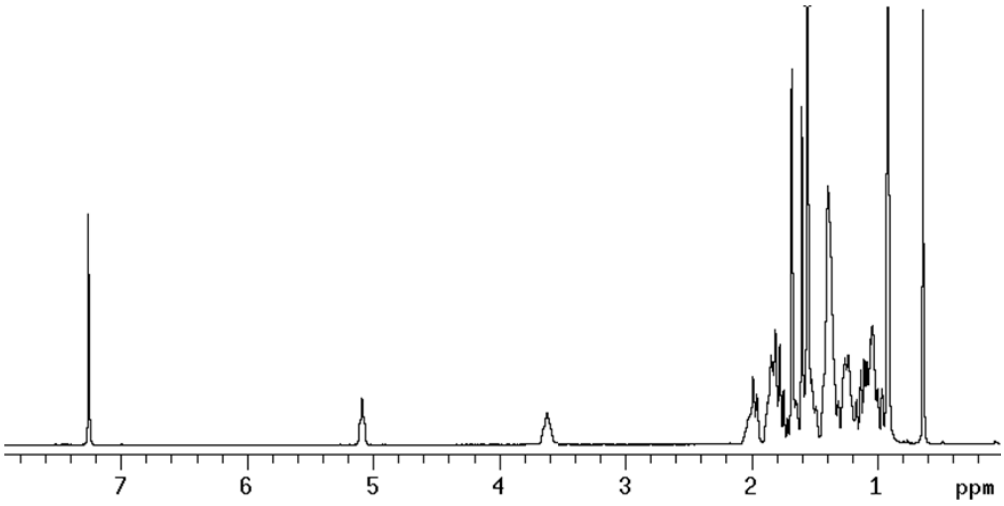

^{1}H NMR (400 MHz, $CDCl_3$) of compound **74**

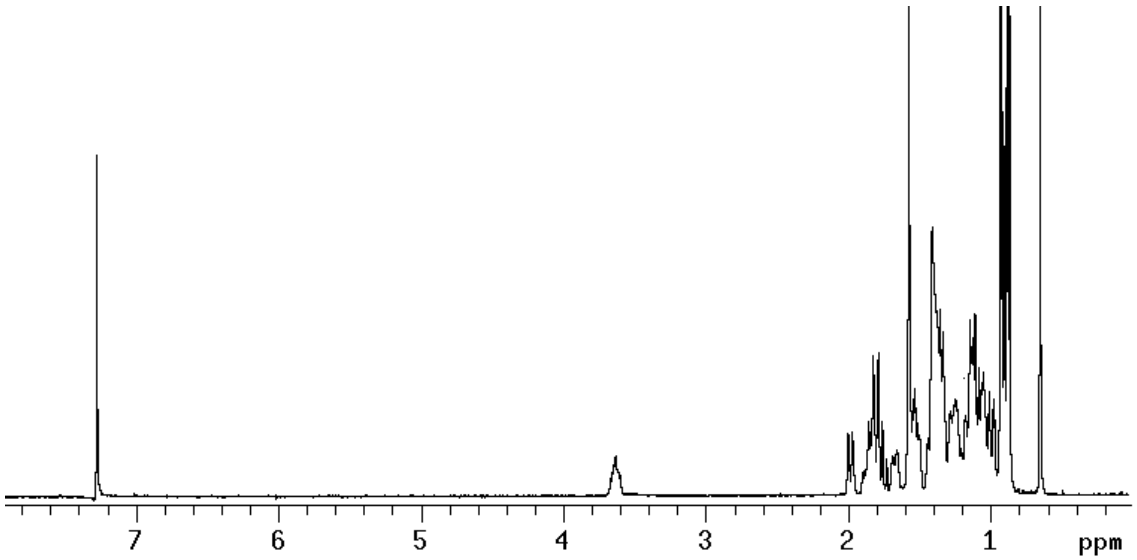

^{1}H NMR (400 MHz, $CDCl_3$) of compound **77**

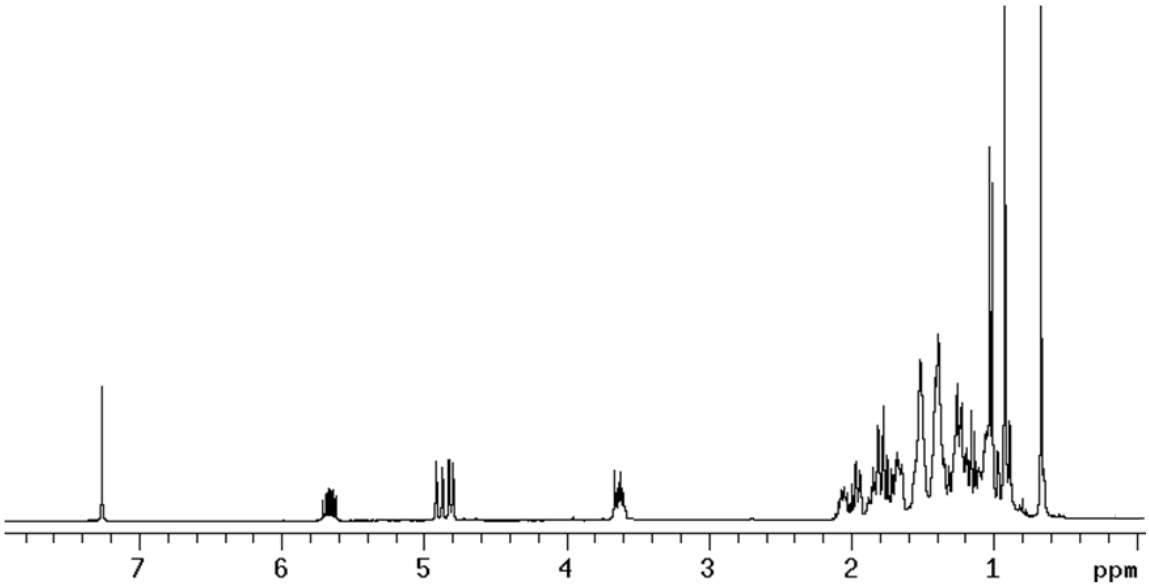

^{1}H NMR (400 MHz, $CDCl_3$) of compound **78**

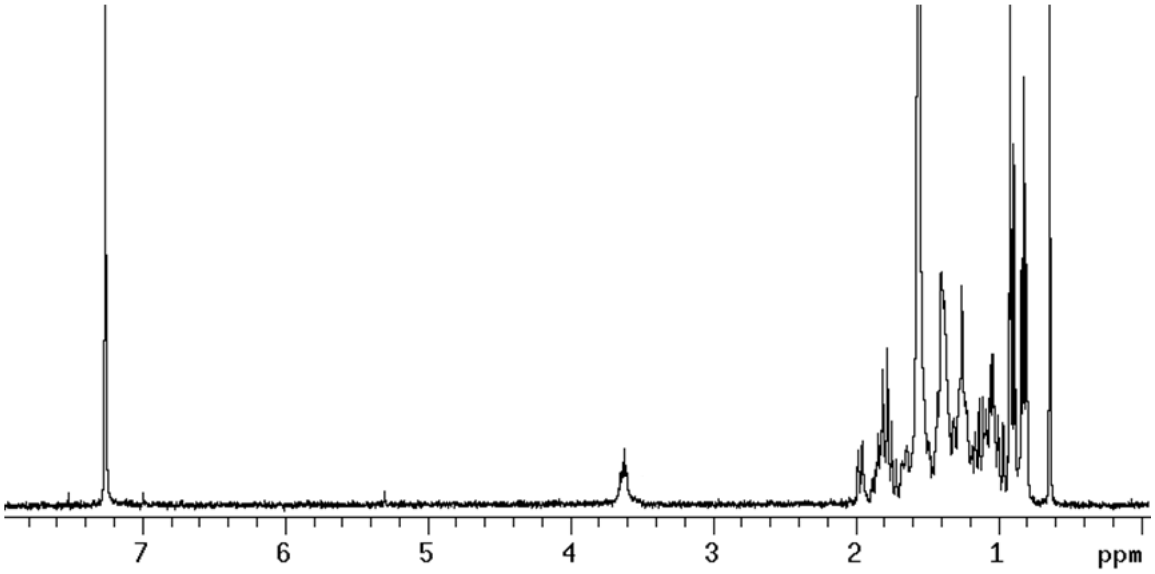

^{1}H NMR (400 MHz, $CDCl_3$) of compound **82**

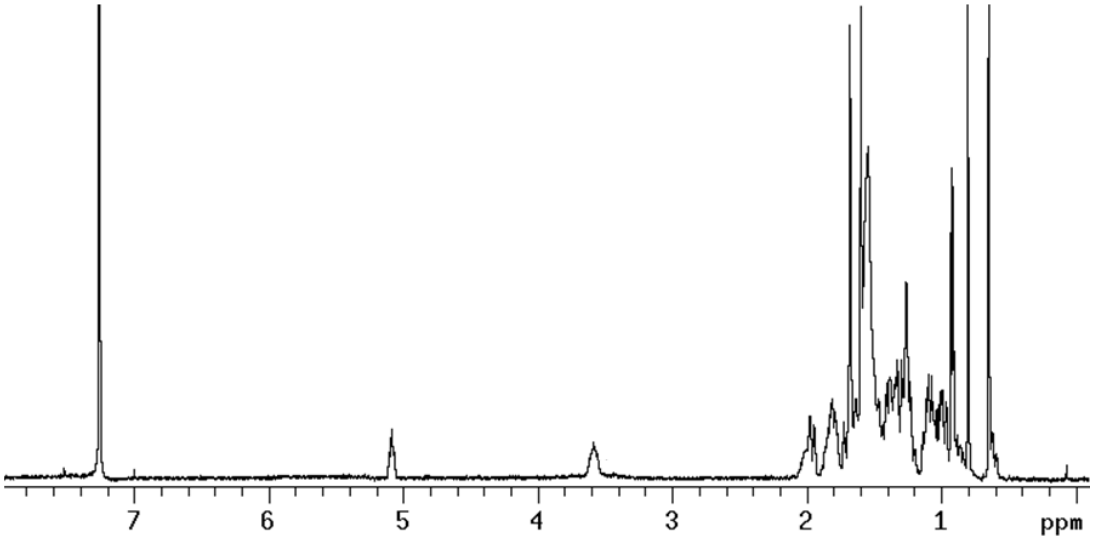

^{1}H NMR (400 MHz, $CDCl_3$) of compound **84**

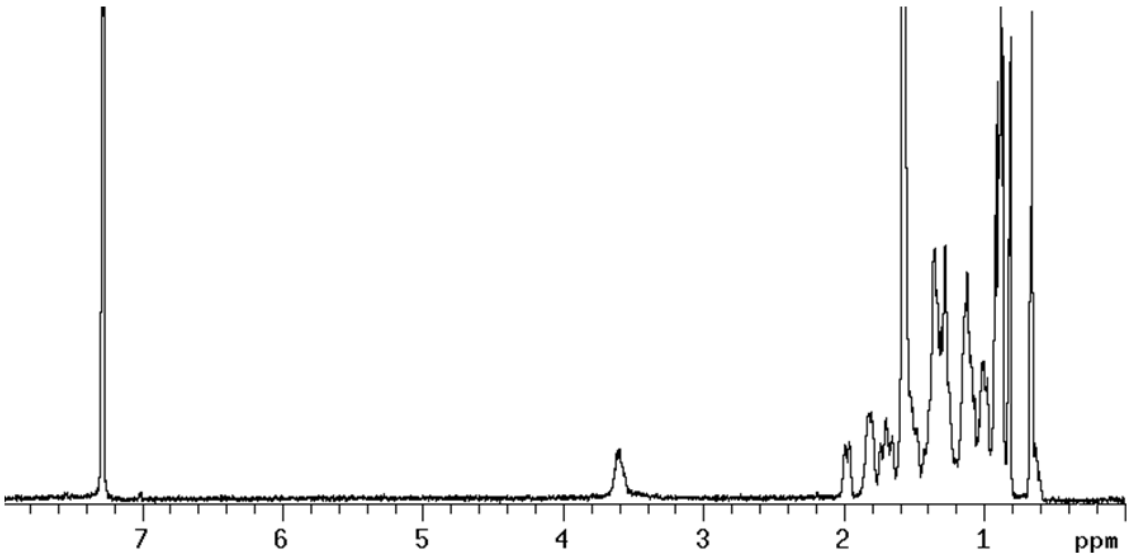

^{1}H NMR (400 MHz, $CDCl_3$) of compound **81**

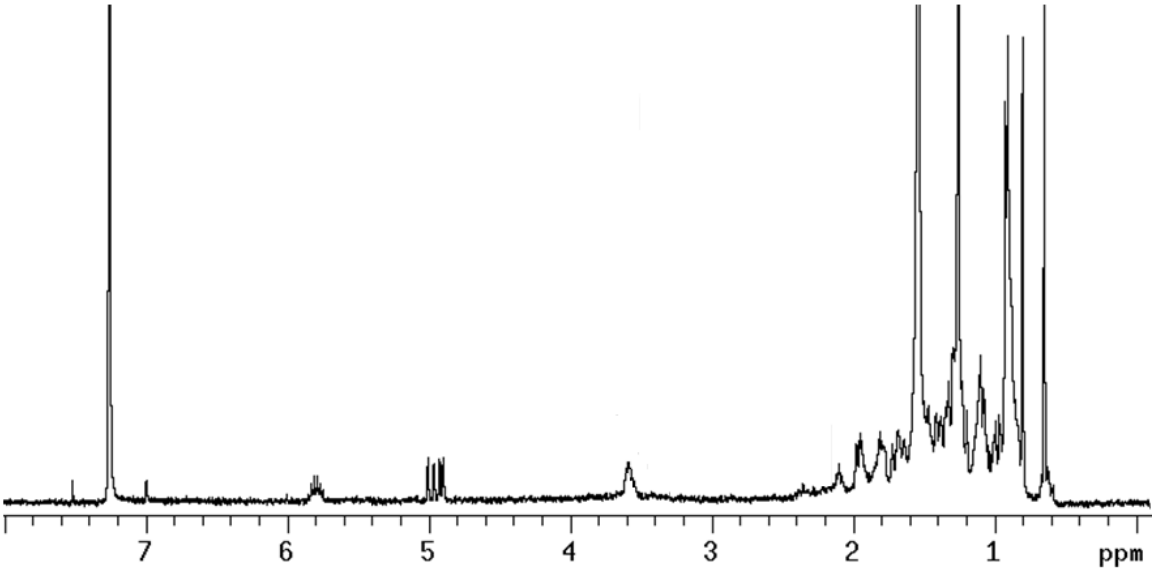

^{1}H NMR (400 MHz, $CDCl_3$) of compound **83**

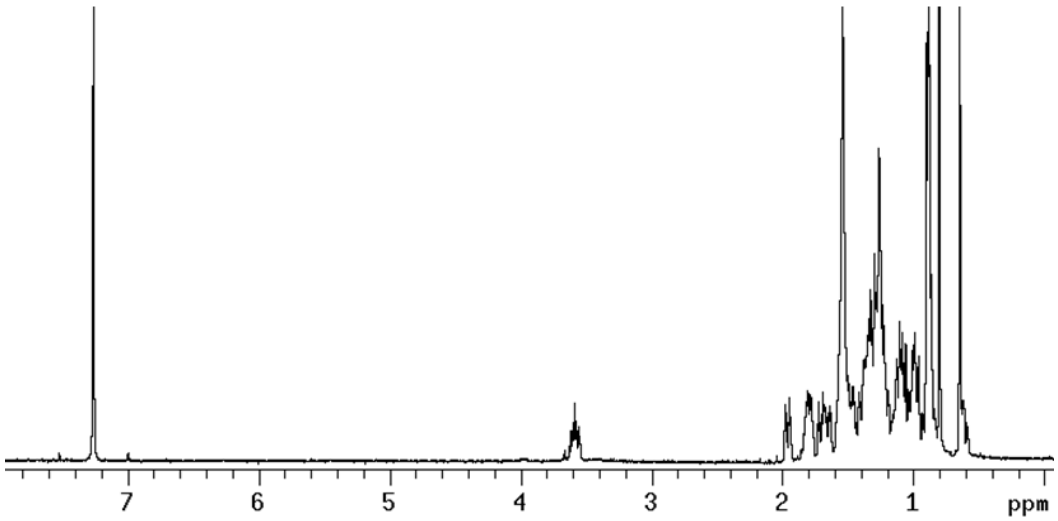

^{1}H NMR (400 MHz, CD_3OD) of compound **86**

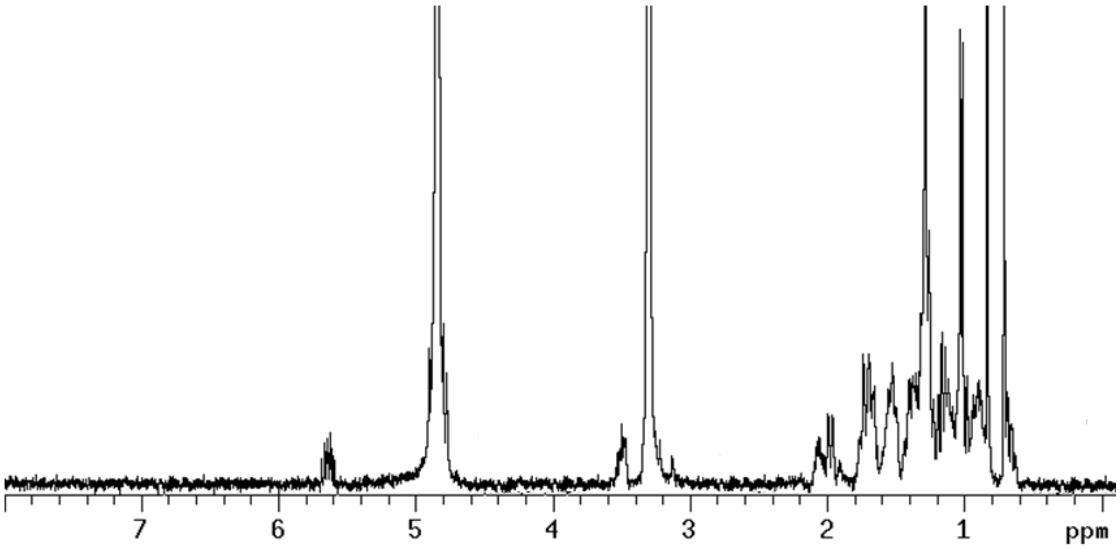

^{1}H NMR (400 MHz, CD_3OD) of compound **87**

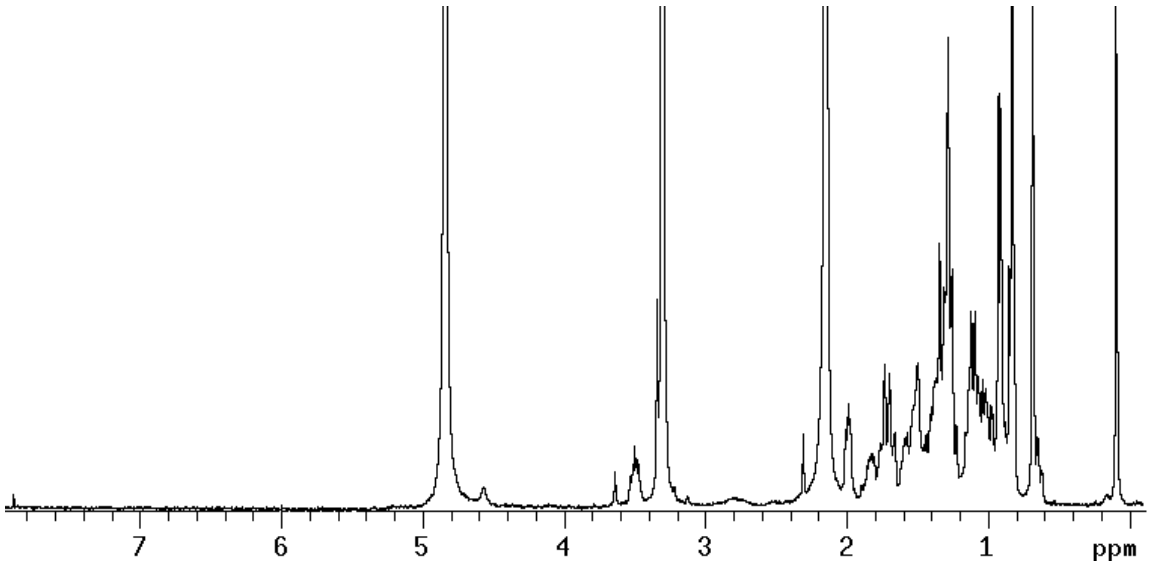

V. Experimental section of SHP agonists.

3-(2,6-dichlorophenyl)-4-carboethoxy-5-isopropyl-isoxazole (91): 1.2 g compound **88** (5.6 mmol) was obtained starting from 1 g of 2,6-dichlorobenzaldehyde (5.7 mmol) using a procedure found in literature[107] with a 97.5% yield over three steps of reaction. Selected ^{1}H NMR (400 MHz $CDCl_3$): δ 7.4-δ 7.3 (3H, m), 4.1 (2H, dd, *J* = 7.25 Hz), 3.88 (m), 1.44 (6H, d, *J* = 6.9 Hz), 1.02 (3H, t, *J* = 6.98 Hz). ^{13}C NMR (100 MHz $CDCl_3$): δ 183.31, 161.08, 158.56, 135.4, 130.9 (2C), 127.84 (3C), 107.57, 60.44, 27.72, 20.16 (2C), 13.56. HR ESIMS *m/z* 328.1890 $[M+H]^+$, $C_{15}H_{16}Cl_2NO_3$ requires 328.1894.

3-(2,6-dichloro-phenyl)-4-carboxyl-5-isopropyl-isoxazole acid (92): Crude compound 9**1** (200 mg, 0.6 mmol) was refluxed in *ca*. 50 mL of methanol-water 1:l with 30% NaOH. After stirring for 12 h, the basic aqueous solution was neutralized with HCl 6 N. Then methanol was evaporated and the residue was extracted with EtOAc (3 x 30 mL). The combined organic layers were washed with brine, dried and evaporated to dryness to give white solid residue, that was purified by silica gel chromatography, eluted with CH_2Cl_2 100% (154 mg, 84.3% yield). Selected ^{1}H NMR (400 MHz $CDCl_3$): δ 7.36-7.3 (3H, m), 3.85 (1H, m), 1.44 (6H, d, *J* = 6.95). ^{13}C NMR (100 MHz $CDCl_3$): δ 184.81, 166.34, 158.65, 135.33, 131.06 (2C), 127.81 (3C), 106.79, 27.82, 20.18 (2C). HR ESIMS *m/z* 298.0116 $[M-H]^-$, $C_{13}H_{10}Cl_2NO_3$ requires 298.0119.

3-(2,6-dichlorophenyl)-4-hydroxymethyl-5-isopropyl-isoxazole (93): a solution of 3-(2,6-dichlorophenyl)-4-carbomethoxy-5-isopropyl-isoxazole (800 mg, 2.5 mmol) in tetrahydrofurane (10 ml) was cooled to 0 °C under a nitrogen atmosphere while a solution of diisobutylammonium hydride (3.8 ml, 1.5 M in

toluene) was added dropwise. The reaction was allowed to warm slowly to ambient temperature over several hours and stirred at room temperature for 48 h. The flask was again cooled to 0 °C and methanol (4 ml) was carefully added over a 10 minutes period. Water (20 ml) was added dropwise and a gelatinous mixture formed. Sodium Hydroxide (30 ml, 2 N) was added and the mixture was filtered over a plug of celite. After the solids were nearly dry, they were extracted with ethyl acetate (3x30 ml) and the filtrates were combined. The organic layer was washed with water (2x30 ml) brine (30 ml), dried over anhydrous magnesium sulphate, filtered and condensed to give compound **3** (481 mg, 69% yield). An analytic sample was obtained by silica gel chromatography eluting with *n*-hexane: EtOAc 97:3. Selected ^{1}H NMR (400 MHz $CDCl_3$): δ 7.45-7.35 (3H, m), 4.35 (2H, s), 3.35 (1H, m), 1.44 (6H, d, J = 7.08 Hz). ^{13}C NMR (100 MHz $CDCl_3$): δ 176.27, 159.05, 135.69, 131.32 (2C), 128.16 (3C), 112.53, 53.63, 26.95, 20.9 (2C). HR ESIMS *m/z* 286.1520 $[M+H]^+$, $C_{13}H_{14}Cl_2NO_2$ requires 286.1522.

3-(2,6-dichlorophenyl)-4-ethylacrylate-5-isopropyl-isoxazole (94): DMSO (994 μl, 14 mmol) was added dropwise for 5 min to a solution of oxalyl chloride (3.5 ml, 7 mmol) in dry CH_2Cl_2 (5 ml) at −78°C under argon atmosphere. After 30 min, a solution of **93** (400 mg, 1.4 mmol) in dry CH_2Cl_2 (5 ml) was added dropwise and the mixture was stirred at −78 °C. After 30 min, Et_3N dry (1.9 ml, 14 mmol) was added dropwise to the solution and the mixture was allowed to warm to room temperature. After 1 h, the reaction was quenched by addition of aqueous $NaHSO_4$ (1 M, 50 ml). The layers were separated, and the aqueous phase was extracted with CH_2Cl_2 (3x30 mL). The combined organic layers were washed with saturated aqueous $NaHSO_4$, saturated aqueous $NaHCO_3$, and brine. The organic phase was then dried over Na_2SO_4 and concentrated to give the

corresponding aldehyde (475 mg, quantitative yield) as a colorless oil, which was used without any further purification. To a solution of aldehyde (1.7 mmol) in THF dry (10 ml) was added LiOH (94 mg, 3.9 mmol) and TEPA (triethylphosphonoacetate, 742 μl, 3.9 mmol). The reaction mixture was stirred for 45 min at room temperature and then quenched with water (10 ml). The mixture was then extracted with EtOAc (3×30 mL), and the organic phase was concentrated *in vacuo*. Silica gel chromatography (CH_2Cl_2 100%) afforded pure **94** (415 mg, 84% over two steps). Selected ^{1}H NMR (400 MHz $CDCl_3$): δ 7.45-7.35 (3H, m), 7.38 (1H, d, *J* = 16.1 Hz), 5.51 (1H, d, *J* = 16.1 Hz), 4.17 (2H, dd, *J* = 7.38 Hz), 3.43 (1H, m), 1.46 (6H, d, *J* = 6.8 Hz), 1.27 (3H, t, *J* = 6.9 Hz). HR ESIMS *m/z* 354.2270 $[M+H]^+$, $C_{17}H_{18}Cl_2NO_3$ requires 354.2269.

3-(2,6-dichlorophenyl)-4-acrilic-5-isopropyl-isoxazole acid (95): A portion of compound **94** (100 mg, 0.3 mmol) was hydrolyzed with lithium hydroxide (14 mg, 0.6 mmol) in a solution of THF:H_2O 1:1 v/v (5 mL). The resulting solution was then acidified with HCl 6N and extracted with ethyl acetate (3x30 mL). The collected organic phases were washed with brine, dried over Na_2SO_4 anhydrous and evaporated under reduced pressure to give **95** (85 mg, 93% yield). An analytic sample was obtained by silica gel chromatography eluting with CH_2Cl_2 100%. Selected ^{1}H NMR (400 MHz $CDCl_3$): δ 7.45-7.35 (3H, m), 7.41 (1H, d, *J* = 16.1 Hz), 5.4 (1H, d, *J* = 16.1 Hz), 3.43 (1H, m), 1.46 (6H, d, *J* = 6.9 Hz). ^{13}C NMR (100 MHz $CDCl_3$): δ 178.71, 171.63, 157.44, 133.57, 131.82 (2C), 128.42 (2C), 127.00 (3C), 116.92, 109.64, 27.0, 20.68 (2C). HR ESIMS *m/z* 326.1730 [M-H], $C_{15}H_{12}Cl_2NO_3$ requires 326.1732.

3-(2,6-dichlorophenyl)-4-prop-2-en-1-ol-5-isopropyl-isoxazole (96): a solution of compound **94** (300 mg, 0.9 mmol) in tetrahydrofurane (5 ml) was cooled to 0

°C under a nitrogen atmosphere while a solution of diisobutylammonium hydride (2.8 ml, 1.5 M in toluene) was added dropwise. The reaction was allowed to warm slowly to ambient temperature over several hours and stirred at room temperature for 48 h total. The flask was again cooled to 0 °C and methanol (3 ml) was carefully added over a 10 minutes period. Water (10 ml) was added dropwise and a gelatinous mixture formed. Sodium Hydroxide (30 ml, 2 N) was added and the mixture was filtered over a plug of celite. After the solids were nearly dry, they were extracted with ethyl acetate (3x50ml) and the filtrates were combined. The organic layer was washed with water (2x50 ml) brine (50 ml), dried over anhydrous magnesium sulphate, filtered and condensed to give compound **96** (201 mg, 76% yield). An analytic sample was obtained by silica gel chromatography eluting with CH_2Cl_2 100%. Selected ^1H NMR (400 MHz $CDCl_3$): δ 7.45-7.35 (3H, m), 7.35 (1H, d, *J* = 16.1 Hz), 6.27 (1H, d, *J* = 16.1 Hz), 4.13 (1H, d, *J* = 5.89 Hz), 3.55 (1H, t, *J* = 6.0 Hz), 3.22 (1H, m), 1.4 (6H, d, *J* = 7.1 Hz). HR ESIMS *m/z* 312.1900 $[M+H]^+$, $C_{15}H_{16}Cl_2NO_2$ requires 312,1903.

3-(2,6-dichlorophenyl)-4-(*E*)-ethyl penta-2,4-dienoate-5-isopropyl-isoxazole (97): DMSO (455 µl, 1.6 mmol) was added dropwise for 5 min to a solution of oxalyl chloride (1.6 ml, 6.4 mmol) in dry dichloromethane (5 ml) at −78 °C under argon atmosphere. After 30 min, a solution of **96** (100 mg, 0.3 mmol) in dry CH_2Cl_2 (5 ml) was added dropwise and the mixture was stirred at −78 °C. After 30 min, Et_3N dry (892 µl, 6.4 mmol) was added dropwise to the solution and the mixture was allowed to warm to room temperature. After 1 h, the reaction was quenched by addition of aqueous $NaHSO_4$ (1 M, 10 ml). The layers were separated, and the aqueous phase was extracted with CH_2Cl_2 (3×20 ml). The combined organic layers were washed with saturated aqueous $NaHSO_4$, saturated

aqueous $NaHCO_3$, and brine. The organic phase was then dried over Na_2SO_4 and concentrated to give the corresponding aldehyde (150 mg, quantitative yield) as a colorless oil, which was used without any further purification. To a solution of aldehyde (0.5 mmol) in THF dry (5 ml) was added LiOH (24 mg, 1.0 mmol) and TEPA (triethylphosphonoacetate, 175 μl, 0.9 mmol). The reaction mixture was stirred for 30 min at room temperature and then quenched with water (5 ml). The mixture was then extracted with EtOAc (3×30 ml), and the organic phase was concentrated *in vacuo*. The solution was poured over a C18 silica gel column. Fraction eluted with *n*-hexane: EtOAc 99:1 gave a mixture that was further purified by HPLC on a Nucleodur 100-5 C18 (5 μm; 4.6 mm i.d. x 250 mm) with MeOH/H_2O (80:20) as eluent (flow rate 1 mL/min), to give 8 mg (6% yield, over two steps) of compound **97** (t_R=16.2 min). Selected ^{1}H NMR (400 MHz $CDCl_3$): δ 7.48-7.39 (3H, m), 6.56 (2H, d, *J* = 16.8 Hz), 5.94 (1H, t, *J* = 14.8 Hz), 5.67 (1H, d, *J* = 15.24 Hz), 4.19 (2H, dd, *J* = 7.38 Hz), 3.37 (1H, m), 1.46 (6H, d, *J* = 3.63 Hz), 1.29 (3H, t, *J* = 7.1 Hz).HR ESIMS *m/z* 380.2650 $[M+H]^+$, $C_{19}H_{20}Cl_2NO_3$ requires 380.2654.

VI. Experimental section 2-AAQ derivatives.

Compound 99. To a suspension of Menadione (**98**, 15.7 g, 89 mmol) in ethyl acetate (Volume: 129 ml) was added a solution of sodium hydrosulfite (36.6 g, 179 mmol) in water (Volume: 145 ml) at rt. The resulting mixture was stirred for 30 min at the same temperature. The organic layer was separated, washed with water (2×110 mL), and concentrated under reduced pressure. The residue was triturated with *n*-heptane (160 mL). The resulting crystals were collected by filtration, washed with *n*-heptane (50 mL), and dried under reduced pressure to give 2-methylnaphthalene-1,4-diol **99** (14.8 g, 85 mmol, 96 % yield) as a pale purple crystalline powder.

Compound 100. To a solution of 2-methylnaphthalene-1,4-diol (14.8 g, 85 mmol) and dimethylsulfate (43.1 g, 342 mmol) in isopropanol (Volume: 231 ml), sodium methoxide (65.9 g of a 28 wt.% solution in methanol, 342 mmol) was added dropwise at rt. The resulting mixture was stirred for 30 min at 63°C and cooled to 20 °C. Water (500 ml) was added and the mixture was extracted using EtOAc (2×500 ml). The organic layers were combined and washed successively with water (4×125 ml), dried with $MgSO_4$, filtered through a glass filter (Por. 4), rinsed with EtOAc and concentrated under reduced pressure to give 1,4-dimethoxy-2-methylnaphthalene **100** (17 g, 84 mmol, 98% yield) as a brown solid, which was used directly in further reactions without purification.

Compound 101. To a solution of 1,4-dimethoxy-2-methylnaphthalene (17 g, 84 mmol) in DCM (Volume: 232 ml) at 0 °C under a nitrogen atmosphere, there was slowly added (dropwise with a pipet) bromine (14.8 g, 92 mmol). The mixture was stirred under nitrogen for 1 h at 0 °C, and for an additional 1 h at room temperature. Then, 230 ml of water was added to the reaction mixture, the layers

were separated, and the aqueous phase was extracted with another 230 ml of CH_2Cl_2. The combined organic layers were washed with 230 ml brine, dried with $MgSO_4$, filtered through a glass filter (Por. 4) and the solvents were removed *in vacuo* to yield 2-bromo-1,4-dimethoxy-3-methylnaphthalene **101** (23.5 g, 83 mmol, 99% yield).

Compound 102. In a dry 500 ml RB flask (oven dried, cooled under Ar), an ethyl acetate (Volume: 228 ml) solution of the 2-bromo-1,4-dimethoxy-3-methylnaphthalene (16 g, 57.1 mmol) was added. Next, N-Bromosuccinimide (13.2 g, 74.3 mmol) and (E)-Azobis(isobutyronitrile) (657 mg, 4 mmol) were added. The reaction mixture was then stirred and heated to reflux temp. When the reaction was finished, the reaction mixture was concentrated *in vacuo*. The crude product was then diluted with heptane, and the resulting crystals were separated by filtration. The filtrate was then concentrated to obtain 2-bromo-3-(bromomethyl)-1,4-dimethoxynaphthalene **102** (19.4 g, 53.8 mmol, 94% yield).

Compound 103. To an oven dried Ar-filled 500 mL RB flask there was added Sodiumhydride (2.1 g, 86 mmol) in 190 mL DMSO. After applying a nitrogen blanket, N-Ethenylacetamide (7.3 g, 86 mmol) in 25 mL of DMSO was added and the mixture was stirred at room temperature until a clear mixture was obtained. The nitrogen blanket could then be removed. A solution of 2-bromo-3-(bromomethyl)-1,4-dimethoxynaphthalene (20.6 g, 57.1 mmol) in 70 ml dry DMSO was added dropwise over 1 hour and the mixture was stirred further at room temperature for 1 hour. After completation, the reaction was poured in 500 mL of water and extracted with (2x500 mL) EtOAc. Combined organic fractions were washed with water (2x300 mL) and 150 mL brine. The combined organic fractions were then dried with $MgSO_4$, filtered over a glass filter (Por. size 4) and

the solvents were removed *in vacuo* to obtain N-((3-bromo-1,4-dimethoxynaphthalen-2-yl)methyl)-N-vinylacetamide **103** (19.4 g, 5.,3 mmol, 93% yield).

Compound 104. N-((3-bromo-1,4-dimethoxynaphthalen-2-yl)methyl)-N-vinylacetamide (5 g, 13.7 mmol) was loaded in a flame dried pressure tube as a solid. Palladium(II)acetate (154 mg, 0.7 mmol) and tert-Butyldicyclohexylphosphonium tetrafluoroborate (470 mg, 1.4 mmol) were weighed each in an NMR vial and closed with a cap with a septum. Cesium carbonate (4.92 g, 15.1 mmol) was weighed in an NMR vial without cap and was oven-dried for at least one hour. The needed amount of solvent was taken with a syringe. This was then used to dissolve the reagents sequentially in the different vials by dissolving the first reagent (e.g. $Pd(OAc)_2$), add this to the ligand, and so on. The mixture of all the reagents, except for Cs_2CO_3, was then added to the oven-dried MW vial under Ar atmosphere. The oven-dried cesium carbonate was, after cooling, added to the mixture (without Ar atmosphere). The mixture was then bubbled with Ar for at least ten minutes. The pressure tube was closed with a screw cap, and was then heated to 130 °C under an Ar atmosphere until the reaction was complete (overnight). The solution was then poured onto 40 g of ice and extracted with (3x100 ml) EtOAc. The combined layers were washed with water (2x200 ml) and brine (200 ml). The combined organic layers were then dried with $MgSO_4$, filtered over a glass filter through a pad of celite (Por. size 4) and the solvents were removed *in vacuo* to obtain 1-(5,10-dimethoxybenzo[*g*]isoquinolin-2(1H)-yl)ethanone **104** (3.9 g, 13.8 mmol, 100 % yield).

Compound 105. 1-(5,10-dimethoxybenzo[*g*]isoquinolin-2(1H)-yl)ethanone (3,9 g, 13.8 mmol) in a two-necked round-bottomed flask was dissolved in Methanol (Volume: 332 ml), and sodiumhydroxide (83 mL of a 5 M aq. solution, 413 mmol) was added. The mixture was heated at reflux, while pressurized air was bubbled through the reaction mixture until the reaction was finished (both deprotection and oxidation of C-N bond). After this time the mixture was made neutral with an aq. HCl solution and the mixture was concentrated *in vacuo*. The crude mixture was then extracted with (3x200 ml) DCM and the combined organic layers were washed with water (200 ml) and brine (200 ml). The combined organic layers were dried with $MgSO_4$ and filtered through a glass filter (Por. size 4), and the solvents were removed *in vacuo* to obtain 5,10-dimethoxybenzo[*g*]isoquinoline **105** (3.6 g, 14.9 mmol, quantitative). Purification by silica gel chromatography eluting with heptane: ethyl acetate 8:2 afforded 1.8 g of pure **105.**

Compound 106. To a solution of 5,10-dimethoxybenzo[*g*]isoquinoline (1.8 g, 7.5 mmol) in a mixture of ACN/H_2O (2:1) was added Cerium(IV)diammoniumnitrate (8.7 mg, 15.8 mmol) portionwise over 5 minutes at 0 °C. The mixture was stirred at 0 °C until the reaction was complete. Next, the solution was quenched with water (200 ml), ACN was removed *in vacuo* and the mixture was then extracted with DCM (3x200 ml). The combined organic phases were dried over $MgSO_4$, filtered over a glass filter (Por. 4) through a pad of Celite and the solvents were removed *in vacuo* to obtain benzo[*g*]isoquinoline-5,10-dione **106** (1.6 g, 7.5 mmol, 87 % yield) .

Compound 107. To a solution of benzo[*g*]isoquinoline-5,10-dione (1.6 g, 7.5 mmol) in DCM (Volume: 75 ml), m-Chloroperbenzoicacid (75% wt, 2.1 g , 9.0

mmol) was added at room temperature while stirring. The reaction mixture was stirred at room temperature until the reaction was complete. When the reaction was finished, the solvent was removed *in vacuo*, after which a saturated $NaHCO_3$ solution (400 ml) was added and was allowed to stir for about 1 hr. The water layer was then separated and extracted with DCM (2x400 ml) and the combined organic layers were washed with brine (200 mL), dried with $MgSO_4$, filtered through a glass filter (Por. 4) and the solvents were removed *in vacuo* furnishing compound **107** (1.5 g, 6.6 mmol, 88%yield).

^{1}H NMR (400 MHz $CDCl_3$): δ 8.89 (1H, s), 8.43 (1H, d, J = 6.8 Hz), 8.33 (2H, m), 8.14 (1H, d, J = 6.7 Hz), 7.8 (2H, m).

^{13}C NMR (100 MHz $CDCl_3$): δ 180.4, 179.6, 143.7,137.4, 135.3, 134.8, 133.1, 132.9, 131.1, 128.0, 127.7, 127.6, 123.9. HR ESIMS *m/z* 226.2030 $[M+H]^+$, $C_{13}H_7NO_3$ requires 226.2033

General amination procedure

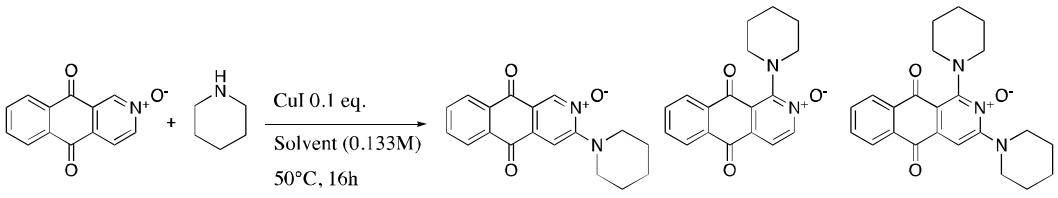

108 **109** **110**

To a solution of compound **107** (30 mg, 0.1 mmol) in the choosen solvent (0.1 M), CuI (2.5 mg, 10% mmol) was added (when required). The reaction was capped and an oxygen balloon was insert. Then, piperidine was added and the reaction was let stir for the selected time. After completion, the mixture was cooled down to room temperature, then H_2O (10 ml) was added and the mixture

was extracted with DCM (3x30 ml). The combined organic layers were dried over $MgSO_4$ and evaporated to give the desired product.

Entry 1. Following the general procedure, toluene was used as solvent. Piperideine (91 mg, 1.1 mmol) was added and the reaction was let stir for 16 h. Purification by silica gel chromatography (from 100% heptane to 50% heptane:ethyl acetate) yielded compound **108** (3.7 mg, 0,012 mmol, 9%) and compound **110** (1.5 mg, 0.004 mmol, 2%).

Entry 2. Following the general procedure, DMSO was used as solvent. Piperideine (91 mg, 1.1 mmol) was added and the reaction was let stir for 16 h. Purification by silica gel chromatography (from 100% heptane to 50% heptane:ethyl acetate) yielded compound **108** (9 mg, 0,029 mmol, 16%) and compound **110** (2.8 mg, 0.007 mmol, 4%).

Entry 3. Following the general procedure, DMF was used as solvent. Piperideine (91 mg, 1.1 mmol) was added and the reaction was let stir for 16 h. Purification by silica gel chromatography (from 100% heptane to 50% heptane:ethyl acetate) yielded compound **108** (18 mg, 0.045 mmol, 34%) and compound **110** (5 mg, 0.017 mmol, 13%).

Entry 4. Following the general procedure, CH_3CN was used as solvent. Piperideine (91 mg, 1.1 mmol) was added and the reaction was let stir for 16 h. Purification by silica gel chromatography (from 100% heptane to 50% heptane:ethyl acetate) yielded compound **108** (4 mg, 0.013 mmol, 10%).

Entry 5. Following the general procedure, toluene was used as solvent. Piperideine (91 mg, 1.1 mmol) was added and the reaction was let stir for 10 days. Purification by silica gel chromatography (from 100% heptane to 50%

heptane:ethyl acetate) yielded compound **108** (4 mg, 0.013 mmol, 10%) and compound **110** (3 mg, 0.007 mmol, 5%).

Entry 6. Following the general procedure, an excess of piperideine was added and the reaction was let stir for 16 h. Purification by silica gel chromatography (from 100% heptane to 50% heptane:ethyl acetate) yielded compound **110** (2 mg, 0.006 mmol, 4%).

Entry 7. Following the general procedure, toluene was used as solvent. Cs_2CO_3 (43 mg, 0.1 mmol) was used as additive and piperideine (91 mg, 1.1 mmol) was added and the reaction was let stir for 16 h. Purification by silica gel chromatography (from 100% heptane to 50% heptane:ethyl acetate) yielded compound **108** (13 mg, 0.04 mmol, 32%) and compound **110** (31 mg, 0.08 mmol, 60%).

Entry 8. Following the general procedure, without adding CuI, toluene was used as solvent. Cs_2CO_3 (43 mg, 0.1 mmol) was used as additive and piperideine (91 mg, 1.1 mmol) was added and the reaction was let stir for 5h.

Entry 9. Following the general procedure, without adding CuI, toluene was used as solvent. Cs_2CO_3 (43 mg, 0,.1 mmol) was used as additive and piperideine (23 mg, 0.3 mmol) was added and the reaction was let stir for 16 h.

Entry 10. Following the general procedure, without adding CuI, toluene was used as solvent. Cs_2CO_3 (43 mg, 0.1 mmol) was used as additive and piperideine (45 mg, 0.5 mmol) was added and the reaction was let stir for 16 h.

Entry 11. Following the general procedure, without adding CuI, toluene was used as solvent. Cs_2CO_3 (43 mg, 0.1 mmol) was used as additive and piperideine (91 mg, 1.1 mmol) was added and the reaction was let stir for 72 h. Purification by silica gel chromatography (from 100% heptane to 50% heptane:ethyl acetate)

yielded compound **108** (11 mg, 0.03 mmol, 23%) and compound **110** (2 mg, 0.0065 mmol, 5%).

Entry 12. Following the general procedure, toluene was used as solvent. Cs_2CO_3 (43 mg, 0.1 mmol) was used as additive and piperideine (91 mg, 1.1 mmol) was added and the reaction was let stir for 5 h. Purification by silica gel chromatography (from 100% heptane to 50% heptane:ethyl acetate) yielded compound **108** (4 mg, 0.014 mmol, 10%), compound **109** (6 mg, 0.018 mmol, 14%) and compound **110** (28 mg, 0.07 mmol, 53%).

Entry 13. Following the general procedure, toluene was used as solvent. Cs_2CO_3 (43 mg, 0.1 mmol) was used as additive and piperideine (91 mg, 1.1 mmol) was added and the reaction was let stir for 5 h. Purification by silica gel chromatography (from 100% heptane to 50% heptane:ethyl acetate) yielded compound **108** (5 mg, 0.016 mmol, 9%), compound **109** (19 mg, 0.062 mmol, 32%) and compound **110** (20 mg, 0.05 mmol, 26%).

GENERAL REDUCTION PROCEDURE

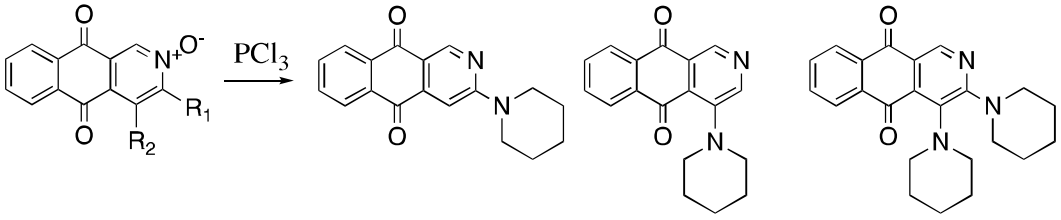

111 **112** **113**

To a stirred mixture of The N-oxide in toluene (0.2 M), was dropwise added Phosphorustrichloride (1.2 eq.). The reaction mixture was stirred for 1h at room temperature. Saturated solution of $NaHCO_3$ (5 mL) was added and then stirred for additional 5 min. The aqueous layer was then washed with CH_2Cl_2 (3x20 ml). The combined organic layers were dried over $MgSO_4$, filtered, and concentrated under reduced pressure to give the de-oxygenated product in quantitative yields.

SPECTROSCOPIC DATA

Compound 108.

^{1}H NMR (400 MHz $CDCl_3$): δ 8.88 (1H, s), 8.28 (2H, broad t), 7.82 (2H, m), 7.6 (1H, s), 3.52 (4H, t, *J* = 5.0 Hz), 1.82 (4H, m), 1.73 (2H, m).

^{13}C NMR (100 MHz $CDCl_3$): δ 180.9, 180.0, 139.5, 134.6, 134.4, 133.5, 133.4, 129.4, 127.5, 127.3, 122.3, 110.2, 49.5 (2-C), 25.6 (2-C), 24.3. HR ESIMS *m/z* 309.3370 $[M+H]^+$, $C_{18}H_{16}N_2O_3$ requires 309.3372

Compound 109.

^{1}H NMR (400 MHz $CDCl_3$): δ 8.48 (1H, s), 8.27 (1H, d, *J* = 7.75 Hz), 8.22 (1H, d, *J* = 7.75 Hz), 8.18 (1H, d, *J* = 1.67 Hz), 7.83 (1H, t, *J* = 7.12 Hz), 7.77 (1H, t, *J* = 7.35 Hz), 3.18 (4H, t, *J* = 5.1 Hz), 1.77 (4H, m), 1.69 (2H, m).

^{13}C NMR (100 MHz $CDCl_3$): δ 181.5, 178.9, 150.4, 135.0, 134.9, 134.7, 133.6, 132.9, 131.6, 130.2, 127.7, 126.8, 118.0, 53.5 (2-C), 25.6 (2-C), 23.7. HR ESIMS *m/z* 309.3371 $[M+H]^+$, $C_{18}H_{16}N_2O_3$ requires 309.3374

Compound 110

^{1}H NMR (400 MHz $CDCl_3$): δ 8.6 (1H, s), 8.18 (2H, m), 7.79 (1H, t, *J* = 7.3 Hz), 7.74 (1H, t, *J* = 7.3 Hz), 3.34 (4H, broad d), 1.77-1.68 (12H, m).

^{13}C NMR (100 MHz $CDCl_3$): δ 181.4, 180.6, 157.9, 148.3, 135.9, 134.7, 133.8, 133.4, 132.6, 127.0 (2-C), 126.6, 124.4, 52.1 (2-C), 49.0 (2-C), 26.6 (2-C), 26.1 (2-C), 24.0, 23.9. HR ESIMS *m/z* 391.4710 $[M+H]^+$, $C_{23}H_{25}N_3O_3$ requires 391.4709

Compound 111.

^{1}H NMR (400 MHz $CDCl_3$): δ 9.12 (1H, s), 8.32 (1H, d, *J* = 7.5 Hz), 8.26 (1H, d, *J* = 7.7 Hz), 7.81 (1H, t, *J* = 7.6 Hz), 7.28 (1H, s), 3.83 (4H, t, *J* = 4.9 Hz), 1.74 (2H, m), 1.69 (4H, m).

^{13}C NMR (100 MHz $CDCl_3$): δ 183.8, 180.8, 161.1, 151.4, 134.7, 134.5, 1343.6, 133.2, 127.1 (2-C), 116.1, 100.9, 46.4 (2-C), 25.6, 24.6 (2-C). HR ESIMS *m/z* 293.3380 $[M+H]^+$, $C_{23}H_{25}N_3O_3$ requires 293.3383

Compound 112.

^{1}H NMR (400 MHz $CDCl_3$): δ 9.01 (1H, s), 8.83 (1H, s), 8.25 (2H, m), 7.8 (2H, m), 3.27 (4H, t, *J* = 5.4 Hz), 1.88 (4H, q, *J* = 5.6 Hz), 1.77 (2H, q, *J* = 5.7 Hz).

^{13}C NMR (100 MHz $CDCl_3$): δ 184.1, 181.7, 148.4, 145.2, 140.0, 134.8, 134.5, 133.6, 132.2, 127.4, 127.3, 126.5, 126.8124.5, 53.5, 25.8, 24.1. HR ESIMS *m/z* 293.3382 $[M+H]^+$, $C_{23}H_{25}N_3O_3$ requires 293.3385

Compound 113.

^{1}H NMR (400 MHz $CDCl_3$): δ 8.95 (1H, s), 8.19 (1H, m), 8.09 (1H, m), 7.73 (2H, m), 3.57 (4H, t, *J* = 5.1 Hz), 3.11 (4H, broad t), 1.75-1.69 (12H, m).

^{13}C NMR (100 MHz $CDCl_3$): δ 185.6, 182.2, 164.8, 143.0, 138.0, 133.8, 133.6, 133.4, 133.2, 126.4, 126.3, 121.5, 50.3 (2-C), 49.7 (2-C), 26.3, 26.1, 24.6 (2-C), 24.1 (2-C). HR ESIMS *m/z* 376.4720 $[M+H]^+$, $C_{23}H_{25}N_3O_3$ requires 376.4724

Compound 114.

^{1}H NMR (400 MHz $CDCl_3$): δ 8.15 (1H, d, *J* = 7.6 Hz), 7.93 (1H, d, *J* = 7.6 Hz), 7.66 (1H, dt, *J* = 7.6 Hz, *J* = 0.8 Hz), 7.57 (1H, dt, *J* = 7.5 Hz, *J* = 1.0 Hz), 3.71 (4H, broad t), 3.57 (4H, broad t), 2.91 (4H, broad t), 1.68-1.62 (18H, m).

^{13}C NMR (100 MHz $CDCl_3$): δ 190.6, 176.6, 161.7, 155.5, 140.9, 135.5, 134.7, 133.5, 131.6, 129.1, 126.3, 124.9, 101.9, 50.6 (2-C), 50.2 (2-C), 49.9 (2-C), 26.5, 26.4, 26.3 (2-C), 24.9 (2-C), 24.8, 24.0 (2-C). HR ESIMS *m/z* 459.6060 $[M+H]^+$, $C_{23}H_{25}N_3O_3$ requires 459.6063.

^{1}H NMR (400 MHz, $CDCl_3$) of compound **107**

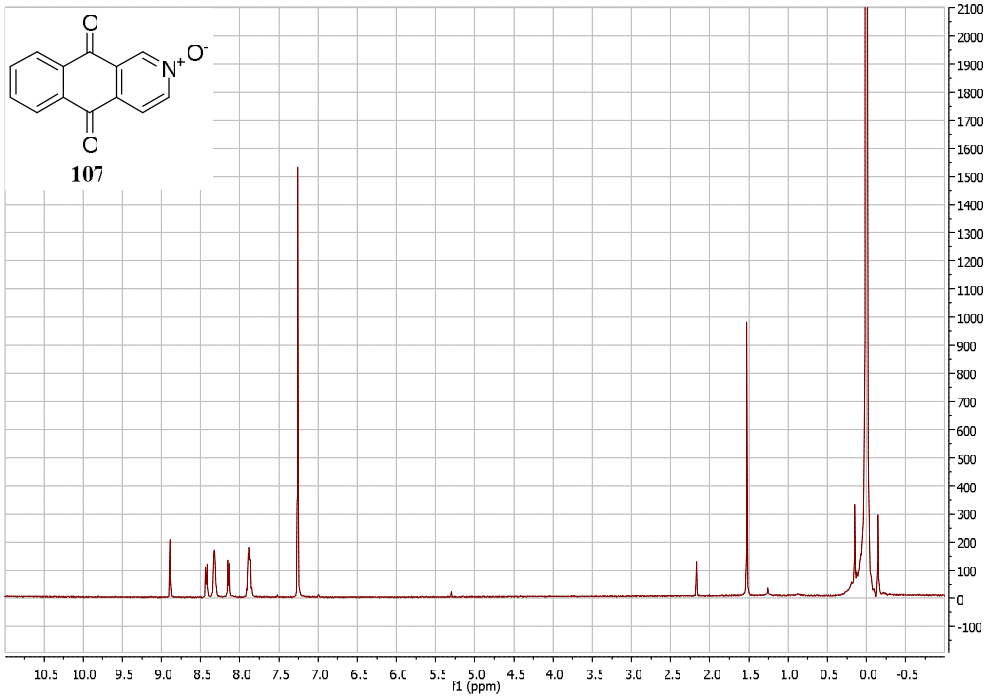

^{1}H NMR (400 MHz, $CDCl_3$) of compound **108**

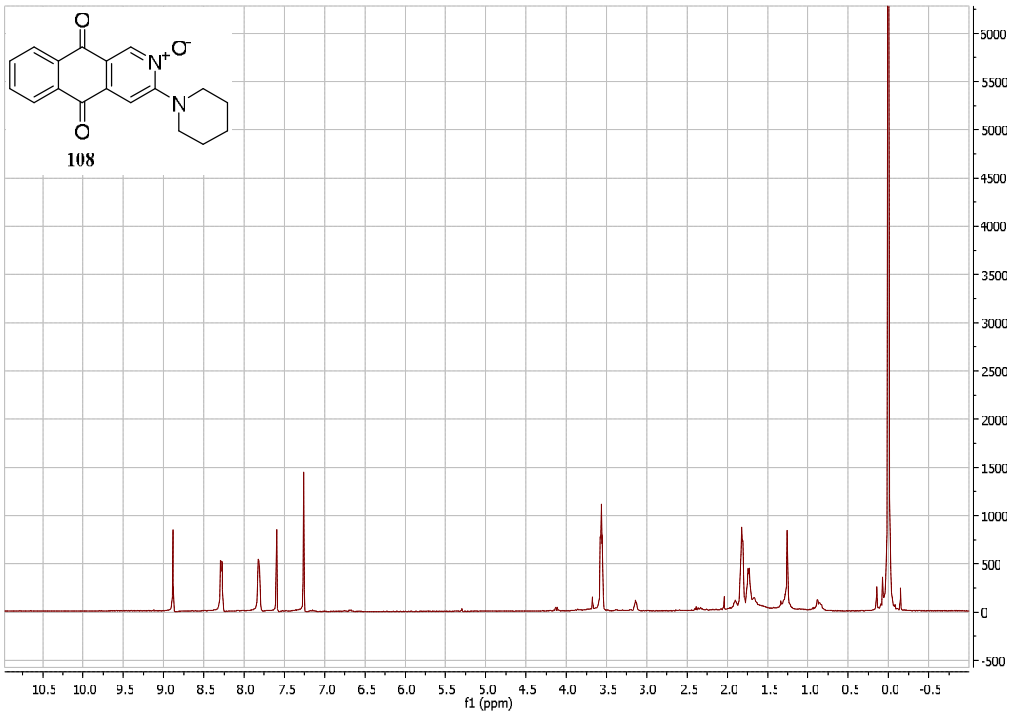

^{1}H NMR (400 MHz, $CDCl_3$) of compound **109**

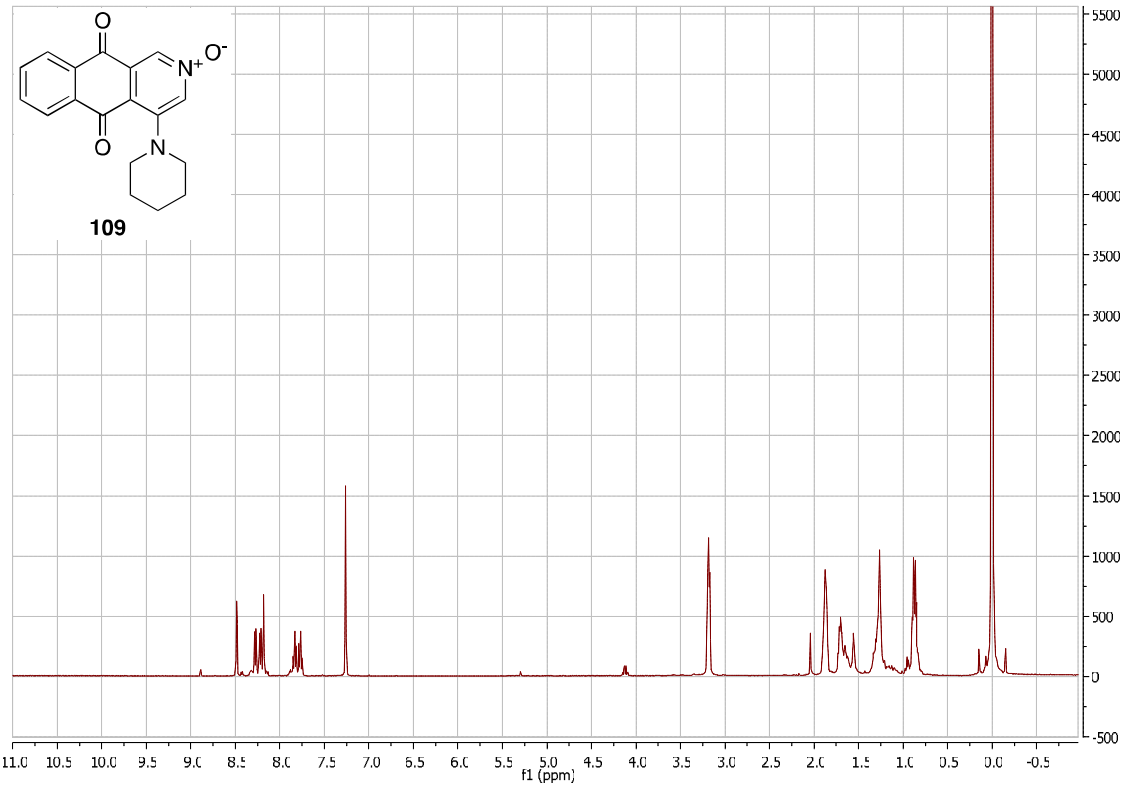

^{1}H NMR (400 MHz, $CDCl_3$) of compound **110**

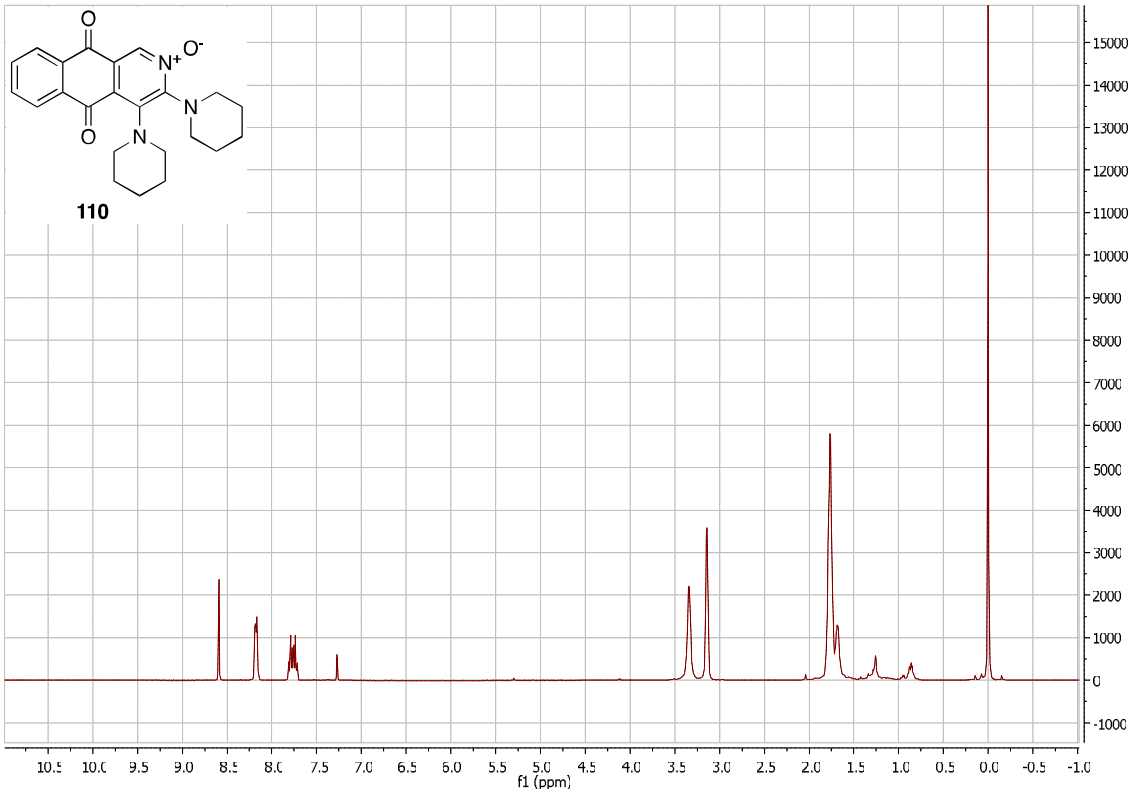

^{1}H NMR (400 MHz, $CDCl_3$) of compound **111**

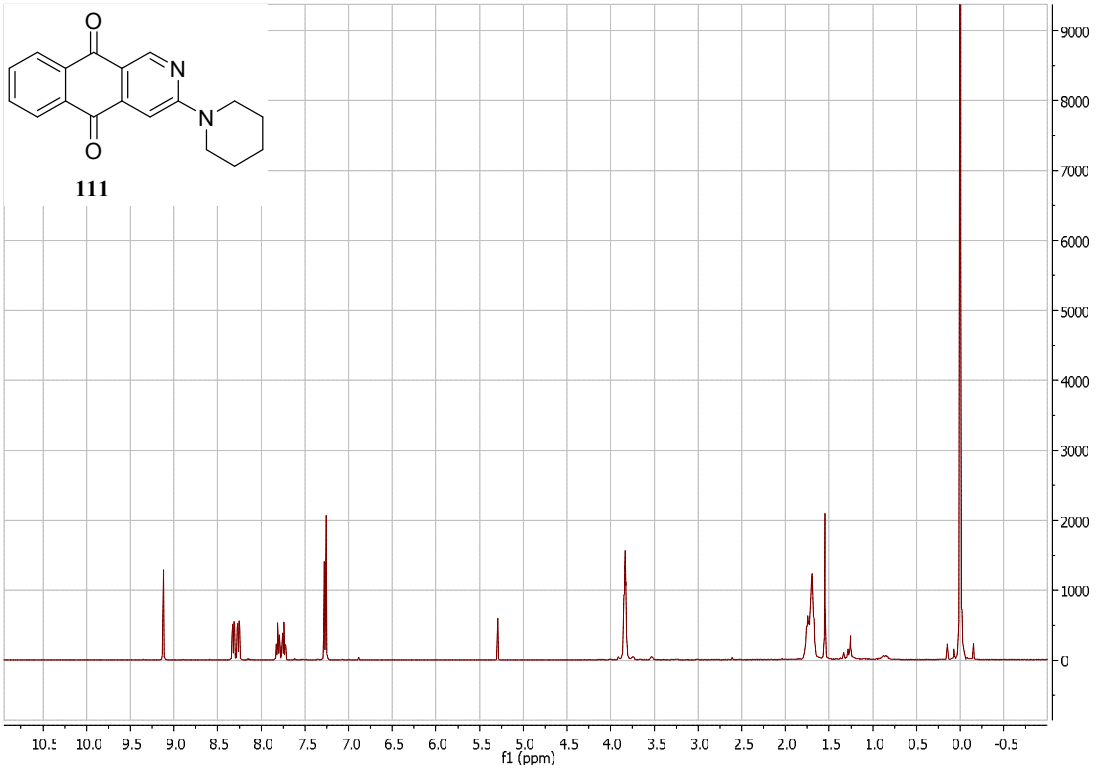

^{1}H NMR (400 MHz, $CDCl_3$) of compound **112**

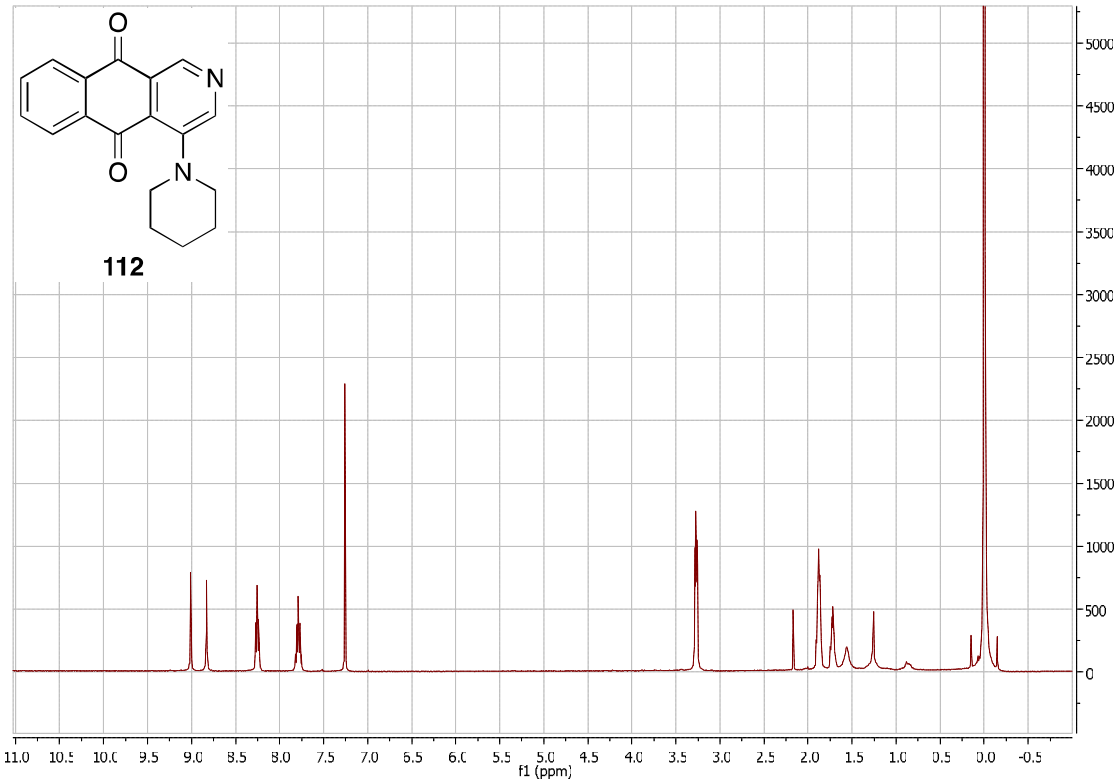

^{1}H NMR (400 MHz, $CDCl_3$) of compound **113**

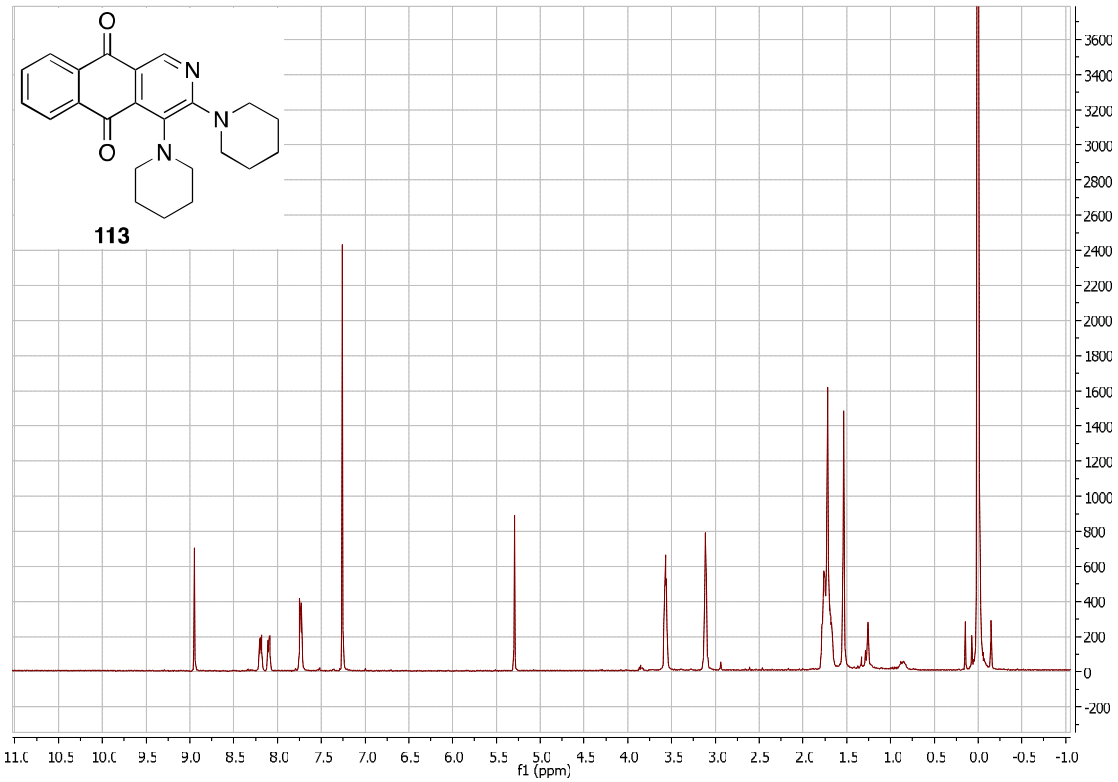

^{1}H NMR (400 MHz, $CDCl_3$) of compound **114**

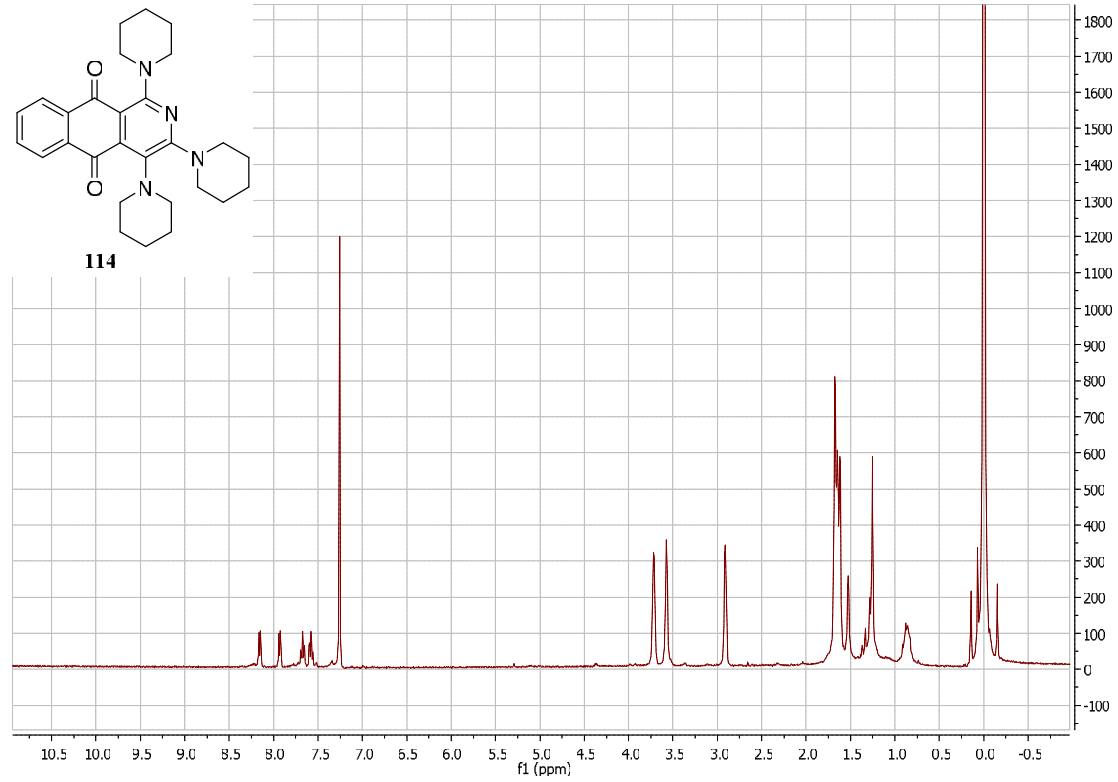

REFERENCES

[1] Kaur J. *Cardiology research and*. **2014**: 943162

[2] Alberti K.G.M.M. et al. Definition, Diagnosis, and Classification of Diabetes Mellitus and its Complications. *World Health Organization*. **1999**, pp. 32–33

[3] Obesity and Overweight. WHO, 28 Nov. 2012

[4] Alberti K.G.M.M. et al. The IDF Consensus Worldwide Definition of the Metabolic Syndrome. *Publication. Ed. Scott M. Grundy. Brussels, Belgium: International Diabetes Federation*, **2006**. Web. 29 Nov

[5] National Cholesterol Education Program (NCEP) Expert Panel on Detection, Evaluation, and Treatment of High Blood Cholesterol in Adults (Adult Treatment Panel III). *Circulation*, **2002.** 106, 25, pp. 3143–3421

[6] Wilson P. W. F. et al. The metabolic syndrome practical guide to origins and treatment: part I. *Circulation*. **2003.** 108, 12, pp. 1422–1424,

[7] Mills E. et al. The safety of overthe- counter niacin. A randomized placebo-controlled trial [ISRCTNI8054903]. *BMC Clinical Pharmacology*, **2003,** vol. 3, article 4

[8] Grundy S. M. et al. Efficacy, safety, and tolerability of once-daily niacin for the treatment of dyslipidemia associated with type 2 diabetes: results of the Niaspan trial. *Archives of Internal Medicine*, **2002,** vol. 162, no. 14, pp. 1568–1576

[9] Streja D. Combination therapy for the treatment of dyslipidemia. *Current Opinion in Investigational Drugs*, **2004,** vol. 5, no. 3, pp. 306–312

[10] Israili Z. H. et al. Metabolic syndrome: treatment of hypertensive patients. *The American Journal of Therapeutics*, **2007,** vol. 14, no. 4,pp. 386–402

[11] Abuissa H. et al. Angiotensin-converting enzyme inhibitors or angiotensin receptor blockers for prevention of type 2 diabetes: a metaanalysis of randomized clinical trials. *Journal of the American College of Cardiology*, **2005,** vol. 46, no. 5, pp. 821–826

[12] Bosch J. et al. Effect of ramipril on the incidence of diabetes. *The New England Journal of Medicine*, **2006,** vol. 355, no. 15, pp. 1551–1562

[13] Knowler W.C. et al. Reduction in the incidence of type 2 diabetes with lifestyle intervention or metformin. *The New England Journal of Medicine*, **2002,** vol. 346, no. 6, pp. 393 403

[14] Knowler W. C. et al. Prevention of type 2 diabetes with troglitazone in the Diabetes Prevention Program. *Diabetes*, **2005** vol. 54, no. 4, pp. 1150–1156

[15] Chiassonet J.L. al. Acarbose for prevention of type 2 diabetes mellitus: the STOP-NIDDM randomised trial. *The Lancet*, **2002,** vol. 359, no. 9323, pp. 2072–2077

[16] Chiasson J-L. et al. Acarbose treatment and the risk of cardiovascular disease and hypertension in patients with impaired glucose tolerance: the STOP-NIDDM trial. *Journal of the American Medical Association*, **2003**, vol. 290, no. 4, pp. 486–494.

[17] Novac N. et al Nuclear Receptors: Overview and Classification. *Current Drug Targets - Inflammation & Allergy*, **2004**, 3, 335-346

[18] Makishima M. et al. Identification of a nuclear receptor for bile acids. *Science* **1999**; 284:1362-1365

[19] Parks D.J. et al. Bile acids: natural ligands for an orphan nuclear receptor. *Science* **1999**; 284:1365-1368

[20] Wang H. et al. Endogenous bile acids are ligands for the nuclear receptor FXR/BAR. *Mol Cell* **1999**;3:543-553

[21] Moore D.D. et al. The NR1H and NR1I receptors: constitutive androstane receptor, pregnene X receptor, farnesoid X receptor α, farnesoid X receptor β, liver X receptor α, liver X receptor β, and vitamin D receptor. *Pharmacol. Rev.* **2006**, *58*, 742–759

[22] Wang Y. D. et al. FXR: a metabolic regulator and cell protector. *Cell Res*. **2008**, *18*, 1087–1095

[23] Goodwin B. et al. A regulatory cascade of the nuclear receptors FXR, SHP-1, and LRH-1 represses bile acid biosynthesis. *Mol. Cell* **2000,** 6, 517–526

[24] Lu T.T. et al. Molecular basis for feedback regulation of bile acid synthesis by nuclear receptors. *Mol. Cell* **2000**, 6, 507–515

[25] Ballatori N. et al. OSTa–OSTb: a major basolateral bile acid and steroid transporter in human intestinal, renal, and biliary epithelia. *Hepatology* **2005,** 42, 1270–1279

[26] Zollner G. et al. Role of nuclear receptors in the adaptive response to bile acids and cholestasis: pathogenetic and therapeutic considerations. *Mol. Pharm.* **2006,** 3, 231–250

[27] Fiorucci S. et al. Farnesoid X receptor agonists in biliary tract disease. *Curr. Opin. Gastroenterol*. **2009**, 25 252–259

[28] Fiorucci S. et al. Farnesoid X receptor agonist for the treatment of liver and metabolic disorders: focus on 6-ethyl-CDCA. *Mini Rev. Med. Chem*. **2011,** 11 753–762

[29] Watanabe M. et al. Bile acids lower triglyceride levels via a pathway involving FXR, SHP, and SREBP-1c. *J. Clin. Invest*. **2004,** 113, 1408–1418

[30] Yamagata K. et al. Bile acids regulate gluconeogenic gene expression via small heterodimer partner-mediated repression of hepatocyte nuclear factor 4 and Foxo1. *J. Biol. Chem*. **2004**, 279, 23158–23165

[31] Duran-Sandoval D. et al. The farnesoid X receptor modulates hepatic carbohydrate metabolism during the fasting–refeeding transition. *J. Biol. Chem*. **2005**, 280, 29971–29979

[32] Duran-Sandoval D. et al. Glucose regulates the expression of the farnesoid X receptor in liver. *Diabetes* **2004**, 53, 890–898

[33] Maloney P.R. et al. Identification of a chemical tool for the orphan nuclear receptor FXR. *J. Med. Chem*. **2000**, 43, 2971-2974

[34] Nicolaou K.C. et al. Discovery and optimization of non-steroidal FXR agonists from natural product-like libraries. *Org. Biol. Chem*. **2003**, 1, 908-920

[35] Pellicciari R et al. 6alpha-ethyl-chenodeoxycholic acid (6-ECDCA), a potent and selective FXR agonist endowed with anticholestatic activity. *J. Med. Chem*. **2002**, 45, 3569-3572

[36] Joseph S.B. et al. LXRs: new therapeutic targets in atherosclerosis? *Curr. Opin. Pharmacol*. **2003**, 3, 192-197

[37] Edwards P.A. et al. LXRs; oxysterol-activated nuclear receptors that regulate genes controlling lipid homeostasis. *Vascul. Pharmacol*. **2002**, 38 (4): 249–56.

[38] Repa J.J. et al. Regulation of absorption and ABC1-mediated efflux of cholesterol by RXR heterodimers. *Science*, **2000**, 289, 1524-1529

[39] Repa J.J. et al. Regulation of mouse sterol regulatory element-binding protein-1c gene (SREBP-1c) by oxysterol receptors, LXR alpha and LXR beta. *Genes Dev*. **2000**, 14, 2819-2830

[40] Alberti S. et al. Hepatic cholesterol metabolism and resistance to dietary cholesterol in LXRβ-deficient mice. *J. Clin. Invest*. **2001**, 107 (5): 565–73

[41] Joseph S.B. et al. Synthetic LXR ligand inhibits the development of atherosclerosis in mice. *Proc. Natl. Acad. Sci. U.S.A*. **2001**, 99 (11): 7604–9

[42] Song C. et al. Auto-oxidized cholesterol sulfates are antagonistic ligands of liver X receptors: implications for the development and treatment of atherosclerosis. *Steroids*. 2001, **66** (6): 473–9

[43] Kratzer A. et al. Synthetic LXR agonist attenuates plaque formation in apoE-/- mice without inducing liver steatosis and hypertriglyceridemia. *J. Lipid Res*. **2009**, 50 (2): 312–26

[44] Laffitte B.A. et al. Activation of liver X receptor improves glucose tolerance through coordinate regulation of glucose metabolism in liver and adipose tissue. *Proc. Natl. Acad. Sci. U.S.A*. **2003**, 100 (9): 5419–24

[45] Joseph S.B. et al. Reciprocal regulation of inflammation and lipid metabolism by liver X receptors. *Nat. Med*. **2003**, **9** (2): 213–9

[46] Fukuchi J. et al. Antiproliferative effect of liver X receptor agonists on LNCaP human prostate cancer cells. *Cancer Res*. **2004**, 64 (21): 7686–9

[47] Chuu C.P. et al. Inhibition of tumor growth and progression of LNCaP prostate cancer cells in athymic mice by androgen and liver X receptor agonist. *Cancer Res*. **2006**, 66 (13): 6482–6

[48] Schultz, J.R. et al. Role of LXRs in control of lipogenesis. *Genes Dev*. **2000**, 14, 2831-2838

[49] Cha, J.Y. et al. The carbohydrate-response elementbinding protein is a target gene of LXR. *J. Biol. Chem*. **2007**, 282, 743-751

[50] Uyeda K. et al. Carbohydrate response element binding protein, ChREBP, a transcription factor coupling hepatic glucose utilization and lipid synthesis. *Cell Metab*. **2006**, 4, 107-110

[51] Yamashita H. et al. A glucoseresponsive transcription factor that regulates carbohydrate metabolism in the liver. *Proc. Natl. Acad. Sci. U.S.A*. **2001**, 98, 9116-9121

[52] Janowski B.A et al. Structural requirements of ligands for the oxysterol liver X receptors LXRalpha and LXRbeta. *Proc. Natl. Acad. Sci. U.S.A.* **1999** , 96 , 266-271

[53] Letasiová S. et al. Antiproliferative activity of berberine in vitro and in vivo. *Biomed. Pap.* **2005**, 149, 461-463

[54] Chen Q.M. et al. Studies on the hypoglycemic effect of Coptis chinensis and berberine. *Xue Xue Bao*, **1986** , 21 , 401-406

[55] Leng S.H. et al. Therapeutic effects of berberine in impaired glucose tolerance rats and its influence on insulin secretion. *Acta Pharmacol. Sin*. **2004**, 25 , 496-502

[56] D'Amore C. et al. Design, synthesis, and biological evaluation of potent dual agonists of nuclear and membrane bile Acid receptors. *J. Med. Chem*. **2014**, 57, 937-954

[57]Duboca H. et al. *Digestive and Liver Disease* **2014** 46, 4, 302–312

[58] Keitel V. et al. The membrane-bound bile acid receptor TGR5 (Gpbar-1) is localized in the primary cilium of cholangiocytes. *Biological Chemistry*. **2010**, 391, pp. 785–789

[59] Keitel V. et al. TGR5 in the biliary tree. *Digestive Diseases*. **2011**, 29, pp. 45–47 V.

[60] Keitel M. et al. Expression and function of the bile acid receptor TGR5 in Kupffer cells. *Biochemical and Biophysical Research Communications*, **2008**, 372, pp. 78–84

[61] Watanabe M. et al. . Bile acids induce energy expenditure by promoting intracellular thyroid hormone activation. *Nature*, **2006**, *439*, 484-489

[62] Pols T.W. H.et al. The bile acid membrane receptor TGR5 as an emerging target in metabolism and inflammation. *Review journal of hepatology*, **2011**, 54, 1263-1272

[63] Thomas C. et al. TGR5-mediated bile acid sensing controls glucose homeostasis. *Cell Metabolism*. **2009**, 10, pp. 167–177

[64] Harach T. et al. TGR5 potentiates GLP-1 secretion in response to anionic exchange resins. *Science Reporter* **2012**, 2, p. 430

[65] Potthoff M.J. et al. Colesevelam suppresses hepatic glycogenolysis by TGR5-mediated induction of GLP-1 action in DIO mice. *American Journal of Physiology – Gastrointestinal and Liver Physiology*. **2013**, 304 pp. G371–G380

[66] Wu T. et al. Effects of rectal administration of taurocholic acid on glucagon-like peptide-1 and peptide YY secretion in healthy humans. *Diabetes, Obesity and Metabolism.* **2013**, 15, pp. 474–477

[67] Sato H. et al. Anti-hyperglycemic activity of a TGR5 agonist isolated from *Olea europaea* .*Biophysical Research Communications* **2007**, 362, pp. 793–798

[68] Wang Y.D. et al. The G-protein-coupled bile acid receptor, Gpbar1 (TGR5), negatively regulates hepatic inflammatory response through antagonizing nuclear factor kappa light-chain enhancer of activated B cells (NF-κB) in mice. *Hepatology*, 54 (**2011**), pp. 1421–1432

[69] Keitel V. et al. Expression and function of the bile acid receptor TGR5 in Kupffer cells. *Biochemical and Biophysical Research Communications*, 372 (**2008**), pp. 78‑84

[70] Cipriani S. et al. The bile acid receptor GPBAR-1 (TGR5)modulates integrity of intestinal barrier and immune response to experimentalcolitis. PLoS ONE **2011**;6:e25637

[71] Yoneno K. et al. TGR5 signalling inhibits theproduction of pro-inflammatory cytokines by in vitro differentiated inflammatory and intestinal macrophages in Crohn's disease. *Immunology* **2013**;139:19–29.

[72] Karlsen T.H. et al Genome-wide association analysis in primary sclerosing cholangitis. *Gastroenterology*, 138 (**2010**), pp. 1102–1111

[73] Loftus E.V. et al PSC-IBD: a unique form of inflammatory bowel disease associated with primary sclerosing cholangitis. *Gut*, 54 (**2005**), pp. 91–96

[74] Boyer J.L. Bile formation and secretion. *Compr Physiol* **2013**;3: 1035-1078

[75] Schaap F.G. et al. Bile acid receptors as targets for drug development. *Nature Rev. Gastroenterol. Hepatol*. **2014**, 1, 55−67

[76] Azzaroli F. et al. Ursodeoxycholic acid diminishes Fas-ligand-induced apoptosis in mouse hepatocytes. *Hepatology* **2002**, 36, 49−54

[77] Keene C.D. et al. Tauroursodeoxycholic acid, a bile acid, is neuroprotective in a transgenic animal model of Huntington's disease. *Proc. Natl. Acad. Sci. U.S.A*. **2002**, 99, 10671−10676

[78] Alberts D.S. et al. Phase III trial of ursodeoxycholic acid to prevent colorectal adenoma recurrence. *J. Natl. Cancer Inst*. **2005**, 97, 846−853

[79] Alemi F. et al. The TGR5 receptor mediates bile acid-induced itch and analgesia *J. Clin. Invest.* 123 (**2013**) 1513–1530

[80] Vassileva G. et al. *Biochem J*. **2006**;398:423–430

[81] Li et al. *Molecular Endocrinology*. **2011**, 25(6):1066-71

[82] Festa C. et al. Exploitation of cholane scaffold for the discovery of potent and selective farnesoid X receptor (FXR) and G-protein coupled bile acid receptor 1 (GPBAR1) ligands. *J Med Chem* **2014**; 57; 8477-8495

[83] Sepe V. et al. Insights on FXR selective modulation. Speculation on bile acid chemical space in the discovery of potent and selective agonists. *Scientific Reports* 6:19008

[84] Pellicciari R. et al. Non genomic actions of bile acids. Synthesis and preliminary characterization of 23- and 6,23-alkyl-substituted bile acid derivatives as selective modulators for the G-protein coupled receptor TGR5. *J. Med. Chem*. 50 (**2007**) 4265–4268

[85] Neuschwander-Tetri B.A. et al. Farnesoid X nuclear receptor ligand obeticholic acid for non-cirrhotic, non-alcoholic steatohepatitis (FLINT): a multicentre, randomised, placebo-controlled trial *Lancet* 385 (**2015**) 956–965

[86] Hirschfield G.M. et al. Efficacy of obeticholic acid in patients with primary biliary cirrhosis and inadequate response to ursodeoxycholic acid *Gastroenterology* 148 (**2015**) 751–761

[87] Carino A. et al. The bile acid receptor GPBAR1 (TGR5) is expressed in human gastric cancers and promotes epithelial-mesenchymal transition in gastric cancer cell lines. *Oncotarget*. **2016**. 7, 38, 61021-61035

[88] Song C. et al. Selective activation of liver X receptor alpha by 6-alpha-hydroxy bile acids and analogs. *Steroids* (**2000**) 65**,** 423-427

[89] Eyssen H.J. et al. Formation of hyodeoxycholic acid from muricholic acid and hyocholic acid by an unidentified gram-positive rod termed HDCA-1 isolated from rat intestinal microflora. *Appl. Environ. Microbiol.* (**1999**) 65**,** 3158-3163

[90] Sacquet E. et al. Intestinal absorption, excretion, and biotrnsformation of hyodeoxycholic acid in man. *J. Lipid Res*. **1983,** 24 (5): 604–13. PMID:6875384.

[91] Song C. et al. Selective activation of liver X receptor alpha by 6-alpha-hydroxy bile acids and analogs. *Steroids*. **2000**, 65, 423-427

[92] Singhal A.K. et al. Role of hydrophilic bile acids and of sterols on cholelithiasis in the hamster. *J. Lipid Res.* **1984,** 25, 564-570

[93] Shih D.M. et al. Hyodeoxycholic acid improves HDL function and inhibits atherosclerotic lesion formation in LDLR-knockout mice. *FASEB J.* **2013**, 9, 3805-3817

[94] Fujita K. Dietary hyodeoxycholic acid exerts hypolipidemic effects by reducing farnesoid X receptor antagonist bile acids in mouse enterohepatic tissues. *Lipids* (**2014**), 49, 963-973.

[95] Sato H. et al. . Novel potent and selective bile acid derivatives as TGR5 agonists: biological screening, structure-activity relationships, and molecular modeling studies. *J. Med. Chem.* **2008***,* 51, 1831-1841

[96] Svensson S. et al. Crystal structure of the heterodimeric complex of LXRα and RXRβ ligand-binding domains in a fully agonistic conformation. *EMBO J.* **2003**, 22, 4625-4633

[97] Sepe V. et al. Total synthesis and pharmacological characterization of solomonsterol A, a potent marine pregnane-X-receptor agonist endowed with anti-inflammatory activity. *J. Med. Chem*. **2011**, 54, 4590-4599

[98] Bełtowski J. Liver X receptors (LXR) as therapeutic targets in dyslipidemia. *Cardiovasc. Ther*. **2008**, 26(4):297-316

[99] Fradera X. et al. X-ray structures of the LXRα LBD in its homodimeric form and implications for heterodimer signaling. *J. Mol. Biol.* **2010**, 399, 120-132

[100] Seol W. et al. An orphan nuclear hormone receptor that lacks a DNA binding domain and heterodimerizes with other receptors. *Science* **1996,** 272, 1336–1339

[101] Lee H. K. et al. Structure and expression of the orphan nuclear receptor SHP gene. *J Biol Chem* **1998**, 273, 14398–14402

[102] Johansson L. et al. The orphan nuclear receptor SHP inhibits agonist-dependent transcriptional activity of estrogen receptors ERα and ERβ *Journal of Biological Chemistry*. **1999,** 274, 1, 345–353

[103] Kemper J. K. et al. Role of an mSin3A-Swi/Snf chromatin remodeling complex in the feedback repression of bile acid biosynthesis by SHP *Molecular and Cellular Biology*. **2004,** 24, 17, 7707–7719

[104] Gabriella G. et al. A Pleiotropic Role for the Orphan Nuclear Receptor Small Heterodimer Partner in Lipid Homeostasis and Mtabolic Pathways. *Journal of Lipids,* **2012**. Article ID 304292

[105] Zou A. et al. New Insights into Orphan Nuclear Receptor SHP in Liver Cancer. *Nucl Receptor Res*. **2015**; 2: 101162

[106] Fiorucci S. et al. The nuclear receptor SHP mediates inhibition of hepatic stellate cells by FXR and protects against liver fibrosis. *Gastroenterology.* **2004,** 127, 1497–1512

[107] Moreira R.K. Hepatic stellate cells and liver fibrosis. *Arch Pathol Lab Med*. **2007,** 131(11):1728-34.

[108] Farhana L. et al. Adamantyl-substituted retinoid-related molecules bind small heterodimer partner and modulate the Sin3A repressor *Cancer Research.* **2007**, 67, 318–325

[109] Maloney P. R. et al. Identification of a Chemical Tool for the Orphan Nuclear Receptor FXR. *J. Med. Chem.*, **2000**, *43* (16), pp 2971–2974

[110] Renga B. et al. SHP-dependent and -independent induction of peroxisome proliferator-activated receptor-γ by the bile acid sensor farnesoid X receptor counter-regulates the pro-inflammatory phenotype of liver myofibroblasts. *Inflamm Res*. **2011,** 60, 577–87

[111] Jacobs J. et al. A survey of synthetic routes towards 2-azaanthraquinones. *Tetrahedron* **2011,** 67, 9459e9471

[112] Arsenault G.P. The structure of bostrycoidin, a β-aza-anthraquinone from Fusarium solani D_2 purple *Tetrahedron Lett*. **1965**, 45, 4033e4037

[113] Parisot D. et al. Conversion of anhyro-fusarubin lactol into the antibiotic Bostrycoidin. *M. J. Antibiot*. **1989**, 42, 1189e1190

[114] Visconti A. et al. Produzione di pigmenti da parte di isolati di Fusarium Moniliforme Sheld. da cereali in Italia e loro attività antibatterica *Phytopathol. Mediterr*. **1983**, 22, 150-156.

[115] Miljkovic A. et al. Scorpinone: A New Natural Azaanthraquinone Produced by a *Bispora*-like Tropical Fungus *J. Nat. Prod.* **2001**, 64, 1251-1253

[116] Moriyasu Y. et al. 5-Deoxy-7-methylbostrycoidin from cultured mycobionts from Haematomma sp. *Phytochemistry* **2001**, 58, 239-241

[117] Cimanga R.K. et al. *Recent Prog. Med. Plants* **2008**, 13, 337-349

[118] Burckhardt G. et al. Binding of 2-Azaanthraquinone Derivatives to DNA and Their Interference with the Activity of DNA Topoisomerases in Vitro *Biochemistry* **1998**, 37, 4703-4711

[119] El-Helw L.M. et al. Pixantrone: a promising drug in the treatment of non-Hodgkin lymphomas *Future Oncol*. **2009**, 5, 445-453

[120] Gonsette R.E. Subcellular localization of the tumor suppressor protein APC in developing cultured neurons *J. Neurosci*. **2004**, 223, 81-86

[121] Moore M.H. et al. DNA-drug interactions. The crystal structure of d(CGATCG) complexed with daunomycin. *J. Mol. Biol*. **1989**, 206, 693-705

[122] Perkins W. et al. Myocardial effects of mitoxantrone and doxorubicin in the mouse and guinea pig. *Cancer Treat. Rep*. **1984**, 68, 841

[123] Potts K.T. et al. Cycloaddition routes to azaanthraquinone derivatives. 1. Use of azadienophiles. *J. Org. Chem*. **1986**, 51, 2011-2021

[124] Krapcho A.P. et al. 6,9-Bis[(aminoalkyl)amino]benzo[g]isoquinoline-5,10-diones. A Novel Class of Chromophore-Modified Antitumor Anthracene-9,10-diones: Synthesis and Antitumor Evaluations. *J. Med. Chem*. **1994**, 37, 828-837

[125] Goldstein D.M. et al. *PCT Int. Appl*. WO 2008028860, **2008**

[126] Maiti D. et al. Orthogonal Cu- and Pd-Based Catalyst Systems for the O- and N-Arylation of Aminophenols. *J. Am. Chem. Soc*. **2009**, 131, 17423–17429

[127] Keith J.M. One-Step Conversion of Azine *N*-Oxides to α-1,2,4-Triazolo-, 1,2,3-Triazolo, Imidazolo-, and Pyrazoloheteroarenes. *J. Org. Chem*. **2010**, 75, 2722–2725

[128] Bremner D.H. et al. A Comparison of Methods for N-Oxidation of Some 3-Substituted Pyridines. *Synthetic Communications*. **1997**. 27:9, 1535-1542

[129] Londregan A.T. et al. General and Mild Preparation of 2-Aminopyridines. *Organic Letters*. **2010**. 12, 22, 5254-5257

[130] Crisenza G.E.M. et al. C2-Alkenylation of N-heteroaromatic compounds via Brønsted acid catalysis *Org. Biomol. Chem.* **2016**,14, 5820-5825

[131] Zhu et al. Copper-Catalyzed Direct Amination of Quinoline N−Oxides via C−H Bond Activation under Mild Conditions. *Org. Lett*. **2014**, 16, 1840−1843

[132] Mori-Quiroz et al. Exploiting Alkylquinone Tautomerization: Amine Benzylation. *Org. Lett.* **2016**. 18 (14), 3446-3449

[133] Sepe, V. et al. The first total synthesis of solomosterol B, a marine pregnane X receptor agonist. *Eur. J. Org. Chem.* **2012**, 5187–5194.

AKNOWLEDGMENTS

In the end, I would like to express my gratitude to the following people for their different contribution in reaching this important goal.

I would like to express my deep gratitude to Professor Angela Zampella, my research supervisor, for her patient guidance, encouragement and useful critiques.

I would like to thank Prof. Maria Valeria D'Auria, the Ph.D. coordinator, for her scientific and personal advices.

Dr. Valentina Sepe, the N20 lab guidance; I would like to thank her for the valuable and constructive suggestions during the planning and development of this research work.

I wish to thank also Prof. Franco Zollo and Dr. Simona De Marino, two of the kindest people I have met during this Ph.D. Our discussion about chemistry or instrument maintenance have taught a lot.

A special mention to Prof. Kourosch Abbaspour Tehrani, my supervisor at Antwerp University, that very kindly accepted me in his lab.

Special thanks goes to my colleagues and friends Dr. Carmen Festa and Dr. Claudia Finamore. I am very proud to have spent this three years with two strong, smart, positive girls like you. I wish you all the best.

I wish to thank my parents and my brother, whose unconditional love and support were fundamental for me. To you, I dedicate this thesis.

Finally, I would like to thank my girlfriend Roberta, a source of inspiration for me. Her love, patience and encouragement have supported me constantly throughout this Ph.D. To you, I dedicate all of my love.